Synthesis and Characterization of Multi-Component Polymeric Materials Prepared via Free Radical Polymerization

Anthony J. Pasquale

Dissertation submitted to the Faculty of the
Virginia Polytechnic Institute and State University
in partial fulfillment of the requirements for the degree of

Doctor of Philosophy
in
Chemistry

Timothy E. Long, Chair
James E. McGrath
Judy S. Riffle
Mark R. Anderson
Robert D. Allen

April 22, 2002
Blacksburg, Virginia

Keywords: Alternating Copolymerization, Maleic Anhydride, Norbornene, Nitroxide Mediated Free Radical Polymerization, *In situ* FTIR Spectroscopy

Synthesis and Characterization of Multi-Component Polymeric Materials Prepared via Free Radical Polymerization

Anthony J. Pasquale

ABSTRACT

High molecular weight star-shaped polystyrenes were prepared via the coupling of 2,2,6,6-tetramethyl-1-piperidinyloxy (TEMPO) terminated polystyrene oligomers with divinylbenzene (DVB) in *m*-xylene at 138 °C. Linear polystyrene oligomers (M_n = 19,300 g/mol, M_w/M_n = 1.10) were synthesized in bulk styrene using benzoyl peroxide in the presence of TEMPO at approximately 130 °C. *In situ* mid-infrared spectroscopy was successfully utilized to follow initiation, monomer conversion, and polymer formation. Real-time data allowed for the determination of apparent rate constants ($k_{app}=k_p[P_n\bullet]$) of 2.1 x 10^{-5} s^{-1} at 132 °C and 1.2 x 10^{-5} s^{-1} at 126 °C from the profile of the decaying styrene vinyl carbon-hydrogen (=CH_2) absorbance at 907 cm^{-1}. Coupling of the TEMPO terminated oligomers under optimum conditions resulted in a compact and dense product with a number average molecular weight exceeding 300,000 g/mol (M_w/M_n = 3.03) after 24 h, suggesting the formation of relatively well-defined star-shaped polymers.

Synthetic factors that affected the molecular weight, yield, and composition of maleic anhydride (MAH), norbornene (Nb), and *tert*-butyl 5-norbornene-2-carboxylate (NbTBE) terpolymers were investigated. Pseudo first order kinetic analysis using *in situ* FTIR indicated that the observed rate of reaction (k_{obs}) was a strong function of the Nb/NbTBE ratio with a maximum of 6.7 x 10^{-5} s^{-1} for a 50/0/50 Nb/NbTBE/MAH monomer ratio and a minimum of 1.1 x 10^{-5} s^{-1} for a 0/50/50 Nb/NbTBE/MAH ratio. Polymer yields were also observed to be a function of the Nb/NbTBE ratio and also decreased with increasing NbTBE. Calculated work of adhesion values (W_{adh}) values were observed to increase as the content of NbTBE was increased. 193 nm photoresist formulations incorporating polymers with high NbTBE content showed increased imaging performance using 193 nm

light and successfully produced sharp and defined features as small as 110 nm, which was demonstrated via scanning electron microscopy (SEM). Additional functionality was introduced via the copolymerization of MAH with several norbornene (Nb) derivatives that were synthesized from facile Diels-Alder cycloaddition reactions of cyclopentadiene with α-olefins containing electron withdrawing groups. Subsequent hydrolysis of the anhydride offered further versatility and provided an avenue to introduce aqueous base solubility into Nb/MAH copolymers.

Acknowledgements

I would first like to thank my advisor, Dr. Timothy E. Long for his direction and instruction throughout my graduate career at Virginia Tech. I feel very fortunate to have learned all that I have from him. I would also like to thank the members of my advisory committee: Dr. James E. McGrath, Dr. Judy S. Riffle, Dr. Mark R. Anderson, and Dr. Robert D. Allen for their time and guidance through my graduate study at Virginia Tech.

Special thanks are owed to the Center for Adhesive and Sealant Science (CASS) at Virginia Tech and the Adhesive and Sealant Council (ASC) Education Foundation for financial support through a fellowship. This interaction allowed me to gain valuable experiences through collaborations with other CASS colleagues as well as the opportunity to attend several outstanding conferences in the area of adhesive science. I would also like to thank all of the faculty and staff associated with CASS who it has been a pleasure to interact with and learn from: Ms. Tammy J. Hiner, Ms. Linda A. Haney, Dr. Thomas C. Ward, Dr. James P. Wightman, Dr. David A. Dillard, Dr. John G. Dillard, Dr. Charles E. Frazier, and Dr. Ritchey M. Davis. I would also like to thank IBM, which provided financial support for the norbornene/maleic anhydride copolymerization project.

Special thanks go to Mr. Tom Glass for all his help with NMR. Dr. Alan Esker for his assistance with spin coating polymer films onto silicon wafers. Frank Cromer for help with surface analysis. Hoa Truong (IBM Almaden) for her time spent performing lithographic analysis and also spending several days training me in lithographic characterization while I was at the IBM Almaden Research Center. Thanks to Ms. Esther Brann, Ms. Laurie Good, and Ms. Millie Ryan in the NSF office for all of their help and patience whenever I had a question or needed help with an administrative issue. In addition, Ms. Jan McGinty is acknowledged for her help with the chemistry stockroom and special orders.

Much thanks go out to all of my colleagues (both current and former) in the Long group. In particular, I would like to thank those with whom I have the pleasure of sharing

the Davidson lab: Phil Madison, Jeremy Lizotte, Koji Yamauchi, Ann Fornof, Matt McKee, and the undergrads: Kayleen Gloor, Jen Kelly, Heather Brooks, and Sara Anderson. I would also like to acknowledge group members from the Hahn Lab: Sebnem Kara, Qin Lin, Huaiying Kang, Dave Williamson, Lars Kilian, Casey Hudelson, Youngtai Yoo, and Zhenhe Wang. A special thanks goes out to the daily lunch crowd with whom it was always nice to get a break from the lab.

Lastly, I would like express my deepest gratitude to my parents for their guidance, support, and encouragement throughout my life.

Table of Contents

List of Schemes

List of Figures

List of Tables

CHAPTER 1

Introduction

1.1 BACKGROUND AND OBJECTIVES

The synthesis of macromolecules with controlled and functional architecture is becoming an increasingly important field of polymer science. For example, star-shaped polymers have received significant attention due to their desirable properties (*e.g.* low melt viscosity) that arise from having a highly branched structure. A star structure is described as a nonlinear polymer composed of multiple backbone chains emanating from junction points. Branching results in a more compact structure than analogous linear structures on account of high segment density, which dramatically affects crystalline, mechanical, and viscoelastic properties. Macromolecules with controlled architectures are typically prepared using living polymerization methodologies such as anionic, cationic, and group transfer polymerization. In addition to conventional living polymerization methods, recent advancements in controlled free radical polymerization routes have further increased the synthetic methods that are available to the polymer chemist to prepare macromolecules with well-defined features and architectures. The goal of this research was to synthesize star-shaped polystyrene using nitroxide-mediated controlled free radical polymerization. Linear polystyrene oligomers were prepared in bulk styrene using benzoyl peroxide in the presence of 2,2,6,6-tetramethyl-1-piperidinyloxy (TEMPO) at approximately 130 °C. High molecular weight star-shaped polystyrenes were then synthesized by means of coupling the TEMPO terminated polystyrene oligomers with divinylbenzene (DVB) in *m*-xylene at 138 °C.

Alternating copolymerization is an example of chain copolymerization where each of the comonomers adds preferentially to the other. The most widely studied electron-

deficient comonomer for producing alternating copolymers is maleic anhydride (MAH). MAH contains an electron poor double bond and has been shown to homopolymerize poorly via free radical methods. However, MAH will copolymerize with a number of electron rich olefins to form alternating copolymers. Many 1,2-disubstituted and cyclic olefins that do not readily homopolymerize using free radical initiators will form alternating copolymers with MAH. This has been attributed to the low radical reactivity of the electron rich 1,2-disubstituted double bond. Recently, main-chain alicyclic macromolecules produced from the alternating free radical copolymerization of MAH with norbornene and norbornene derivatives have received attention as photoresist materials for 193 nm lithography (Figure 1.1**)**. MAH serves to incorporate polar carbonyl oxygen, which provides necessary adhesion and solubility that are required for acceptable imaging performance. In addition, the alicyclic backbone resulting from copolymerization with norbornene provides for excellent etch resistance, surpassing even phenol based materials.

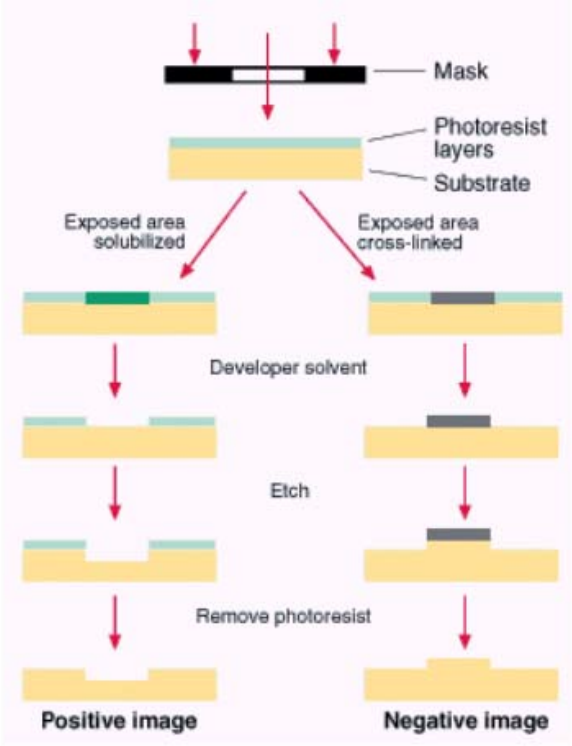

Chem. Eng. News **1999**, *77(37)*, **37**.

Figure 1.1 Photolithography imaging process.

Despite the abundance of scientific and patent literature describing the alternating copolymerization of maleic anhydride with electron-rich olefins, copolymerizations with norbornene proceed via a complex polymerization mechanism resulting in the uncontrolled formation of low molecular weight oligomers. The goal of the research described herein was to focus on fundamental studies to elucidate the free radical alternating copolymerization of maleic anhydride with norbornene and norbornene derivatives. This was achieved using a unique combination of experimental variation, *in situ* infrared spectroscopy, and nuclear magnetic resonance spectroscopy. This fundamental mechanistic understanding provided the basis for the development of a polymerization system that resulted in more predictable molecular weights and higher polymerization yields. Special attention was devoted to kinetic investigations to understand the relative

rates of propagation versus copolymerization reaction variables. It is proposed that the development of this better defined polymerization mechanism for maleic anhydride with norbornene and norbornene derivatives will also result in viable manufacturing processes and improved 193 nm lithographic performance for these materials.

Research efforts have also focused on the synthesis of functionalized macromolecules based on alternating copolymers of MAH and Nb derivatives. MAH offers exceptional versatility in the compositional design of new macromolecules due to both inherent polarity and potential reactivity of the anhydride functionality. For example, hydrolysis of the anhydride functionality yielded two acid functionalities per anhydride repeat unit. In addition, facile Diels-Alder reactions of cyclopentadiene with functional olefins offered further versatility and further provides for a myriad of potential copolymer compositions that can be produced via alternating copolymerizations of MAH with norbornene derivatives.

In all areas of the research, the application of *in situ* infrared spectroscopy was applied as a real-time analytical reaction-monitoring tool. The use of *in situ* infrared spectroscopy (FTIR) is well suited to obtain real-time structural and kinetic information of polymerization reactions. Controlled polymerization routes such as stable free radical polymerization (SFRP) and living anionic polymerization permit the synthesis of well-defined macromolecules with controlled chemical composition, predictable molecular weight based on the initiator concentration and monomer conversion, and narrow molecular weight distribution. Demonstration of the controlled nature of a polymerization is traditionally accomplished from a linear plot of number-average molecular weight versus conversion, narrow molecular weight distributions, and ability to target number average molecular weights. *In situ* FTIR provides real-time data without multiple reactor samplings and subsequent analyses. The utility of this state of the art reaction-monitoring tool was evaluated for its application to the monitoring of a variety of polymerization processes. The objective for these initial *in situ* IR studies was to determine polymer structural information real-time as the polymerization proceeds. It is anticipated that this tool will soon become a very valuable instrument to process and mechanistic chemists in both industry and academia. The ability to follow monomer conversion, polymer end

groups, and deleterious side reactions provides a better understanding and control of polymerization pathways. Initial efforts were focused upon the *in situ* monitoring of the stable free radical polymerization (SFRP) of styrene. SFRP is a relatively new controlled polymerization route that permits the synthesis of well-defined macromolecules with controlled chemical composition, predictable molecular weight, and narrow molecular weight distribution. The ability to control polymer architecture is essential in advanced technological applications where well-defined macromolecular architectures are required. The kinetic and mechanistic understanding of SFRP is in its infancy and presented an excellent opportunity for the application of *in situ* IR to evaluate this controlled polymerization chemistry. In addition, *in situ* IR was employed to evaluate the synthesis of complex star-shaped polymer architectures via SFRP using an "arm-first" method.

CHAPTER 2

Literature Review

2.1 INTRODUCTION

An increasingly important area of polymer science research is the preparation of macromolecules with controlled and functional architecture. The preparation of controlled architectures has traditionally been achieved using living polymerization pathways such as anionic, cationic, and group-transfer polymerization. Recent years have seen new developments in free radical chemistry that permit the synthesis of these controlled and functional architectures. The following review chapter will highlight select developments in the field of preparing macromolecules with controlled architecture via free radical polymerization methodologies. The first section presents a discussion on the use of stable nitroxide additives, which act as reversible terminating agents and allow for molecular weight control, narrow molecular weight distributions, and controlled topologies during free radical polymerization processes. This next section will focus on the synthesis of star-shaped macromolecules via controlled-polymerization methodologies. Following that, a review on fundamental aspects of free radical alternating copolymerizations will be presented. Developments in polymeric materials for 193 nm photolithography with a specific emphasis on cyclic olefin/maleic anhydride (COMA) copolymers prepared via free radical alternating copolymerization will also be discussed. The last section of this review will highlight the use of *in situ* FTIR spectroscopy to monitor polymerization reactions in real-time.

2.2 STABLE FREE RADICAL POLYMERIZATION

2.2.1 Introduction

Free radical polymerization is a very important polymerization pathway for the synthesis of commercial polymer products due to both economic and practical advantages.[1] However, a recognized disadvantage of free radical polymerization is the apparent lack of control over polymer features such as molecular weight, molecular weight distribution, topology, *etc*. The ability to synthesize controlled polymer architectures is becoming increasingly more important for the preparation of materials that are to be used in advanced technological applications where well-defined macromolecular architectures are required. A limited degree of control and functionality can be introduced using free radical polymerization via the addition of agents such as functionalized initiators or chain-transfer agents,[2] but typically living polymerization methods are utilized to prepare macromolecules with controlled architectures.

Living chain polymerization techniques used to control polymer architecture traditionally include living anionic,[3] cationic,[4] or group-transfer[5] polymerization procedures. Living polymerization mechanisms offer advantages that include the ability to control molecular weight, molecular weight distribution, architecture (such as well-defined block copolymers), and end group functionalization.[6] However, living chain polymerization chemistries typically require stringent reaction conditions such as the

---

[1] Rosen, S. L. *Fundamental Principles of Polymeric Materials*; Wiley-Interscience: New York, 1993.
[2] Odian, G. *Principles of Polymerization*, 3rd ed.; Wiley-Interscience: New York, 1991; Chapter 3.
[3] Szwarc, M. *Nature* **1956**, *178*, 1168. *Anionic Polymerization: Kinetics, Mechanisms, and Synthesis*; McGrath, J. E., Ed.: ACS Symposium Series 166; American Chemical Society: Washington, DC, 1981.
[4] Matyjaszewski, K. *Cationic Polymerizations: Mechanisms, Synthesis and Applications*; Marcel Dekker: New York, 1996.
[5] Sogah, D. Y.; Hertler, W. R.; Webster, O. W.; Cohen, G. M. *Macromolecules* **1987**, *20*, 1473.

complete absence of oxygen and water impurities as well as ultra-pure solvents and reactants. In addition, living chain polymerization methods are incompatible with a number of functionalities.[3] As a consequence of these factors, the commercial application of living chain polymerization has been limited. A desirable alternative has been the development of free radical polymerization chemistry that allows for the production of controlled polymer structures similar to what can be achieved using living polymerization techniques. Recent developments in controlled free radical polymerization methods that include stable free radical polymerization (SFRP),[7] atom transfer radical polymerization (ATRP),[8] and radical addition-fragmentation transfer (RAFT)[9] have significantly enhanced the ability to produce well-defined polymer architectures using free radical methods.

2.2.2 Controlled Polymerization of Styrene via Stable Free Radical Polymerization (SFRP)

The basic feature of controlled polymerization is the absence of transfer and termination processes in chain growth reactions. Szwarc first defined such systems as "living polymerizations" in 1956 based upon his work on anionic polymerizations.[2] Szwarc found that even after 100% conversion of monomer had been reached, the "living" anionic chain ends could further propagate via addition of more monomer. Furthermore, Szwarc found that the monomer added quantitatively to propagating chain ends, resulting in nearly monomodal molecular weight distributions. Several decades later, Otsu and coworkers extended the idea of living polymerizations to free radical systems. They reported the use of initiator-transfer-agent-terminators, or iniferters, to reduce irreversible

---

[6] Webster, O. W. *Science* **1991**, *251*, 887.
[7] Hawker, C. J. *ACC. Chem. Res.* **1997**, *30*, 373.
[8] Patten, T. E.; Matyjaszewki, K. *Adv. Mater.* **1998**, *10*, 901.
[9] Chiefari, J.; Chong, Y. K.; Ercole, F.; Krstina, J.; Jeffery, J.; Le, T. P. T.; Mayadunne, R. T. A.; Meijs, G. F.; Moad, C. L.; Rizzardo, E.; Thang, S. H. *Macromolecules* **1998**, *31*, 5529.

chain termination in free radical polymerization processes.[10] The reversible radical termination step helped to control irreversible chain termination and resulted in polymerization behavior that resulted in a linear molecular weight increase with time similar to living anionic polymerizations. However, the iniferter mechanism resulted in polydispersities that were inferior compared to those that could be achieved via anionic polymerization. These broad polydispersities resulted from yielded radicals that would initiate new chains throughout the reaction as well as a significant loss of active end groups resulting in chain-chain coupling termination.[11]

Following the earlier work of Rizzardo and coworkers in nitroxide mediated stable free radical polymerization of methyl acrylate,[12] Georges *et al.* first reported the preparation of polystyrene with low polydispersity using bulk free radical polymerization of styrene initiated by a conventional free radical initiator, benzoyl peroxide (BPO), in the presence of the stable nitroxide free radical, 2,2,6,6-tetramethyl-1-piperidinyloxy (TEMPO) at 125 °C.[13] The SFRP process involves a desirable reversible equilibrium between nitroxide capped polymer chains and uncapped polymer radicals. The uncapped polymer radicals are then able to chain extend via styrene monomer addition (Scheme 2.1). The success of this method arises from the unique feature that the nitroxide radicals will react with carbon radicals at near diffusion controlled rates, but will not react with other oxygen centered radicals or initiate additional polymer chains.

---

[10] Otsu, T.; Yoshida, M. *Makromol. Chem., Rapid Commun.* **1982**, *3*, 127. Otsu, T.; Yoshida, M.; Tazaki, T. *Makromol. Chem., Rapid Commun.* **1982**, *3*, 133.
[11] Turner, S. R.; Blevins, R. W. *Polym. Prepr. (Am. Chem. Soc., Div. Polym. Chem.)* **1988**, *29*, 6. Lambrinos, P.; Tardi, M.; Poulton, A.; Sigwalt, P. *Eur. Polym. J.* **1990**, *26*, 1125.
[12] Moad, G.; Rizzardo, E.; Solomon, D. H. *Macromolecules* **1982**, *15*, 909.
[13] Georges, M. K.; Veregin, R. P. N.; Kazmaier, P. M.; Hamer, G. K. *Macromolecules* **1993**, *26*, 2987.

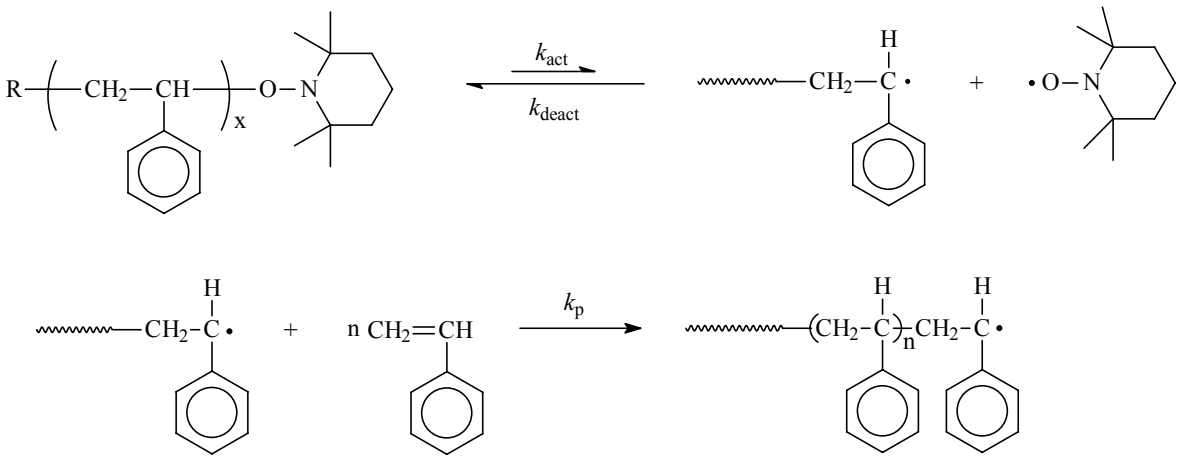

Scheme 2.1 Styrene SFRP reaction scheme.

2.2.3 Rate Accelerating Additives for SFRP

A drawback of the SFRP process illustrated in Scheme 2.1 was that long reaction times were required to achieve high conversion and molecular weights. To address this issue, Georges and coworkers have investigated alternative reaction conditions for SFRP in an attempt to increase the reaction rate and still achieve controlled polymerization. One of their findings that they reported was that addition of camphorsulfonic acid not only suppressed autopolymerization, but it also increased the polymerization rate and high yields could be achieved with reaction times less than six hours.[14] Hawker and coworkers have also investigated the use of rate-accelerating additives for nitroxide-mediated SFRP.[15] They found that addition of acylating agents such as acetic anhydride to styrene SFRP also dramatically reduced reaction time. As a potential explanation of the rate enhancement, they proposed a reversible acylation reaction of the alkoxyamine end group on the growing polymers chains (Scheme 2.2).

---

[14] Georges, M. K.; Veregin, R. P. N.; Kazmaier, P. M.; Hamer, G. K.; Saban, M. *Macromolecules* **1994**, *27*, 7228.
[15] Malmström, E.; Miller, R. D.; Hawker, C. J. *Tetrahedron* **1997**, *53*, 15225.

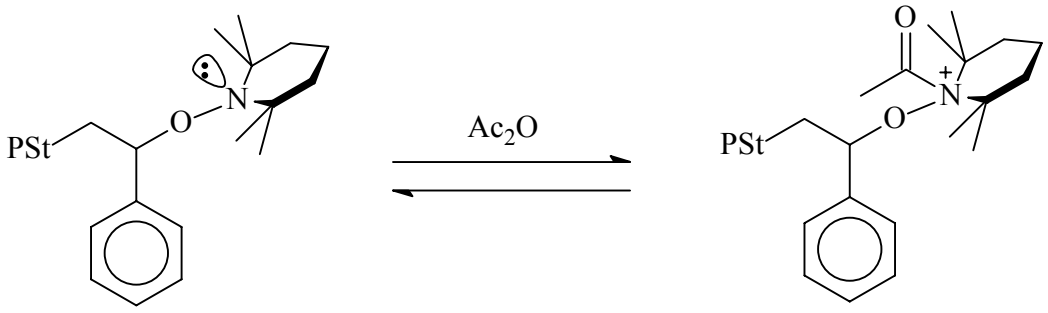

Scheme 2.2 Proposed acylation of alkoxyamine end group.

2.2.4 Unimolecular Initiators for SFRP

An important area of SFRP that has been investigated extensively by Hawker and coworkers is the development of unimolecular initiators for SFRP.[16] The original initiating system used by Georges was bimolecular and consisted of benzoyl peroxide as the initiating radical together with TEMPO as the mediating radical. Disadvantages of the bimolecular initiating system included lack of control over structural features such as molecular weight, chain ends, and architecture. To overcome these shortcomings, Hawker first reported the use of a unimolecular alkoxyamine initiator for SFRP in 1994.[17] The unimolecular initiator was synthesized in a one-step reaction from benzoyl peroxide, TEMPO, and styrene (Scheme 2.3). The synthesis of the initiator was similar to the original bi-molecular styrene SFRP method originally reported by Georges. However, the reaction was conducted at a low enough temperature (80 ºC) that once a benzoyl radical added to one unit of styrene, it would be trapped immediately by a TEMPO molecule and not react further. After column purification to isolate the desired monoadduct, a yield of

---

[16] Hawker, C. J. *J. Am. Chem. Soc.* **1994**, *116*, 11185. Benoit, D.; Chaplinski, V.; Braslau, R.; Hawker, C. J. *J. Am. Chem. Soc.* **1999**, *121*, 3904.
[17] Hawker, C. J. *J. Am. Chem. Soc.* **1994**, *116*, 11185.

42% of the initiator was obtained. Using this unimolecular initiator and derivatives of it, Hawker and coworkers have reported the synthesis of a variety of narrow polydispersity materials with controlled molecular weights,[18] chain ends,[19] and chain architectures.[20]

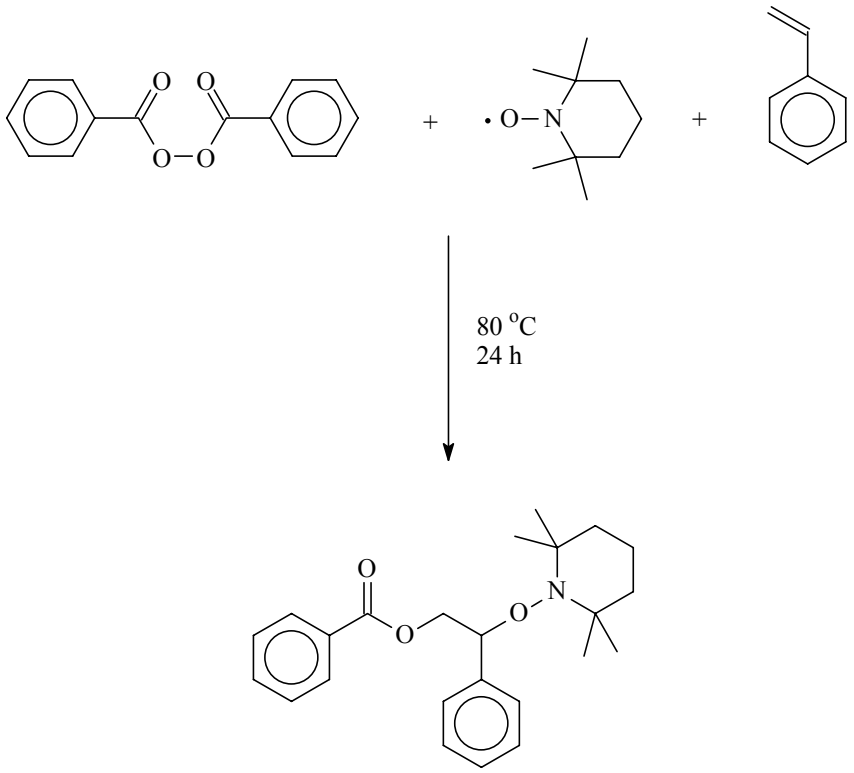

Scheme 2.3 Synthesis of unimolecular initiator for SFRP.

The SFRP methods using TEMPO as the mediating radical, including the universal initiator synthesized by Hawker, have been limited to the controlled polymerization of

---

[18] Hawker, C. J.; Hedrick, J. L. *Macromolecules* **1995**, *28*, 2993.
[19] Hrank, B.; Gast, A. P.; Russell, T. P.; Brown, H. R.; Hawker, C. J. *Macromolecules* **1996**, *29*, 6531.
[20] Hawker, C. J. *Angew. Chem. Int. Ed. Engl.* **1995**, *34*, 1456.

styrene-based systems. Georges and coworkers have attempted to use a TEMPO derivative, 4-oxo-TEMPO,[21] as well as the reducing additives acetone and glucose to polymerize acrylates and dienes.[22] Both of these methods showed improvement over the traditional BPO/TEMPO system. However, polydispersities of the resulting materials were still greater than 1.40. A very successful approach to the controlled nitroxide-mediated polymerization of acrylates using a β-phosphonate substituted nitroxide (Figure 2.1) with 2,2'-azobisisobutyronitrile (AIBN) as the initiating radical source was reported by Gnanou and coworkers.[23] They reported the polymerization of acrylates with polydispersities as low as 1.11 using this initiating system. Two major structural features of the β-phosphonate substituted nitroxide distinguished it from previously studied nitroxides. First, it was acyclic; and second, it contained a α-hydrogen to the nitroxide functionality. Both of these features are expected to decrease the stability of nitroxide and increase decomposition. It has been proposed that the limitation of nitroxide-mediated polymerization of acrylates and other monomer families is the control of excess free nitroxide that accumulates during polymerization.[22] Therefore, Gnanou and coworkers concluded that the decreased stability of the acyclic β-phosphonate substituted nitroxide bearing a α-hydrogen led to decreased accumulation of excess nitroxide during reaction and resulted in improved control over the polymerization of acrylates.

---

[21] Listigovers, N. A.; Georges, M. K.; Odell, P. G.; Keoshkerian, B. *Macromolecules* **1996**, *29*, 8992.

[22] Keoshkerian, B.; Georges, M. K.; Quinlan, M.; Veregin, R.; Goodbrand, B. *Macromolecules* **1998**, *31*, 7559.

[23] Benoit, D.; Grimaldi, S.; Finet, J. P.; Tordo, P.; Fontanille, M.; Gnanou, Y. *Polym. Prep. (Am. Chem. Soc., Div. Polym. Chem.)* **1997**, *38*, 729.

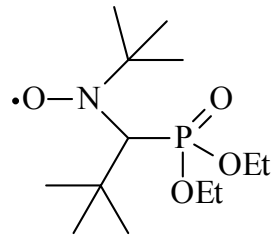

Figure 2.1 Acyclic β-phosphonate substituted nitroxide.

Following the findings of Gnanou *et al*., Hawker and coworkers recently investigated a series of α-hydrogen bearing alkoxyamines in an attempt to develop a "universal" unimolecular initiator to be used for nitroxide-mediated stable free radical polymerization.[23] They synthesized a library of twenty alkoxyamine unimolecular initiators consisting of both cyclic and acyclic structures as well as with and without α-hydrogens to the nitrogen. They then evaluated this library of compounds as initiators for nitroxide-mediated stable free radical polymerization of a variety of monomers. Consistent with the earlier findings of Gnanou, several of the acyclic α-hydrogen bearing alkoxyamines successfully provided controlled polymerization of both styrene and acrylates. Two of the alkoxyamine initiating structures (Figure 2.2) were found to be particularly very robust and successfully polymerized styrene, acrylate, acrylamide, and acrylonitrile based monomers with controlled molecular weights ranging from 1,000 to 200,000 g/mol and polydispersities of 1.05 to 1.15. They also reported the successful synthesis of narrow polydispersity block and random copolymer based on combinations of the above monomers.

Hawker has also applied the unimolecular "universal" initiators to controlled free radical alternating copolymerizations. Recently he has described the one-pot controlled synthesis of a block polymer consisting of an alternating styrene/maleic anhydride block

and a styrene block.[24] The one-pot synthesis was accomplished using an excess concentration of styrene to maleic anhydride in the presence of one of the "universal" initiators. He reported that the controlled alternating copolymerization of styrene and maleic anhydride proceeded until the supply of maleic anhydride had been exhausted, at which point styrene monomer continued to polymerize in a controlled manner (Scheme 2.4**)**.

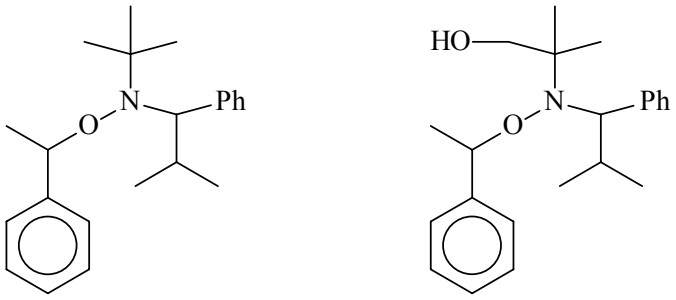

Figure 2.2 Hawker's "universal" acyclic α-hydrogen bearing alkoxyamine initiators.

[24] Hawker, C. J.; Benoit, D.; Rivera, F.; Piotti.; Rees, I.; Hedrick, J. L.; Zech, C.; Maier, G.; Voit, B.; Braslau, R.; Fréchet, J. M. J. *Polym. Prep. (Am. Chem. Soc. Div. Polym. Chem.)* **1999**, *40(2)*, 315. Information pertaining to alternating copolymerization was disclosed during presentation.

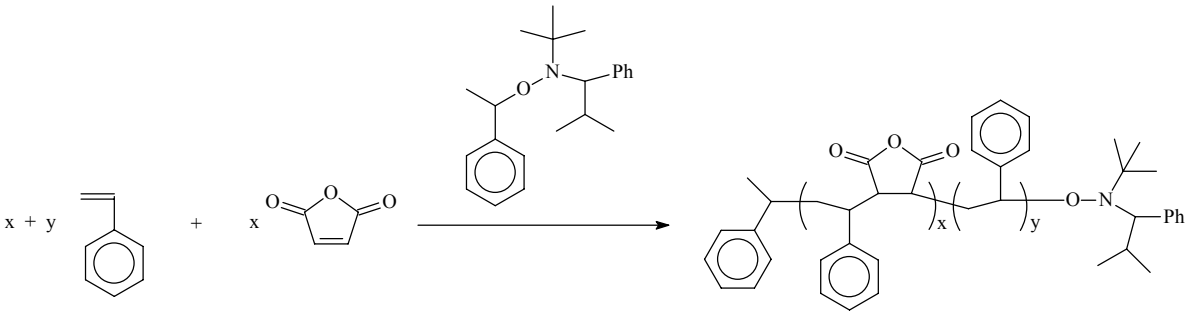

Scheme 2.4 Controlled synthesis of poly(styrene-*alt*-maleic anhydride-*block*-styrene) via SFRP.

2.2.5 Probing the SFRP Process

An indication of the controlled polymerization mechanism via SFRP of styrene is typically accomplished from the demonstration of a linear increase in molecular weight with conversion.[13,16] Kinetic information has commonly been obtained from withdrawing samples and analyzing for residual monomer with gravimetric and chromatographic methods.[25] Recently, more sophisticated analytical methods have also been applied to study the SFRP reaction. Georges *et al*. have recently utilized *in situ* ESR spectroscopy to study the SFRP process.[26] ESR provided a means to follow the time-dependent concentration of stable TEMPO nitroxide radicals *in situ* during the polymerization and provide a better understanding of the formation of narrow polydispersity, high molecular weight polystyrene via SFRP. In addition, Hawker has applied ^{1}H NMR to evaluate initiator efficiency for SFRP processes using deuterated styrene. ^{1}H NMR of the

---

[25] Veregin, R. P. N.; Odell, P. G.; Michalak, L. M.; Georges, M. K. *Macromolecules* **1996**, *29*, 2746.

[26] Veregin, R. P. N.; Georges, M. K.; Kazmaier, P. M.; Hamer, G. K. *Macromolecules* **1993**, *26*, 5316. Veregin, R. P. N.; Odell, P. G.; Michalak, L. M.; Georges, M. K. *Macromolecules* **1996**, *29*, 4161. MacLeod, P. J.; Veregin, R. P. N.; Odell, P. G.; Georges, M. K. *Macromolecules* **1998**, *31*, 530. Moffat, K. A.; Hamer, G. K.; Georges, M. K. *Macromolecules* **1999**, *32*, 1004.

deuterated polystyrenes prepared using SFRP enabled characterization of molecular weights (with time) and also permitted end group characterization that provided confirmation of the initiation and termination processes that occur during styrene SFRP.[27]

[27] Hawker, C. J. *J. Am. Chem. Soc.* **1994**, *116*, 11185.

2.3 SYNTHESIS OF STAR SHAPED POLYMERS *VIA* CONTROLLED POLYMERIZATION METHODS

2.3.1 Introduction

Star-shaped polymers have received significant attention due to their desirable properties that arise from having a highly branched structure.[28] A branched structure is described as a nonlinear polymer composed of multiple backbone chains emanating from junction points.[29] Branching results in a more compact structure than analogous linear structures because of high segment density, which dramatically affects crystalline, mechanical, and viscoelastic properties. The synthesis of star-shaped polymers has generally been accomplished using controlled polymerization pathways such as group transfer,[30] ring opening metathesis,[31] transition metal catalysis, cationic,[32] and anionic.[33] The two approaches to star-shaped polymers using controlled polymerization methods are known as "arm-first" and "core-first".[34] The "core-first" approach involves the use of a multifunctional initiator that initiates the polymerization of multiple linear polymer chains (Scheme 2.5). The "arm-first" approach involves the coupling of preformed linear

---

[28] *Star and Hyperbranched Polymers*, Mishra, M. K., Kobayashi, S., Eds.; Marcel Dekker: New York, 1999.

[29] Roovers, J. in *Encyclopedia of Polymer Science and Engineering*, 2nd ed., Kroschwitz, J. I., Ed.; Wiley: New York, 1985, Vol. 2, p. 478.

[30] Webster, O. W. *Macromol. Chem. Macromol. Symp.* 1990, *33*, 133.

[31] Bazan, G. C.; Shrock, R. R. *Macromolecules* 1991, *24*, 817.

[32] Kennedy, J. P.; Iván, B. *Designed Polymers by Carbocationic Macromolecular Engineering: Theory and Practice*; Hanser Publishers: New York, 1992.

[33] Martin, M. K., Ph.D. Dissertation, Virginia Polytechnic Institute and State University, Blacksburg, VA, 1980. Quack, G.; Fetters, L. J.; Hadjichristidis, N.; Young, R. N. *Ind. Eng. Chem. Prod. Res. Dev.* 1980, *19*, 587. Martin, M. K.; Ward, T. C.; McGrath, J. E. In *Anionic Polymerization: Kinetics, Mechanisms, and Synthesis*, McGrath, J. E., Ed.; ACS Symposium Series 166; American Chemical Society: Washington, DC, 1981. Hsieh, H. L.; Quirk, R. P. *Anionic Polymerization: Principles and Practical Applications*; Marcel Dekker: New York, 1996.

[34] Rempp, P.; Franta, E.; Herz, J. *Adv. Polym. Sci.* 1988, *86*, 145.

polymer chains containing functionality at the chain end with a multifunctional coupling agent such as divinylbenzene (DVB) (Scheme 2.6). This approach results in a material with a network-like hub of the coupling agent with the preformed linear polymers attached to the hub. The number of arms resulting from the "arm-first" approach is controlled by varying the molar ratio of the multifunctional coupling agent to the preformed linear polymer chains.

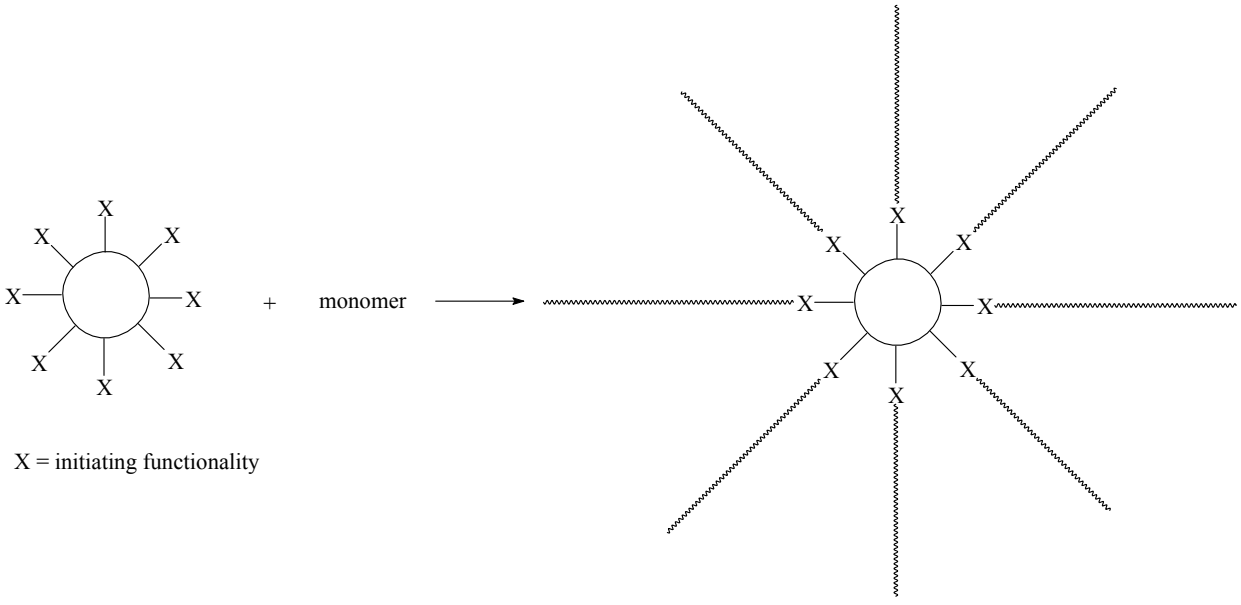

Scheme 2.5 Star-shaped polymer synthesis via a "core-first" approach.

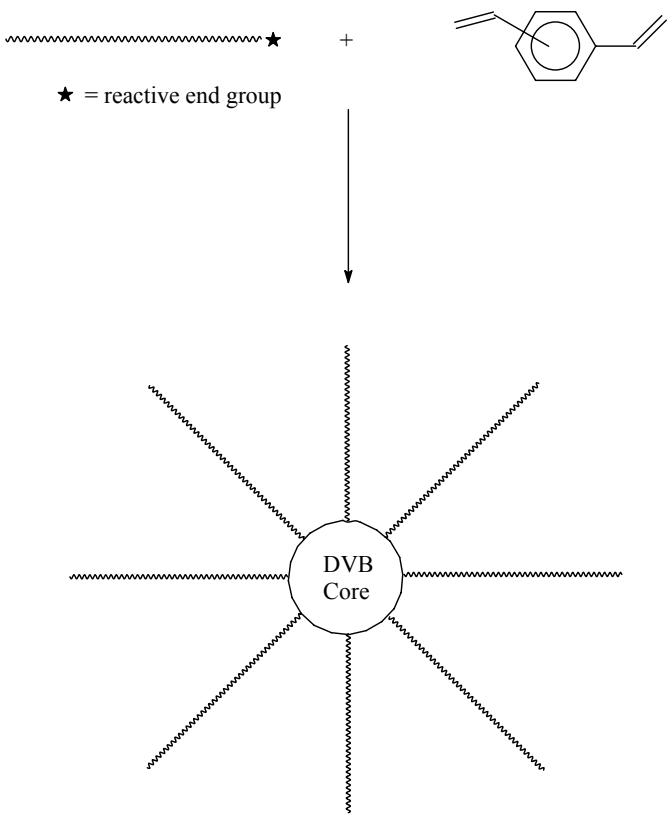

Scheme 2.6 Synthesis of star polymer via the "arm first" method.

2.3.2 Group-transfer Polymerization

The synthesis of acrylic and methacrylic monomers using group-transfer polymerization (GTP) methodologies was first reported by Webster and coworkers at Dupont.[35] GTP gives living polymers at room temperature and above that are free of chain terminating reactions and works best for methacrylic monomers. While the living polymerization of acrylic monomers is feasible, it is a great deal more complex than for methacrylics. The mechanism for GTP is the Michael addition of a silyl ketene to an α,β-

[35] Webster, O. W.; Hertler, W. R.; Sogah, D. H.; Farnham, W. B.; Rajanbabu, T. V. *J. Am. Chem. Soc.* **1983**, *105*, 5706.

unsaturated carbonyl (Scheme 2.7). The net effect is the transfer of the silyl ketene acetal center from initiator to monomer. Chain propagation then proceeds via the repeated transfer of the silyl group to additional monomer.

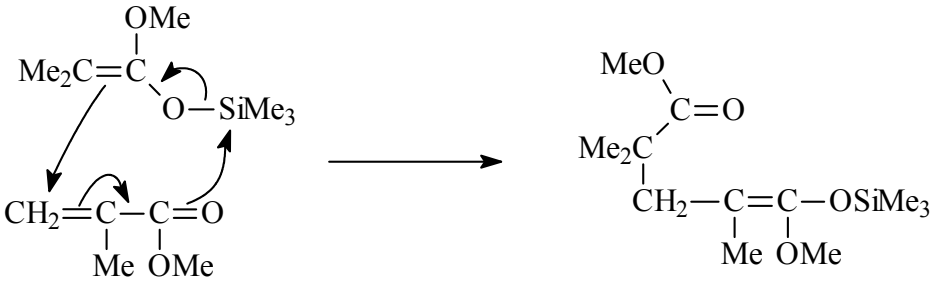

Scheme 2.7 Group transfer polymerization reaction scheme.[35]

The living nature of GTP lends itself as a useful method in which to synthesize star-shaped and branched acrylic and methacrylic polymer architectures. Both "arm-first" and "core-first" methods of star polymer synthesis via GTP have been reported. For example, an "arm-first" reaction of a poly(methyl methacrylate) living GTP polymer chain end with 1,3,5-tris(bromo)methylbenzene was reported to give a three-arm poly(methyl methacrylate) star structure.[36] In addition, "core-first" approaches can also be used to synthesize star-shaped architectures by means of the polymerization of an acrylic or methacrylic monomer initiated by a compound containing two or more silyl ketene acetal initiating functionalities.[37]

---

[36] Webster, O. W. *Macromol. Chem. Macromol. Symp.* **1990**, *33*, 133. Jenkins, A. D. *Macromol. Chem. Macromol. Symp.* **1992**, *53*, 267.

[37] Haddleton, D. M.; Crossman, M. C. *Macromol. Chem. Phys.* **1997**, *198*, 871. Sannigrahi, B.; Wadgaonkar, P. P.; Sehra, J. C.; Sivaram, S. *J. Polym. Sci., Part A: Polym. Chem.* **1997**, *35*, 1999.

2.3.3 Ring Opening Metathesis Polymerization (ROMP)

Cycloalkenes, such as norbornene, will undergo ring-opening polymerization to give a polymer product containing a double bond (Scheme 2.8) .[38] The process is referred to as metathesis polymerization in correlation with the olefin metathesis reaction. The initiating and propagating species are metal-carbene complexes from transition-metal compounds, which are typically molybdenum or tungsten. Developments in the design of ROMP catalysts has permitted the synthesis of more complex architectures such as block copolymers using ROMP.[39] New catalysts have also been shown to be practical for the synthesis of star-shaped macromolecules. For example, Bazan and Schrock have described ROMP for the preparation of well-defined poly(norbornene) type star-shaped polymers via an "arm-first" approach.[40] They employed ROMP catalyst systems that are relatively inactive for metathesis of acyclic olefins, but is useful for living ROMP of especially reactive cyclic olefins such as norbornene. The coupling of living arms prepared from various norbornene monomers were coupled with norbornadiene dimer (Figure 2.3), which was prepared via the catalytic dimerization of norbornadiene.[41]

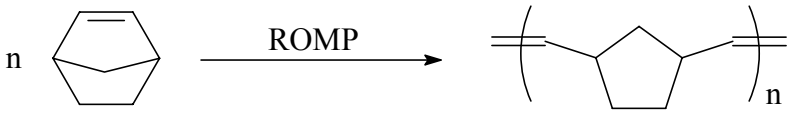

Scheme 2.8 Ring opening metathesis polymerization (ROMP) of norbornene.

---

[38] Gilliom, L. R.; Grubbs, R. H. *J. Am. Chem. Soc.* **1986**, *108*, 733.
[39] Schrock, R. R. *Acc. Chem. Res.* **1990**, *23*, 158.
[40] Bazan, G. C.; Schrock, R. R. *Macromolecules* **1991**, *24*, 817.
[41] Arnold, D. R.; Trecker, D. J.; Whipple, E. B. *J. Am. Chem. Soc.* **1965**, *87*, 2596.

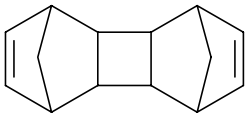

Figure 2.3 Norbornadiene dimer ROMP coupling agent.

2.3.4 Cationic Polymerization

Living cationic polymerization of monomers containing electron-donating substituents can be initiated by both protonic Brønsted acids and also Lewis acids such as $AlCl_3$ and $SnCl_4$.[42] The initiated ion pair species that results from formation of a carbocation upon addition of the acidic initiator to monomer then propagates from successive additions of monomer molecules. Cationic systems are very sensitive and detrimental transfer and termination reactions are difficult to eliminate while still enabling propagation. Monomers commonly polymerized using living cationic methods include styrenics, isobutylene, and vinyl ethers. [42] Because of living nature of cationic polymerization, although very sensitive, controlled polymer architectures such as block-copolymers can be produced. In addition, appropriately chosen coupling agents or multi-functional initiators for cationic polymerization enables the synthesis of star-shaped architectures. For example, Storey and Shoemake have reported on the synthesis of poly(styrene-*b*-isobutylene) star-shaped block copolymers.[43] They first prepared linear living polystyrene-polyisobutylene block copolymer arms using a $CCl/TiCl_4$/pyridine initiating system at –80 ºC. Star-shaped polymers were then synthesized via the rapid addition of divinyl benzene coupling agent to the living arms (Scheme 2.9). Living cationic polymerization has also been applied to prepare star-shaped polymers by means of a "core-first" approach. For example, Kennedy and coworkers have described the

---

[42] Kennedy, J. P.; Iván, B. *Designed Polymers by Carbocationic Macromolecular Engineering: Theory and Practice*; Hanser Publishers: New York, 1992.
[43] Storey, R. F.; Shoemake, K. A. *J. Polym. Sci., Part A: Polym. Chem.* **1999**, *37*, 1629.

synthesis of an eight arm polyisobutylene star that was prepared via the living cationic polymerization of isobutylene initiated from a multi-functional calixarene core molecule.[44]

[44] Jacob, S.; Majoros, I.; Kennedy, J. P. *Macromolecules* **1996**, *29*, 8631.

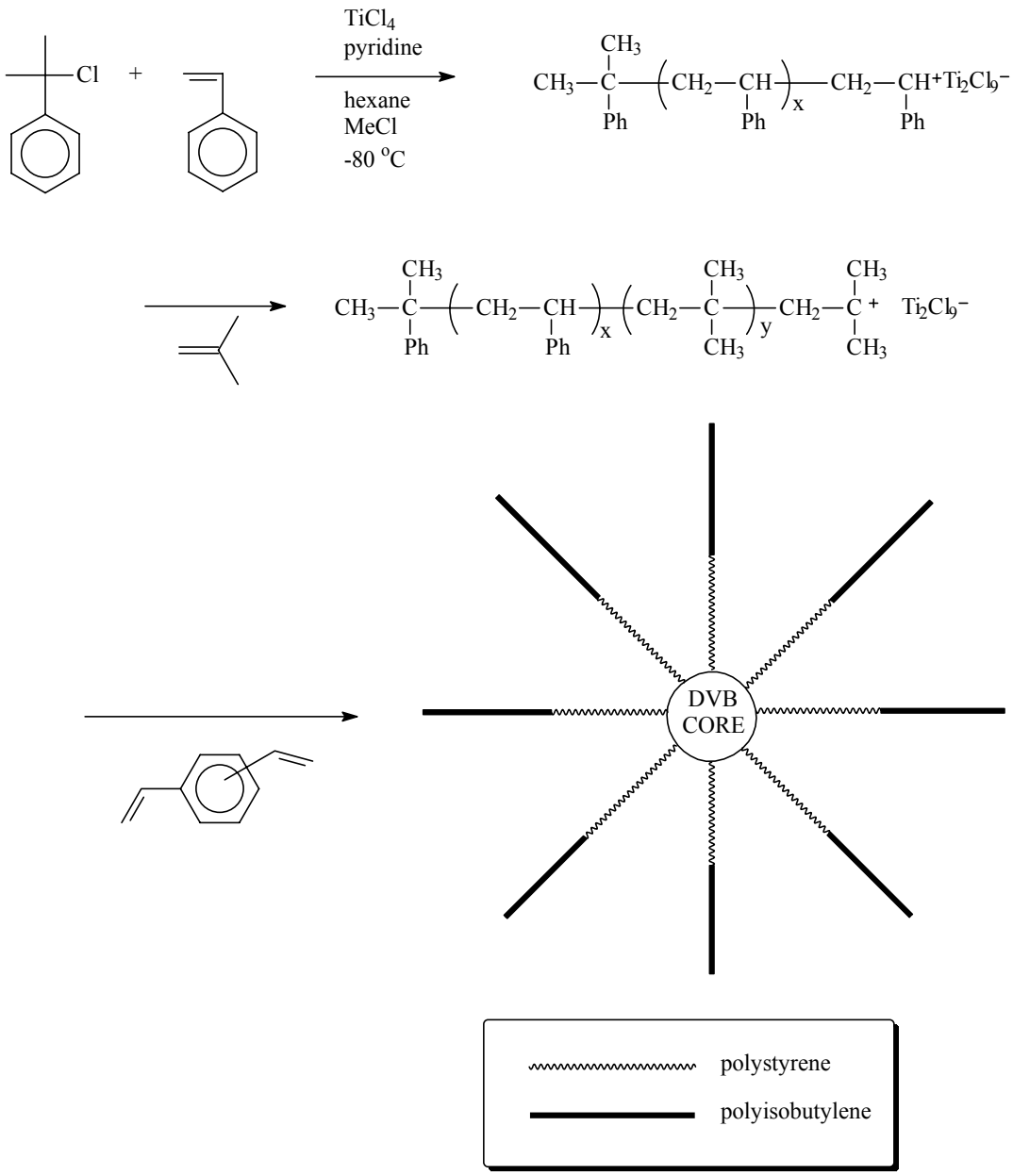

Scheme 2.9 Synthesis of poly(styrene-*b*-isobutylene) star-shaped polymers.[43]

2.3.5 Anionic Polymerization

Living anionic polymerization is similar to cationic polymerization in that it involves the propagation of an ionic chain end in the absence of termination reactions. Anionic polymerization differs from cationic polymerization in that there is an appreciable difference in reactivities and stabilities of ion pairs. In addition, anionic polymerizations are not as temperature sensitive as cationic polymerizations and can be conducted at room temperatures and above.[45] Anionic polymerization methods are well suited for the preparation of advanced 3-dimensional architectures via the coupling of reactive end groups.[46] Advantages include the precise control of molecular weight and polydispersity. Furthermore, anionic polymerization methods also provide for a great deal of control of the functionality of controlled architectures such as star-shaped polymers.

"Arm-first" methods have been carried out by means of using living polymer chains to initiate the subsequent polymerization of a bi-functional coupling agent such as divinyl benzene or ethylene glycol dimethacrylate (EGDMA).[47] Another useful "arm-first" approach to star polymers using anionic polymerization has been to employ chlorosilane coupling agents.[48] For example, the use of trichlorosilane coupling agents (Figure 2.4) that were separated by ethylene spacers has enabled the quantitative coupling of living anionic chains and resulted in the synthesis of well-defined star-shaped polymers containing up to 128 arms.[49]

---

[45] Odian, G. *Principles of Polymerization*, 3rd ed.; Wiley-Interscience: New York, 1992; Chapter 5.
[46] Hadjichristidis, N.; Fetters, L. J. *Macromolecules* **1980**, *13*, 191. Rempp, P.; Franta, E. *Adv. Polym. Sci.* **1984**, *58*, 1.
[47] Worsfold, D. J.; Zillox, J. G.; Rempp, P. *Can. J. Chem.* **1969**, *47*, 3379. Martin, M. K. Ph.D. Dissertation, Virginia Polytechnic Institute and State University, Blacksburg, VA, 1980. Sheridan, M. M.; Hoover, J. M.; Ward, T. C.; McGrath, J. E. *Polymer Preprints* **1984**, *25*(2), 102.
[48] Hadjichristidis, N.; Guyot, A.; Fetters, L. J. *Macromolecules* **1978**, *11*, 668.
[49] Roovers, J.; Zhou, L.; Toporowski, P. M.; Zwan, M.; Iatrou, H.; Hadjichristidis, N. *Macromolecules* **1993**, *26*, 4324.

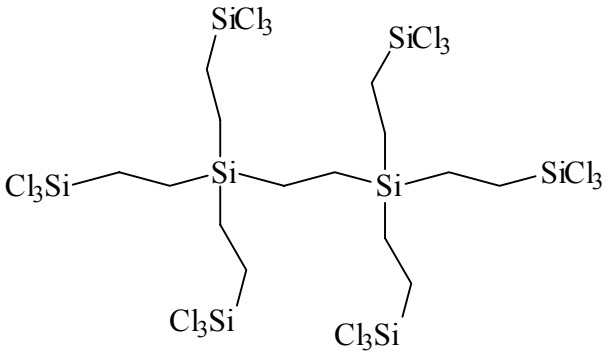

Figure 2.4 Trichlorosilane coupling agent.

Long and coworkers have also utilized living anionic polymerization in combination with terminal functionalization using trialkoxysilanes. Subsequent polycondensation using acid catalyzed sol-gel reaction conditions resulted in the formation of narrow molecular weight distribution, star-shaped polymers.[50] Anionic polymerization has also been employed for the synthesis of functional star-shaped polymers. For example, the use of a tertiary amine initiator, ((3-dimethylamino)propyl)lithium, afforded star-polymers containing amine functionality at the periphery of the star.[51] Reaction of these amine functionalized stars with appropriate bifunctional compounds resulted in reversible gelation of the reaction solution. Star-shaped polymers composed of polybutadiene and polyisoprene elastomeric arms have also been prepared using DVB coupling compounds.[52] In addition, star polymers with diblock arms have also been prepared using anionic polymerization methods. When the blocks were composed of polystyrene and a rubbery

---

[50] Long, T. E.; Kelts, L. W.; Turner, S. R.; Wesson, J. A.; Mourey, T. H. *Macromolecules* 1991, *24*, 1431.
[51] Burchar, W.; Merkle, G. *J. Phys. Chem.* **1992**, *96*(10), 3915.
[52] Young, R. N.; Fetters, L. J. *Macromolecules* **1978**, *11*, 899. Rein, D. H.; Rempp, P.; Lutz, P. J. *Macromol. Chem. Phys.* **1998**, *199*, 569.

block, such as polyisoprene or polybutadiene, the resulting star-shaped polymers behaved as thermoplastic elastomers.[53]

"Core-first" approaches have also been investigated using anionic polymerization methods. Unlike "arm-first" methods, "core-first" approaches offer the advantage of preparing periphery functionalized stars without the use of functional initiators. Several workers have described the synthesis of "core-first" star polymers that were prepared via anionic polymerization from multi-functional initiating cores that were soluble in polar solvents appropriate for anionic polymerization (Scheme 2.10).[54] In addition, "core-first" anionic methodology has also been described for the preparation of functional biocompatible poly(ethylene oxide) multi-arm star polymers that represent versatile building blocks for structured polymer networks such as hydrogels and amphiphilic networks.[55]

---

[53] Bi, L. K.; Fetters, L. J. *Macromolecules* **1975**, *8*, 90.
[54] Fujimoto, T.; Tani. S.; Takano, K.; Ogawa, M.; Nagasawa, M. *Macromolecules* **1978**, *11*, 673. Tung, L. H.; Lo, G. Y. *Macromolecules* **1994**, *27*, 1680. Burchard, W.; Eschwey, H. *Polymer* **1975**, *16*, 180.
[55] Knischka, R.; Lutz, P. J.; Sunder, A.; Mulhaupt, R.; Frey, H. *Macromolecules* **2000**, *33*, 315. Gnanou, Y.; Lutz, P.; Rempp, P. *Makromol. Chem.* **1988**, *189*, 2885.

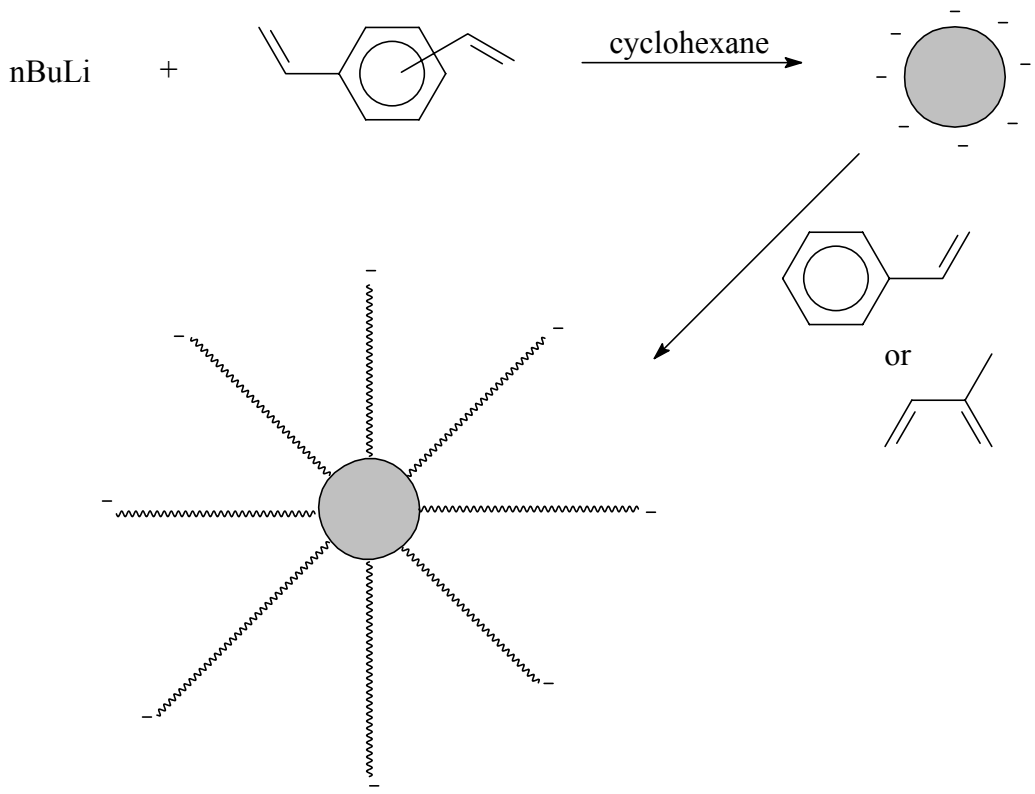

Scheme 2.10 Synthesis of star-shaped polymers via an anionic "core-first" method.

2.3.6 Controlled Free Radical Polymerization

Synthetic methodologies for the preparation of molecules with complex architectures such as star-shaped macromolecules have been expanded with recent developments in stable free radical polymerization (SFRP)[56] and atom transfer radical polymerization (ATRP).[57] Conventional free radical polymerization methods are generally not suitable for synthesizing star shaped polymers due to the occurrence of undesirable radical coupling reactions. During a "core-first" synthesis this would lead to coupling of the growing polymer arms and ultimately result in an cross-linking of the star macromolecules.

---

[56] Hawker, C. J. *ACC. Chem. Res.* **1997**, *30*, 373.

Similarly, a "arm-first" methodology using conventional free radical polymerization would result in core-core reactions after addition of the multifunctional coupling molecule and again result in undesirable cross-linking. However, the reduced concentration of radical centers at the chain ends of these controlled free radical polymerization methods permits the preparation of complex macromolecular architectures such as stars due to the near absence of chain-terminating side reactions. For example, Matyjaszewski and coworkers have recently reported the synthesis of star-shaped polystyrene by an "arm-first" method (Scheme 2.11).[58] Their approach involved the coupling of polystyrene macroinitiators with divinylbenzene by means of copper-mediated ATRP. In addition, nitroxide-mediated SFRP is suitable as a useful controlled free radical polymerization route for the synthesis of branched and star architectures. For example, Ide and Fukuda have demonstrated the nitroxide-mediated (2,2,6,6-tetramethyl-1-piperidinyloxy (TEMPO)) stable free radical copolymerization of styrene with a small amount of 4,4'-divinylbiphenyl to produce a lightly cross-linked homogeneous material (Scheme 2.12).[59] In addition, Solomon and coworkers have previously studied the synthesis of soluble microgels from the nitroxide-mediated stable free radical copolymerization of tert-butylstyrene and DVB.[60]

---

[57] Patten, T. E.; Matyjaszewki, K. *Adv. Mater.* **1998**, *10*, 901.
[58] Xia, J.; Zhang, X.; Matyjaszewski, K. *Macromolecules* 1999, *32*, 4482.
[59] Ide, N.; Fukuda, T. *Macromolecules* **1999**, *32*, 95.
[60] Abrol, S.; Kambouris, P. A.; Looney, M. G.; Solomon, D. H. *Macromol. Rapid Commun.* **1997**, *18*, 755.

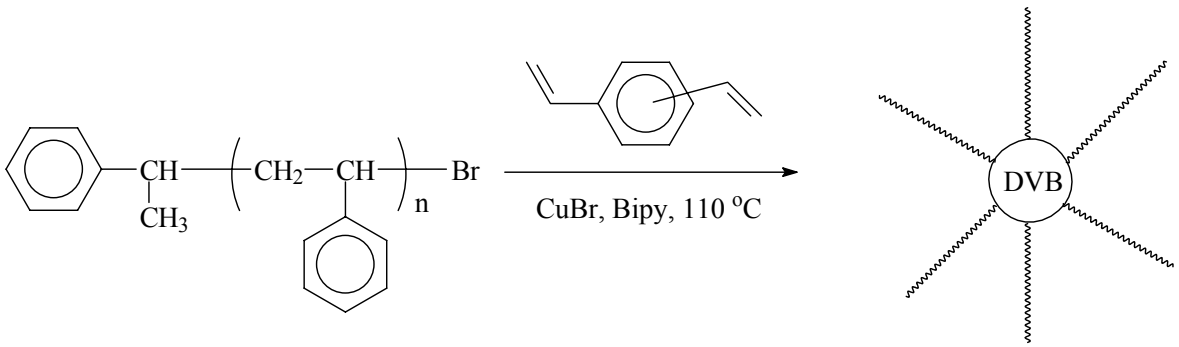

Scheme 2.11 ATRP of star-shaped polystyrene via an "arm-first" method.

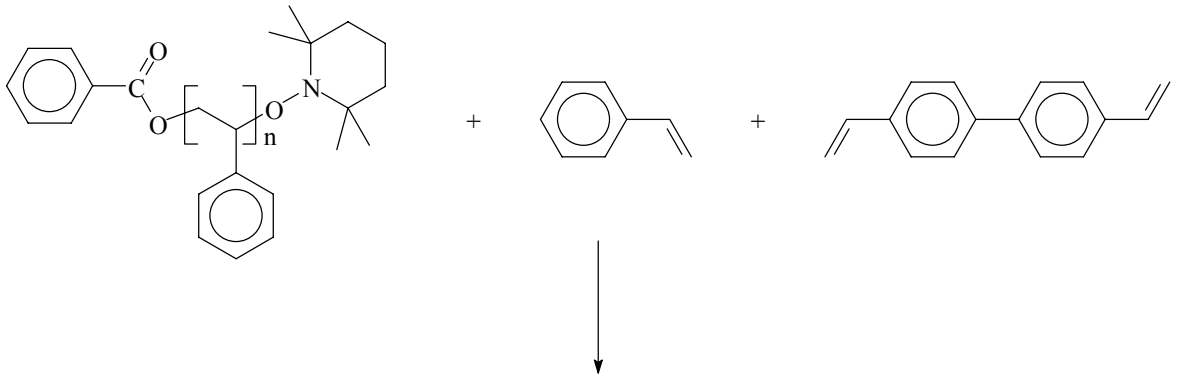

Scheme 2.12 Controlled polystyrene network formation via nitroxide-mediated stable free radical polymerization.

2.4 FREE RADICAL CHAIN COPOLYMERIZATION

2.4.1 Introduction

The demand for new and improved materials often can be achieve as a result of altering the properties of existing polymeric materials. For example, the use of additives can incorporate desirable properties into an existing polymer material that is to be used for specialized applications. Common additives include plasticizers, stabilizers, flame retardants, fillers, colorants, processing aids, and impact modifiers.[61] Another approach is to combine the beneficial properties of different known polymer structures. One known technique to achieve this is to simply blend two individual polymers to give a material whose mechanical properties exceed those of the individual blend components (*i.e.*, synergism). A few advantages of blending include reducing the cost of expensive high performance polymers, improving the processability of a high temperature material, and improving impact resistance of materials. However, because few polymers are miscible, their blends form immiscible phase separated materials. These immiscible blends often have poor physical properties due to inadequate interfacial strength between the phases.[62] A desirable alternative is to copolymerize different monomer structures into a single polymeric material (Scheme 2.13).[63] Prime examples include the important commercial materials produced from vinyl chloride/vinyl acetate and styrene/butadiene copolymers.[61] Careful consideration of such factors as the selection of the comonomers and the copolymerization reaction conditions allows one to precisely tailor the properties of the resulting copolymer and provides a useful method of synthesizing an almost unlimited number of polymeric structures with a wide range of properties and applications.

---

[61] *Polymer Blends and Alloys*; Folkes, M. J., Hope, P. S., Eds.; Chapman & Hall: London, England, 1993.
[62] Olabisi, O.; Robeson, L. M.; Shaw, M. T. *Polymer-Polymer Miscibility*; Academic Press: New York, N. Y., 1979.
[63] Gao, J.; Penlidid, A. J. *Macromol. Sci., Rev. Macromol. Chem. Phys.* **1998**, *C38*(4), 651-780.

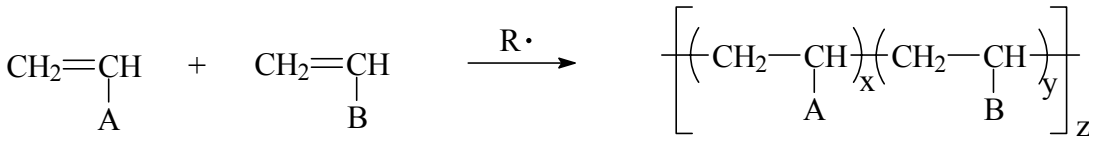

Scheme 2.13 Generalized free radical chain copolymerization reaction scheme.

Copolymer structures can be described in a variety of ways. Different types of copolymers include statistical, alternating, block, and graft copolymers (Figure 2.5). Statistical copolymers result from a single process where the incorporation of the comonomers follow some statistical law that is due solely to kinetic factors.[64] Alternating copolymerization, which will be focused in the preceding sections, is an example of chain copolymerization where each of the monomers adds preferentially to the other and homopropagation is effectively nonexistent.[65] Block and graft copolymers differ in that they contain long sequences of each comonomer either along the backbone or as side chains (grafts) and are often the result of a multi-step process.[66]

---

[64] Kuchanov, S. I. *Adv. Polym. Sci.* **1992**, *103*, 1. Tirrell, D. A. In *Comprehensive Polymer Science and Engineering*, 2nd ed.; Eastmond, G. C., Ledwith, A., Russo, S., Sigwalt, P., Eds.; Pergamon: London, 1989; Vol. 3, p 195.

[65] Odian, G. *Principles of Polymerization*, 3rd ed.; Wiley & Sons: New York, 1991; Chapter 6.

[66] Rempp, P. F., Lutz, P. J. In *Comprehensive Polymer Science*; Eastmond, G. C, Ledwith, A., Russo, S., Sigwalt, P., Eds.; Pergamon: London, 1989, Vol. 4, p 403.

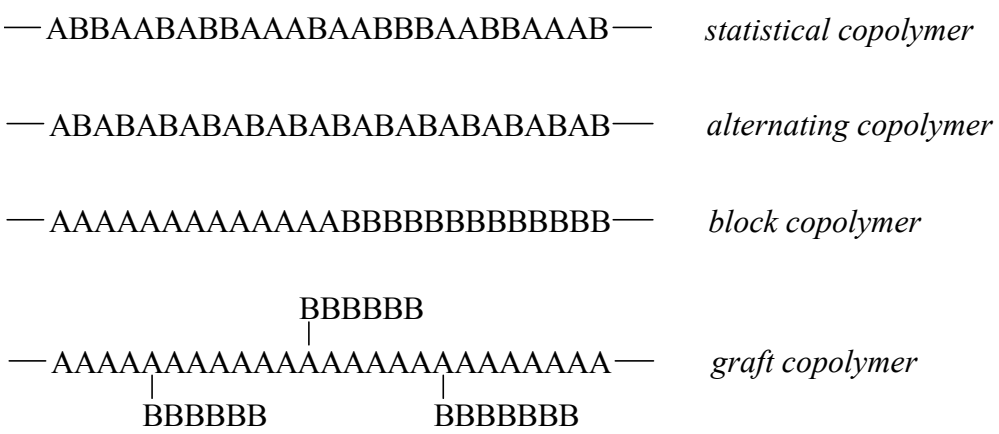

Figure 2.5 Types of copolymer topologies.

The manner in which comonomer repeat units are incorporated into the polymer backbone is determined from the reactivities of the monomers and radicals involved in the reaction. Reaction conditions such as solvent and temperature can also have a marked effect on the monomer reactivities and will contribute to the copolymer composition. Therefore, in only a few select cases of chain copolymerization will the copolymer composition be directly proportionate to the monomer feed. More typically, both the comonomer feed and instantaneous copolymer composition vary throughout the copolymerization, which results in heterogeneity.

2.4.2 Copolymerization Models

2.4.2.1 Terminal Model

The simplest quantitative statistical treatment for the determination of copolymerization composition, which is generally referred to as the terminal model, was

first hypothesized by Dostal[67] in 1936 and later elucidated by others.[68] The terminal model is based upon the assumption that the chemical reactivity of a propagating polymer chain is independent of the size or composition of the chain and is only influenced by the active end group.[69] Though the terminal model is dependent on several assumptions and may not be the most accurate model to describe a copolymer process, it is relatively simple to apply and provides a facile starting point when evaluating copolymerizations of various monomer pairs. When two monomers, M_1 and M_2 are copolymerized by free radical methods, four reactions are feasible according to the terminal model:

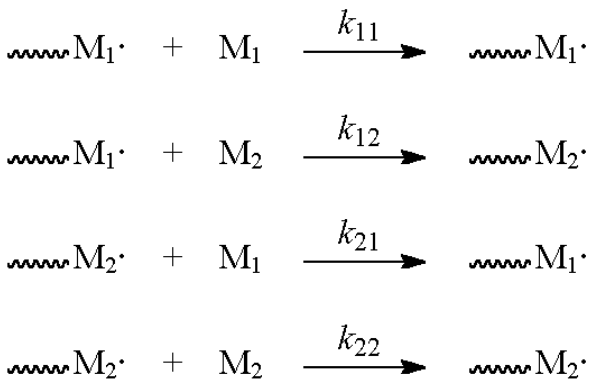

Figure 2.6 Terminal model of copolymerization.

Where k_{11} is the rate constant for the addition of a propagating chain ending in M_1 adding to monomer M_1, k_{12} is the rate constant for the addition of a propagating chain ending in M_1 adding to monomer M_2, and so on. The rate constants can then be expressed in terms of the monomer reactivity ratios, r_1 and r_2, where $r_1 = k_{11}/k_{12}$ and $r_2 = k_{22}/k_{21}$. Monomer

---

[67] Dostal, H. *Monatsh. Chem.* **1936**, *69*, 424.
[68] Mayo, F. R.; Lewis, F. M. *J. Am. Chem. Soc.* **1944**, *66*, 1594. Alfrey, T., Jr.; Goldfinger, G. *J. Chem. Phys.* **1944**, *12*, 115. Wall, F. T. *J. Am. Chem. Soc.* **1944**, *66*, 2050.

reactivity ratios may either be experimentally[70] determined or estimated[71] and for free radical polymerizations are generally independent of initiator and solvent with only slight temperature dependence. The different types of copolymerization behaviors can then be described based upon the values of the monomer reactivity ratios. "Random copolymerization" results when $r_1 = r_2 = 1$ due to the equal reactivity of the monomers toward both types of propagating chain ends and the resulting copolymer composition will directly reflect the comonomer feed. When $r_1 r_2 = 1$, the two different types of propagating chain ends both add preferentially to one of the monomers, and is described as "ideal copolymerization". The case when r_1 and r_2 are much greater than one results in a tendency to form blocks of both monomers and is appropriately termed "block copolymerization". The copolymerization behavior focused upon in this review, which describes the situation when $r_1 = r_2 = 0$, is referred to as "alternating copolymerization".

The mechanism of most typical copolymerizations fall somewhere between the extremes of "ideal copolymerization" and "alternating copolymerization". The mechanism of becomes increasingly "alternating" as the $r_1 r_2$ product decreases from one toward zero. For polymerizations where the $r_1 r_2$ product lies somewhere between zero and one, the composition of the copolymer can be controlled to some extent by variation of the monomer feed ratio. However, as $r_1 r_2$ approaches very close to zero, the "alternating" behavior of the polymerization mechanism becomes the dominating factor and a 1:1 alternating copolymer can be formed independent of the monomer feed ratio.

The terminal model also provides a useful means to approximate copolymer compositions that are dependent on such factors as the comonomer feed ratio and the reactivities of the comonomers according to the model. The Mayo-Lewis equation,[72]

---

[69] Morris, L. M.; Davis, T. P.; Chaplin, R. P. *Polymer* **2000**, *42*, 941.
[70] *Polymer Handbook,* 3rd ed.; Brandrup, J., Immergut, E. H., Eds.; Wiley & Sons: New York, 1989; Chapter 2, p 153.
[71] Alfrey, T., Jr.; Price, C. C. *J. Polym. Sci.* **1947**, *2*, 101.
[72] Mayo, F. R.; Lewis, F. M. *J. Am. Chem. Soc.* **1944**, *66*, 1594.

which is derived from the terminal model using the assumption of the steady-state radical approximation, can be used to describe the instantaneous copolymer composition:

$$\frac{d[M_1]}{d[M_2]} = \frac{[M_1](r_1[M_1]+[M_2])}{[M_2]([M_1]+r_2[M_2])}$$

Figure 2.7 Mayo-Lewis copolymer composition equation.

Where r_1 and r_2 are the respective monomer reactivity ratios. $[M_1]$ and $[M_2]$ describe the beginning concentrations in the comonomer feed. The instantaneous mole fractions of the two repeating units in the copolymer is then defined as $d[M_1]/d[M_2]$. The terminal model, therefore, allows one to predict the instantaneous copolymer composition for a given comonomer feed simply on the basis of the comonomer reactivity ratios. Although the terminal model relies on several assumptions and may not be the most reliable model to describe of a copolymerization process, it is has the advantages of being simple to apply and very useful as a starting point to study a given copolymerization reaction.

2.4.2.2 Penultimate Model

It has been shown that the behavior of the propagating species of some comonomer pairs is significantly influenced by the penultimate monomer unit.[73] The principal feature of the penultimate model is that the penultimate unit (Figure 2.8) in a propagating polymer

[73] Coote, M. L.; Davis, T. P. *Prog. Polym. Sci.* **2000**, *24*, 1217. Cywar, D. W.; Tirrell, D. A. *J. Am. Chem. Soc.* **1989**, *111*, 7544. Tanaka, H.; Sasai, K.; Sato, T.; Ota, T. *Macromolecules* **1988**, *21*, 3534. Hill, D. J. T.; Lang, A. P.; O'Donnell, J. H.; O'Sullivan, P. W. *Eur. Polym. J.* **1989**, *25*, 911.

chain will affect the reactivity of the terminal reactive radical. The exact nature of the penultimate unit of the propagating species will determine the magnitude of this effect. For example, Tirrell and coworkers have reported that in copolymerizations of styrene and acrylonitrile, there is little effect of the terminal radical reactivity when the penultimate units is styrene unit, but there is an appreciable effect when the penultimate unit is acrylonitrile.[74]

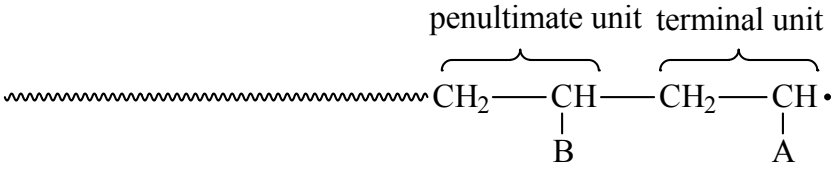

Figure 2.8 Penultimate and terminal units of propagating copolymer chain.

The effect of the penultimate unit on the kinetic of copolymerization was first reported by Merz et al.[75] and later by Ham[76] and Barb.[77] The mathematical model for the penultimate effect involves the use of eight propagating reactions (Figure 2.9) from which four reactivity ratios are defined (Figure 2.10):

[74] Jones, S. A.; Prementine, G. S.; Tirrell, D. A. *J. Am. Chem. Soc.* **1985**, *107*, 5275.
[75] Merz, E.; Alfrey, T.; Goldfinger, G. *J. Polym. Sci.* **1946**, *1*, 75.
[76] Ham, G. E. *J. Polym. Sci.* **1954**, *14*, 87.
[77] Barb, W. G. *J. Polym. Sci.* **1953**, 11, 117.

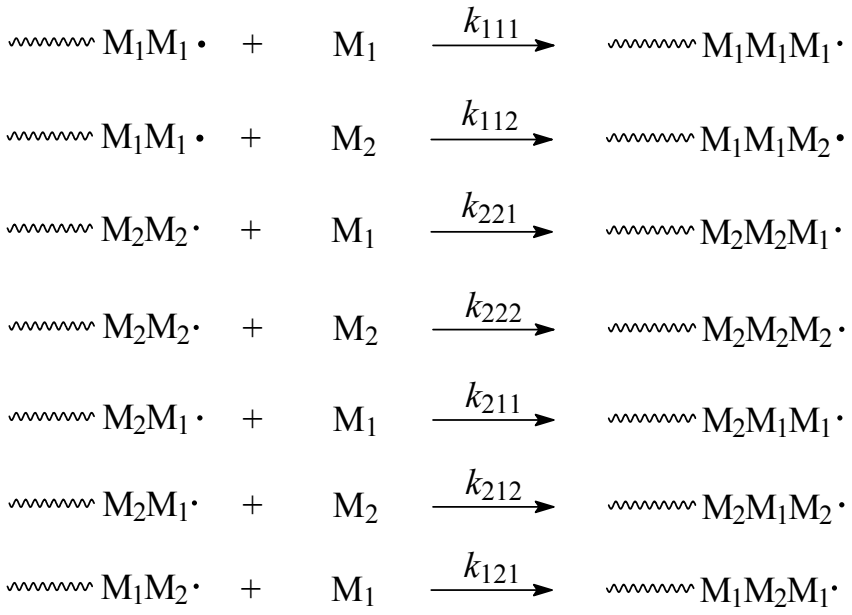

Figure 2.9 Penultimate kinetic model for copolymerization.

$$r_{11} = \frac{k_{111}}{k_{112}} \qquad r_{12} = \frac{k_{122}}{k_{121}} \qquad r_{22} = \frac{k_{222}}{k_{221}} \qquad r_{21} = \frac{k_{211}}{k_{212}}$$

Figure 2.10 Comonomer reactivity ratios based upon the penultimate model.

Each monomer is thus characterized by two monomer reactivity ratios. One reactivity ratio (r_{11} and r_{22}) that represents the propagating species in which the penultimate and terminal monomer units are the same. The other represents the propagating species in which the penultimate and terminal units differ (r_{12} and r_{21}).

Several copolymerization processes have been studied where the experimental data agreed better with the penultimate model that the terminal model. However, application of

the penultimate model to study copolymerization behavior is significantly more complicated and time consuming than application of the terminal model. Consequently, the study of copolymerizations has been primarily limited to analysis in terms of the terminal model. Comonomers that have been studied using the penultimate model include acrylonitrile,[78] butadiene,[79] maleic anhydride,[80] and vinyl chloride.[81]

2.4.2.3 Complex Model

The complex model assumes that no free monomers are involved in the kinetic rate of the reaction, but rather the polymer chains propagate by the head-to-tail homopolymerization of comonomer complexes. Copolymerization mechanisms involving complexed comonomers were first introduced to help explain the high degree of alternation observed for some copolymerization reactions.[82] One proposed mechanism is that there is a charge-transfer-complex (CTC) that exists between electron poor/electron rich comonomer pairs and propagation of the copolymer then proceeds via the polymerization of the CTC and not of the individual comonomers.[83] The most studied system is that of styrene-maleic anhydride. The idealized structure of the proposed CTC of the styrene-maleic anhydride comonomer pair is illustrated in Figure 2.11.[84] The validity of complex copolymerization models has been thoroughly debated over the years. The existence of complexes between certain comonomer pairs using spectroscopic techniques has been well documented and accepted. Donor-accepter interactions between monomer pairs can lead to highly colored complexes and the appearance of new absorption bands in the UV-visible

---

[78] Hill, D. J. T.; Lang, A. P., O'Donnell, H. H.; O'Sullivan, P. W. *Eur. Polym. J.* **1989**, *25*, 911.
[79] Van Der Meer, R.; Alberti, J. M.; German, A. L.; Linssen, H. N. *J. Polym. Sci., Part A: Polym. Chem.* **1979**, *17*, 3349.
[80] Hill, D. J. T.; O'Donnell, J. H.; O'Sullivan, P. W. *Macromolecules* **1985**, *18*, 9.
[81] Guillot, J.; Vialle, J.; Guyot, A. *Macromol. Sci. Chem.* **1971**, *A5*, 735.
[82] Cowie, J. M. G. In *Alternating Copolymers*; Cowie, J. M. G., Ed.; Plenum: New York, 1985, Ch. 1.
[83] Ellinger, L. P. *Advances in Macromolecular Chemistry*; Academic Press: New York, 1968; Vol. 1, p 169.

spectrum are observed.[85] In addition, charge transfer complexes have been characterized by small chemical shifts in the NMR spectra.[86] However, evidence for the involvement of these complexes in the actual propagation step has been less conclusive and thus undeniable proof for a copolymerization mechanism via a CTC has not been presented.[87]

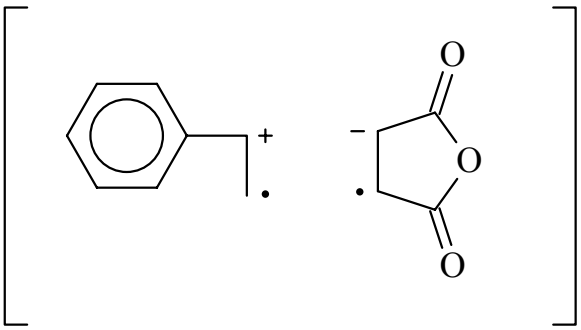

Figure 2.11 Charge-transfer-complex of styrene and maleic anhydride**.**

Complex copolymerization models have been applied to the study of many electron donor-acceptor comonomer pairs.[88] Electron donating monomers studied include linear dienes, heterocyclic dienes, vinylbenzenes, vinyl esters, vinyl ethers, and vinyl sulfides. Electron accepting monomers include maleic anhydride, maleimides, acrylate esters, cinnamate esters, cyanoethylenes, and fumarate esters. Characteristic features of copolymerizations involving electron donor-accepter pairs include high degrees of

---

[84] Cais, R. E.; Farmer, R. G.; Hill, D. J. T.; O'Donnell, J. H. *Macromolecules* **1979**, *12*, 835.
[85] Vosburgh, W. C.; Cooper, G. R. *J. Am. Chem. Soc.* **1941**, *63*, 437. Butler, G. B.; Badgett, T.; Sharabash, M. *J. Macromol. Sci., Chem.* **1970**, *A4*, 51.
[86] Hanna, M. W.; Ashbaugh, A. L. *J. Phys. Chem.* **1964**, *68*, 811. Sandoval, A. A.; Hanna, M. W. *J. Phys. Chem.* **1966**, *70*, 1203.
[87] Hall, H. K.; Padias, A. B. *J. Polym. Sci., Part A: Polym. Chem.* **2001**, *39*, 2069. Jones, S. A.; Tirrell, D. A. *J. Polym. Sci., Part A: Polym. Chem.* **1987**, *25*, 3177.

alternation, faster copolymerization rates than either homopolymerization rate, and in many cases the strongly electron donating or accepting monomers will not undergo homopolymerization to an appreciable extent. Several complex copolymerization models have been reported to help explain the behavior of copolymerizations involving donor-acceptor comonomer pairs. For example, the complex participation model assumes that the comonomer complex that is formed is much more reactive than the uncomplexed monomers and as a result the comonomers are incorporated into the chain as pairs and result in perfectly alternating sequences.[89] The complex participation model considers both propagation of complexed comonomer pairs and also competing propagation of uncomplexed monomers. An alternative model is called the complex dissociation model,[90] which also considers propagation of uncomplexed monomers. However, where the complex dissociation model differs is that it assumes the complexed monomer pairs dissociate upon addition to a growing polymer chain and as a result only a single monomer unit is incorporated into the polymer chain. These complex models have been successful in describing the copolymerization behavior of certain donor-acceptor comonomer pairs. However, it is often difficult to differentiate between these models and other higher order models such as the penultimate model, which do not consider the existence of comonomer complexes.[91] In addition, application of complex copolymerization models have been further complicated due to the feature that many of these donor-acceptor pairs undergo spontaneous initiation.[92]

---

[88] Cowie, J. M. G. In *Alternating Copolymers*; Cowie, J. M. G., Ed.; Plenum: New York, 1985, Ch. 2.

[89] Cais, R. E.; Farmer, R. G.; Hill, D. J. T.; O'Donnell, J. H. *Macromolecules* **1979**, *12*, 835. Seiner, J. A.; Litt, M. *Macromolecules* **1971**, *4*, 308. Pittman, C. U.; Rounsefell, T. D. *Macromolecules* **1975**, *8*, 46.

[90] Hill, D. J. T.; O'Donnell, J. H.; O'Sullivan, P. W. *Macromolecules* **1983**, *16*, 1295.

[91] Hill, D. J. T.; O'Donnell, J. H.; O'Sullivan, P. W. *Macromolecules* **1985**, *18*, 9.

[92] Hall, H. K.; Padias, A. B. *Acc. Chem. Res.* **1990**, *23*, 3.

2.4.3 Principles of Alternating Copolymerization

When two monomers are mixed together in the presence of an initiator there are several ways that the monomers may combine to form a copolymer. In general, the composition of the product rarely follows the monomer feed ratio. Furthermore, the composition resulting from a copolymerization reaction cannot directly be predicted from knowledge of the homopolymerization rates of the monomers.[93] Therefore, the factors that determine the incorporation of repeating units into a copolymer chain are not as trivial as those in homopolymerization reactions. Not only does the homopolymerization rate of the comonomers have an effect, but the rate at which comonomers react with each other is also a determining factor.

Alternating copolymerization is an example of chain copolymerization where each of the monomers adds preferentially to the other, which results in an alternating monomer sequence distribution along the backbone.[94] Monomers that are difficult to homopolymerize are often found to be capable of alternating copolymerization. For example, if a strong electron acceptor is added together with a strong electron donor, regular alternating copolymers may result from either spontaneous initiation or a free radical source.[95]

The most widely studied comonomers for producing alternating copolymers is maleic anhydride. Maleic anhydride is a very strong electron acceptor that has been shown to homopolymerize poorly,[96] but will react with a number of electron donating monomers to

---

[93] Staudinger, H.; Schneiders, J. *Ann. Chim.* **1939**, *541*, 151.
[94] Odian, G. *Principles of Polymerization*, 3rd ed.; Wiley & Sons: New York, 1991; Chapter 6.
[95] Cowie, J. M. G. In *Comprehensive Polymer Science*; Allen, G., Bevington, J. C., Eastmond, G. C., Ledwith, A., Russo, S., Sigwalt, P., Eds.; Pergamon: Oxford, England, 1989; Vol. 4, Chapter 22.
[96] Gaylord, N. G. *J. Macromol. Sci. Rev. Macromol. Chem.* **1975**, *13*, 235. Regel, W.; Schneider, C. *Makromol. Chem.* **1981**, *182*, 237. Trivedi, B. C.; Culbertson, B. M. *Maleic Anhydride*; Plenum Press: New York, 1982.

form alternating copolymers.[97,98] Of particular interest is that many 1,2-disubstituted and cyclic olefins that do not homopolymerize by free-radical methods, will form alternating copolymers with maleic anhydride. The copolymerization of *trans*-stilbene with maleic anhydride was first described in 1930.[99] Later, Bartlett and Nozaki reported that the radical initiated copolymerization of allyl acetate and maleic anhydride resulted in a material with equimolar incorporation of allyl acetate and maleic anhydride into the copolymer regardless of monomer feed.[100] This result led the authors to propose the possibility that electron transfer in an activated charge-transfer-complex (CTC) could account for the observed alternating behavior of these comonomers.

The CTC proposed by Bartlett and Nozaki has been thoroughly debated over the years. Early on, several researches supported[101] the CTC while others challenged its existence.[102] The existence of a CTC between donor-acceptor comonomer pairs has typically been illustrated from characterization using ultraviolet-visible spectroscopy[103] and nuclear magnetic resonance spectroscopy.[104] In addition, experiments studying the

---

[97] Walling, C.; Briggs, E. R.; Wolfstirn, K. B.; Mayo, F. R. *J. Am. Chem. Soc.* **1948**, *70*, 1537. Barb, W. G. *J. Polym. Sci.* **1953**, *11*, 117. Seymour, R. B.; Garner, D. P. *Polymer* **1976**, *17*, 21. Block, H.; Cowd, M. A.; Walker, S. M. *Polymer* **1972**, *13*, 549. Gaylord, N. G.; Maiti, S.; Patnaik, B. K.; Takahashi, A. *J. Macromol. Sci., Chem.* **1972**, *A6*, 1459. Gaylord, N. G.; Maiti, S. *J. Macromol. Sci., Chem.* **1972**, *A6*, 1481. Fujimori, K. *J. Macromol. Sci., Chem.* **1975**, *A9*, 495. Caze, C.; Loucheux, C. *J. Macromol. Sci., Chem.* **1975**, *A9*, 29.

[98] Trivedi, B. C.; Culbertson, B. M. *Maleic Anhydride*; Plenum Press: New York, 1982; Chapter 10.

[99] Wagner-Jaruegg, T. *Ber.* **1930**, *63B*, 3213.

[100] Bartlett, P. D.; Nozaki, K. *J. Am. Chem. Soc.* **1946**, *68*, 1495.

[101] Booth, D.; Dainton, F. S.; Ivin, K. J. *Trans. Faraday Soc.* **1959**, *55*, 1293. Barb, W. G. *Proc. R. Soc. London, Ser. A* **1952**, *212*, 66. Dainton, F. S.; Ivin, K. J. *Proc. R. Soc. London, Ser. A* **1952**, *212*, 96, 207. Dainton, F. S.; Bristow, G. M. *Proc. R. Soc. London, Ser. A* **1955**, *229*, 509, 525. Tokura, N.; Matsuda, M. *Kogyo Kagaku Zasshi* **1961**, *64*, 501. Tokura, N.; Matsuda, M. *Kogyo Kagaku Zasshi* **1962**, *65*, 1095. Ito, I.; Hayshi, H.; Saegusa, T.; Furukawa, J. *Kogyo Kagaku Zasshi* **1962,** *65*, 703. Ito, I.; Saegusa, T.; Furukawa, J. *Kogyo Kagaku Zasshi* **1962**, *65*, 1878.

[102] Walling, C.; Briggs, E. R.; Wolfstirn, K. B.; Mayo, F. R. *J. Am. Chem. Soc.* **1948**, *70*, 1537. Price, C. C. *J. Polym. Sci.* **1948**, *3*, 772. Mayo, F. R.; Walling, C. *Chem. Rev.* **1950**, *46*, 191.

[103] Vosburgh, W. C.; Cooper, G. R. *J. Am. Chem. Soc.* **1941**, *63*, 437.

[104] Hanna, M. W.; Ashbaugh, A. L. *J. Phys. Chem.* **1964**, *68*, 811. Sandoval, A. A.; Hanna, M. W. *J. Phys. Chem*. **1966**, *70*, 1203.

effects of temperature and solvent polarity have been utilized to study the effect of the CTC on the behavior of alternating copolymerizations.[105]

Following the earlier work of Bartlett and Nozaki, several others have reported the synthesis of materials produced via the alternating copolymerization of maleic anhydride and electron donating comonomers including. Electron donating comonomers that were successfully copolymerized with maleic anhydride include furan,[106] conjugated dienes,[107] divinyl ether,[108] styrene,[109] allyl cycloalkenes,[110] and methyl vinyl silanes.[111] The results of these investigations demonstrated that the comonomers copolymerized via an alternating copolymerization mechanism. Furthermore, the authors generally supported the CTC concept proposed by Bartlett and Nozaki concluding that propagation occurred following the formation of a CTC between maleic anhydride and the electron donating monomer.

---

[105] Case, C.; Loucheux, C. *J. Macromol. Sci., Chem.* **1975**, *A9*, 29. Seymour, R. B.; Garner, D. P. *J. Coatings Technol.* **1976**, *41*, 612. Seymour, R. B.; Garner, D. P. *Polymer* **1976**, *17*, 21. Seymour, R. B.; Garner, D. P.; Sanders, L. J. *J. Macromol. Sci., Chem.* **1979**, *A13,* 173. Tsuchida, E.; Tomono, T.; Sano, H. *Makromolek. Chem.* **1972**, *151*, 245. Butler, G. B.; Fujimori, K. *J. Macromol. Sci., Chem.* **1972**, *A6*, 1533.

[106] Gaylord, N. G.; Maiti, S.; Patnaik, B. K.; Takahashi, A. *J. Macromol. Sci., Chem.* **1972**, *A6*, 1459. Gaylord, N. G.; Maiti, S. *J. Macromol. Sci., Chem.* **1972**, *A6*, 1481. Butler, G. B.; Badgett, J. T.; Sharabash, M. *J. Macromol. Sci., Chem.* **1970**, *A4*, 51. Ragab, Y. A.; Butler, G. B. *J. Polym. Sci., Part A: Polym. Chem.* **1981**, *19*, 1175.

[107] Butler, G. B.; Vanhaeren, G.; Ramadier, M. *J. Polym. Sci.* **1967**, *5*, 1265. Butler, G. B.; Joyce, K. C. *J. Polym. Sci. Part C* **1968**, *22*, 45. Gaylord, N. G.; Maiti, S. *J. Polym. Sci., Polym. Lett. Ed.* **1971**, *9*, 359. Gaylord, N. G.; Stolka, M.; Takahashi, A.; Maiti, S. *J. Macromol. Sci., Chem.* **1971**, *A5*, 867. Gaylord, N. G.; Tomono, T.; Mandal, B. M. *J. Polym. Sci., Part A: Polym. Chem.* **1976**, *14*, 1283.

[108] Butler, G. B.; Fujimori, K. *J. Macromol. Sci., Chem.* **1972**, *A6*, 1533. Barton, J. M.; Butler, G. B.; Chapin, E. C. *J. Polym. Sci.* **1965**, *3*, 501. Butler, G. B. *J. Macromol. Sci., Chem.* **1971**, *A5*, 219.

[109] Tsuchida, E.; Tomono, T. *Makromolek. Chem.* **1971**, *141*, 265. Tsuchida, E.; Tomono, T.; Sano, H. *Makromolek. Chem.* **1972**, *151*, 245. Tsuchida, E.; Ohtani, Y.; Nakadai, H.; Shinohara, I. *J. Chem. Soc. Jpn., Ind. Chem. Sect.* **1967**, *70*, 573. Tsuchida, E.; Tsumuji, T.; Tomono, T.; Shinohara, I. *J. Chem. Soc. Jpn., Ind. Chem. Sect.* **1969**, *72*, 765. Tsuchida, E.; Tomono, T.; Sano, H. *J. Chem. Soc. Jpn., Ind. Chem. Sect.* **1970**, *73*, 2031.

[110] van Heiningen, J. J.; Butler, G. B. *J. Macromol. Sci., Chem.* **1974**, *A8*, 1175.

[111] Butler, G. B.; Campus, A. F. *J. Polym. Sci.* **1970**, *8*, 523.

2.5 CYCLIC OLEFIN/MALEIC ANHYDRIDE (COMA) ALTERNATING COPOLYMERS FOR 193 NM PHOTORESIST MATERIALS

2.5.1 Introduction

Photolithography using 193 nm (Ar-F laser) light has emerged for the production of the next generation of microelectronic devices.[112] Current technology (Kr-F laser), including ultraviolet (UV) and deep-UV photolithography, employs aromatic materials based upon phenolic polymers.[113] However, the photon energy of 193 nm light is approximately 150 kcal/mol, which is high enough for aromatic polymers to absorb strongly at this wavelength, resulting in opaque materials that are not practical for 193 nm lithography.[114] Therefore, recent years have seen a large effort devoted to the design of materials that are optically transparent at 193 nm and also have the desirable etch-resistant and image-forming properties of phenolic based materials.[115]

A number of approaches to materials with high transparency at 193 nm have been reported.[116] Initially, acrylic-based polymers seemed promising as new materials for 193 nm lithography. Acrylates were desirable materials due to only a weak $n \rightarrow \pi^*$ carbonyl absorption at 193 nm, which resulted in good transparency when exposed to this

---

[112] Nozaki, N.; Kaimoto, M.; Takahashi, S.; Takeshi, S.; Abe, N. *Chem. Mater.* **1994**, *6*, 1492. Kunz, R. R.; Palmateer, A. R; Forte, A. R.; Allen, R. D.; Wallraff, G. M.; DiPietro, R. A.; Hofer, D. C. *Proc. SPIE-Int. Soc. Opt. Eng.* **1996**, *2724*, 365. Allen, R. D.; Opitz, J.; Larson, C. E.; Wallow, T. I.; Hofer, D. C. *Microlithography World* **winter 1999**, 5. Jung, M. H.; Jung, J. C.; Lee, G.; Baik, K. H. *Jpn J. Appl. Phys., Part 1* **1998**, *37*, 6889. Nalamasu, O.; Houlihan, R. A.; Cirelli, A. G.; Watson, G. P.; Hutton, R. S.; Kometani, J. M.; Reichmanis, E. *J. Vac. Sci. Technol., B* **1998**, *16*, 3716. Okoroanyanwu, U.; Byers, J.; Shimokawa, T.; Willson, C. G. *Chem. Mater.* **1998**, *10*, 3328.

[113] Ito, H. *Solid State Technol.* **1996**, *36(7)*, 164. Willson, C. G. *Introduction to Microlithography*, 2nd ed.; ACS Professional Reference book; American Chemical Society: Washington, DC, 1994; Ch. 3.

[114] Kunz, R. R.; Allen, R. D.; Wallraff, G. M. *Polym. Prepr. (Am. Chem. Soc., Div. Polym. Chem.)* **1994**, *35(2)*, 939.

[115] Allen, R. D.; Wallraff, G. M.; Hofer, D. C.; Kunz, R. R. *IBM J. Res. Dev.* **1997**, *41*, 95.

[116] Nonogaki, S.; Ueno, T.; Ito, T. Chemistry of Photoresist Materials. In *Microlithography Fundamentals in Semiconductor Devices and Fabrication Technology*; Marcel Dekker: New York, 1999; pp 115-119.

wavelength of light.[117] In 1991, IBM described successful 193 nm patterning using an all-acrylic terpolymer made up of methylmethacrylate, *tert*-butylmethacrylate and methacrylic acid (Figure 2.12).[118] This material successfully provided positive imaging via aqueous base development after photo-generated acid catalyzed deprotection of the *tert*-butyl functionality to yield methacrylic acid groups. A major disadvantage, however, of this and other acrylic materials is poor reactive-ion etch resistance under the etching conditions used widely in the semiconductor industry.[119]

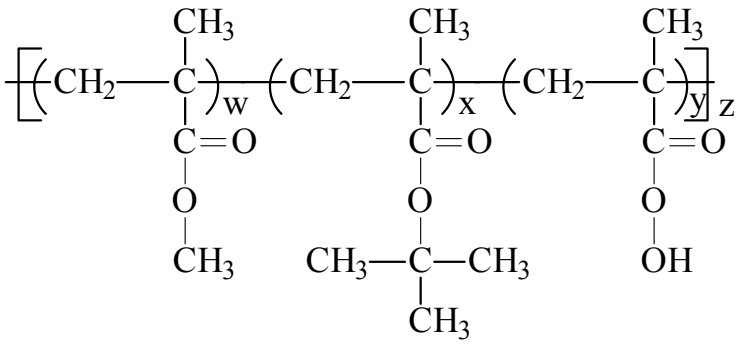

Figure 2.12 IBM acrylic terpolymer for 193 nm photolithography.

The primary design challenge that has emerged in the development of new materials for 193 nm photolithography is the trade off between imaging performance (broadly defined as resolution, process latitude, adhesion, sensitivity, and compatibility with

---

[117] Wallraff, G. M.; Hinsberg, W. D. *Chem. Rev.* **1999**, *99*, 1801.
[118] Allen, R. D.; Wallraff, G. M.; Hinsberg, W. D.; Simpson, L. L. *J. Vac. Sci. Technol., B* **1991**, *9*, 3357.
[119] Wallow, T. I.; Brock, P. J.; Dipietro, R. A.; Allen, R. D.; Opitz, J.; Sooriyakumaran, R.; Hofer, D. C; Meute, J.; Byers, J. D.; Rich, G. K.; McCallum, M.; Schuetze, S.; Jayaraman, S.; Hullihen, K.; Vicari, R.; Rhodes, L. F.; Goodall, B. L.; Shick, R. A. *Proc. SPIE-Int. Soc. Opt. Eng.* **1998**, *3333*, 92.

industry standard aqueous-base developers) and reactive-ion etch resistance.[120] For acrylic materials, the chemical modifications that were used to tailor imaging performance also deleteriously influenced reactive-ion etch resistance.[121] Previously, it has been determined that there is a correlation between increased reactive-ion etch resistance and a high carbon to hydrogen (C/H) ratio,[122] explaining why phenolic materials that are currently used as resist materials, which have a high C/H ratio, exhibit good plasma etch resistance. Therefore, to improve the reactive-ion etching properties of acrylic based materials by increasing the C/H ratio, a number of acrylic-based materials containing pendant alicyclic adamantane or norbornane functionality have been investigated.[123] Incorporation of the pendant alicyclic functionalities greatly improved the etch resistance of acrylic based materials. However, the increase in etch resistance was also accompanied by decreased image performance, which has hindered the development of a 193 nm photolithography acrylic resist material with both etch resistant and image performing properties required for industrial application.

The main drawback of the acrylic materials for use in lithography was the poor etch stability of the oxygen rich linear backbone, which could be improved by incorporation of

---

[120] Nonogaki, S.; Ueno, T.; Ito, T. Chemistry of Photoresist Materials. In *Microlithography Fundamentals in Sumiconductor Devices and Fabrication Technology*; Marcel Dekker: New York, 1999; pp 115-119.

[121] Wallow, T. I.; Brock, P. J.; Dipietro, R. A.; Allen, R. D.; Opitz, J.; Sooriyakumaran, R.; Hofer, D. C; Meute, J.; Byers, J. D.; Rich, G. K.; McCallum, M.; Schuetze, S.; Jayaraman, S.; Hullihen, K.; Vicari, R.; Rhodes, L. F.; Goodall, B. L.; Shick, R. A. *Proc. SPIE-Int. Soc. Opt. Eng.* **1998**, *3333*, 92.

[122] Kunz, R. R.; Palmateer, A. R; Forte, A. R.; Allen, R. D.; Wallraff, G. M.; DiPietro, R. A.; Hofer, D. C. *Proc. SPIE-Int. Soc. Opt. Eng.* **1996**, *2724*, 365. Gokhan, H.; Esho, S.; Ohnishi, Y. *J. Electrochem. Soc.* **1983**, *130*, 143.

[123] Kaimoto, Y.; Nozaki, K.; Takechi, M.; Abe, N. *Proc. SPIE-Int. Soc. Opt. Eng.* **1992**, *1672*, 66. Nozaki, K.; Kaimoto, Y.; Takahashi, M.; Takechi, Abe, N. *Chem. Mater.* **1994**, *6*, 1492. Takechi, S.; Takahashi, M.; Kotachi, A.; Nozaki, K.; Yano, E.; Hanyu, I. *J. Photopolym. Sci. Technol.* **1996**, *9*, 475. Yamashita, K.; Endo, M.; Sasago, M.; Nomura, N.; Nagano, H.; Mizuguchi, S.; Ono, T.; Sato, T. *J. Vac. Sci. Technol., B* **1993**, *11*, 2692. Nakano, K.; Maeda, K.; Iwasa, S.; Yano, J.; Ogura, Y.; Hasegawa, E. *Proc. SPIE-Int. Soc. Opt. Eng.* **1994**, *2195*, 194. Maeda, K.; Nakano, K.; Ohfuji, T.; Hasegawa, E. *Proc. SPIE-Int. Soc. Opt. Eng.* **1996**, *2724*, 377. Allen, R. D.; Wallraff, G. M.; DiPietro, R. A.; Hofer, D. C.; Kunz, R. R. *J. Photopolym. Sci. Technol.* **1994**, *7*, 507.

alicyclic pendant groups along the backbone. However, the amount of alicyclic incorporation required to achieve necessary etch resistance also tended to produce a material that had poor film forming and adhesion properties as well as limited aqueous base solubility. An alternative approach to increase the C/H ratio was to incorporate alicyclic structures directly into the polymer backbone.[124] A variety of synthesis routes for producing resist materials with alicyclic backbones have been investigated. They include cyclic olefin alternating free radical copolymerization,[125] metal catalyzed vinyl addition polymerization,[126] and ring opening metathesis polymerization (ROMP) followed by hydrogenation.[127] In recent years, the most promising of these methods that has emerged for synthesizing alicyclic materials for 193 nm lithography is the alternating copolymerization of maleic anhydride with cyclic olefin monomers such as norbornene. Materials made using this method exhibit excellent etch resistance similar to hydroxystyrene materials that are currently used as photoresist materials. In addition, the ability to modify the polymer properties via incorporation of cyclic olefin monomer

---

[124] Wallraff, G. M.; Hinsberg, W. D. *Chem. Rev.* **1999**, *99*, 1801.

[125] Okoroanyanwu, U.; Shimokawa, T.; Byers, J.; Medeiros, D.; Willson, C. G.; Niu, Q, J.; Fréchet, J. M. J.; Allen, R. D. *Proc. SPIE-Int. Soc. Opt. Eng.* **1997**, *3049*, 92. Okoroanyanwu, U.; Shimokawa, T.; Byers, J.; Willson, C. G. *Chem Mater.* **1998**, *10*, 3319. Nozaki, K.; Yano, E. *J. Photopolym. Sci. Technol.* **1997**, *10*, 545. Patterson, K.; Okoroanyanwu, U.; Shimokawa, T.; Cho, S.; Byers, J.; Willson, C. G. *Proc. SPIE-Int. Soc. Opt. Eng.* **1998**, *3333*, 425. Wallow, T. I.; Houlihan, F. M.; Nalamasu, O.; Chandross, E. A. Neenan, T. X.; Reichmanis, E. *Proc. SPIE-Int. Soc. Opt. Eng.* **1996**, *2724*, 355. Houlihan, F. M.; Wallow, T. I.; Nalamasu, O.; Reichmanis, E. *Macromolecules* **1997**, *30*, 6517. Patterson, K.; Yamchika, M.; Cho, S.; Rager, T.; Yamada, S.; Byers, J.; Willson, C. G. *Polym. Mat. Sci. Eng.* **1999**, *81*, 43. Gabor, A. H.; Dimov, O.; Medina, A. N.; Bowden, M. J.; Neisser, M. O.; Houlihan, F. M.; Cirelli, R. A.; Dabbagh, G.; Hutton, R. S.; Rushkin, I. L.; Sweeney, J. R.; Nalamasu, O.; Reichmanis, E. *Polym. Mat. Sci. Eng.* **1999**, *81*, 41.

[126] Okoroanyanwu, U.; Shimokawa, T.; Byers, J.; Medeiros, D.; Willson, C. G.; Niu, Q, J.; Fréchet, J. M. J.; Allen, R. D. *Proc. SPIE-Int. Soc. Opt. Eng.* **1997**, *3049*, 92. Okoroanyanwu, U.; Shimokawa, T.; Byers, J.; Willson, C. G. *Chem Mater.* **1998**, *10*, 3319. Allen, R. D.; Sooriyakumaran, R.; Opitz, J.; Wallraff, G. M.; DiPietro, R. A.; Breyta, G.; Hofer, D. C. *Proc. SPIE-Int. Soc. Opt. Eng.* **1996**, *2724*, 334. Allen, R. D.; Opitz, J.; Wallow, T. I.; DiPietro, R. A.; Hofer, D. C.; Jayaraman, S.; Hullihan, K. A.; Rhodes, L. F.; Goodall, B. L.; Shick, R. A. *Proc. SPIE-Int. Soc. Opt. Eng.* **1998**, *3333*, 463. Opitz, J.; Allen, R. D.; Wallow, T. I.; Wallraff, G. M.; Hofer, D. C. *Proc. SPIE-Int. Soc. Opt. Eng.* **1998**, *3333*, 571.

[127] Okoroanyanwu, U.; Shimokawa, T.; Byers, J.; Medeiros, D.; Willson, C. G.; Niu, Q, J.; Fréchet, J. M. J.; Allen, R. D. *Proc. SPIE-Int. Soc. Opt. Eng.* **1997**, *3049*, 92. Okoroanyanwu, U.; Shimokawa, T.; Byers, J.; Willson, C. G. *Chem Mater.* **1998**, *10*, 3319.

derivatives to improve lithographic performance has further made this a very attractive route to new materials for 193 nm lithography.

2.5.2 Cyclic Olefin/Maleic Anhydride Alternating Copolymers for 193 nm Photoresist Materials

One of the most promising and generally accepted routes for main-chain alicyclic 193 nm resist materials is the alternating free radical copolymerization of maleic anhydride with cyclic olefin comonomers, such as norbornene (Scheme 2.14). Cyclic olefins will homopolymerize poorly via free radical methods. However, when cyclic olefins are reacted with maleic anhydride, which is a strong electron acceptor, in the presence of a free radical initiator, they copolymerize in an alternating manner. In addition, maleic anhydride also serves to incorporate oxygen into the material, providing necessary adhesion and solubility properties that are required for imaging performance while still retaining sufficient etch resistance to be successfully demonstrated as 193 nm resist materials. The cyclic olefin character of these materials provides for excellent etch resistance, surpassing even currently utilized phenol based resists. Furthermore, the increased etch resistance is of great importance because of the decreasing film thickness necessary for the achievement of increasingly smaller feature sizes.[128] Several routes have emerged as methods for the synthesis of maleic anhydride/cyclic olefin resist materials for 193 nm lithography. Major contributors in this area have been Reichmanis and coworkers at AT&T (Lucent Technologies), Willson and coworkers at the University of Texas, Allen and coworkers at IBM, and Jung and coworkers at Hyundai Electronics.

---

[128] Allen, R. D.; Opitz, J.; Larson, C. E.; Wallow, T. I.; Hofer, D. C. *Microlithography World* **winter 1999**, 5.

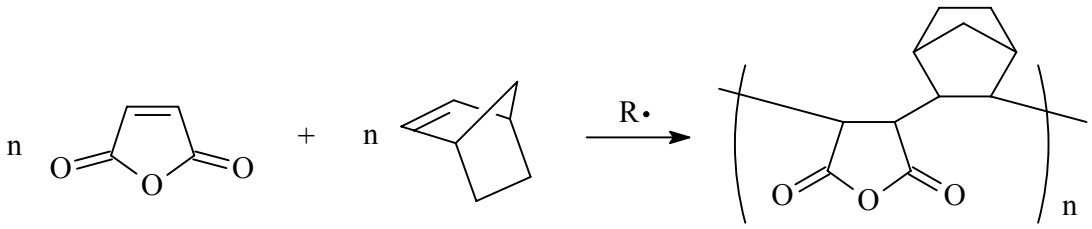

Scheme 2.14 Free radical alternating copolymerization of maleic anhydride and norbornene.

Workers at AT&T (Lucent Technologies) have focused upon 193 nm resist materials consisting of norbornene, maleic anhydride, acrylic acid, and *t*-butyl acrylate monomer units polymerized by free radical methods.[129] A key feature of maleic anhydride/norbornene alternating polymerization first described in a patent is that small percentages (reported to be less than 10%) of other vinyl monomers can be incorporated without disrupting the alternating nature of the polymerization.[130] These workers utilized this feature to incorporate acrylic acid and *tert*-butyl acrylate monomer units into the norbornene/maleic anhydride alternating copolymer polymer backbone. Initially, they performed terpolymerization studies of norbornene and maleic anhydride with either acrylic acid or *tert*-butyl acrylate, and they found that they could incorporate even greater amounts (from 0 to 0.3) of the acrylate monomers into the polymer without disrupting the 1:1 ratio of norbornene and maleic anhydride. In addition, they showed that the acrylate monomers could be uniformly incorporated into the materials as a linear function of the

[129] Nalamasu, O.; Houlihan, R. A.; Cirelli, A. G.; Watson, G. P.; Hutton, R. S.; Kometani, J. M.; Reichmanis, E. *J. Vac. Sci. Technol., B* **1998**, *16*, 3716. Wallow, T. I.; Houlihan, F. M.; Nalamasu, O.; Chandross, E. A. Neenan, T. X.; Reichmanis, E. *Proc. SPIE-Int. Soc. Opt. Eng.* **1996**, *2724*, 355. Houlihan, F. M.; Wallow, T. I.; Nalamasu, O.; Reichmanis, E. *Macromolecules* **1997**, *30*, 6517. Gabor, A. H.; Dimov, O.; Medina, A. N.; Bowden, M. J.; Neisser, M. O.; Houlihan, F. M.; Cirelli, R. A.; Dabbagh, G.; Hutton, R. S.; Rushkin, I. L.; Sweeney, J. R.; Nalamasu, O.; Reichmanis, E. *Polym. Mat. Sci. Eng.* **1999**, *81*, 41.

[130] Potter, G. H.; Zutty, N. L. U. S. Patent 3 280 080, 1966.

mole fraction of the monomers in the feed.[131] They found that incorporation of acrylic acid provided a controlled method of providing aqueous base solubility for development. Furthermore, the materials incorporating *tert*-butyl acrylate possessed thermal, optical, and organic solubility's similar to poly(norbornene-*alt*-maleic anhydride) copolymers, but showed improved adhesion to silicon wafer substrates and the *t*-butyl ester functionality provides a site to afford base solubility via acid hydrolysis of the acrylate ester functionality (Scheme 2.15). In subsequent publications, they reported the synthesis of poly(norbornene-*alt*-maleic anhydride-*co*-acrylic acid-*co*-*tert*-butyl acrylate) materials, which incorporated both acrylic acid and *t*-butyl acrylate into the same norbornene/maleic anhydride alternating copolymer (Figure 2.13).[132] They reported that lithographic evaluation of the materials showed potential for use as 193 nm resist materials.

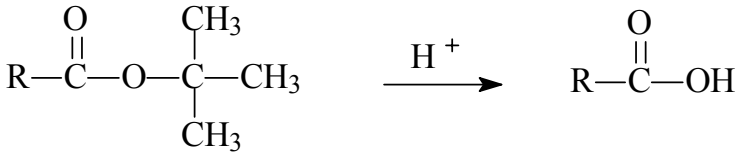

Scheme 2.15 Acid catalyzed hydrolysis of *tert*-butyl ester functionality.

[131] Houlihan, F. M.; Wallow, T. I.; Nalamasu, O.; Reichmanis, E. *Macromolecules* **1997**, *30*, 6517.
[132] Nalamasu, O.; Houlihan, R. A.; Cirelli, A. G.; Watson, G. P.; Hutton, R. S.; Kometani, J. M.; Reichmanis, E. *J. Vac. Sci. Technol., B* **1998**, *16*, 3716. Wallow, T. I.; Houlihan, F. M.; Nalamasu, O.; Chandross, E. A. Neenan, T. X.; Reichmanis, E. *Proc. SPIE-Int. Soc. Opt. Eng.* **1996**, *2724*, 355. Gabor, A. H.; Dimov, O.; Medina, A. N.; Bowden, M. J.; Neisser, M. O.; Houlihan, F. M.; Cirelli, R. A.; Dabbagh, G.; Hutton, R. S.; Rushkin, I. L.; Sweeney, J. R.; Nalamasu, O.; Reichmanis, E. *Polym. Mat. Sci. Eng.* **1999**, *81*, 41.

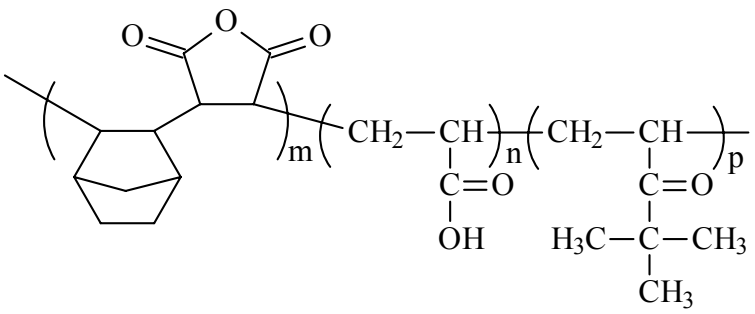

Figure 2.13 Poly(norbornene-*alt*-maleic anhydride-*co*-acrylic acid-*co*-*tert*-butyl acrylate).

Willson and coworkers at the University of Texas have focused upon the synthesis of cycloaliphatic co- and terpolymers using Pd(II) metal catalyzed polymerization, ring opening metathesis polymerization (ROMP), and free radical copolymerization with maleic anhydride (Scheme 2.16).[133] In conjunction with workers from IBM, they reported that polymers made up solely of cycloaliphatics, which were prepared via Pd(II) catalyzed addition polymerization, exhibited excellent image contrast. However, these materials showed cracking and poor adhesion to silicon substrates at low dimensions (< 0.6 μm).

[133] Okoroanyanwu, U.; Byers, J.; Shimokawa, T.; Willson, C. G. *Chem. Mater.* **1998**, *10*, 3328. Okoroanyanwu, U.; Shimokawa, T.; Byers, J.; Medeiros, D.; Willson, C. G.; Niu, Q, J.; Fréchet, J. M. J.; Allen, R. D. *Proc. SPIE-Int. Soc. Opt. Eng.* **1997**, *3049*, 92.

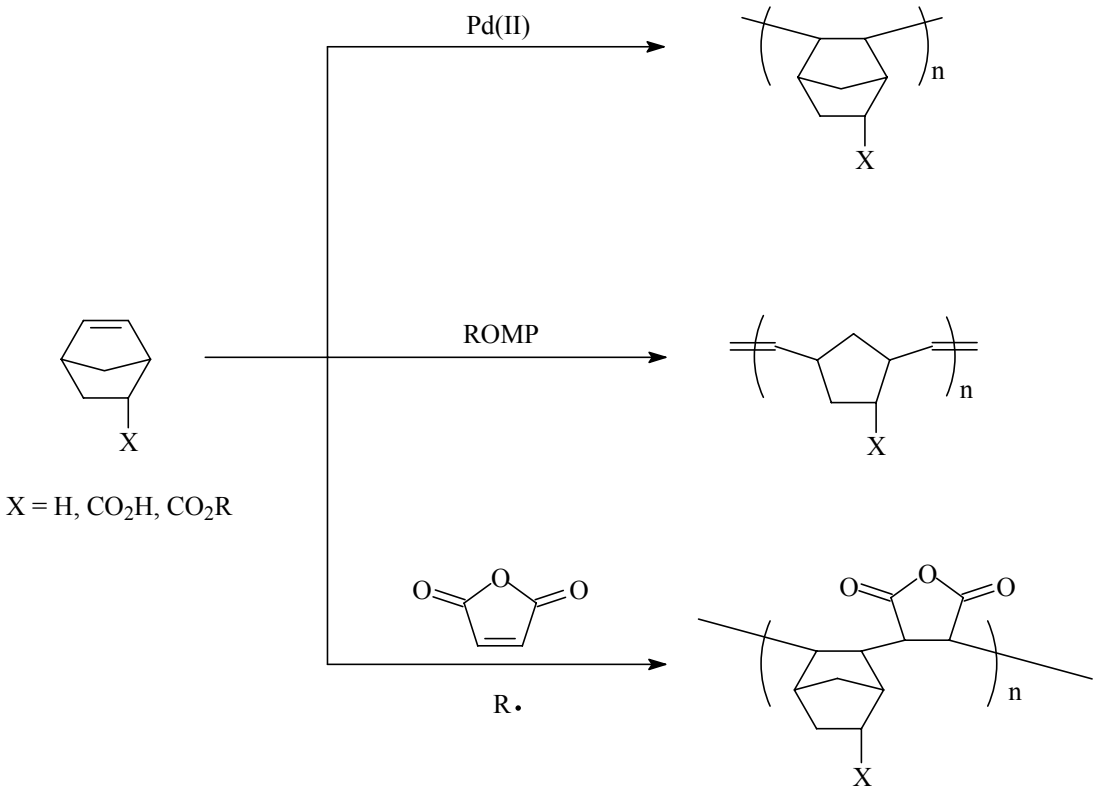

Scheme 2.16 Nb polymerization pathways for 193 nm photoresist materials.

The cracking and adhesion problem could be dramatically improved through incorporation of maleic anhydride, via free radical alternating copolymerization with the cycloaliphatic olefin monomers. In addition, excellent resolution (down to 0.16 μm) was achieved with the materials incorporating maleic anhydride. In addition to norbornene and norbornene derivatives, these workers have investigated the free radical alternating copolymerization of the tetracyclic monomer, *tert*-butyl tetracyclo[4.4.0.1.1]dodec-3-ene-8-carboxylate (DBNC) (Scheme 2.17).[134] While these materials demonstrated good lithographic performance and dry etch resistance, the post exposure delay stability

[134] Patterson, K.; Yamchika, M.; Cho, S.; Rager, T.; Yamada, S.; Byers, J.; Willson, C. G. *Polym. Mat. Sci. Eng.* **1999**, *81*, 43.

remained inadequate. The post exposure delay is the period between the exposure step (photogeneration of a strong acid) and the post exposure baking step (where the acid cleaves the *tert*-butyl esters to yield base soluble acid functionality). During the post exposure delay, any diffusion of the photogenerated acid to unexposed film area will alter the pattern, leading to undesirable variation in the final developed image. During the spin-coating process of the polymer films, free volume is created as solvent molecules quickly evaporate. The trapped free volume within the film allows for increase diffusion of small molecules, such as the photogenerated acid, resulting in decreased post exposure delay stability. Heating the polymer to near the glass transition temperature anneals the polymer, allowing the chains to relax and fill the free volume. However, poly(DBNC-*alt*-MAH) cannot be annealed, as the glass transition temperature of the material is greater than the decomposition temperature of the ester functional group. To address this issue, Willson and coworkers prepared a series of materials incorporating variations of the tetracyclic monomer with the general structure shown in Figure 2.14. The aliphatic groups that were incorporated act to plasticize the resulting polymers and effectively lower the glass transition temperature to allow for annealing, while retaining good lithographic performance and dry etch resistance.

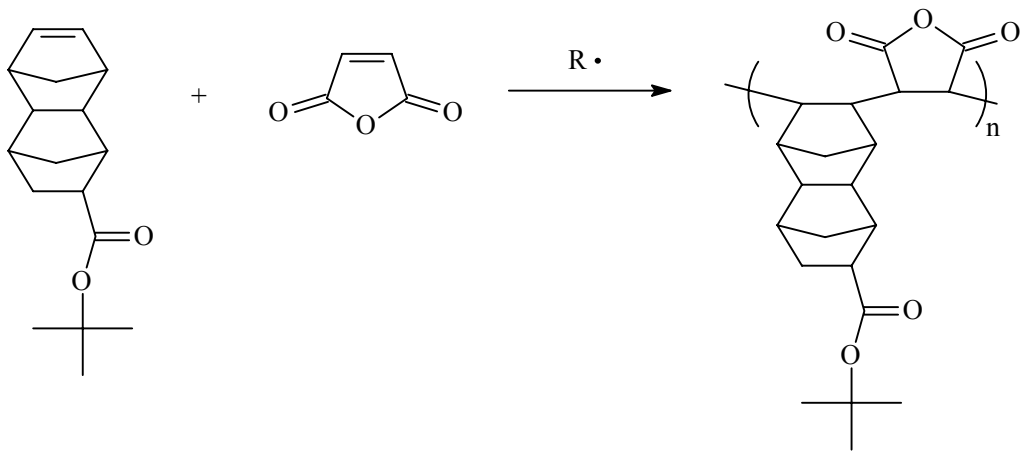

Scheme 2.17 Synthesis of poly(DBNC-*alt*-MAH) via free radical copolymerization.

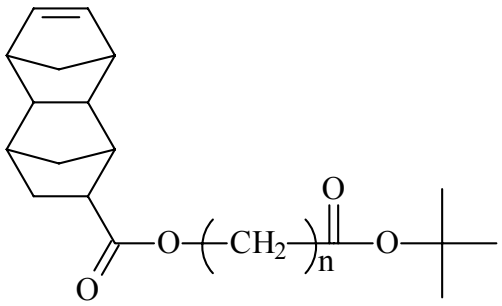

Figure 2.14 Annealable tetracyclic bi-norbornene monomer.

Workers at Hyundai have reported on the copolymerization maleic anhydride/cyclic olefins using substituted norbornenes with the goal of improving adhesion to Si substrates.[135] They first synthesized a polymer consisting of 2-(*tert*-butoxycarbonyl)-5norbornene (BNOR), 5-norbornene-2-carboxylic acid (NORA), and maleic anhydride (MAH). From evaluation of this material, they found that poor adhesion of the material to the silicon substrate was limiting its lithographic performance. To improve the adhesion of the photoresist to the silicon substrate, they introduced the polar monomer, 2-hydroxyethyl acrylate (HEA), into the material. The structure of the multi-component polymer made from HEA, BNOR, NORA, and MAH is illustrated in Figure 2.15. Each of the monomer units served a specific purpose to the lithographic performance of the material. The BNOR was introduced as a dissolution inhibitor, the NORA to increase sensitivity, and HEA to promote adhesion to the silicon substrate. They found that introduction of HEA greatly improved adhesion to the substrate and resulted in improved lithographic performance of the material. In a subsequent publication, the authors reported the synthesis of a similar material that included enhancements to the previously reported

[135] Lee, K. K.; Jung, J. C.; Jhon, M. S. *Polymer* **1998**, *39*, 4457. Jung, M. H.; Jung, J. C.; Lee, G.; Baik, K. H. *Jpn. J. Appl. Phys.* **1998**, *37*, 6888.

poly(HEA/BNOR/NORA/MAH).[136] To further improve the etch resistance, they substituted the hydrophilic monomer previously used, HEA, with 2-hydroxyethyl 5-norbornene-2-carboxylate (HNC), an alicyclic norbornene derivative containing a hydrophilic pendant functionality analogous to HEA. Furthermore, the NORA monomer, which was incorporated to increase sensitivity, was replaced with a dicarboxylic acid norbornene derivative, 5-norbornene-2,3-dicarboxylic acid (NDCA). Based upon their earlier experiments, they found that NORA exhibited a very strong odor and that there are problems with its treatment and preservation for large-scale production. Furthermore, NORA is synthesized from acrylic acid, which is also very malodorous and toxic. NDCA was found to be solid, nontoxic, and to have a long shelf life. Also beneficial was that NDCA could be synthesized via hydrolysis of the Diels-Alder product of cyclopentadiene and maleic anhydride. In addition, the two carboxylic acid functionalities provided for increased sensitivity and contrast than the NORA monoacid monomer. Lithographic evaluation demonstrated that the final material, poly(HNC/BNOR/NDCA/MAH) (Figure 2.16), exhibited excellent adhesion, etch resistance, sensitivity, resolution, and aqueous base development. These results were very promising and showed great potential for this material to be applied as a 193 nm resist material.

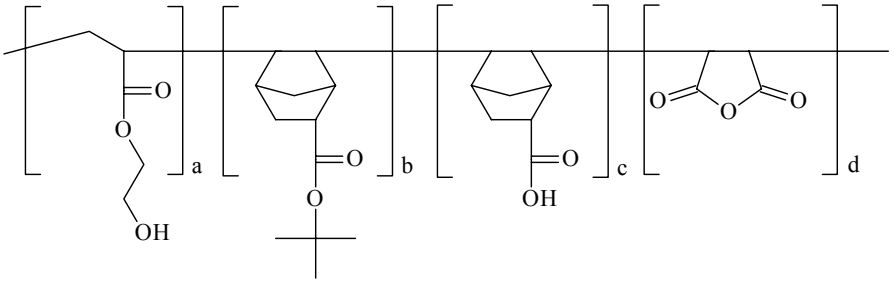

Figure 2.15 Poly(HEA/BNOR/NORA/MAH).

[136] Jung, M. H.; Jung, J. C.; Lee, G.; Baik, K. H. *Jpn. J. Appl. Phys.* **1998**, *37*, 6888.

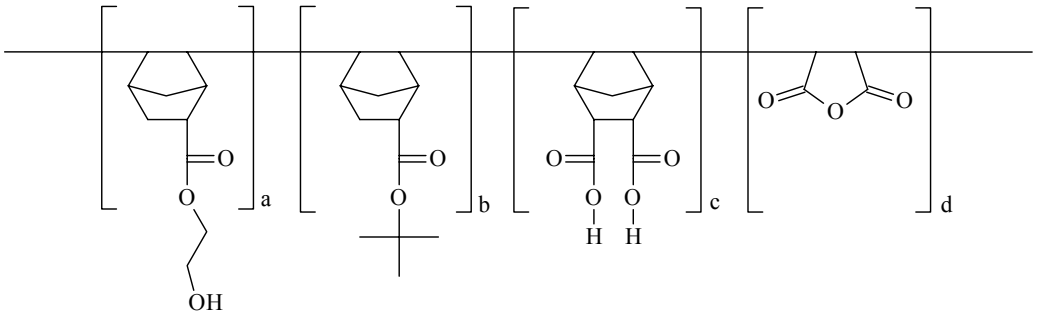

Figure 2.16 Poly(HNC/BNOR/NDCA/MAH).

2.5.3 New Directions for 157 nm Photoresist Polymers

Photolithography using 157 nm F_2 lasers represents the next generation in microlithography. The initial requirements for 157 nm photoresist polymer materials are that they must be capable of 100 nm resolution and be extendable to less than 70 nm.[137] As has been the case with other transitions to shorter wavelengths, the photoresist polymers that have been developed previously for 248 and 193 nm resist platforms are not transparent enough when imaged with 157 nm light for practical use in traditional single layer resists.[138] Recently, fluoropolymers and siloxane-based polymers have emerged as leading candidates towards highly transparent 157 nm photoresist materials due to their high transparency at 157 nm and the ability to achieve base solubility through modification of the polymers. For example, Ober and coworkers have recently reported on the synthesis

---

[137] Bloomstein, T. M.; Rothschild, M.; Kunz, R. R.; Hardy, D. E.; Goodman, R. B.; Palmacci, S. T. *J. Vac. Sci. Technol. B* **1999**, *16*, 3154.
[138] Kunz, R. R.; Bloomstein, T. M.; Hardy, D. E.; Goodman, R. B.; Downs, D. K.; Curtin, J. E. *J. Vac. Sci. Technol. B* **1999**, *17*, 1999.

of fluorocarbinol-containing acrylic copolymers with high transparency at 157 nm (Scheme 2.18).[139]

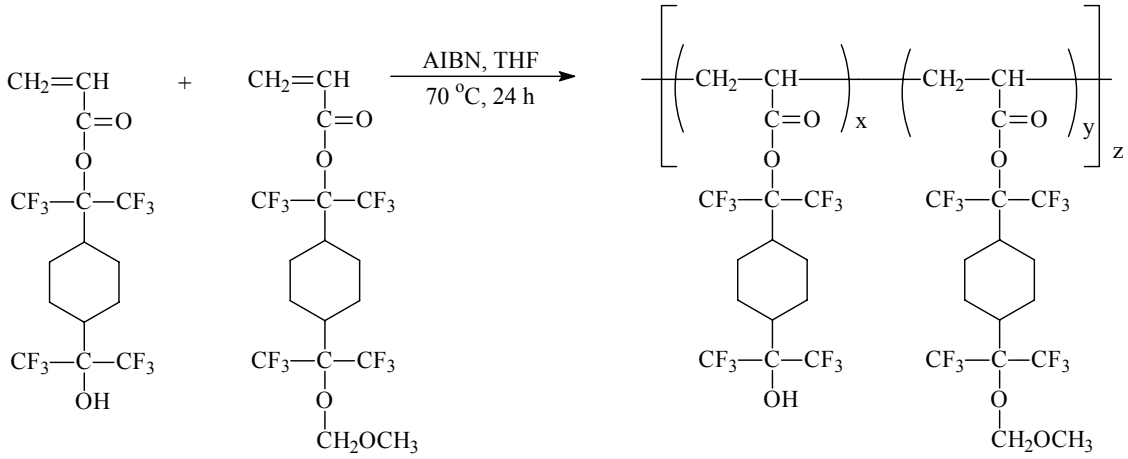

Scheme 2.18 Fluorocarbinol containing acrylic copolymers for 157 nm lithography.

[139] Bae, Y. C.; Ober, C. K. *Polymer Preprints* **2002**, *42*(2), 403.

2.6 EXPANDABLE MICROSPHERES VIA FREE RADICAL SUSPENSION COPOLYMERIZATION

Expandable thermoplastic microspheres have been commercially produced for several years. Thermoplastic microspheres were first described in US Patent 3,615,972[140] and later by others.[141] They are produced by suspension (bead) polymerization where a liquid monomer or comonomer mixture containing a low boiling organic solvent and cross-linkable monomer is dispersed in an aqueous medium containing a suspending agent (Scheme 2.19). As the polymerization proceeds, the low boiling solvent acts as a solvent for the monomer and a non-solvent for the forming cross-linked polymer. The forming polymer network migrates to the oil/water interface and encapsulates the organic expanding agent. The resulting structure of the microsphere consists of a polymer shell containing the liquid, volatile propellant (Figure 2.17). The spheres expand by heating to a temperature above the boiling point of the propellant and the softening point of the polymer.

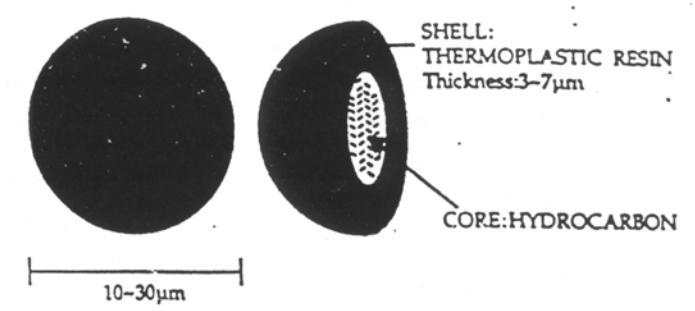

Figure 2.17 Expandable microsphere diagram.

---

[140] Morehouse, D. S. Jr. Expansible thermoplastic polymer particles containing volatile fluid foaming agent and method of foaming the same. U.S. Patent 3,615,972, October 26, 1971.

[141] Lundqvist, J. Expandable thermoplastic microspheres and a method for the production and use thereof. Eur. Patent EP 0 486 080, January 31, 1991. Sueo Kida, K.; Kenichi Kitano, O.; Kyuno Seiji, I. Thermoexpandable microcapsule and production. U.S. Patent 5,536,756, July 16, 1996.

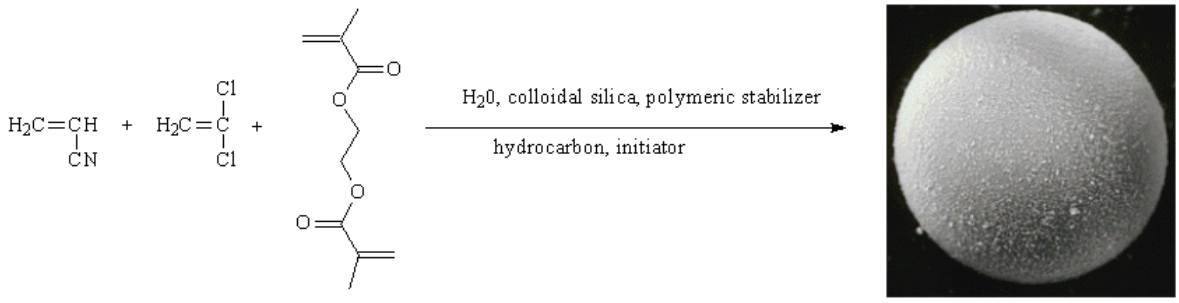

Scheme 2.19 Suspension free radical copolymerization of expandable microsphere.

The thermoplastic shell of the spheres may consist of polymers or copolymers of vinyl chloride, vinylidene chloride, acrylonitrile, methacrylonitrile, methyl methacrylate and styrene. The particle size of the unexpanded and expanded spheres may vary within wide limits. The particle size of the unexpanded spheres may be 1 μm to 1 mm, but is more typically 5 μm to 50 μm. Upon expansion, the diameter of the microspheres can increase by as much as a factor of 5. A diagram of showing the idealized expansion mechanism is shown in (Figure 2.18). As the softening temperature of the microsphere is reached, it begins to expand due to the internal pressure of the volatile organic propellant. The propellant then begins to leak through voids in the shell that are created as the shell expands. Once the propellant has completely egressed and the internal and external pressures have equalized, the shell contracts to its final shape. The desired propellant is typically a low boiling hydrocarbon such as n-pentane, isopentane, neopentane, butane, isobutene, hexane, etc. The propellant typically makes up 5-30 % by weight of the microspheres. An example commercial product is Expancel® (Casco Nobel), which has a thermoplastic shell made up of vinylidene chloride/acrylonitrile copolymer and contains isobutene propellant.

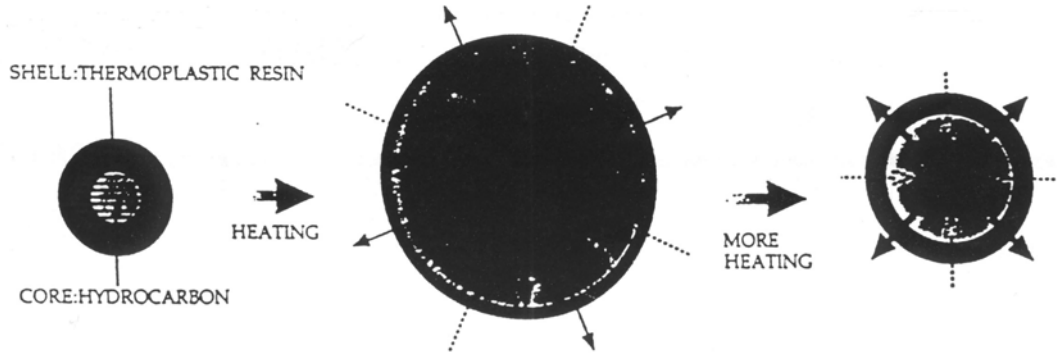

Figure 2.18 Microsphere expansion mechanism.

Thermoplastic expandable microspheres have several desirable properties including weight reduction, lower volume cost, and lower VOC emissions in fiber reinforced polyester (FRP) applications. These properties make them very attractive for a wide variety of industrial applications such as FRP products (bathtubs, showers, spas, architectural columns, etc.), expandable printing ink, moldable plastics, PVC foam, paint, and automotive underbody coatings.[142]

[142] Pierce & Stevens Dualite Homepage. http://www.piercestevens.com/dualite.htm (accessed March 2002).

2.7 REAL-TIME MONITORING OF POLYMERIZATION PROCESSES VIA *IN SITU* FTIR SPECTROSCOPY

2.7.1 Introduction

Polymerization reaction data is traditionally obtained by careful sampling techniques followed by gravimetric and molecular weight analysis. Alternatively, samples can be withdrawn from the reactor and analyzed for residual monomer in solution at various times by chromatographic or spectroscopic techniques. Sample removal techniques can be very difficult, especially since many reactions are extremely sensitive to oxygen and other impurities that can be introduced during sampling. *In situ* infrared spectroscopy is a state-of-the-art, real-time, monitoring technique that is well suited to obtain real-time structural and kinetic information of polymerization processes without sampling. In addition, reactions are analyzed without complicated reactor modifications or expensive deuterated monomers.

Advantages of *in situ* reaction monitoring include evaluating reaction variables for the determination of reaction performance and optimization of reaction conditions, analyzing reactions that use hazardous or air-sensitive reagents, and elimination of experimental uncertainties associated with reactor sampling. Furthermore, *in situ* monitoring provides for the following of instantaneous changes in reactants, intermediates, and products, essentially allowing one to "watch" a reaction as it proceeds. This allows for the facile tracking of reaction trends, concentration changes, reaction end-points, and percent conversions for a wide range of reactions. Kinetic information can easily be obtained and evaluated from the concentration monitoring of key reaction components. Deleterious side reactions can be followed and evaluated. In addition, the time normally required to acquire analytical results is minimized and the data is more comprehensive (*i.e.* more data points). All of the information of a reaction obtained by *in situ* monitoring can be combined and evaluated to provide an in-depth understanding of reaction pathways.

2.7.2 Near-Infrared (NIR) Investigations

Living polymerization processes permit the synthesis of well-defined macromolecules with controlled chemical composition, predictable molecular weight, and narrow molecular weight distribution.[143] Long and coworkers have described the utility of *in situ* near-infrared spectroscopy for the analysis of well established living anionic polymerizations in various organic solvents and at various polymerization conditions.[144] These initial investigations served as a demonstration of the applicability of *in situ* near-infrared spectroscopy. Scheme 2.20 depicts the living anionic polymerization of a mixed monomer system, i.e. styrene and para-substituted styrenes (where R = $Si(CH_3)_2C(CH_3)_3$), in a polar solvent. Despite the insertion of the near-infrared probe, the living nature of the anionic propagating intermediate was not affected as evidenced by the preservation of a narrow molecular weight distribution and predictable molecular weight (as determined using GPC). These block copolymers were routinely prepared in one-step, and exhibited characteristic two-phase morphologies and thermal properties. The ability to form a diblock copolymer in only one-step has important implications in the industrial arena. This one-step block copolymer formation relies on controlling the electron density and relative reactivities of the unsaturated sites. In addition, first-order polymerization kinetics were determined for each monomer homopolymerization as expected based on many earlier comprehensive studies using more complicated analyses.[145] Figure 2.19 illustrates the potential rate of *in situ* data acquisition at a single near-infrared wavelength.

---

[143] Hogen-Esch, T. E.; Smid, J. In *Recent Advances in Anionic Polymerization*, Elsevier, New York, 1987. *Anionic Polymerization: Kinetics, Mechanisms, and Synthesis*; McGrath, J. E., Ed.; ACS Symposium Series 166; American Chemical Society: Washington, DC, 1981.
[144] Long, T. E.; Liu, H. Y.; Schell, B. A.; Teegarden, D. M. *Macromolecules* **1993**, *26*, 6237.
[145] Ishizone, T.; Ohnuma, K.; Okazawa, Y.; Hirao, A.; Nakahama, S. *Macromolecules* **1998**, *31*, 2797. Maurer, A.; Marcarian, X.; Mueller, A. H. E.; Navarro, C.; Vuillemin, B. *Polym. Prepr.* **1997**, *38*, 467 (1997).

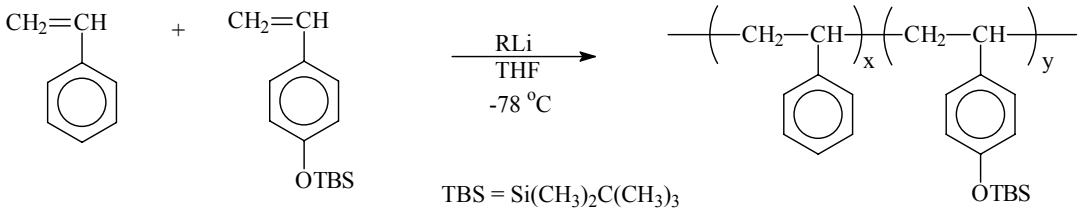

Scheme 2.20 Mixed-Monomers for the one-step synthesis of block copolymers.

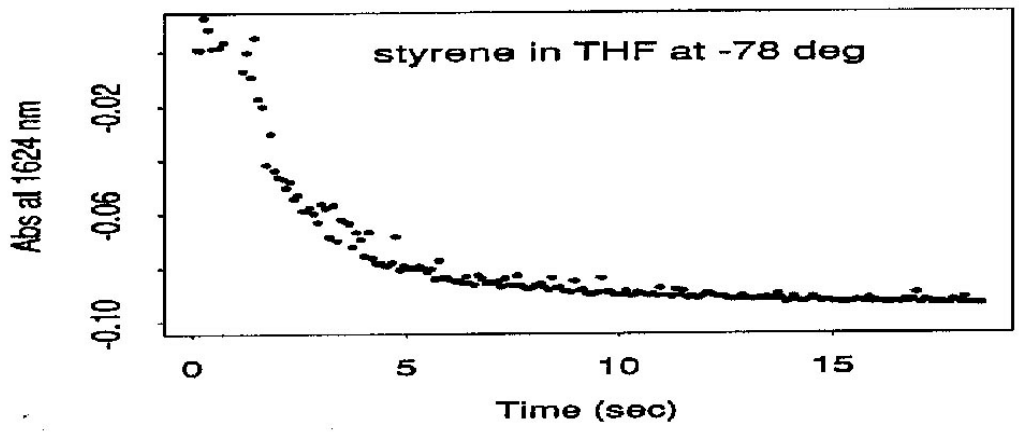

Figure 2.19 Absorbance at 1624 nm (NIR) vs. Time for a styrene polymerization in THF at –78 ºC.

The NIR *in situ* process also allowed for the determination of intermediate sequence distribution in styrene/isoprene copolymers, poly(diene) stereochemistry quantification, and identification of complete monomer conversion. The classic one-step, anionic, tapered block copolymerization of isoprene and styrene in hydrocarbon solvents is shown in Scheme 2.21. The ultimate sequence distribution is defined using four rate constants involving the two monomers. NIR was successfully utilized to monitor monomer conversion during conventional, anionic solution polymerization.[145] The conversion of the

vinyl protons in the monomer to methylene protons in the polymer was easily monitored under conventional (10-20% solids) solution polymerization conditions. Despite the presence of the NIR probe, the "living" nature of the polymerizations was maintained in all cases. Both styrene and isoprene polymerization kinetics were investigated in nonpolar and polar solvents, and relative rate constants were compared to values previously reported in the literature. In addition to the requirement for an inert probe, high sampling frequencies were required since polymerization times ranged from 5 s in tetrahydrofuran to 20 min in cyclohexane. Figure 2.20 depicts the monomers and near-infrared spectra for a mixed styrene and isoprene anionic polymerization as a function of time, and the inflection point was consistent with sequence tapering. The residual absorbance at 1.67 microns indicates the presence of residual pendant unsaturated sites.

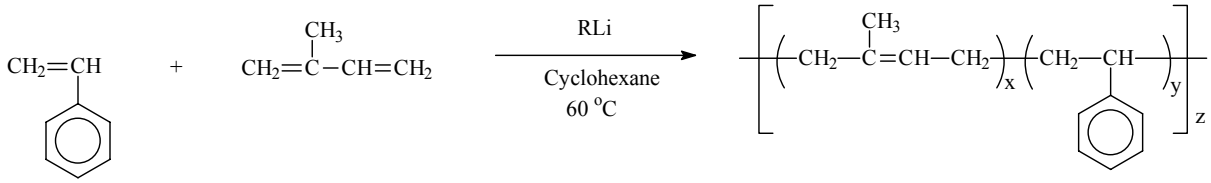

Scheme 2.21 Living anionic polymerization of one-step tapered block copolymers.

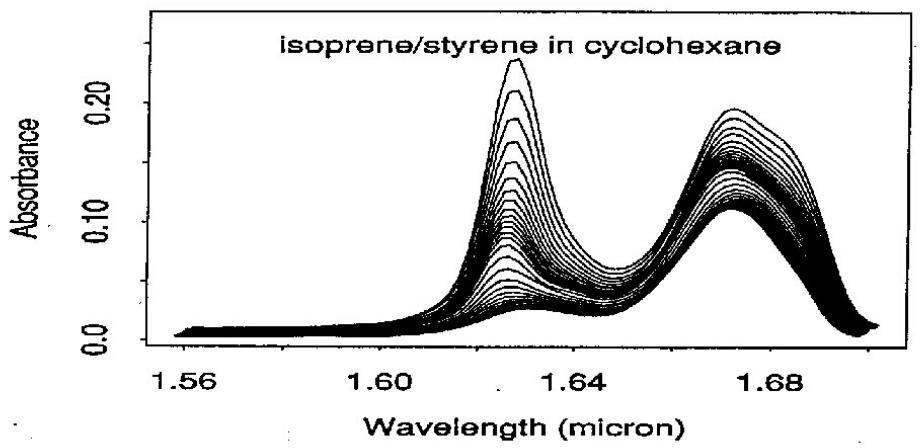

Figure 2.20 Mixed isoprene-styrene copolymerization: near-infrared spectra vs. time.

2.7.3 Cyclohexadiene Anionic Polymerization

Various polymerization techniques were utilized in the mid-1960's and early 1970's in an attempt to find a viable polymerization methodology for 1,3-cyclohexadiene.[146] In addition, in the late 1970's a series of patents were issued to Phillips Petroleum that described the process and composition of 1,3-cyclohexadiene containing polymers.[147] The effects of various ligating agents on the resulting composition were also investigated. The ligating agents investigated were TMEDA, dimethoxyethane (DME), and tetrahydrofuran (THF). The compositions were limited to "random" copolymers containing poly(1,3-cyclohexadiene), poly(styrene), poly(isoprene), or poly(butadiene) and prepared using

---

[146] Sharaby, Z.; Jagur-Grodzinski, J.; Martan, M.; Vofsi, D. *Journal of Polymer Science: Part A* **1982**, *20*, 901. Lefebvre, G.; Dawans, F. *Journal of Polymer Science Polymer Chemistry* **1964**, *A2*, 3277. Sharaby, Z.; Martan, M.; Jagur-Grodzinski, J. *Macromolecules* **1982**, *15*, 1167. Mango, L. A.; Lenz, R. W. *Polymer Preprints* **1972**, *12*, 402.

[147] Hsieh, H. L., Phillips Petroleum Co. U.S. Patent 4127710, 1980. Hsieh, H. L., Phillips Petroleum Co. U.S. Patent 4131653, 1979. Hsieh, H. L., Phillips Petroleum Co. U. S. Patent 4020251, 1978. Hsieh, H. L., Phillips Petroleum Co. U. S. Patent 4138356, 1978. Hsieh, H. L., Phillips Petroleum Co. U. S. Patent 4237246, 1977.

various ligating agents. Despite these early attempts to polymerize 1,3-cyclohexadiene in a controlled fashion, the resulting polymers exhibited unpredictable molecular weights and broad molecular weight distributions. Natori and coworkers recently reported the successful living anionic polymerization of 1,3-cyclohexadiene utilizing n-butyllithium (nBuLi) in combination with a single ligation agent (tetramethylethylene diamine (TMEDA)).[148] The resulting homopolymers exhibited relatively narrow molecular weight distributions and modest molecular weights. In addition to the elucidation of the relative reactivities of the monomer pairs, they have also reported the synthesis of di- and tri-block copolymers composed of various combinations of styrene, butadiene, and isoprene.[149]

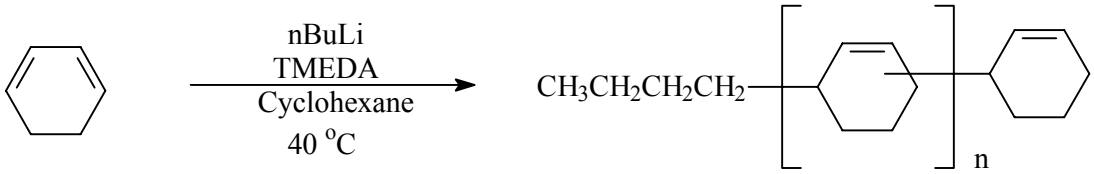

Scheme 2.22 Living anionic polymerization of 1,3-cyclohexadiene.

Recently, Williamson and coworkers have reported the use of *in situ* mid-infrared spectroscopy to monitor the anionic synthesis of a 5000 g/mol poly(1,3-cyclohexadiene) homopolymer (Scheme 2.22).[150] The resulting polymer was characterized using GPC and found to be a single peak with a molecular weight of 5,200 g/mol and a molecular weight distribution of 1.01. *In situ* near-FTIR spectroscopy has been previously employed for determination of the kinetics of the anionic homopolymerization of styrene and isoprene.[151] However, this was the first reported use of *in situ* mid-FTIR spectroscopy to

---

[148] Natori, I. *Macromolecules* **1997**, *30*, 3696.
[149] Natori, I.; Inoue, S. *Macromolecules* **1998**, *1998*, 982. Natori, I.; Inoue, S. *Macromolecules* **1998**, *31*, 4687.
[150] Williamson, D. T.; Elman, J. F.; Madison, P. H.; Pasquale, A. J.; Long, T. E. *Macromolecules*, **2001**, *34*, 2108.
[151] Long, T. E.; Liu, H. Y.; Schell, B. A.; Teegarden, D. M. *Macromolecules* **1993**, *26*, 6237.

study the kinetics of a living anionic polymerization. The monomer and polymer peaks in the spectrum must be clearly resolved as shown in Figure 2.21 in order to ensure accurate analysis. The decrease in the absorbance of the monomer peak found at 657 cm^{-1} and the increase in the absorbance of the polymer peak at 703 cm^{-1} resulting from the out of plane bending vibration of the carbon to hydrogen bond of the alkene are shown in Figure 2.21. The polymer was synthesized using a 10 wt. % monomer/cyclohexane solution at 40 °C using the TMEDA/nBuLi ratio of 5/4. The polymerization was then initiated with nBuLi and the solution became heterogeneous within five minutes. Despite the heterogeneity of the polymerization solution, molecular weights are predictable and molecular weight distributions are relatively narrow. Figure 2.22 is a waterfall plot of the polymerization indicating that complete conversion of the monomer occurred within 13 minutes. The polymerization kinetics did not change as the polymerization proceeded from a homogenous solution to a heterogeneous solution as is shown in Figure 2.22. Due to the excellent resolution of both the monomer and polymer absorbances, the spectral data was utilized in the generation of a pseudo first order kinetic plot with monomer concentration plotted against time as shown in Figure 2.23. The calculated rate constant for propagation was 0.31 L/mol·s. Values for the polymerization rate constant of an anionic polymerization are dependant upon the temperature, monomer concentration, and the presence of additives.[152] An understanding of the propagation rate facilitated the minimization of any termination/transfer steps occurring after quantitative polymerization of 1,3-cyclohexadiene monomer.

---

[152] *Anionic Polymerization: Kinetics, Mechanisms, and Synthesis*; McGrath, J. E., Ed.; ACS Symposium Series 166; American Chemical Society: Washington, DC, 1981.

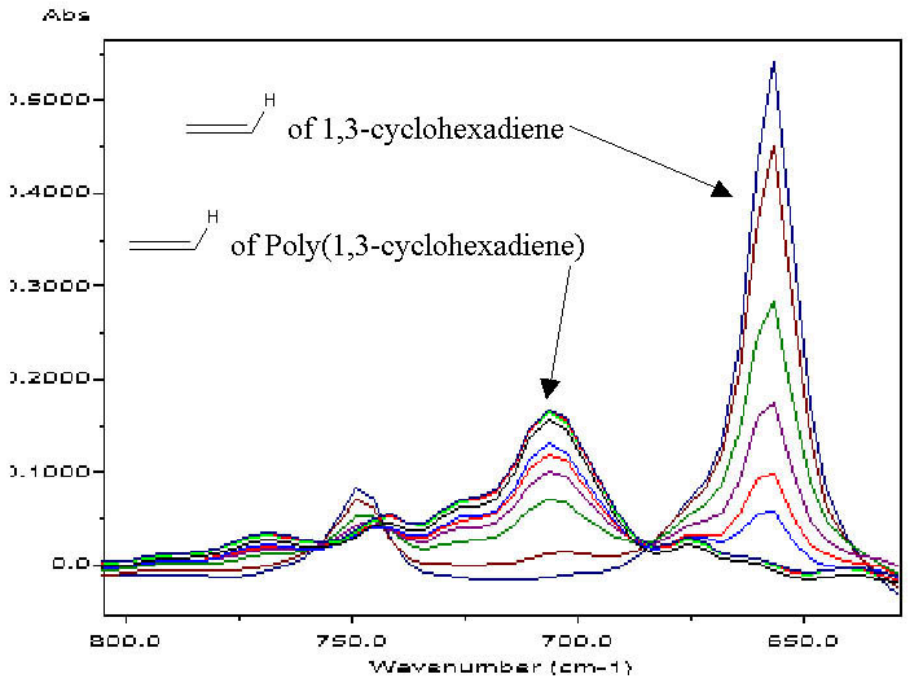

Figure 2.21 *In situ* FTIR spectra illustrating the disappearance of the monomer absorption at 657 cm^{-1} and simultaneous polymer absorption increase at 703 cm^{-1}.

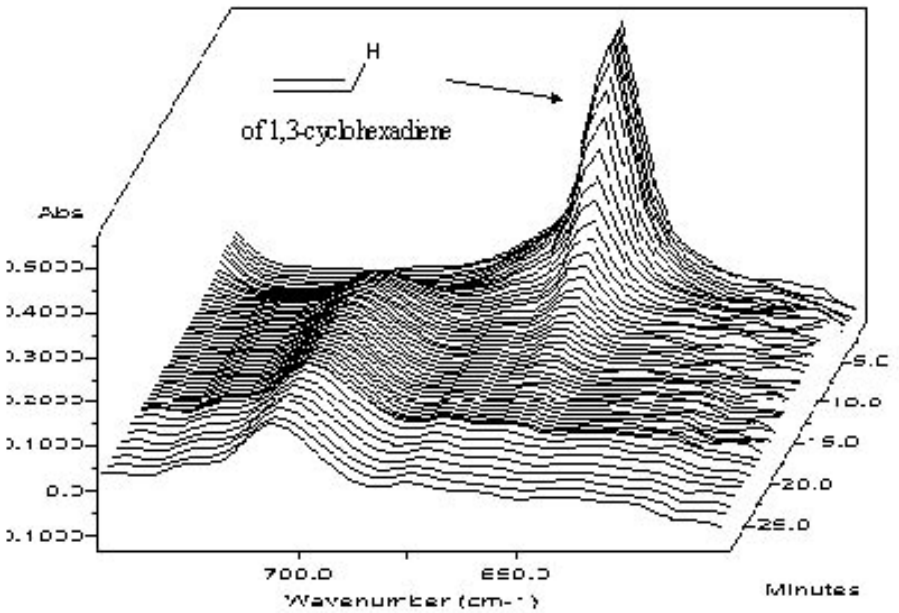

Figure 2.22 *In situ* FTIR "waterfall" plot of 1,3-cyclohexadiene living anionic polymerization.

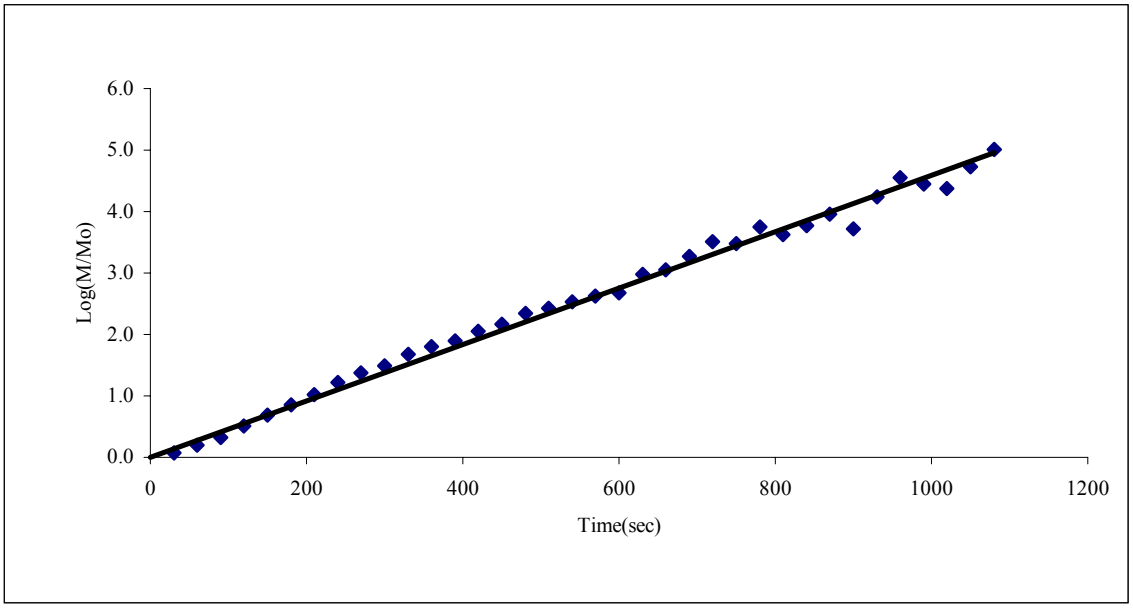

Figure 2.23 Psuedo first order kinetic plot of 1,3-cyclohexadiene living anionic polymerization.

2.7.4 Nitroxide Mediated Stable Free Radical Polymerization

Control of chain-growth polymer architecture has been traditionally achieved using living anionic,[152] cationic,[153] or group transfer[154] polymerization procedures. Synthetic methodologies for controlled polymerization have been expanded with recent developments in both stable free radical polymerization (SFRP)[155] and atom transfer radical polymerization (ATRP).[156] Based on the earlier work of Rizzardo et al.[157] in

[153] Matyjaszewski, K. *Cationic Polymerizations: Mechanisms, Synthesis and Applications*; Marcel Deker: New York, 1996.
[154] Sogah, D. Y.; Hertler, W. R.; Webster, O. W.; Cohen, G. M. *Macromolecules* **1987**, *20*, 1473.
[155] Hawker, C. J. *ACC. Chem. Res.* **1997**, *30*, 373.
[156] Patten, T. E.; Matyjaszewki, K. *Adv. Mater.* **1998**, *10*, 901.
[157] Moad, G.; Rizzardo, E.; Solomon, D. H. *Macromolecules* **1982**, *15*, 909.

nitroxide mediated stable free radical polymerization, Georges et al.[158] first reported the preparation of polystyrene with low polydispersity using bulk free radical polymerization of styrene initiated by a conventional free radical initiator, benzoyl peroxide (BPO), in the presence of the stable nitroxide free radical, 2,2,6,6-tetramethyl-1-piperidinyloxy (TEMPO) at 125 °C. The SFRP process involves a desirable equilibrium between nitroxide capped polymer chains and uncapped polymer radicals. The uncapped polymer radicals are then able to chain extend via styrene monomer addition (Scheme 2.23). The success of this method arises from the unique feature that the nitroxide radicals will react with carbon radicals at near diffusion controlled rates, but will not react with other oxygen centered radicals or initiate additional polymer chains. An indication of the controlled nature of the SFRP of styrene is typically accomplished by the demonstration of a linear increase in molecular weight with conversion.[159] Kinetic information is commonly obtained by withdrawing samples and analyzing for residual monomer with gravimetric and chromatographic methods.[160] In addition, more sophisticated analytical methods have recently been applied to study SFRP kinetics. For example, Georges et al. have utilized *in situ* ESR spectroscopy to study the SFRP process,[161] and Hawker et al. have applied ^{1}H NMR to evaluate initiator efficiency for SFRP processes using deuterated styrene.[162]

---

[158] Georges, M. K.; Veregin, R. P. N.; Kazmaier, P. M.; Hamer, G. K. *Macromolecules* **1993**, *26*, 2987.
[159] Hawker, C. J. *J. Am. Chem. Soc.* **1994**, *116*, 11185.
[160] Veregin, R. P. N.; Odell, P. G.; Michalak, L. M.; Georges, M. K. *Macromolecules* **1996**, *29*, 2746.
[161] Veregin, R. P. N.; Georges, M. K.; Kazmaier, P. M.; Hamer, G. K. *Macromolecules* **1993**, *26*, 5316. Veregin, R. P. N.; Odell, P. G.; Michalak, L. M.; Georges, M. K. *Macromolecules* **1996**, *29*, 4161. MacLeod, P. J.; Veregin, R. P. N.; Odell, P. G.; Georges, M. K. *Macromolecules* **1998**, *31*, 530. Moffat, K. A.; Hamer, G. K.; Georges, M. K. *Macromolecules* **1999**, *32*, 1004.
[162] Hawker, C. J.; Barclay, G. G.; Orellana, A.; Dao, J.; Devonport, W. *Macromolecules* **1996**, *29*, 5245.

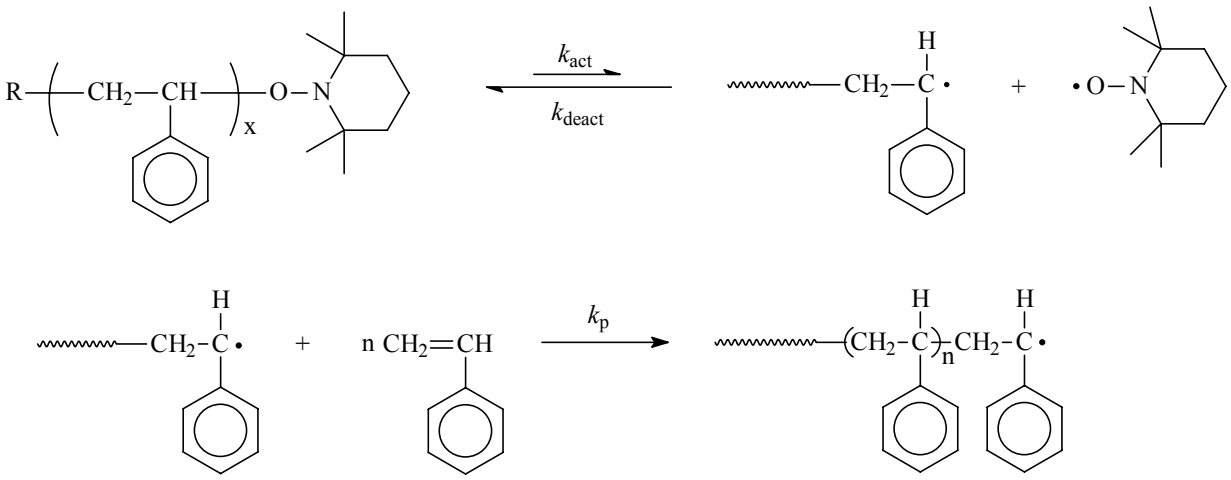

Scheme 2.23 Styrene stable free radical polymerization (SFRP) scheme.

In situ mid-infrared spectroscopy was used to monitor the bulk SFRP reaction of styrene (Aldrich, vacuum distilled from calcium hydride) initiated by BPO (Aldrich, used as received) in the presence of TEMPO (Aldrich, used as received). An example procedure for the polymerization at 132 °C is as follows. The reaction was carried out in a 100 mL, round-bottomed, 2-necked flask that was fitted with the DiComp probe. To the flask was added a magnetic stir bar, 35 mL of styrene (350 mmoles), and 0.368 g of TEMPO (2.36 mmoles). Although a magnetic stir bar did not provide adequate agitation at higher conversions due to the extremely high bulk viscosity, it facilitated the intimate contact of the reaction mixture with the probe tip and reduced the likelihood of spurious oxygen ingress. The flask was sealed under nitrogen with a rubber septum and a thermocouple was inserted through the septum to simultaneously monitor the temperature of the reaction mixture. The ReactIR 1000 was programmed to collect spectra every minute for the first 90 minutes and then every 5 minutes for the remaining 24 hours. An oil bath at 142 °C was raised to the reaction flask and IR data acquisition was initiated. After several minutes the temperature of the styrene/TEMPO solution in the reaction flask stabilized at 132 °C (the large temperature difference between the oil bath and reaction

mixture is speculated to be due to the heat loss due to the stainless steel DiComp probe). Infrared analysis indicated that the styrene/TEMPO solution was stable in the absence of benzoyl peroxide and appreciable thermal polymerization was not observed during this short period. After the temperature of the reaction stabilized at 132 °C, a solution of 0.440 g BPO (1.818 mmoles) dissolved in 5 mL of styrene was added via syringe. After 14 h the viscosity of the reaction increased dramatically and stirring stopped due to the high bulk viscosity. In addition, the infrared absorbances associated with the styrene monomer stabilized and stopped decreasing. The polymer product was cooled to room temperature, dissolved in chloroform, precipitated into methanol, and dried overnight under vacuum to yield 30.54 g (84% conversion) TEMPO-terminated polystyrene of M_n = 20,600 (M_w/M_n = 1.04) determined by size exclusion chromatography (Waters GPC with external 410 RI detector and Viscotek 150R viscometer, NMP/ P_2O_5 (0.02 M) solvent at 60 °C and 1.0 mL/min flow rate). Styrene polymerization at 126 °C yielded 26.6 g (73.2% conversion) TEMPO-terminated polystyrene of M_n = 18,000 (M_w/M_n = 1.04) after a reaction time of 16 h. NMR analysis of the vacuum dried TEMPO-terminated polystyrenes indicated the absence of appreciable residual monomer and/or precipitation solvent. The reproducibly low molecular weight distributions were indicative that the presence of the probe did not adversely affect the controlled polymerization process. In order to eliminate concerns associated with the polymer isolation process, samples were directly removed from the reaction mixture, dried to a constant weight, and analyzed using size exclusion chromatography. In all cases, the molecular weight distributions obtained using the NMP/ P_2O_5 (0.02 M) solvent system exhibited M_w/M_n values ranging from 1.04 to 1.09.

Styrene monomer exhibited two strong infrared absorbances that were easily monitored. The ReactIR 1000 with light conduit technology allowed for the generation of real-time mid-IR spectra from 4000 cm^{-1} to 650 cm^{-1}. "Waterfall" plots of the C=C (1628 cm^{-1}) and $=CH_2$ (907 cm^{-1}) absorbances for styrene polymerization at 132 °C are shown in Figure 2.24. Both monomer and polymer infrared absorbances were analyzed to produce a symmetrical x-shaped plot, which is characteristic of a controlled polymerization process such as SFRP. The x-plot produced from three alkyl C-H absorbances (2925, 2929, and

3028 cm^{-1}), exhibited by the forming polymer, and the two vinyl absorbances (907 and 1628 cm^{-1}), exhibited by the disappearing monomer, for the polymerization at 132 °C is shown in Figure 2.25. The absorbance peak height (y-axis) was auto-scaled so that the relative changes in each of the monitored absorbances were directly comparable. As one can see, the profiles for the three polymer alkyl absorbances as well as the two monomer vinyl absorbances overlap and agree favorably with each other as expected for a controlled polymerization process.

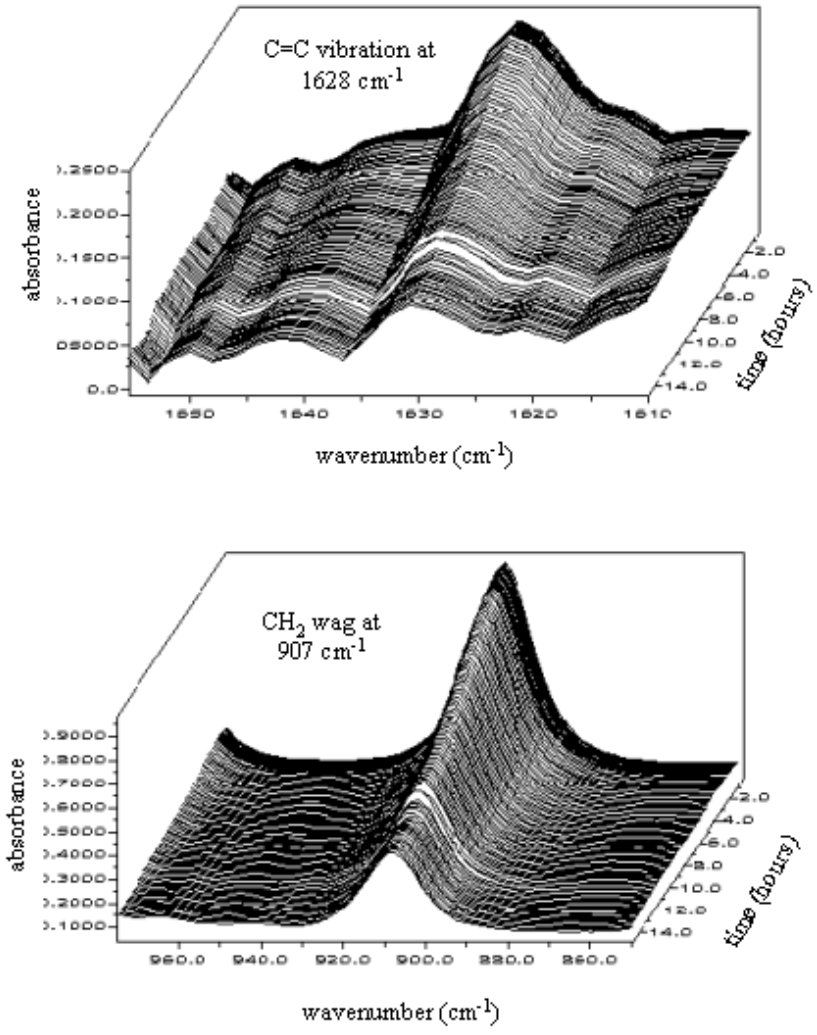

Figure 2.24 Real-time FTIR "waterfall" plots of styrene monomer: C=C stretch at 1628 cm^{-1} (top) and $=CH_2$ wag at 907 cm^{-1} (bottom).

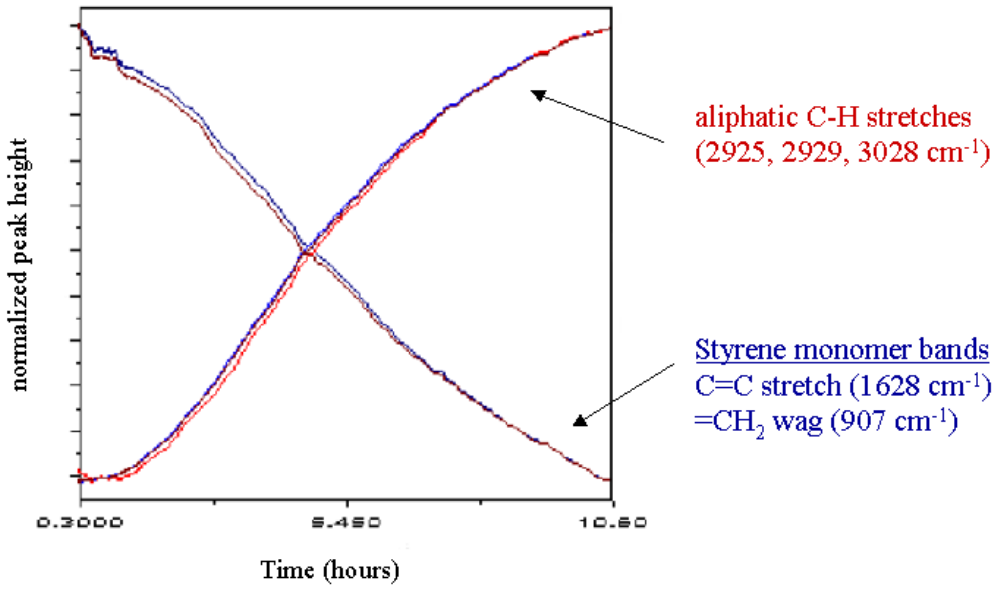

Figure 2.25 Real-time profiles of increasing alkyl C-H polymer peak heights (2925, 2929, and 3028 cm^{-1}) and decreasing vinyl monomer peak heights (907 and 1628 cm^{-1}).

To demonstrate the sensitivity of this technique, the initiation step of the polymerization was monitored by profiling the initiator, BPO, as well as the ester end group that is formed from addition of the initiating radical to one styrene monomer. The profiles of two BPO absorbances, C=O (1767 cm^{-1}) and C-O-C (1223 cm^{-1}), were compared with two polymer ester end group absorbances, C=O (1725 cm^{-1}) and C-O-C (1268 cm^{-1}), and are shown in Figure 2.26. The absorbance peak heights (y-axis) were again auto-scaled to allow for visual comparison. After an elapsed time of 29 minutes and 9 seconds of data collection, the BPO/styrene solution was added to the TEMPO/styrene solution at 132 °C. The BPO absorbances appeared after addition of the BPO to the reaction and then rapidly decayed completely. From the profile of BPO decay, the half-life of BPO in the presence of styrene and TEMPO at 132 °C was estimated to be approximately 50 seconds. In addition, during the same time period as the BPO decay, the formation of the ester polymer end groups was observed as the initiating radicals added to

styrene monomer. The ester end group absorbances at 1725 cm^{-1} and 1268 cm^{-1} increased upon BPO addition and leveled upon complete consumption of BPO. Efforts continue to also identify and follow an absorbance associated with the formation of the nitroxide chain end.

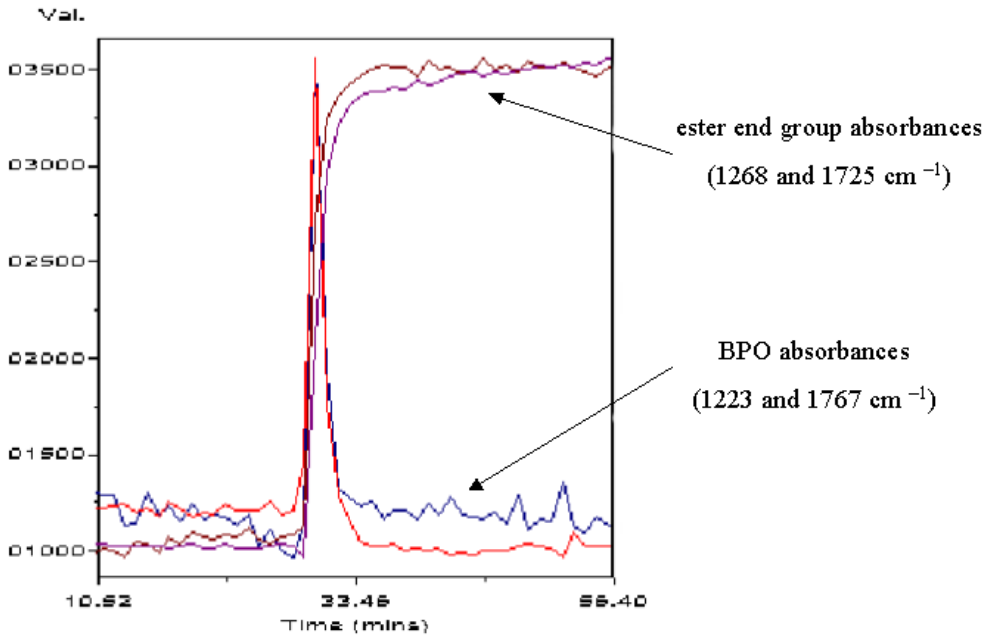

Figure 2.26 Real-time profiles of BPO (C=O at 1767 cm^{-1} and C-O-C at 1223 cm^{-1}) and polymer ester end group (C=O at 1725 cm^{-1} and C-O-C at 1268 cm^{-1}).

Apparent rate constants were also determined from the real-time decay profiles of the styrene monomer. Figure 2.27 depicts the first order kinetic plot constructed from the real-time profile for the decay of the $=CH_2$ absorbance (907 cm^{-1}) of the styrene monomer for the polymerization at 132 °C. Data points were collected every minute for the first 90 minutes and then every 5 minutes for the remainder of the reaction. The initial steep decrease in the absorbance seen in Figure 2.27 was due to the increasing temperature of the

reaction mixture since BPO was not added until constant temperature and constant $=CH_2$ absorbance was observed. Once the reactor temperature stabilized, BPO was added to the reactor and the monomer $=CH_2$ absorbance decreased at a constant rate. Data from the real-time profile of the $=CH_2$ absorbance allowed for the calculation of an observed first order rate constant from the slope, which is equal to the rate of propagation times the concentration of growing polymer radicals ($k_{obs}=k_p[P_n\bullet]$), assuming no termination or side reactions occur. From the first order kinetic plot, the apparent rate constant for the reaction was determined to be 2.1 x 10^{-5} s^{-1} at 132 °C and 1.2 x 10^{-5} s^{-1} at 126 °C. It is important to note that the rate constants determined using the $=CH_2$ absorbance (907 cm^{-1}) were in good agreement with the rate constants determined using the C=C absorbance (1628 cm^{-1}). Although a stable baseline was difficult to identify for the lower intensity C=C absorbance at 1628 cm^{-1}, the observed rate constant at 132 °C was 2.0 x 10^{-5} s^{-1}, which agreed favorably with the value determined using the $=CH_2$ absorbance. Interestingly, it was observed that the slope of the line in Figure 2.27 was not completely linear over the entire polymerization process. It appeared that the rate of the reaction was slower earlier in the reaction and then increased later. Georges et al. observed a similar phenomenon and developed a germination efficiency factor to account for this initial non-linearity.[163] In addition, it was observed that at high conversion, the rate appeared to decrease. This decrease in rate at higher conversions may be attributed to the increasing solution viscosity and the inability of the magnetic stirrer to eliminate temperature gradients. In addition, propagation rate constants may decrease at high conversions due to radical termination reactions that result in a reduced radical concentration.

---

[163] Veregin, R. P. N.; Odell, P. G.; Michalak, L. M.; Georges, M. K. *Macromolecules* **1996**, *29*, 2746.

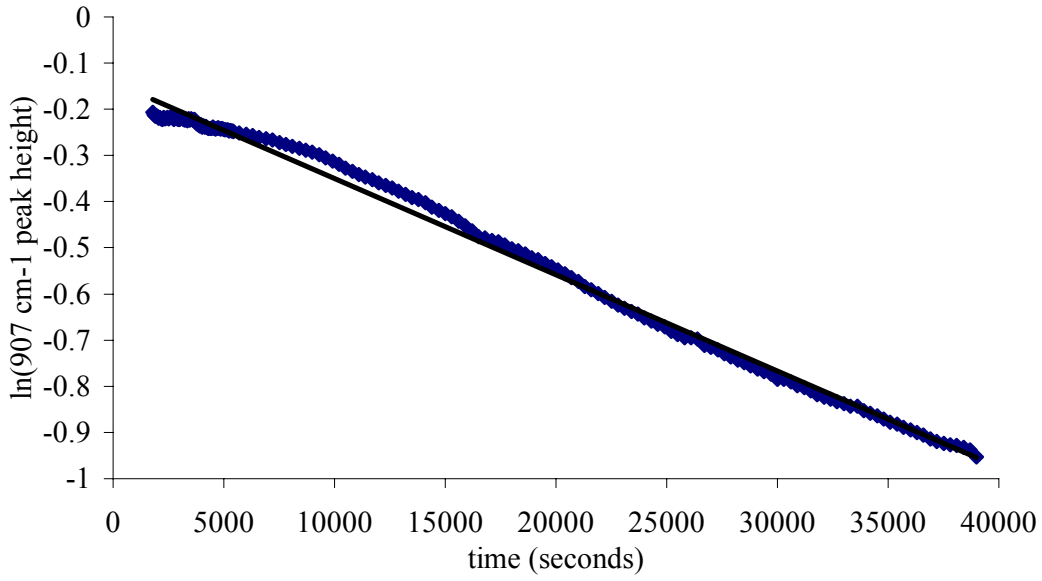

Figure 2.27 First order kinetic plot for styrene SFRP polymerization at 132 °C (determined from the real-time FTIR profile of the styrene $=CH_2$ absorbance (907 cm^{-1})).

Kinetic investigations were also performed to study the living nature of the stable free radical polymerization of 2-vinylnaphthalene. 2-Vinylnaphthalene (VN) has been previously polymerized using anionic methods,[164] conventional free radical techniques,[165] and recently via stable free radical polymerization.[166] However, the SFRP efficiency of 2VN using stable free radical methods remains relatively unexplored. Poly(2-vinylnaphthalene) (P2VN) is of particular interest due to its luminescent properties. A short chain of 2VN units can be linked to the end of a polymer chain to fluorescently label the polymer. 2VN was polymerized via three routes; thermally, conventional free radical, and stable free radical polymerization (Scheme 2.24).

---

[164] Nossarev, C. G.; Hogen-Esch, T. E. *Polymer Preprints* **2000**, *41*(1), 137.
[165] Ryou, J. H.; Ha, C. S.; Cho, W. J. *J. Polym. Sci., Part A: Polym. Chem.* **1993**, *31*, 325.
[166] Nowakowska, M.; Zapotoczny, S.; Karewicz, A. *Macromolecules* **2000**, *33*, 7345.

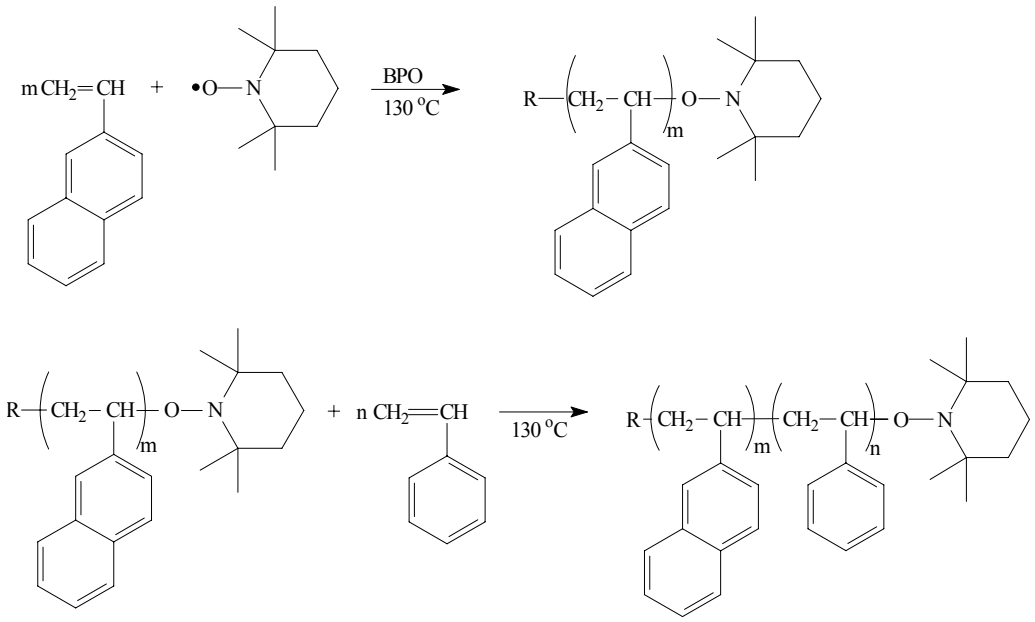

Scheme 2.24 2-Vinylnaphthalene stable free radical polymerization scheme.

In situ monitoring of 2VN polymerization under thermal and SFRP conditions (130 ^{o}C) using FTIR revealed a great deal of similarity in the kinetics for the two reaction systems. All monitored polymerizations were performed in chlorobenzene solution to eliminate exothermic effects associated with bulk thermal polymerization. Monitoring the monomer disappearance demonstrated identical rates of consumption in the thermal and SFRP process (Figure 2.28). Conversion of the monomer disappearance data to kinetic plots of ln[M] versus time exhibited a linear relationship typical of the pseudo first order kinetics associated with NRP and thermal polymerizations. Elucidation of the observed rate constants (k_{obs}) confirmed the identical nature of the two processes indicating that the thermal mechanism dominates initiation of polymerization under SFRP conditions (Figure 2.29). The k_{obs} values for the polymerization of 2VN in thermal and SFRP conditions were 2.5 x 10^{-5} s^{-1} and 2.6 x 10^{-5} s^{-1}, respectively. The difference in observed rate constants is easily attributed to slight variance in experimental procedures and possibly to minimal participation of the TEMPO species in capping the propagating radical.

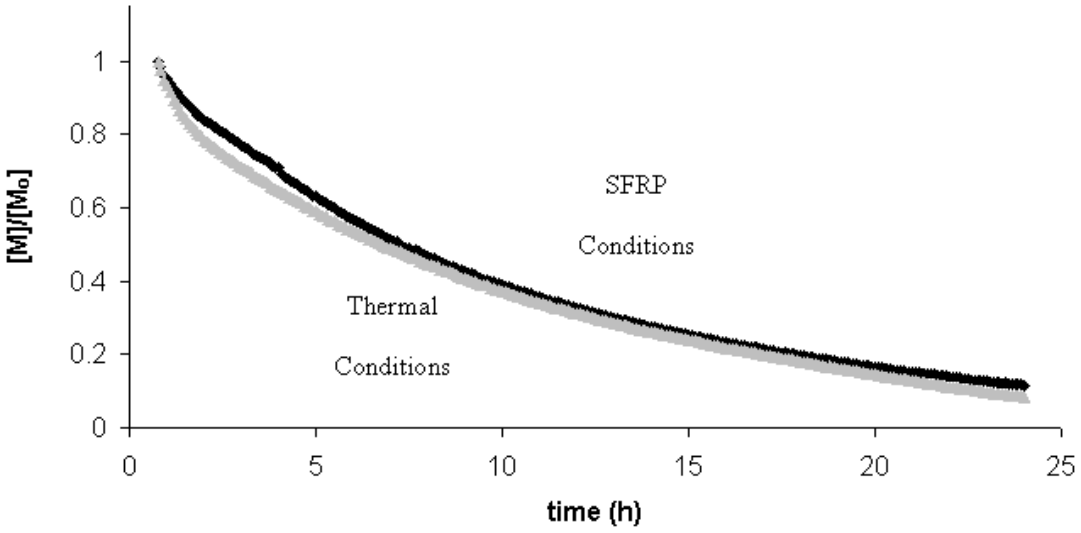

Figure 2.28 Plot of monomer disappearance versus time for SFRP and thermal conditions monitoring the CH bend at 988 cm^{-1} (black=SFRP, gray=thermal).

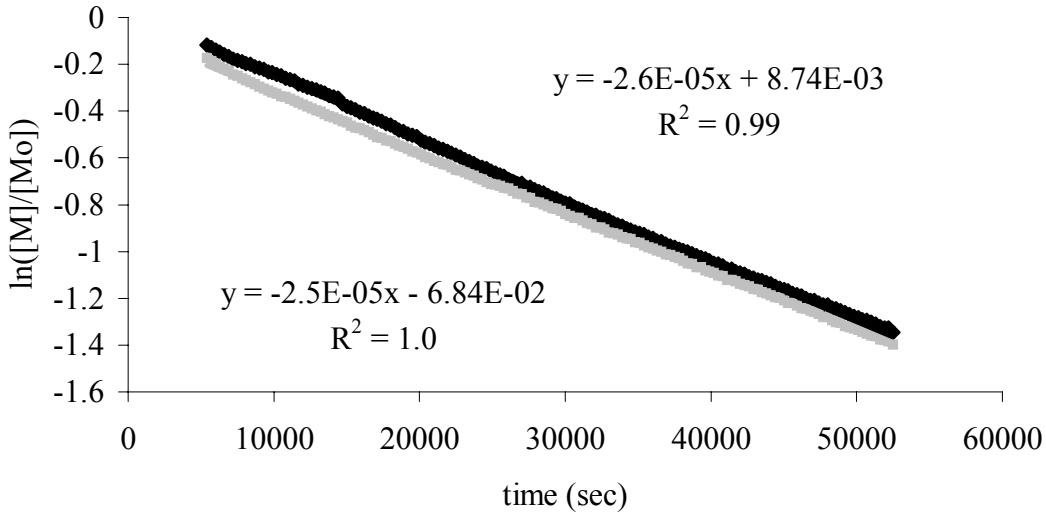

Figure 2.29 Pseudo first order kinetic plot for 2-vinylnaphthalene polymerized under SFRP and thermal conditions (black=SFRP, gray=thermal).

The propensity of styrene to thermally polymerize at reaction temperatures above 100 ^{o}C is well documented.[167] Consequently, *in situ* FTIR was employed to monitor the solution thermal polymerization nature of both styrene and 2-vinylnaphthalene. As expected from the preliminary work, 2VN displayed a marked increase in its tendency to undergo polymerization initiated by a thermal mechanism compared to styrene. The thermal polymerization of both monomers was monitored at 80, 100 and 130 ^{o}C to elucidate the thermal initiation over a range of temperatures (Figure 2.30 and Figure 2.31). Styrene exhibited a steady decrease over the temperature range and monomer disappearance at 80 ^{o}C was almost negligible. On the contrary, 2VN displayed a

[167] Hoyer, H. W.; Santoro, A. V.; Barrett, E. J. *J. Polym. Sci., Polym. Chem.* **1968**, *6*, 1033.

substantial degree of thermal initiation and polymerization at all reaction temperatures although decreasing the reaction temperature resulted in lower monomer conversion.

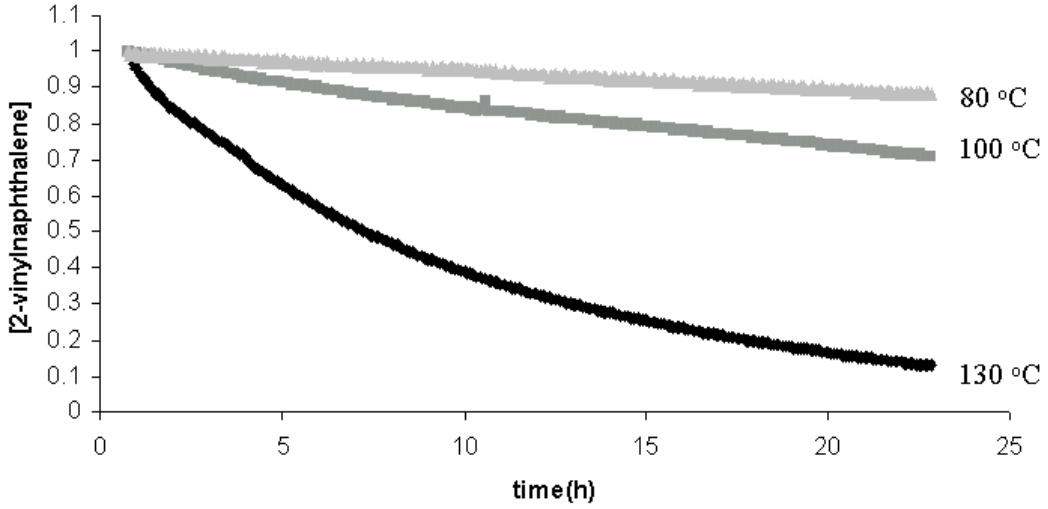

Figure 2.30 Disappearance of 2-vinylnaphthalene monomer at different temperatures in solution polymerization under thermal conditions.

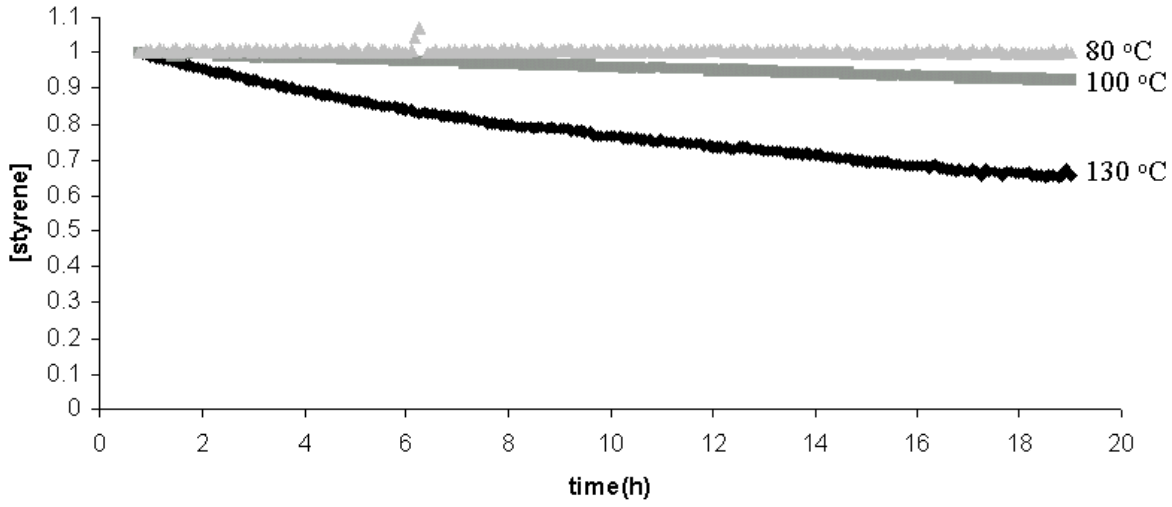

Figure 2.31 Disappearance of styrene monomer at different temperatures in solution polymerization under thermal conditions.

Examination of the observed rate constants determined by pseudo first order kinetics illustrates a large variance in the thermal polymerization of styrene with the rate constants covering a range of two orders of magnitude over the chosen temperature range. On the other hand, 2VN rate constants varied by a single order of magnitude over the range of examined temperatures. Using the observed rate constants, an Arrhenius plot of $\ln[k_{obs}]$ versus 1/T was constructed to determine the energy of activation for each process. Styrene exhibited an activation of 97.7 kJ/mol that closely resembled the value, 89.6 kJ/mol, reported in literature (Figure 2.32).[167] The 2-vinylnaphthalene monomer exhibited an expectedly lower energy of activation at 67.1 kJ/mol demonstrating the greater ease of thermal polymerization for this system compared to styrene (Figure 2.33). The increased propensity for thermal polymerization of 2VN can be attributed to the enhanced stability of radical formed by the Mayo mechanism for thermal initiation. The two fused rings increase the stability of the radicals formed from the thermal initiation process lowering the energy necessary to produce the radicals.

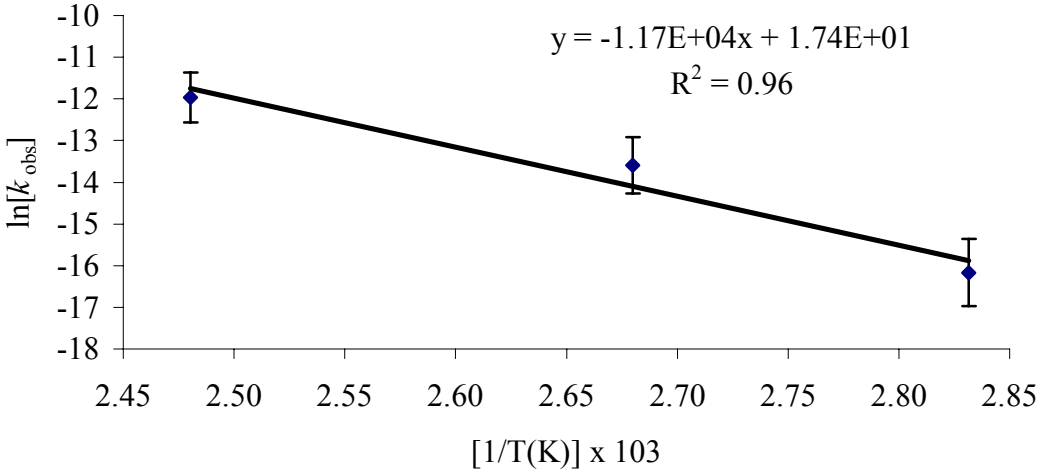

Figure 2.32 Arrhenius plot for the thermal polymerization of styrene in chlorobenzene at 80, 100, and 130 ^{o}C.

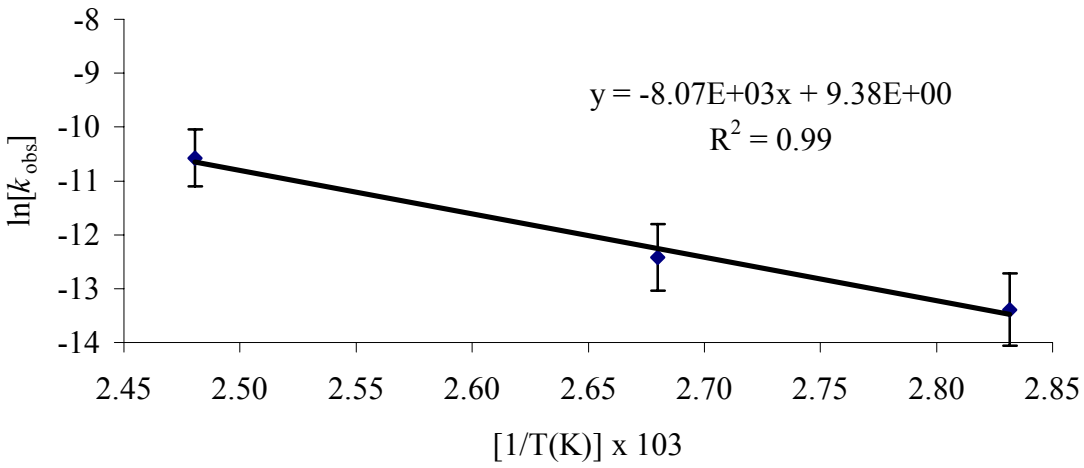

Figure 2.33 Arrhenius plot for the thermal polymerization of 2-vinylnaphthalene in chlorobenzene at 80, 100 and 130 ^{o}C.

2.7.5 Maleic Anhydride/Cyclic Olefin Alternating Copolymers

One of the most promising and generally accepted routes for potential main-chain alicyclic 193 nm resist materials is the alternating free radical copolymerization of maleic anhydride with cyclic olefin comonomers.[168] Cyclic olefins will homopolymerize poorly via free radical methods. However, when cyclic olefins are reacted with maleic anhydride, which is a strong electron acceptor, in the presence of a free radical initiator, copolymerization occurs in an alternating manner.[169] In addition, maleic anhydride also serves to incorporate oxygen into the material, providing necessary adhesion and solubility properties that are required for imaging performance while still retaining sufficient etch

---

[168] Allen, R. D.; Opitz, J.; Larson, C. E.; Wallow, T. I.; Hofer, D. C. *Microlithography World* **winter 1999**, 5.
[169] Houlihan, F. M.; Wallow, T. I.; Nalamasu, O.; Reichmanis, E. *Macromolecules* **1997**, *30*, 6517.

resistance to be successfully demonstrated as 193 nm resist materials.[170] The cyclic olefin character of these materials provides for excellent etch resistance, surpassing even currently utilized phenol based resists. Furthermore, the increased etch resistance is of great importance because of the decreasing film thickness necessary for the achievement of increasingly smaller feature sizes.[169]

Despite the abundance of scientific literature describing the alternating copolymerization of maleic anhydride with electron-rich olefins, multicomponent copolymerizations with norbornene(s) proceed via a complicated polymerization mechanism resulting in the uncontrolled formation of low molecular weight oligomers.[171] Our research objectives have focused on the investigation of synthetic factors that influence the molecular weight, yield, and composition of terpolymers of maleic anhydride (MAH), norbornene (Nb), and *tert*-butyl 5-norbornene-2-carboxylate (NbTBE) (Scheme 2.25). This has been achieved using a unique combination of experimental variation, *in situ* infrared spectroscopy, and nuclear magnetic resonance spectroscopy. *In situ* infrared spectroscopy of alternating copolymerizations has not been reported earlier, and this experimental approach is more facile than conventional NMR approaches. This fundamental understanding will provide the basis for the development of a polymerization system that results in more predictable molecular weights and higher polymerization yields. The development of a fundamental understanding of the polymerization mechanism for maleic anhydride with norbornene and norbornene derivatives will result in viable manufacturing processes and improved 193 nm lithographic performance.

---

[170] Okoroanyanwu, U.; Shimokawa, T.; Byers, J.; Medeiros, D.; Willson, C. G.; Niu, Q. J.; Fréchet, J. M. J. Allen, R. D. *Proc. SPIE-Int. Soc. Opt. Eng.* **1997**, *3049*, 92.

[171] Patterson, K.; Yamchika, M.; Cho, S.; Rager, T.; Yamada, S.; Byers, J.; Willson, C. G. *Polym. Mat. Sci. Eng.* **1999**, *81*, 43. Houlihan, F. M.; Wallow, T. I.; Nalamasu, O.; Reichmanis, E. *Macromolecules* **1997**, *30*, 6517.

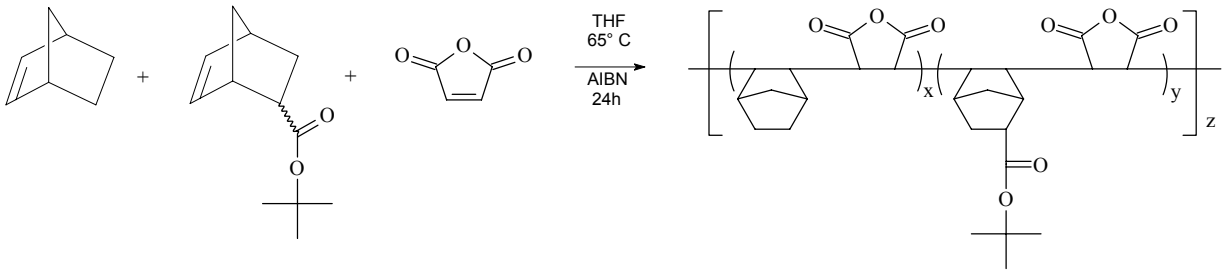

Scheme 2.25 Nb/NbTBE/MAH free radical terpolymerization.

A reaction flask was specifically designed to permit the introduction of the ATR based infrared probe and attention was devoted to ensure the reactor was sealed to eliminate any volatilization of reaction components. Strong vinylene (=C-H) absorbances of the monomers were observed and allowed for kinetic analysis of the terpolymerizations using *in situ* FTIR. The waterfall plot of the vinylene =C-H region for a Nb/NbTBE/MAH (25/25/50 mol ratio) is illustrated in Figure 2.34. The vinylene absorbance of Nb and NbTBE overlapped and were observed at 710 cm^{-1}. The vinylene absorbance of MAH was observed at 695 cm^{-1}. Pseudo first order kinetic plots were constructed from the data obtained via the *in situ* monitoring of the monomer absorbances. Initial kinetic interpretations have focused on the assumption of pseudo first order kinetics for an alternating polymerization mechanism (Figure 2.35). Excellent agreement was observed using these assumptions and linear kinetic plots were observed. A representative kinetic plot of ln[monomer absorbance (total area from 670 to 725 cm^{-1})] vs. time for a Nb/NbTBE/MAH (25/25/50 mol ratio, k_{obs} = 3.8 x 10^{-5} s^{-1}) terpolymerization is shown in Figure 2.36.

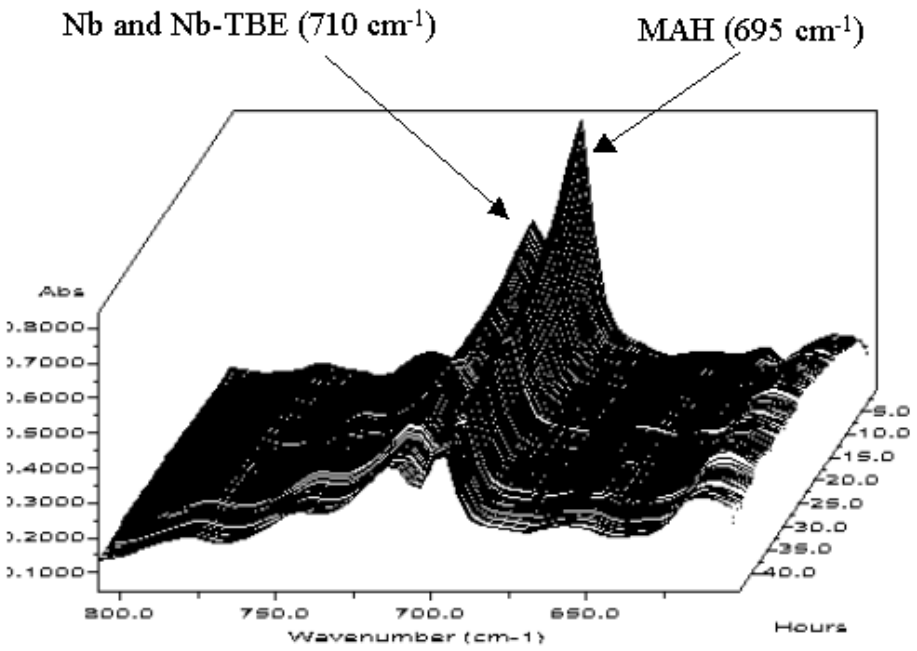

Figure 2.34 Vinylene region of "waterfall plot" for Nb/NbTBE/MAH (25/25/50 mol ratio) terpolymerization (*in situ* FTIR, spectrum acquired every 5 min).

Table 2.1 Summary of Nb/NbTBE/MAH terpolymerizations varying the monomer feed ratio of Nb to NbTBE.

Nb/Nb-TBE/MAH	Observed rate (FTIR) x 10^5 s^{-1} [a]	Yield (%)	M_n[b]	M_w/M_n	Nb/Nb-TBE [c]
50/0/50	6.7	94	7,300	1.63	
35/15/50	5.3	87	6,500	1.46	3.2
25/25/50	3.8	80	6,700	1.64	1.4
15/35/50	2.6	75	6,600	1.49	0.68
0/50/50	1.1	60	6,900	1.59	

[a] Determined from first order kinetic plot using MAH/NB peak area via in-situ FTIR for first 4 h of reaction. [b] Wyatt miniDAWN MALLS detector coupled with Waters GPC with external 410 RI detector viscometer, THF solvent at 40 °C and 1.0 mL/min flow rate. [c] Determined using ^{13}C NMR (Varian Unity-400) at 100 MHz, DMSO-d_6, ambient temperature. Ratio calculated from integration of the quaternary carbon of *tert*-butyl ester group (δ 80 ppm) of Nb-TBE to the total carbonyl region (δ 170-176 ppm). For calculation, a 1:1 ratio of MAH to total cyclic olefin (Nb and Nb-TBE) is assumed.

Free radical terpolymerizations of Nb/NbTBE/MAH with various ratios of Nb to Nb-TBE (while maintaining a 50 % molar feed of maleic anhydride) were performed using previously determined optimum conditions (3.0 mol % AIBN, THF (60 % solids), 24 h). Terpolymerizations were conducted using the following Nb/NbTBE/MAH monomer feed ratios: 50/0/50, 35/15/50, 25/25/50, 15/35/50, 0/50/50. The observed rate constants determined using *in situ* FTIR, percent yields, molecular weights, and Nb/NbTBE composition in the resulting materials are summarized in Table 2.1. Several trends were apparent from the data analysis. First, the observed reaction rate was a strong function of the monomer feed ratio of Nb/NbTBE with a maximum of 6.7 x 10^{-5} s^{-1} at a 50/0/50 Nb/NbTBE/MAH monomer feed ratio. The observed rate decreased with increasing Nb-TBE monomer feed to a minimum of 1.1 x 10^{-5} s^{-1} at a 0/50/50 Nb/NbTBE/MAH monomer feed ratio. In addition, percent yield exhibited a similar trend with a maximum

yield of 94 % for a 50/0/50 Nb/NbTBE/MAH feed ratio and a minimum yield of 60 % observed for a 0/50/50 Nb/NbTBE/MAH feed ratio. The observed decrease in rate with increasing NbTBE was proposed to be due to a combination of steric and electronic effects resulting from the *tert*-butyl ester functionality of Nb-TBE. ^{13}C NMR analysis of terpolymers prepared from a 25/25/50 Nb/NbTBE/MAH monomer feed ratio further indicated that the terpolymers were enriched in Nb and depleted in NbTBE.

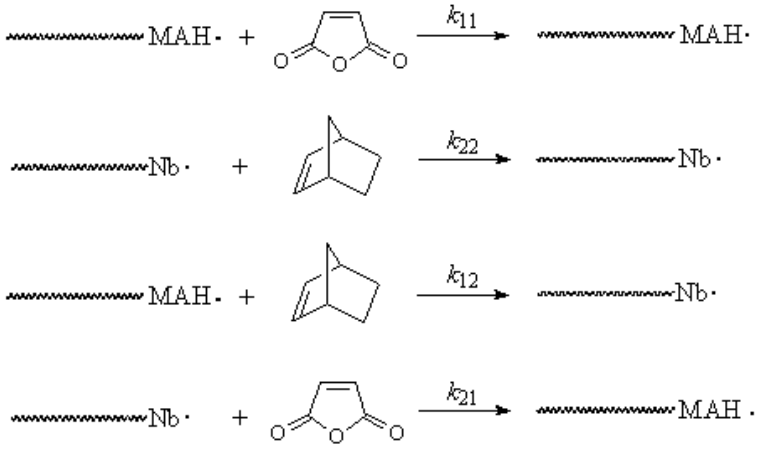

assuming negligible homopolymerization of MAH and Nb, k_{11}=k_{22}=0, overall rate is:

rate = k_{12}[(MAH·)(Nb)] + k_{21}[(Nb·)(MAH)]

assuming a steady state radical concentration and alternating polymerization, rate is:

rate = (k_{12} + k_{21})([P·][M])

where [P·] = conc. of growing polymer radicals and [M] = conc. of MAH or Nb monomer

and therefore an observed rate constant (k_{obs}) is obtained from a plot of ln[M] vs. time

k_{obs} = (k_{12} + k_{21})[P·]

Figure 2.35 Pseudo first order alternating polymerization kinetic assumptions.

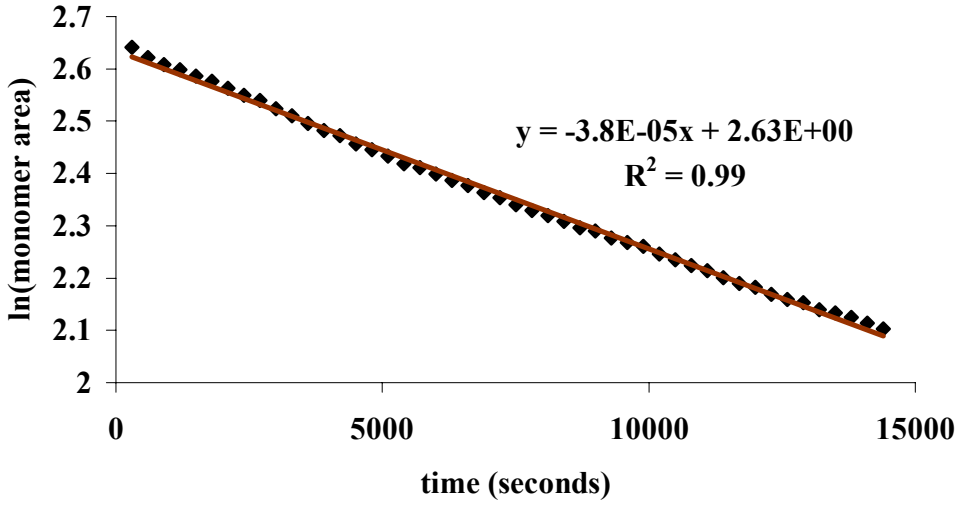

Figure 2.36 Psuedo first order kinetic treatment of convoluted Nb, NbTBE, and MAH (total area from 670 to 725 cm^{-1}) absorbances determined via *in situ* FTIR.

2.7.6 **Polyester Melt Polymerization Processes**

Sampling of conventional melt polymerization processes is often complicated due to high polymerization temperatures, high melt viscosities, the need for precise pressure control, and oxygen sensitivity of the polymerization chemistry.[172] Consequently, it is very desirable to use an *in situ* spectroscopic approach for the analysis of monomer conversion and polymer structure versus time without complicated sampling techniques. The preparation of PET derived from dimethyl terephthalate (DMT) involves ester exchange with ethylene glycol to form bis-hydroxyethylterephthalate (BHET) and

[172] Pilati, F. In *Comprehensive Polymer Science*, G. Allen, J. Bevington, Eds., Pergamon, Vol. 5, 1989, Ch. 17.

polycondensation to form poly(ethylene terephthalate) (PET) (Scheme 2.26).[173] Hydroxyl absorbances are associated with the ethylene glycol monomer, evolved methanol, BHET, and PET end groups. Although the hydroxyl region is often complicated by the presence of water contamination in routine analytical testing, the reaction conditions, i.e. high temperatures and the propensity of water to hydrolyze esters, minimize the presence of water. Initial efforts have focused on DMT based PET polymerization chemistry, however, the utility of *in situ* FTIR for terephthalic acid (PTA) based PET would be an obvious extension. The carbonyl region in the DMT based process does not exhibit obvious differences as the reaction proceeds, however, it is expected that the carbonyl region would be particularly useful in the PTA based process as the dicarboxylic acid is converted to the corresponding ester. In addition, there are significant spectral changes in the carbon-oxygen region that offer the possibility for additional monitoring.

[173] Wilfong, R. E. *J. Polym. Sci.* **1961**, *54*, 385.

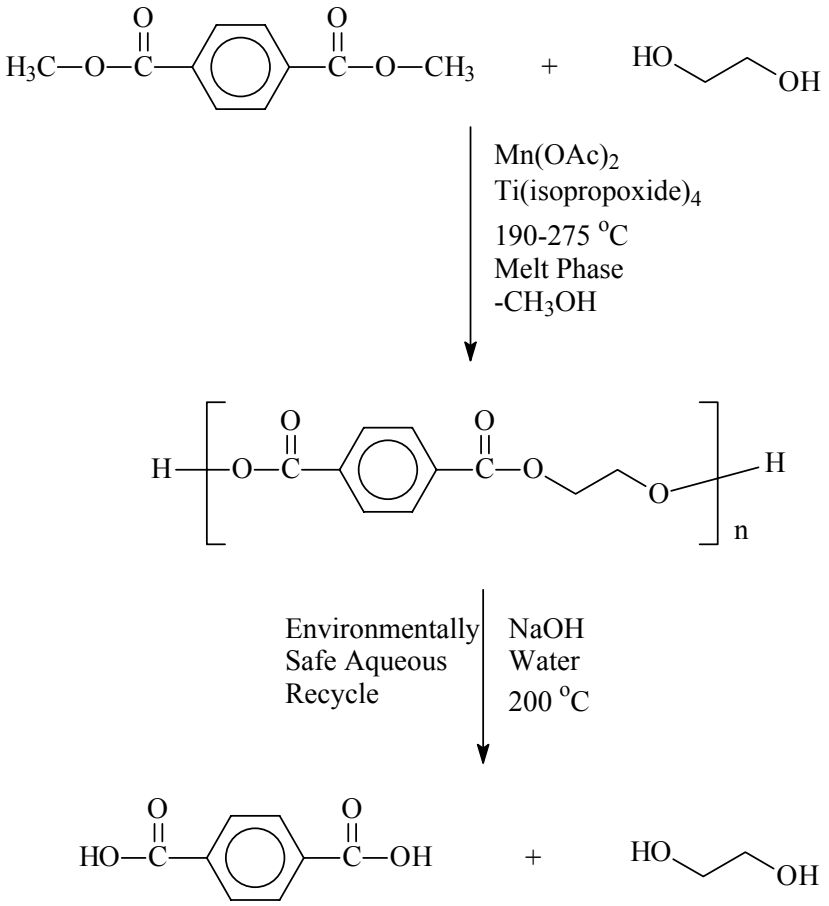

Scheme 2.26 Step-growth polycondensation forming poly(ethylene terephthalate) (PET).

Infrared spectra were obtained as a function of time during the step-growth polymerization of ethylene glycol and dimethyl terephthalate. Scheme 2.26 illustrates the synthetic process, and Figure 2.37 depicts the corresponding infrared spectra as a function of time. Scheme 2.26 refers to the polymer end groups including hydroxyl, carboxylic acid, and methyl carboxylate. Particular attention was devoted to the hydroxyl region (3700-3300 cm^{-1}) in an attempt to determine the polymer end group concentrations as a function of time. In fact, hydroxyl end group concentrations in the final polymer as determined using *in situ* MIR agreed well with values determined using proton nuclear magnetic resonance (^1H NMR). This observation suggested the possibility of determining

molecular weight versus monomer conversion in real-time for polymeric materials with very limited solubility. For example, poly(ethylene terephthalate) (PET) is only soluble in dangerous solvent mixtures such as phenol/tetrachloroethylene (70:30), and liquid crystalline polyesters require hazardous mixtures such as pentafluorophenol/trichlorobenzene. The *in situ* FTIR technique can potentially eliminate the necessity of dissolution for subsequent gel permeation chromatography and inherent viscosity measurements.

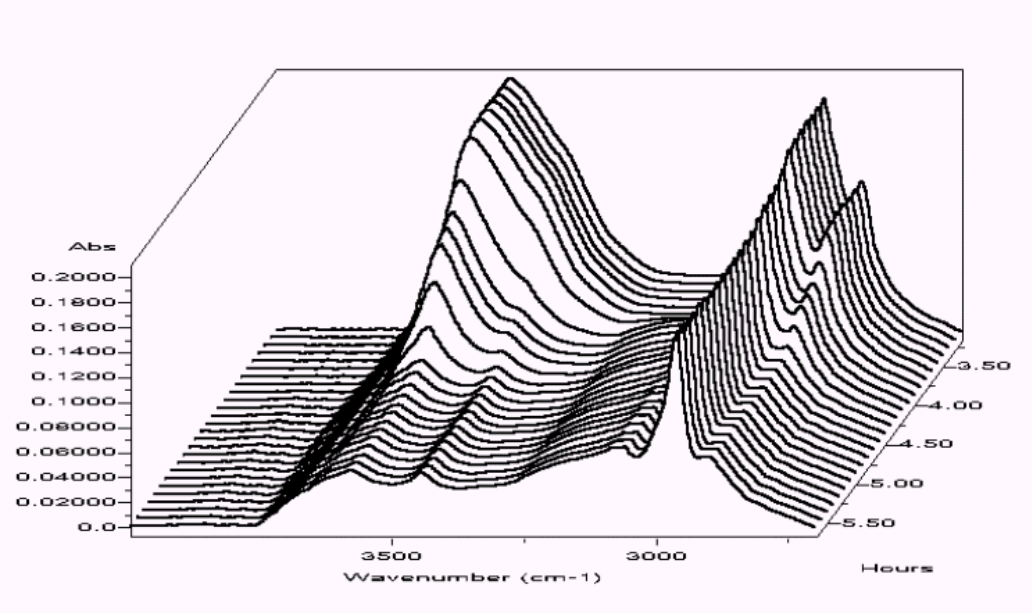

Figure 2.37 Mid-infrared spectra versus time depicting hydroxyl end groups on PET.

CHAPTER 3

Real-Time Monitoring of the Stable Free Radical Polymerization of Styrene via *In situ* Mid-Infrared Spectroscopy

3.1 ABSTRACT

In situ mid-infrared spectroscopy was successfully utilized to follow initiation, monomer conversion, and polymer formation during the stable free radical polymerization (SFRP) of styrene initiated using a conventional free radical initiator, benzoyl peroxide (BPO), in the presence of 2,2,6,6-tetramethyl-1-piperidinyloxy (TEMPO). This method permitted facile acquisition of data at short intervals for relatively long reaction times without the need for time-consuming reaction sampling and subsequent analysis. In addition, the real-time data allowed for the determination of apparent rate constants ($k_{app}=k_p[P_n\bullet]$) of 2.1 x 10^{-5} s^{-1} at 132 °C and 1.2 x 10^{-5} s^{-1} at 126 °C from the profile of the decaying styrene vinyl carbon-hydrogen (=CH_2) absorbance at 907 cm^{-1}. Real-time analysis also indicated the half-life of BPO at 132 °C in the presence of styrene and TEMPO to be approximately 50 seconds.

3.2 INTRODUCTION

Controlled polymerization routes permit the synthesis of well-defined macromolecules with controlled chemical composition, predictable molecular weight, and narrow molecular weight distribution.[1] The ability to control polymer architecture is essential in advanced technological applications where well-defined macromolecular architectures are required. Control of chain-growth polymer architecture has been traditionally achieved using living anionic,[2] cationic,[3] or group-transfer[4] polymerization procedures. Synthetic methodologies for controlled polymerization have been expanded with recent developments in both stable free radical polymerization (SFRP)[5] and atom transfer radical polymerization (ATRP).[6]

Following the earlier work of Rizzardo *et al*.[7] in nitroxide mediated stable free radical polymerization, Georges *et al*.[8] first reported the preparation of polystyrene with low polydispersity using bulk free radical polymerization of styrene initiated by a conventional free radical initiator, benzoyl peroxide (BPO), in the presence of the stable nitroxide free radical, 2,2,6,6-tetramethyl-1-piperidinyloxy (TEMPO) at 125 °C. The SFRP process involves a desirable equilibrium between nitroxide capped polymer chains and uncapped polymer radicals. The uncapped polymer radicals are then able to chain extend via styrene monomer addition (**Scheme 3.1**). The success of this method arises from the unique

---

[1] Webster, O. W. *Science* **1991**, *251*, 887.
[2] Szwarc, M. *Nature* **1956**, *178*, 1168. *Anionic Polymerization: Kinetics, Mechanisms, and Synthesis*, McGrath, J. E., ed.; ACS Symposium Series 166; American Chemical Society: Washington, DC, 1981.
[3] Matyjaszewski, K. *Cationic Polymerizations: Mechanisms, Synthesis and Applications*; Marcel Deker: New York, 1996.
[4] Sogah, D. Y.; Hertler, W. R.; Webster, O. W.; Cohen, G. M. *Macromolecules* **1987**, *20*, 1473.
[5] Hawker, C. J. *ACC. Chem. Res.* **1997**, *30*, 373. Hawker, C. J.; Bosman, A. W.; Harth, E. *Chem. Rev.* **2001**, *101*, 3661.
[6] Patten, T. E.; Matyjaszewki, K. *Adv. Mater.* **1998**, *10*, 901.
[7] Moad, G.; Rizzardo, E.; Solomon, D. H. *Macromolecules* **1982**, *15*, 909.
[8] Georges, M. K.; Veregin, R. P. N.; Kazmaier, P. M.; Hamer, G. K. *Macromolecules* **1993**, *26*, 2987.

feature that the nitroxide radicals will react with carbon radicals at near diffusion controlled rates, but will not react with other oxygen centered radicals or initiate additional polymer chains.

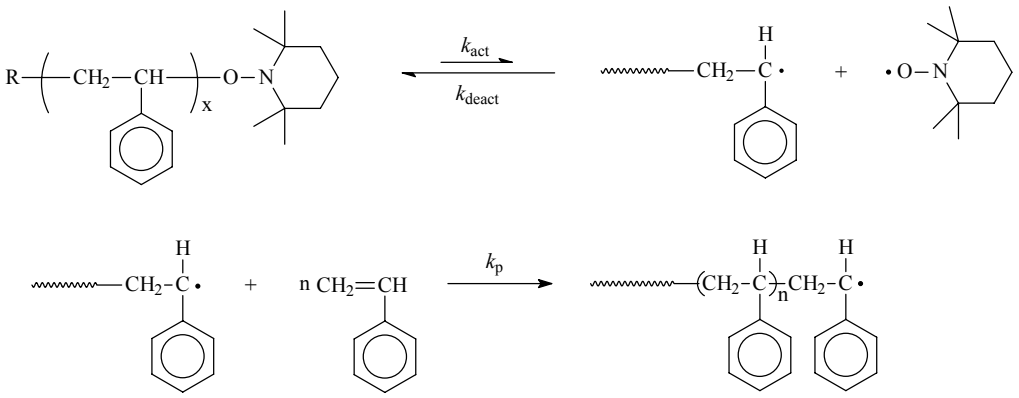

Scheme 3.1 Styrene SFRP reaction scheme.

An indication of the controlled nature of the SFRP of styrene is typically accomplished by the demonstration of a linear increase in molecular weight with conversion.[9] Kinetic information is commonly obtained by withdrawing samples and analyzing for residual monomer with gravimetric and chromatographic methods. In addition, more sophisticated analytical methods have recently been applied to study SFRP kinetics. For example, Georges *et al*. have utilized *in situ* ESR spectroscopy to study the

[9] Hawker, C. J. *J. Am. Chem. Soc.* **1994**, *116*, 11185.

SFRP process,[10] and Hawker *et al*. have recently applied ^{1}H NMR to evaluate initiator efficiency for SFRP processes using deuterated styrene.[11]

In situ mid-infrared spectroscopy is a state-of-the-art, real-time monitoring technique that is well suited to obtain real-time structural and kinetic information of controlled polymerization processes such as SFRP.[12] In addition, reactions are analyzed without complicated reactor modifications or expensive deuterated monomers. Previously, Long *et al*. have utilized *in situ* near-infrared (NIR) (10,000 – 4,000 cm $^{-1}$) spectroscopy using fiber optic probe technology to obtain solution polymerization kinetics of living anionic processes.[13] More recently, Puskas[14] and Storey[15] have reported the application of *in situ* mid-infrared (4000 - 650 cm^{-1}) spectroscopy to monitor living cationic polymerization processes. In addition, Bradley and Long recently applied *in situ* mid-infrared spectroscopy to study melt-phase acidolysis and ester exchange polymerization mechanisms.[16] These previous efforts have demonstrated the versatility of *in situ* infrared spectroscopy and we report herein the application of this instrumentation to monitor the stable free radical polymerization of styrene.

---

[10] Veregin, R. P. N.; Odell, P. G.; Michalak, L. M.; Georges, M. K. *Macromolecules* **1996**, *29*, 2746. Veregin, R. P. N.; Georges, M. K.; Kazmaier, P. M.; Hamer, G. K. *Macromolecules* **1993**, *26*, 5316. Veregin, R. P. N.; Odell, P. G.; Michalak, L. M.; Georges, M. K. *Macromolecules* **1996**, *29*, 4161. MacLeod, P. J.; Veregin, R. P. N.; Odell, P. G.; Georges, M. K. *Macromolecules* **1998**, *31*, 530. Moffat, K. A.; Hamer, G. K.; Georges, M. K. *Macromolecules* **1999**, *32*, 1004.

[11] Hawker, C. J.; Barclay, G. G.; Orellana, A.; Dao, J.; Devonport, W. *Macromolecules* **1996**, *29*, 5245.

[12] Chang, S. Y.; Wang, N. S. In *Multidimensional Spectroscopy of Polymers*; ACS Symposium Series 598; American Chemical Society: Washington, DC, 1995.

[13] Long, T. E.; Liu, H. Y.; Schell, D. M.; Teegarden, D. M.; Uerz, D. S. *Macromolecules* **1993**, *26*, 6237.

[14] Puskas, J. E.; Lanzendörfer, M. G.; Pattern, W. E. *Polym. Bull.* **1998**, *40*, 55. Puskas, J. E.; Lanzendörfer, M. G. *Macromolecules* **1998**, *31*, 8684.

[15] Storey, R. F.; Donnalley, A. B.; Maggio, T. L. *Macromolecules* **1998**, *31*, 1523.

[16] Bradley, J. R.; Long, T. E. *Polymer Preprints* **1999**, *40(1)*, 564.

3.3 EXPERIMENTAL

3.3.1 Materials

Benzoyl peroxide (BPO) and 2,2,6,6-tetramethyl-1-piperidinyloxy (TEMPO) were purchased from Aldrich and used as received. Styrene (Aldrich) was vacuum distilled (0.1 mm Hg) at room temperature from calcium hydride after degassing three times using the traditional freeze-thaw method. After distillation, styrene monomer was stored in a freezer in a septum-sealed bottle under positive nitrogen pressure (4-5 psi).

3.3.2 Characterization

Molecular Weight Characterization

Molecular weights were determined via size exclusion chromatography (SEC) using an Alliance SEC system (Waters Corporation, Milford, MA) with external refractive index detector (Waters 410) and Viscotek T-60A viscometer/90° light scattering dual detector. The mobile phase used for SEC analysis was 1-methyl-2-pyrrolidinone (NMP) containing P_2O_5 (0.02 M) at 60 °C and a flow rate of 1.0 mL/min. Absolute molecular weights and intrinsic viscosities were calculated from SEC using Viscotek SEC^3 Triple Detection software.

Multiple Angle Laser Light Scattering (MALLS) measurements were performed using a miniDAWN (Wyatt Technology, Santa Barbara, CA) with 690 nm laser connected to a Waters SEC (515 pump, 717 autosampler, and 410 refractive index detector). The miniDAWN was connected in series after three 5-μm Plgel mixed-bed columns (Polymer Laboratories, Amherst, MA). Measurements were made at 40 °C with THF as the solvent at a flow rate of 1.0 mL/min. The dn/dc of polystyrene in THF at 40 °C was determined

(via miniDAWN) to be 0.185 mL/g using polystyrene standards of known molecular weight, and was consistent with literature values.[17]

In situ FTIR

In situ mid-FTIR spectra were collected with a ReactIR 1000 (MCT detector, S/N = 7500, resolution = 4) (ASI Applied Systems, Millersville, MD, www.asirxn.com) reaction analysis system equipped with a light conduit and DiComp (diamond-composite) insertion probe. Reaction data was analyzed using ReactIR software.

Thermal Analysis

Polymer glass transition temperatures were determined with a Perkin-Elmer Pyris 1 differential scanning calorimeter (DSC) at a heating rate of 10 °C/min with nitrogen flushing. Glass transition temperatures are reported as the inflection point of the change in heat capacity during the second heat. Thermogravimetric analysis (TGA) was performed using a TA Instruments TGA295 Thermogravimetric Analyzer at a heating rate of 10 °C/min.

3.3.3 Synthesis of Polystyrene via SFRP

In a 100 mL, round-bottomed, two-necked flask that was fitted with the ASI DiComp probe was added a magnetic stir bar, styrene (35.0 mL, 344 mmol), 2,2,6,6-tetramethyl-1-piperidinyloxy (TEMPO) (0.368 g, 2.36 mmol), and benzoyl peroxide (0.440 g, 1.82 mmol) (Scheme 3.2). The flask was sealed under nitrogen with a rubber septum, and a thermocouple was inserted through the septum to simultaneously monitor the temperature of the reaction mixture. A photo of the setup is shown in Figure 3.1. An oil bath at 134 °C was raised to the reaction flask. After several minutes, the temperature of the reaction mixture stabilized at 126 °C (The large temperature difference between the oil bath and

---

[17] Brandrup, J., Immergut, E. H., Grulke, E. A., Eds.; *Polymer Handbook,* 4th ed.; Wiley: New

reaction mixture was speculated to be due to the heat loss due to the stainless steel DiComp probe). The ReactIR was programmed to collect an FTIR spectra of the reaction mixture every minute (64 scans) for 90 minutes and then every 5 minutes (256 scans) for the remainder of the reaction and FTIR data collection was started. A solution of benzoyl peroxide (0.440 g, 1.82 mmol) in styrene (5.0 mL, 5.7 mmol) was then added to the reaction vessel via syringe under a nitrogen atmosphere. After addition of the benzoyl peroxide initiator, the reaction was stirred at 126 °C for 20 h with FTIR monitoring. After the product was cooled to room temperature, it was dissolved in chloroform (50 ML), precipitated into methanol (400 mL), filtered, and dried overnight under vacuum (65 °C) to yield 26.6 g (73% isolated yield) of TEMPO-terminated polystyrene oligomers of M_n = 19,300 g/mol (M_w/M_n = 1.10). NMR analysis of the vacuum-dried TEMPO-terminated polystyrene indicated the absence of appreciable residual monomer and/or precipitation solvent.

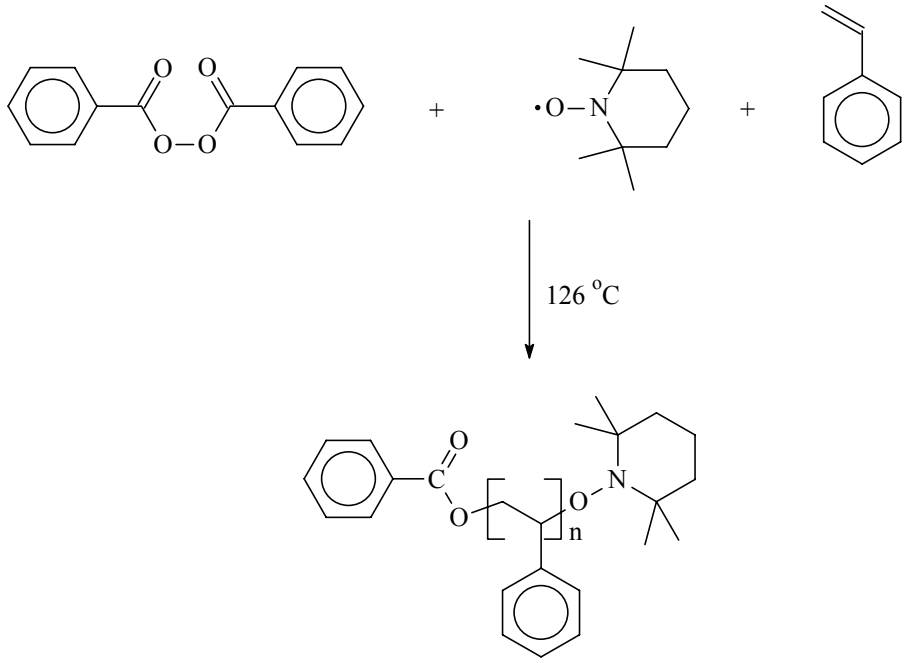

Scheme 3.2 Nitroxide-mediated styrene stable free radical reaction scheme.

York, 1999; pp VII/585-586.

Figure 3.1 Illustration of styrene SFRP reaction with *in situ* FTIR module.

3.4 RESULTS AND DISCUSSION

3.4.1 Styrene SFRP

In situ mid-infrared spectroscopy was utilized to monitor the bulk SFRP reaction of styrene (Aldrich, vacuum distilled from calcium hydride) initiated using benzoyl peroxide (BPO) (Aldrich, used as received) in the presence of 2,2,6,6-tetramethyl-1-piperidinyloxy TEMPO (Aldrich, used as received). A ReactIR 1000 (ASI Applied Systems) reaction analysis system equipped with a light conduit and DiComp (diamond-composite) insertion probe was used to collect mid-FTIR spectra of the polymerization reaction. The reaction was carried out in a 100 mL, round-bottomed, 2-necked flask that was fitted with the DiComp probe (Figure 3.1) and magnetic stir bar. Although a magnetic stir bar did not provide adequate agitation at higher conversions due to the extremely high bulk viscosity, it facilitated the intimate contact of the reaction mixture with the probe tip and reduced the possibility of oxygen ingress. The ReactIR 1000 was programmed to collect an FTIR

spectrum every minute for the first 90 minutes and then every 5 minutes for the remaining 24 hours. After 14 h the viscosity of the reaction increased dramatically and stirring stopped due to the high bulk viscosity. In addition, the infrared absorbances associated with the styrene monomer stabilized and stopped decreasing. The reproducibly low molecular weight distributions obtained after monitoring the reactions with *in situ* FTIR spectroscopy indicated that the presence of the probe did not negatively effect the controlled polymerization process. In order to eliminate concerns associated with the polymer isolation process, samples were directly removed from the reaction mixture, dried to a constant weight, and analyzed using size exclusion chromatography. In all cases, the molecular weight distributions obtained using the NMP/ P_2O_5 (0.02 M) solvent system exhibited M_w/M_n values ranging from 1.04 to 1.09.

3.4.2 FTIR Data Acquisition and Analysis

The ReactIR 1000 with light conduit technology allowed for the generation of real-time mid-IR spectra from 4000 cm^{-1} to 650 cm^{-1}. Styrene monomer exhibited two strong infrared absorbances that were easily monitored in real-time using the ReactIR 1000. The "waterfall" plots illustrating the disappearance of the vinyl carbon-carbon double bond absorbance (1628 cm^{-1}) and vinyl carbon-hydrogen absorbance (907 cm^{-1}) for styrene polymerization at 132 °C are shown in Figure 3.2. In addition, alkyl (sp^3 hybridized) carbon-hydrogen absorbances of the polystyrene backbone that form as polymerization proceeds were also identified and the real-time "waterfall" plot of the alkyl carbon-hydrogen absorbance at 2925 cm^{-1} is shown in Figure 3.3. Both disappearing monomer and forming polymer infrared absorbances were analyzed to produce a symmetrical x-shaped plot, which is characteristic of a polymerization reaction. The x-plot produced from the alkyl C-H absorbances (2925 and 3028 cm^{-1}), exhibited by the forming polymer, and the two vinyl absorbances (907 and 1628 cm^{-1}), exhibited by the disappearing monomer, for the polymerization at 132 °C is shown in Figure 3.4. The absorbance peak height (y-axis) was auto-scaled so that the relative changes in each of the monitored absorbances were directly comparable. The profiles for the three polymer alkyl

absorbances as well as the two monomer vinyl absorbances overlapped and agreed favorably with each other as expected for a controlled polymerization process.

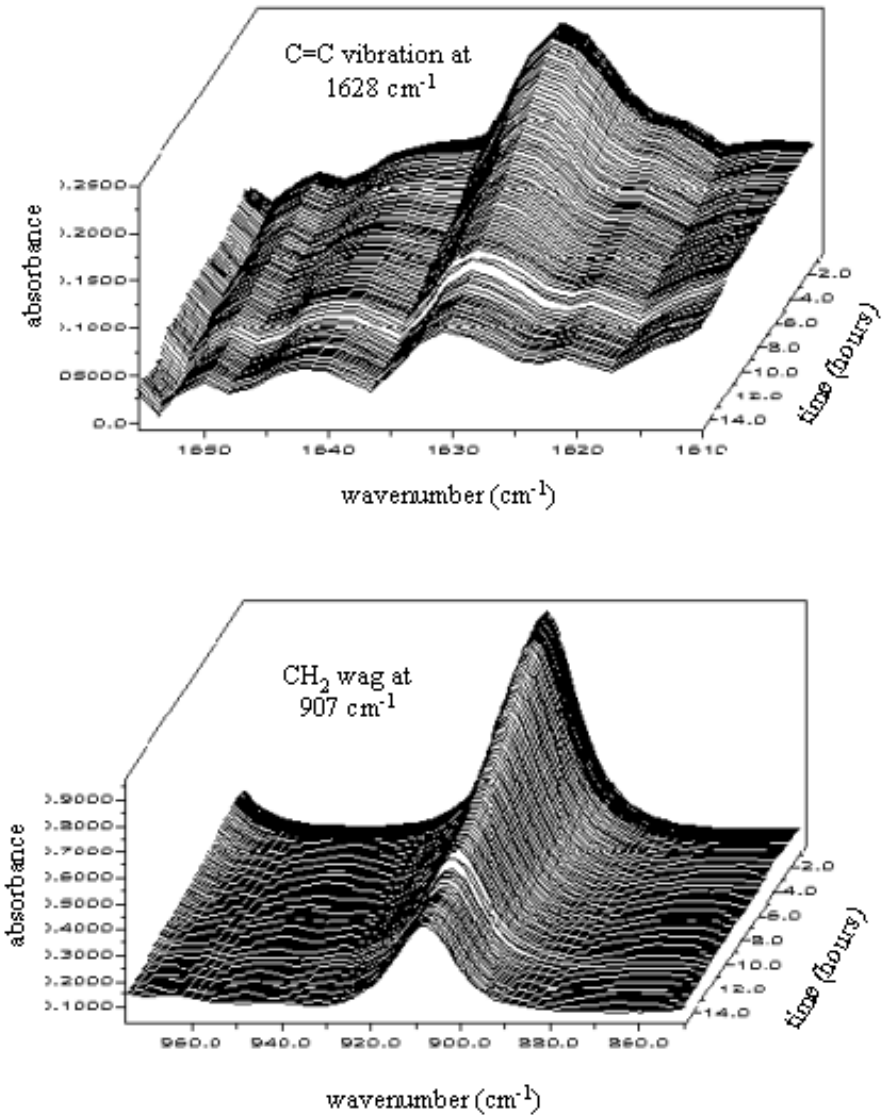

Figure 3.2 Real-time FTIR "waterfall plot" of styrene monomer: vinyl carbon-carbon (C=C) stretch at 1628 cm^{-1} (top) and vinyl carbon-hydrogen (=CH_2) wag at 907 cm^{-1} (bottom).

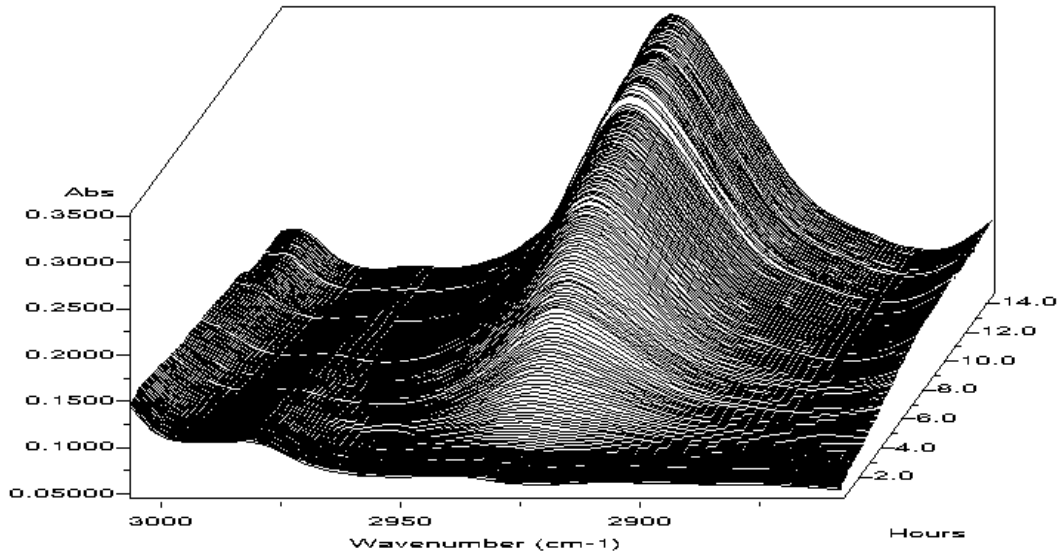

Figure 3.3 Real-time FTIR "waterfall" plot of increasing alkyl carbon-hydrogen absorbance at 2925 cm^{-1} during SFRP of styrene.

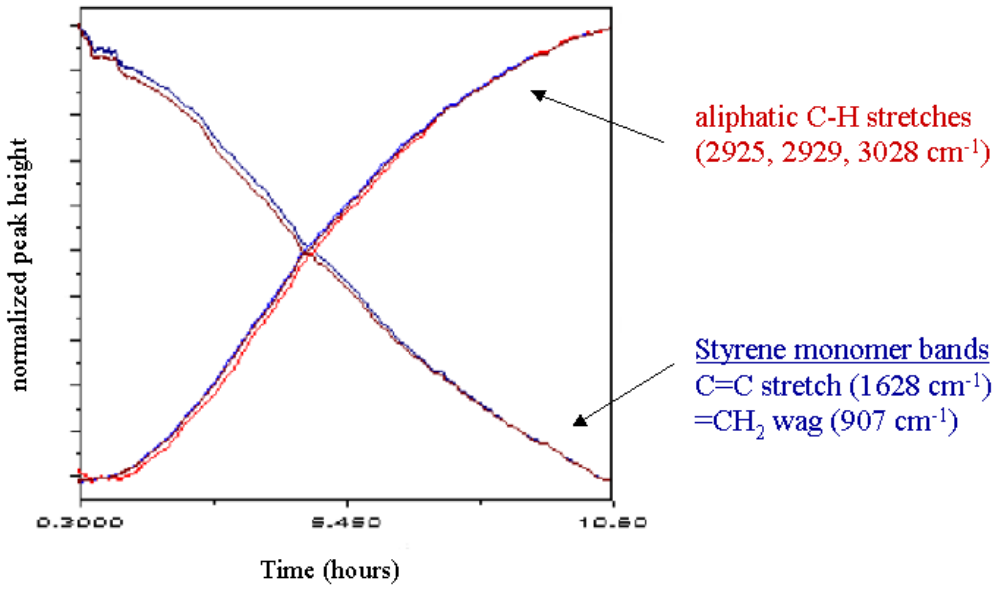

Figure 3.4 Real-time profiles of increasing alkyl carbon-hydrogen polymer peak heights (2925, 2929, and 3028 cm^{-1}) and decreasing vinyl monomer peak heights (907 and 1628 cm^{-1}).

3.4.3 Probing Bimolecular SFRP Initiation via *In situ* FTIR

The sensitivity and real time capability of the ReactIR 1000 allowed for the *in situ* detection of benzoyl peroxide (BPO) initiator decay and formation of the ester end group upon addition of the benzoyl radical to a styrene monomer. Initiation of the polymerization was followed using absorbance profiles of infrared absorbances associated with the initiator, benzoyl peroxide (BPO), as well as the ester end group that is formed from addition of the initiating radical to one styrene monomer. The FTIR absorbance profiles for BPO and the ester end groups are illustrated in Figure 3.5. Fortunately, the carbonyl and carbon-oxygen functionalities of the benzoyl peroxide initiator and ester end groups absorbed infrared light at different wavelengths and did not overlap, which enabled for their separate identification throughout the polymerization reaction using *in situ* FTIR. Two FTIR absorbances that were identified to be associated benzoyl peroxide initiator

were the carbonyl (C=O) stretch at 1767 cm^{-1} and carbon-oxygen-carbon (C-O-C) anti-symmetric stretch at 1223 cm^{-1}. These absorbances were observed to form immediately when benzoyl peroxide initiator was introduced to the reaction flask and then quickly disappear as the benzoyl peroxide dissociated at 132 ºC. Absorbances that were due to the ester groups that formed when the initiating benzoyl radical added to one styrene monomer (carbonyl (C=O) stretch at 1725 cm^{-1} and C-O-C anti-symmetric stretch at 1268 cm^{-1}) were identified and observed to increase during the same time period of benzoyl peroxide decay and then remain constant for the remainder of the reaction.

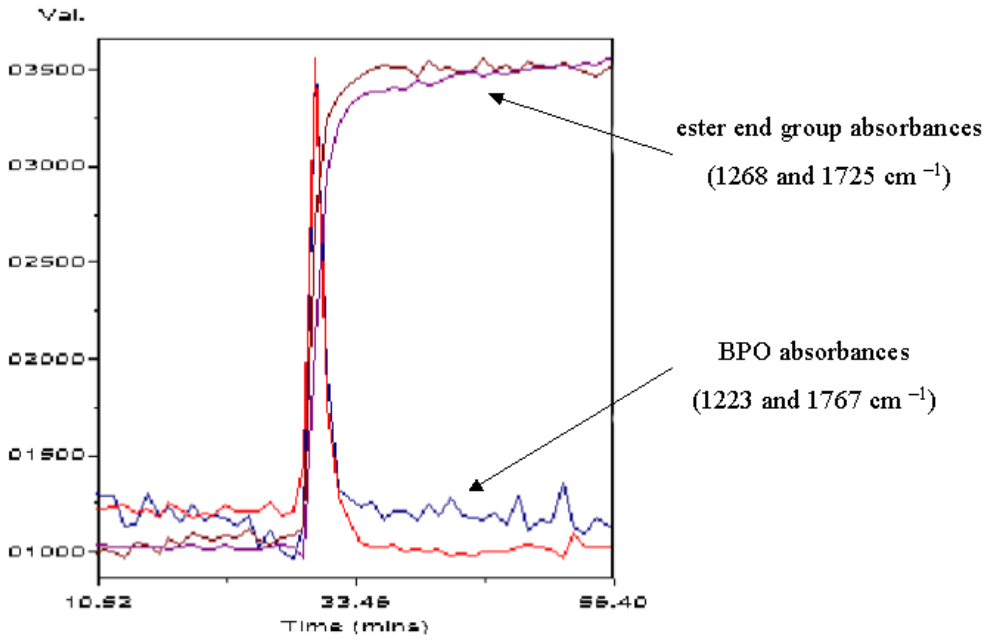

Figure 3.5 Real-time profiles of benzoyl peroxide (C=O at 1767 cm^{-1} and C-O-C at 1223 cm^{-1}) and forming polymer ester end group (C=O at 1725 cm^{-1} and C-O-C at 1268 cm^{-1}) during initiation stage of styrene SFRP.

Absorbance peak height profiles (y-axis) shown in Figure 3.5 were again normalized to allow for facile visual comparison of the multiple FTIR absorbances that were

monitored. After an elapsed time of 29 minutes and 9 seconds of data collection, the BPO/styrene solution was added to the TEMPO/styrene solution when the temperature of the reaction solution had stabilized at 132 °C. At the time of BPO addition to the reaction solution at 132 ºC, the FTIR absorbances due to BPO immediately appeared and then rapidly began to decrease and were completely absent after several minutes. Using the profile of the BPO carbonyl at 1767 cm^{-1}, the half-life of BPO in the presence of styrene and TEMPO at 132 °C was estimated to be approximately 50 seconds (Figure 3.6). An Arrhenius plot (Figure 3.7) constructed using this experimentally determined half-life of benzoyl peroxide at 132 ºC and known values[18] at other temperatures resulted in desirable linear relationship with very good correlation, which provided further confidence of the accurate experimental determination of benzoyl peroxide half-life using *in situ* FTIR.

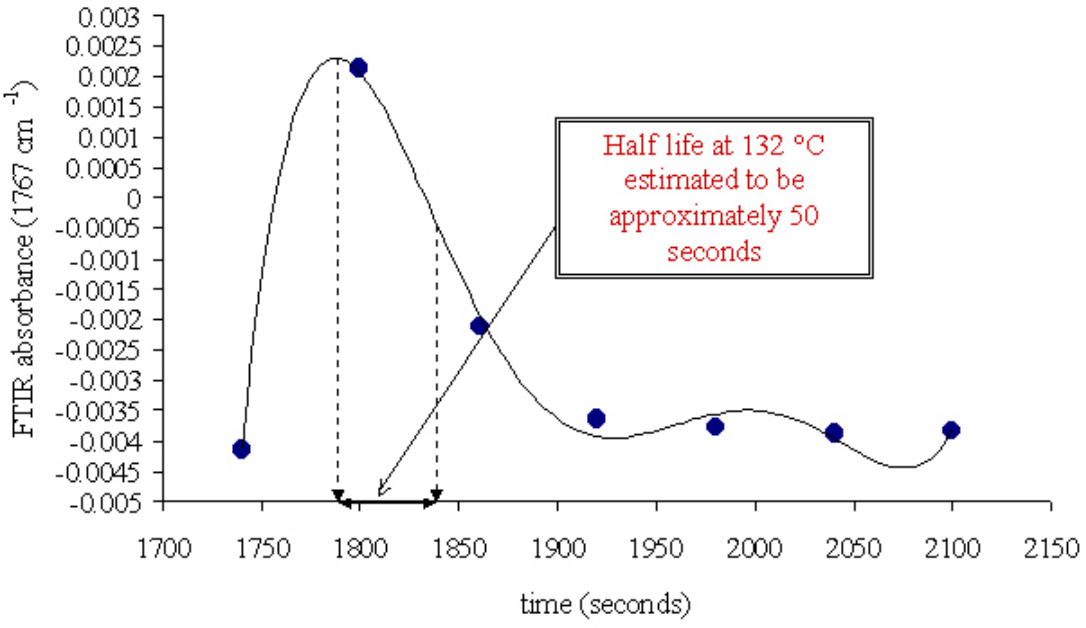

Figure 3.6 Benzoyl peroxide carbonyl FTIR absorbance (1767 cm^{-1}) profile upon addition to styrene monomer at 132 ºC.

[18] Odian, G. *Principles of Polymerization,* 3rd ed; Wiley & Sons: New York, 1991; p 215.

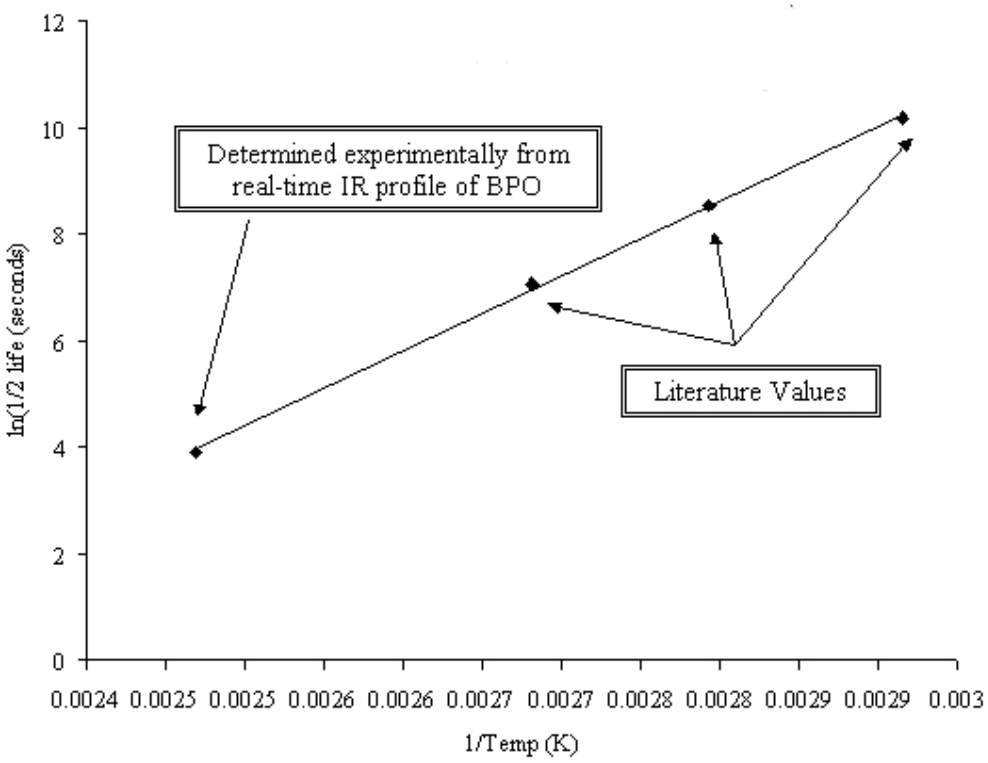

Figure 3.7 Arrhenius plot illustrating correlation of experimentally determined (*in situ* FTIR) half-life of benzoyl peroxide initiator (at 132 ºC) with literature values at various temperatures.

3.4.4 Kinetic Evaluation of SFRP

The kinetics of styrene nitroxide-mediated stable free radical polymerization were evaluated using monomer conversion data that was measured with *in situ* FTIR. The real-time decay profiles of the styrene monomer absorbances, which quantitatively correlates to the concentration of unreacted monomer, was used for calculating observed rate constants. Figure 3.8 depicts the first order kinetic plot constructed from the real-time profile for the decay of the vinyl carbon-hydrogen wag of the styrene monomer at 907 cm^{-1} for the polymerization at 132 °C. FTIR absorbance spectra were collected every minute for the

first 90 minutes and then every 5 minutes for the remainder of the reaction. The initial steep decrease in the absorbance seen in Figure 3.8 was attributed to the increasing temperature of the reaction mixture since benzoyl peroxide (BPO) was not added until a stable temperature was maintained and a constant FTIR absorbance at 907 cm^{-1} was observed. Once the reactor temperature stabilized, BPO was added to the reactor and the styrene vinyl carbon-hydrogen wag (907 cm^{-1}) was observed to decrease at a constant rate. Data from the real-time profile of the FTIR absorbance allowed for the calculation of an apparent first order rate constant from the slope of the line in Figure 3.8, which was equal to the rate of propagation times the concentration of growing polymer radicals ($k_{app}=k_p[P_n\bullet]$), assuming no termination or side reactions occur. From the first order kinetic plot, the apparent rate constant for the reaction was determined to be 2.1 x 10^{-5} s^{-1} at 132 °C and 1.2 x 10^{-5} s^{-1} at 126 °C. It is important to note that the rate constants determined using the $=CH_2$ absorbance (907 cm^{-1}) were in good agreement with the rate constants determined using the carbon-carbon double bond absorbance (1628 cm^{-1}). Although a stable baseline was difficult to identify for the lower intensity carbon-carbon double bond absorbance at 1628 cm^{-1}, the calculated apparent rate constant (k_{app}) at 132 °C was 2.0 x 10^{-5} s^{-1}, which agrees favorably with the value determined using the vinyl carbon-hydrogen absorbance at 907 cm^{-1}. Interestingly, it was observed that the slope of the line in Figure 3.8 was not completely linear over the entire polymerization process. It appeared that the rate of the reaction was slower earlier in the reaction and then increased later. Georges *et al.* observed a similar phenomenon and developed a germination efficiency factor to account for this initial non-linearity.[19] In addition, it was observed that at high conversion, the rate appeared to decrease. This decrease in rate at higher conversions may be attributed to the increasing solution viscosity and the inability of the magnetic stirrer to eliminate temperature gradients. In addition, propagation rate constants may decrease at high conversions due to radical termination reactions that result in decreasing the radical concentration.

---

[19] Veregin, R. P. N.; Odell, P. G.; Michalak, L. M.; Georges, M. K. *Macromolecules* **1996**, *29*, 2746.

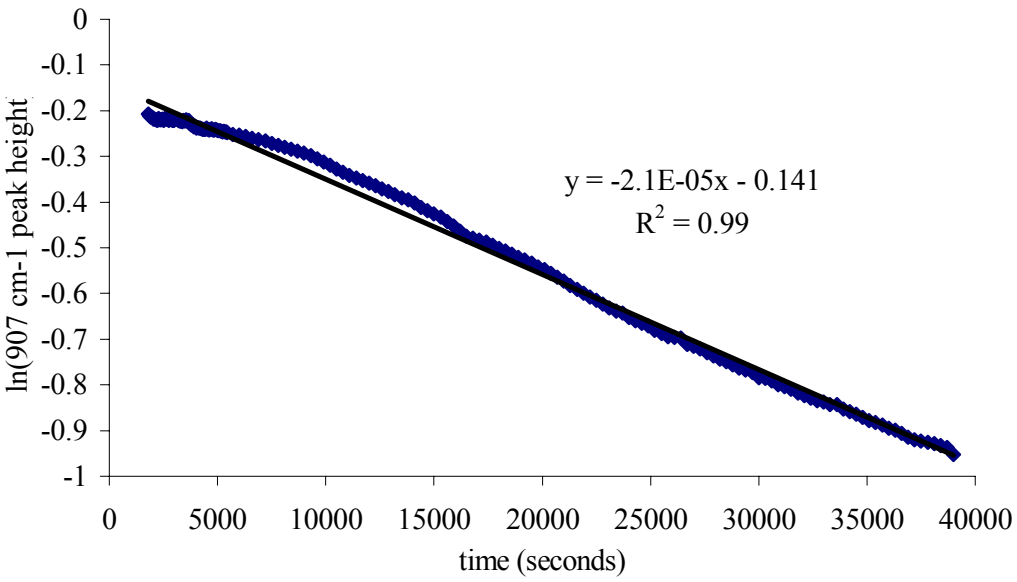

Figure 3.8 First order kinetic plot for styrene SFRP polymerization at 132 °C (determined from the real-time FTIR profile of the styrene $=CH_2$ absorbance (907 cm^{-1})).

3.4.5 Acetic Anhydride as a Rate Enhancing Additive for SFRP

A drawback of the nitroxide-mediated stable free radical polymerization process illustrated in Scheme 3.1 is that long reaction times are required to achieve high conversion and molecular weights (approximately 16 h to synthesize a polystyrene with number average molecular weight of 20,000 and a yield of 80%) using the bimolecular BPO/TEMPO initiator combination as shown in Scheme 3.2. In addition, styrene SFRP typically takes place at extreme reaction temperatures on the order of 125 ºC. At these extreme temperatures thermal initiation becomes an important consideration with respect to the controlled nature of the polymerization.[20] To address some of these issues, Georges and coworkers have investigated alternative reaction conditions for SFRP in an attempt to increase the reaction rate and still achieve controlled polymerization. One of their

[20] Hawker, C. J.; Bosman, A. W.; Harth, E. *Chem. Rev.* **2001**, *101*, 3661.

significant findings that they reported was that addition of camphorsulfonic acid dramatically increased the rate of styrene SFRP and high yields could be achieved with reaction times less than six hours.[21] Hawker and coworkers have also investigated the use of rate-accelerating additives for nitroxide-mediated SFRP.[22] They found that addition of acylating agents such as acetic anhydride to styrene SFRP dramatically reduced reaction time. As a potential explanation of the rate enhancement, they proposed a reversible acylation reaction of the alkoxyamine end group on the growing polymers chains (Scheme 3.3).

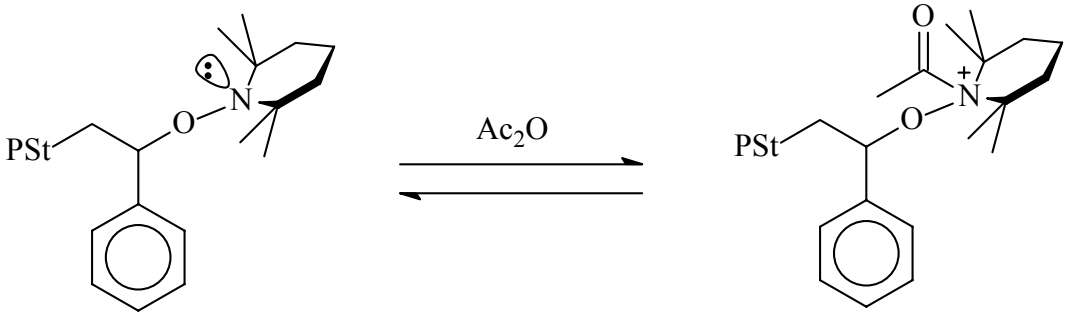

Scheme 3.3 Proposed acylation of alkoxyamine end group.

In situ FTIR was used to measure kinetic information for nitroxide-mediated stable free radical polymerizations of styrene with acetic anhydride added to the reaction to evaluate its rate enhancing effect. A styrene SPRP reaction with *in situ* FTIR monitoring was carried out exactly as described before except for the addition of acetic anhydride (2.0 mol equivalents to benzoyl peroxide) to the reaction mixture. The first-order kinetic plot of the reaction with and without added acetic anhydride is shown in Figure 3.9. Both reactions were carried out at 132 ºC until the viscosity of the bulk polymerizations had

[21] Georges, M. K.; Veregin, R. P. N.; Kazmaier, P. M.; Hamer, G. K.; Saban, M. *Macromolecules* **1994**, *27*, 7228.

increased to the point that notable stirring was no longer occurring. The observed rate constant for SFRP in the presence of acetic anhydride determined from the slope of the line in Figure 3.9 was 4.0 x 10^{-5} s^{-1}. Previously, k_{obs} for the polymerization in the absence of acetic anhydride was measured to be 2.1 x 10^{-5} s^{-1}, which is approximately one-half of the observed rate with added acetic anhydride. This result was consistent with earlier findings of Hawker and coworkers, which was that high conversions were achieved much quicker when acetic anhydride was added, but they did provide a quantitative measure of this rate enhancing effect.[22] As discussed earlier, the success of the controlled nature of nitroxide-mediated SFRP arises from the feature that the reversible nitroxide reaction results in a very low concentration of radicals and greatly decreases the likelihood for termination. The tradeoff of using an additive such as acetic anhydride is that the equilibrium of the capped and uncapped growing polymer radicals is shifted to the uncapped form, which results in increased propensity for radical-radical coupling reactions to occur. This phenomenon was observed to occur as a result of enhancing the rate *via* the addition of acetic anhydride. TEMPO-capped polystyrene that was prepared in the presence of acetic anhydride resulted in slightly less control as the number average molecular weight was measured to be 24,300 with a polydispersity of 1.18, which was not as narrow as the polydispersity (1.04) that was obtained under identical reaction conditions with the exception of acetic anhydride.

---

[22] Malmström, E.; Miller, R. D.; Hawker, C. J. *Tetrahedron* **1997**, *53*, 15225.

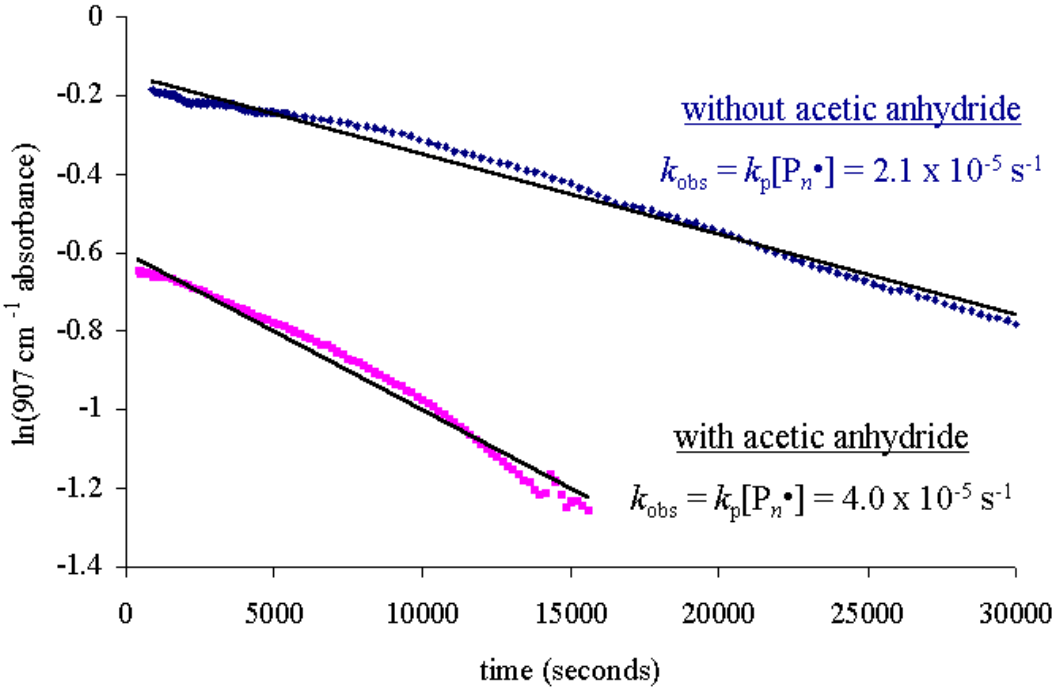

Figure 3.9 Psuedo first order kinetic plots illustrating the rate-enhancing effect of acetic anhydride on the nitroxide-mediated stable free radical polymerization of styrene.

3.5 CONCLUSIONS

Real-time mid-infrared spectroscopy (4000-650 cm^{-1}) monitoring was successfully utilized to follow radical initiation, monomer conversion, and polymer formation during the stable free radical polymerization (SFRP) of styrene initiated by benzoyl peroxide (BPO) in the presence of TEMPO. Apparent rate constants ($k_{app}=k_p[P_n\bullet]$) were calculated from real-time analysis to be 2.1 x 10^{-5} s^{-1} at 132 °C and 1.2 x 10^{-5} s^{-1} at 126 °C from the profile of the decaying absorbance of the monomer vinyl carbon-hydrogen wag at 907 cm^{-1}. The half-life of the benzoyl peroxide initiator at 132 °C in the presence of styrene and TEMPO was also determined from real-time analysis to be approximately 50 seconds. The initial results reported herein demonstrate the utility and application for this real-time analytical technique to provide mechanistic and kinetic information for

polymerization reactions. Furthermore, the ability to detect the initiator decay and formation of ester end groups demonstrates the sensitivity of *in situ* FTIR and the potential for the study of inter- and intra-molecular interactions as well as side reactions.

Acknowledgments. Financial support provided by the National Science Foundation (NSF CRIF 9974632), Jeffress Memorial Trust, and the Virginia Tech NSF Science & Technology Center is gratefully acknowledged.

Recommended future studies:

- Application of *in situ* mid-IR spectroscopy to elucidate polymerization mechanisms, kinetics, sequence distributions, and detrimental side reactions associated with conventional free radical polymerization, other controlled radical polymerization pathways, and anionic solution polymerization processes.
- Investigations of styrene SFRP using unimolecular initiators.
- Star and block shaped architectures using SFRP.
- More detailed investigation of side reactions during SFRP and determination of actual end group concentration at the end of reaction.

CHAPTER 4

Synthesis of Star-Shaped Polystyrene via Stable Free Radical Polymerization Polystyrene via SFRP

4.1 ABSTRACT

High molecular weight star-shaped polystyrenes were prepared via the coupling of 2,2,6,6-tetramethyl-1-piperidinyloxy (TEMPO) terminated polystyrene oligomers with divinylbenzene (DVB) in *m*-xylene at 138 °C. The optimum ratio of the coupling solvent (*m*-xylene) to divinylbenzene coupling agent was empirically determined to be 9 to 1 based on volume. Linear polystyrene oligomers (M_n = 19,300 g/mol, M_w/M_n = 1.10) were prepared in bulk styrene using benzoyl peroxide in the presence of TEMPO at approximately 130 °C under an inert atmosphere. Coupling of the TEMPO terminated oligomers under optimum conditions resulted in a compact and dense product with a number average molecular weight exceeding 300,000 g/mol (M_w/M_n = 3.03) after 24 h, suggesting the formation of relatively well-defined star-shaped polymers. In addition, the intrinsic viscosities and RMS radius of the star-shaped products were lower than calculated values for linear analogs of equivalent molecular weight, which further supported the formation of a star-shaped architecture.

4.2 INTRODUCTION

Star-shaped polymers have received significant attention due to their desirable properties that arise from having a highly branched structure.[1] A star structure is described as a nonlinear polymer composed of multiple backbone chains that emanate from junction points. Branching results in a more compact structure than analogous linear structures on account of high segment density, which dramatically affects crystalline, mechanical, and viscoelastic properties. The synthesis of star-shaped polymers has traditionally been accomplished using living polymerization methods including anionic,[2] cationic,[3] ring opening metathesis,[4] group transfer polymerization,[5] and transition metal catalysis.[6] The two primary approaches to star-shaped polymers using controlled polymerization methods are known as "arm-first" and "core-first".[7] The "core-first" approach involves the use of a multifunctional initiator which initiates the polymerization of multiple linear polymer chains. The "arm-first" approach involves coupling preformed linear polymer chains containing functionality at the chain end with a multifunctional coupling agent such as divinylbenzene (DVB). This approach results in a macromolecule with a network-like hub of the coupling agent and preformed linear polymers attached to the hub. The number of arms resulting from the "arm-first" approach is controlled by varying the molar ratio of the

---

[1] *Star and Hyperbranched Polymers*, Mishra, M. K., Kobayashi, S., Eds.; Marcel Dekker: New York, 1999. Roovers, J. in *Encyclopedia of Polymer Science and Engineering*, 2nd ed., Kroschwitz, J. I., Ed.; Wiley: New York, 1985, Vol. 2, p. 478.

[2] Quack, G.; Fetters, L. J.; Hadjichristidis, N.; Young, R. N. *Ind. Eng. Chem. Prod. Res. Dev.* 1980, *19*, 587. Martin, M. K. Ph.D. Dissertation, Virginia Polytechnic Institute and State University, Blacksburg, VA, 1980. Martin, K. M.; Ward, T. C.; McGrath, J. E. In *Anionic Polymerization: Kinetics, Mechanisms, and Synthesis*, McGrath, J. E., Ed.; ACS Symposium Series 166; American Chemical Society: Washington, DC, 1981. Hsieh, H. L.; Quirk, R. P. *Anionic Polymerization: Principles and Practical Applications*; Marcel Dekker: New York, 1996.

[3] Kennedy, J. P.; Iván, B. *Designed Polymers by Carbocationic Macromolecular Engineering: Theory and Practice*; Hanser Publishers: New York, 1992.

[4] Bazan, G. C.; Shrock, R. R. *Macromolecules* 1991, *24*, 817.

[5] Webster, O. W. *Macromol. Chem. Macromol. Symp.* 1990, *33*, 133.

[6] Kadokawa, J.; Kobayashi, S. *Macromol. Chem. Macromol. Symp.* 1995, *95*, 121.

[7] Rempp, P.; Franta, E.; Herz, J. *Adv. Polym. Sci.* 1988, *86*, 145.

multifunctional coupling agent to the preformed linear polymer chains. Long and coworkers have previously focused on living anionic polymerization in combination with terminal trialkoxysilane functionalization.[8] Subsequent polycondensation using acid catalyzed sol-gel reaction conditions resulted in the formation of narrow molecular weight distribution, star-shaped polymers.[8]

Synthetic methodologies for the preparation of macromolecules with complex architectures have been expanded in recent years as result of developments in controlled free radical polymerization methodologies such as stable free radical polymerization (SFRP)[9] and atom transfer radical polymerization (ATRP).[10] For example, Matyjaszewski and coworkers have recently reported the synthesis of star-shaped polystyrene by an "arm-first" approach via the coupling of polystyrene macroinitiators with divinylbenzene using copper mediated ATRP.[11] SFRP also provides a controlled route for the synthesis of branched architectures. Ide and Fukuda have reported the nitroxide-mediated (TEMPO-2,2,6,6-tetramethyl-1-piperidinyloxy) stable free radical copolymerization of styrene and 4,4'-divinylbiphenyl to produce a lightly crosslinked homogeneous material.[12] In addition, Solomon and coworkers have previously studied the synthesis of soluble microgels from the nitroxide-mediated stable free radical copolymerization of *tert*-butylstyrene and DVB.[13] Previously, our research efforts have included the use of *in situ* mid-infrared spectroscopy to probe psuedo first order kinetics of styrene SFRP.[14] The investigations herein describe the facile synthesis of star-shaped polystyrenes from the reaction of TEMPO-terminated polystyrene oligomers with DVB in *m*-xylene. These efforts represent the first successful solution coupling of TEMPO-terminated polystyrene oligomers using DVB in the absence of other comonomers.

---

[8] Long, T. E.; Kelts, L. W.; Turner, S. R.; Wesson, J. A.; Mourey, T. H. *Macromolecules* 1991, *24*, 1431.
[9] Hawker, C. J. *Acc. Chem. Res.* 1997, *30*, 373.
[10] Patten, T. E.; Matyjaszewski, K. *Adv. Mater.* 1998, *10*, 901.
[11] Xia, J.; Zhang, X.; Matyjaszewski, K. *Macromolecules* 1999, *32*, 4482.
[12] Ide, N.; Fukuda, T. *Macromolecules* 1999, *32*, 95.
[13] Abrol, S.; Kambouris, P. A.; Looney, M. G.; Solomon, D. H. *Macromol. Rapid Commun.* 1997, *18*, 755.
[14] Pasquale, A. J.; Long, T. E. *Macromolecules* **1999**, *32*, 7954.

4.3 EXPERIMENTAL

4.3.1 Materials

Benzoyl peroxide (BPO) and 2,2,6,6-tetramethyl-1-piperidinyloxy (TEMPO) were purchased from Aldrich and used as received. Styrene (Aldrich) was vacuum distilled (0.1 mm Hg) at room temperature from calcium hydride after degassing three times using the traditional freeze-thaw method. After distillation, styrene monomer was stored in a freezer in a septum-sealed bottle under positive nitrogen pressure (4-5 psi). Divinylbenzene (DVB) (80% DVB (mixture of isomers), 20% ethylvinylbenzene) was purchased from Aldrich, purified, and stored according to the procedure described above for styrene. *m*-Xylene (anhydrous, 99%, packaged under nitrogen in Sure/Seal bottle) was purchased from Aldrich and used as received.

4.3.2 Characterization

Molecular Weight Characterization

Molecular weights were determined via size exclusion chromatography (SEC) using an Alliance SEC system (Waters Corporation, Milford, MA) with external refractive index detector (Waters 410) and Viscotek T-60A viscometer/90° light scattering dual detector. The mobile phase used for SEC analysis was 1-methyl-2-pyrrolidinone (NMP) containing P_2O_5 (0.02 M) at 60 °C and a flow rate of 1.0 mL/min. Absolute molecular weights and intrinsic viscosities were calculated from SEC using Viscotek SEC^3 Triple Detection software.

Multiple Angle Laser Light Scattering (MALLS) measurements were performed using a miniDAWN (Wyatt Technology, Santa Barbara, CA) with 690 nm laser connected to a Waters SEC (515 pump, 717 autosampler, and 410 refractive index detector). The miniDAWN was connected in series after three 5-μm Plgel mixed-bed columns (Polymer

Laboratories, Amherst, MA). Measurements were made at 40 °C with THF as the solvent at a flow rate of 1.0 mL/min. The dn/dc of polystyrene in THF at 40 °C was determined (via miniDAWN) to be 0.185 mL/g using polystyrene standards of known molecular weight, and was consistent with literature values.[15]

In situ FTIR Spectroscopy

In situ mid-FTIR spectra were collected with a ReactIR 1000 (MCT detector, S/N = 7500, resolution = 4) (ASI Applied Systems, Millersville, MD, www.asirxn.com) reaction analysis system equipped with a light conduit and DiComp (diamond-composite) insertion probe. Reaction data was analyzed using ReactIR software. The details and capabilities of the ReactIR 1000 reaction analysis system based on attenuated total reflectance (ATR) have been described in detail previously.[16]

Thermal Analysis

Polymer glass transition temperatures were determined with a Perkin-Elmer Pyris 1 differential scanning calorimeter (DSC) at a heating rate of 10 °C/min with nitrogen flushing. Glass transition temperatures are reported as the inflection point of the change in heat capacity during the second heat. Thermogravimetric analysis (TGA) was carried out with a TA Instruments TGA 295Thermogravimetric Analyzer at a heating rate of 10 °C/min.

4.3.3 Synthesis of TEMPO-terminated Linear Polystyrene Oligomers

In a 100 mL, round-bottomed, two-necked flask that was fitted with the ASI DiComp probe was added a magnetic stir bar, styrene (40 mL, 350 mmol), 2,2,6,6-tetramethyl-1-piperidinyloxy (TEMPO) (0.368 g, 2.36 mmol), and benzoyl peroxide (BPO) (0.440 g,

---

[15] Brandrup, J., Immergut, E. H., E. A. Grulke, Eds. *Polymer Handbook,* 4th ed.; Wiley & Sons: New York, 1999; pp VII/585-586.
[16] Storey, R. F.; Donnalley, A. B.; Maggio, T. L. *Macromolecules* **1998**, *31*, 1523.

1.82 mmol). Although a magnetic stir bar did not provide adequate agitation at higher conversions due to the extremely high bulk viscosity, it facilitated (versus an overhead stirrer) the intimate contact of the reaction mixture with the ReactIR 1000 probe tip and reduced the possibility of oxygen intrusion into the reaction vessel. The flask was sealed under nitrogen with a rubber septum, and a thermocouple was inserted through the septum to simultaneously monitor the temperature of the reaction mixture. An oil bath at 134 °C was raised to the reaction flask. After several minutes, the temperature of the reaction mixture stabilized at 126 °C (The large temperature difference between the oil bath and reaction mixture was speculated to be due to the heat loss due to the stainless steel DiComp probe). The ReactIR was programmed to collect an FTIR spectra of the reaction mixture every 5 minutes (256 scans) and the reaction was then stirred at 126 °C for 20 h. The polymer product was cooled to room temperature, dissolved in chloroform, precipitated into methanol, and dried overnight under vacuum (65 °C) to yield 26.6 g (73 % conversion) of TEMPO-terminated polystyrene oligomers of M_n = 19,300 g/mol (M_w/M_n = 1.10). NMR analysis of the vacuum-dried TEMPO-terminated polystyrene indicated the absence of appreciable residual monomer and/or precipitation solvent.

4.3.4 Synthesis of Star-Shaped Polystyrene

A typical procedure for the synthesis of a star-shaped polystyrene *via* an arm-first approach is described. In a 100 mL, round-bottomed, three-necked flask that was fitted with a condenser, nitrogen inlet and outlet, and ASI DiComp probe was added a magnetic stir bar, 19,300 g/mol TEMPO-terminated polystyene (8.0 g, 0.444 mmol), divinyl benzene (DVB) (4.0 mL, 28.1 mmol), and *m*-xylene (36 mL). The ReactIR was programmed to collect an infrared spectrum every 5 minutes (256 scans) and the mixture was heated to the reflux temperature of *m*-xylene (138 °C) using a heating mantle and stirred via magnetic stir plate under a nitrogen atmosphere. After 24 h the viscosity of the reaction mixture had increased dramatically, but remained homogenous. Chloroform (~ 30 mL) was then added to dilute the reaction mixture. The polymer was precipitated into methanol (300 mL) and dried overnight in a vacuum oven (65 °C) to give 10.0 g (approximately 50 % conversion

of DVB assuming 100 % recovery of starting oligomers) of white powder. SEC analysis of the resulting product indicated the presence of unreacted starting oligomers (approximately 23 %, M_n = 19,600 g/mol, M_w/M_n = 1.04) as well as a high molecular weight product (approximately 77 %) of M_n = 319,300 g/mol (M_w/M_n = 3.03).

4.4 RESULTS AND DISCUSSION

4.4.1 Synthesis of Tempo-Terminated Precursor Polystyrene Arms

TEMPO terminated polystyrenes were prepared from the bulk stable free radical polymerization (SFRP) of styrene initiated by benzoyl peroxide (BPO) in the presence of TEMPO at 126 °C for 20 h (Scheme 4.1). Georges and coworkers have previously described in detail the nitroxide mediated free radical bulk polymerization of TEMPO-terminated polystyrene.[17] Linear TEMPO-terminated polystyrene oligomers with a M_n of 19,300 (M_w/M_n = 1.10) were prepared to be used as precursor arms in the synthesis of star polystyrenes using an "arm-first" approach. Previously, we have reported in detail the real-time monitoring of styrene SFRP via *in situ* mid-FTIR.[18] The linear TEMPO-polystyrene oligomers were isolated by precipitation into methanol from chloroform and dried under vacuum at 65 °C overnight. NMR analysis of the vacuum dried TEMPO-terminated polystyrenes indicated the absence of appreciable residual monomer and/or precipitation solvent.

---

[17] Georges, M. K.; Veregin, R. P. N.; Kazmaier, P. M.; Hamer, G. K. *Macromolecules* **1993**, *26*, 2987.
[18] Pasquale, A. J.; Long, T. E. *Macromolecules* **1999**, *32*, 7954.

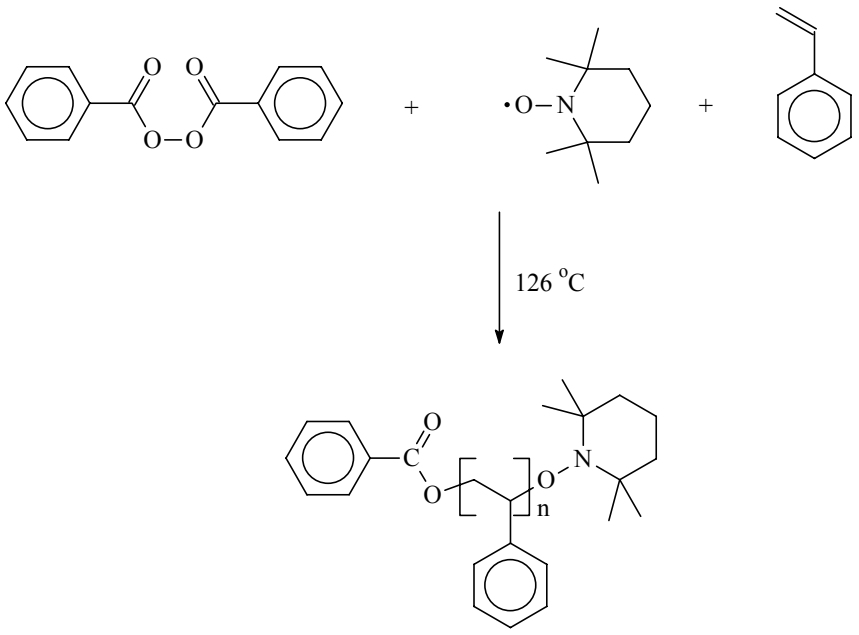

Scheme 4.1 Synthesis of TEMPO-terminated polystyrene oligomers.

4.4.2 Nitroxide Mediated SFRP of Star-Shaped Polystyrene

The synthetic scheme for the generation of star-shaped polystyrenes *via* the coupling of TEMPO terminated polystyrene oligomers with DVB is illustrated in Scheme 4.2. *m*-Xylene was used for the coupling solvent as the starting TEMPO terminated polystyrene oligomers were readily soluble in *m*-xylene. Initially, coupling reactions were attempted in bulk DVB with no solvent. The bulk coupling reaction of oligomers in DVB without *m*-xylene at 138 °C resulted in the rapid thermal polymerization of DVB to form an insoluble product. Coupling reactions were next carried out in *m*-xylene solvent and it was subsequently determined that a well-defined ratio of DVB coupling agent to *m*-xylene was an important consideration for the successful coupling of the starting oligomers with DVB. Experimental evidence indicated that a 90:10 *m*-xylene:DVB (relative volumes) was the optimum ratio based upon SEC analysis of the coupled polymers. Although xylene contains benzylic hydrogens that undergo appreciable chain transfer under free radical conditions, it conveniently has a high enough reflux temperature for homolytic cleavage of

the TEMPO end groups to occur. Subsequent SFRP investigations have compared xylene to chlorobenzene. Chlorobenzene, which has a significantly lower chain transfer, would be expected to give narrower molecular weight distributions and better molecular weight control. However, it was observed that styrene SFRP in both xylene and chlorobenzene solvents gave similar molecular weights and molecular weight distributions.[19] It is suspected that the low concentration of radicals that are present during the SFRP process decreases the occurrence of detrimental chain transfer. In addition, xylene solvent has previously been used successfully for kinetic investigations of the SFRP process.[20]

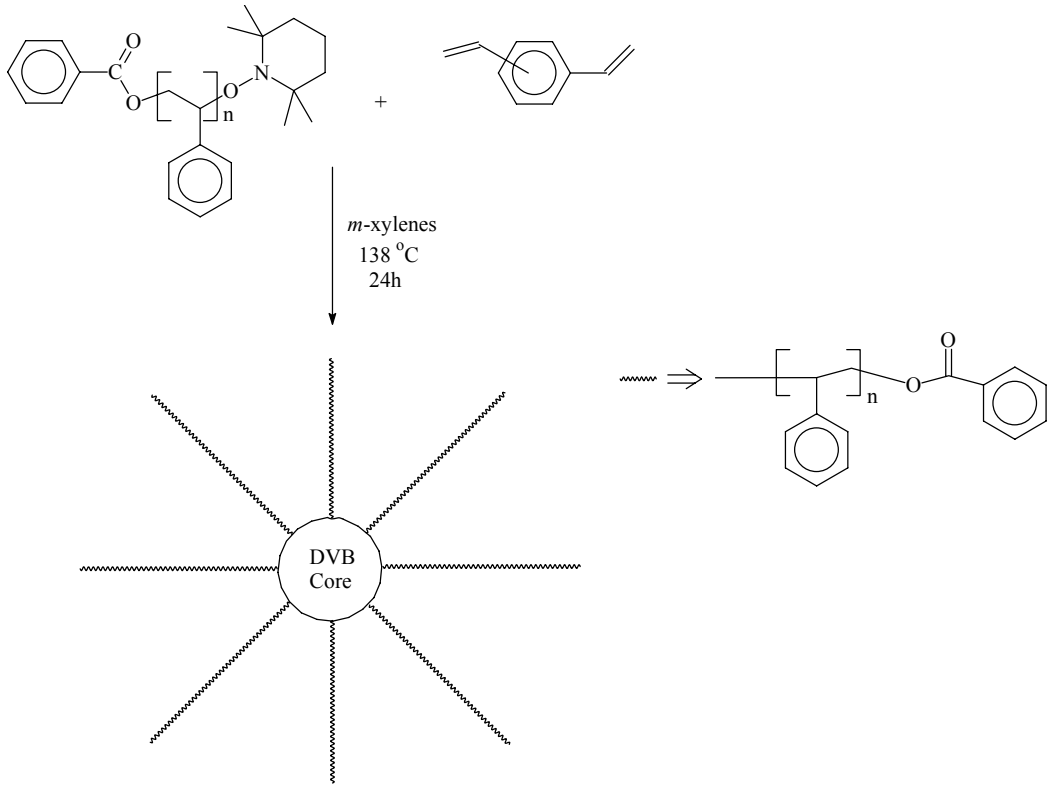

Scheme 4.2 Synthesis of star-shaped polystyrene via divinylbenzene (DVB) coupling of TEMPO terminated oligomers.

[19] Lizotte, J. R.; Long, T. E., unpublished results.
[20] Moffat, K. A.; Hamer, G. K.; Georges, M. K. *Macromolecules* **1999**, *32*, 1004.

Table 4.1 Effect of coupling reaction conditions on star-shaped polystyrene formation.

	Time (hours)	DVB/PS[a]	*m*-xylenes/DVB (mL/mL)	Results
A	24	3.22	176	no reaction
B	24	6.42	88	no reaction
C	24	34.0	18	no reaction
D	24	1360	-	gel
E	24	678	1.0	gel
F	24	67.8	5	gel
G	24	67.8	8	gel
H	24	67.8	9	$M_n = 319{,}000$ ($M_w/M_n = 3.03$)
I	48	67.8	9	$M_n = 874{,}000$ ($M_w/M_n = 5.52$)
J	24	67.8	10	no reaction

[a] Molar ratio of DVB to linear TEMPO-terminated polystyrene chains (based upon a number average molecular weight of 19,300 g/mol). Coupling was performed at the reflux temperature of *m*-xylene (138 °C).

4.4.3 Effect of Solvent to DVB Ratio

Table 4.1 depicts the effect of the *m*-xylene:DVB ratio and polymer concentration on the ability of the TEMPO terminated oligomers to efficiently form coupled star-shaped polymers. Only reactions (**H** and **I**) using a 9.0 to 1.0 volume ratio of *m*-xylene to DVB produced soluble high molecular weight DVB coupled product. Reaction **G**, which was carried out at an 8 to 1 volume ratio of *m*-xylene to DVB produced an insoluble gel while reaction **J** using a 10 to 1 volume ratio of *m*-xylene did not undergo reaction after 24 h. All coupling reactions were degassed using a nitrogen purge and were conducted under a nitrogen atmosphere while refluxing in *m*-xylene (138 ºC). It is proposed that this narrow reaction window may be due to oxygen ingress into the reaction vessel under refluxing conditions and future efforts will involve coupling reactions in an inert closed system below the reflux temperature of the *m*-xylene. The reaction contents remained

homogeneous throughout the coupling process and only a slight discoloration was observed as a function of time. In particular, the formation of gels or insoluble cross-linked particles using a 90:10 *m*-xylene:DVB ratio was not observed. The polymer was readily precipitated into methanol and the white polymer product was dried at 65 °C for 18 hours to ensure the absence of residual solvent.

4.4.4 SEC Analysis

SEC analysis, as depicted in Figure 4.1 and Figure 4.2, confirmed the coupling of TEMPO terminated chain ends with divinylbenzene to form a star-shaped polymer structure. The relative size of the core versus the number of polymer chains is anticipated to be a function of the ratio of DVB to oligomer, and initial investigations have focused on a 1 to 2 weight ratio of DVB to polystyrene oligomer (67.8/1.0 DVB/PS molar ratio based upon a polystyrene number average molecular weight of 19,300 g/mol; see Table 4.1). The effect of oligomer molecular weight will be reported in a subsequent publication. Figure 4.1 and Figure 4.2 indicate that approximately 77% of the polystyrene oligomer chains are coupled to form a higher molecular weight branched product and approximately 23% remains as unreacted starting oligomers. The lower molecular weight peak of the DVB coupled oligomers in the SEC chromatograms was super-imposable with the precursor oligomers indicating the presence of residual, uncoupled, starting oligomer. After 24 h (Figure 4.1) the symmetrical high molecular weight peak had a number average molecular weight of 319,000 g/mol (M_w/M_n = 3.03). It is important to note that the molecular weight reported for the coupled high molecular weight product is the molecular weight calculated using just the high molecular weight peak in the bimodal GPC trace (*i.e.* baseline separation permitted facile analysis of each peak).

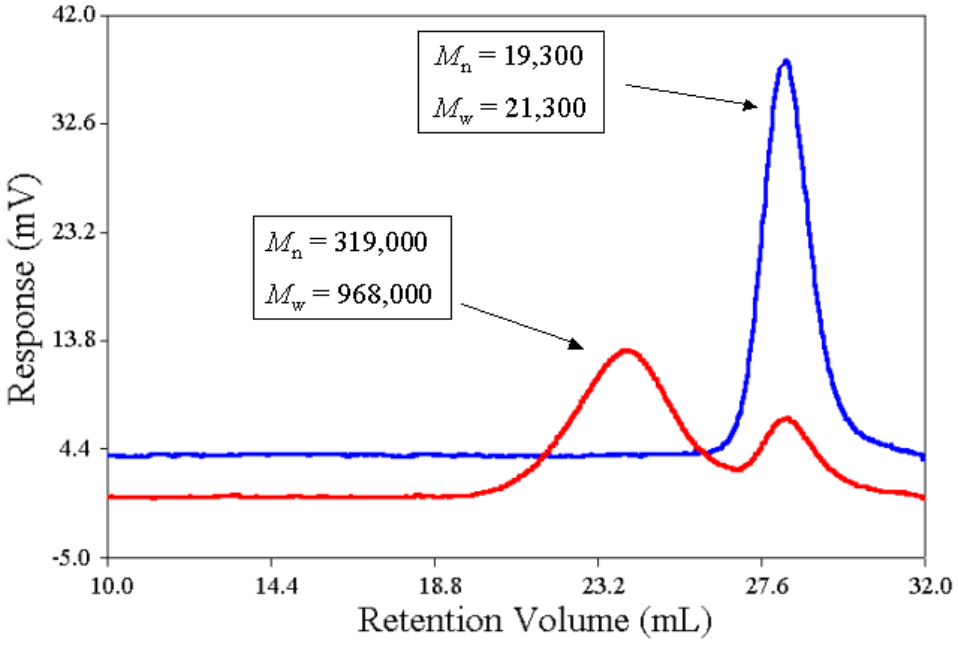

Figure 4.1 Size exclusion chromatographic analysis of precursor arm oligomer and star-shaped polystyrene after 24 h in *m*-xylene at 138 °C.

Figure 4.2 illustrates the broad and unsymmetrical SEC chromatogram of the coupling reaction after 48 h. Approximately the same amount (23%) of the starting oligomers remains after 48 h, indicating that further reaction after 24 h is occurring between the already formed high molecular weight material. It is proposed that during the first 24 h of the coupling reaction, well-defined stars are forming from the coupling of TEMPO-terminated polystyrene oligomers with DVB. The broad molecular weight distribution that results after 48 h is suspected to be due to less-controlled star-star coupling.[21] In addition, the lack of quantitative participation of the starting oligomer in the coupling process may be due to either the absence of TEMPO functionality or less than quantitative coupling.

[21] Martin, M. K. Ph.D. Dissertation, Virginia Polytechnic Institute and State University, Blacksburg, VA, 1980.

Furthermore, only high molecular weight coupled product and starting oligomer were observed in the chromatograms as illustrated in Figure 4.1 and Figure 4.2. In combination with SEC, gravimetric analysis based on isolated yields (50% conversion of DVB assuming 100% recovery of starting oligomers) also supported the coupling of the oligomers with DVB.

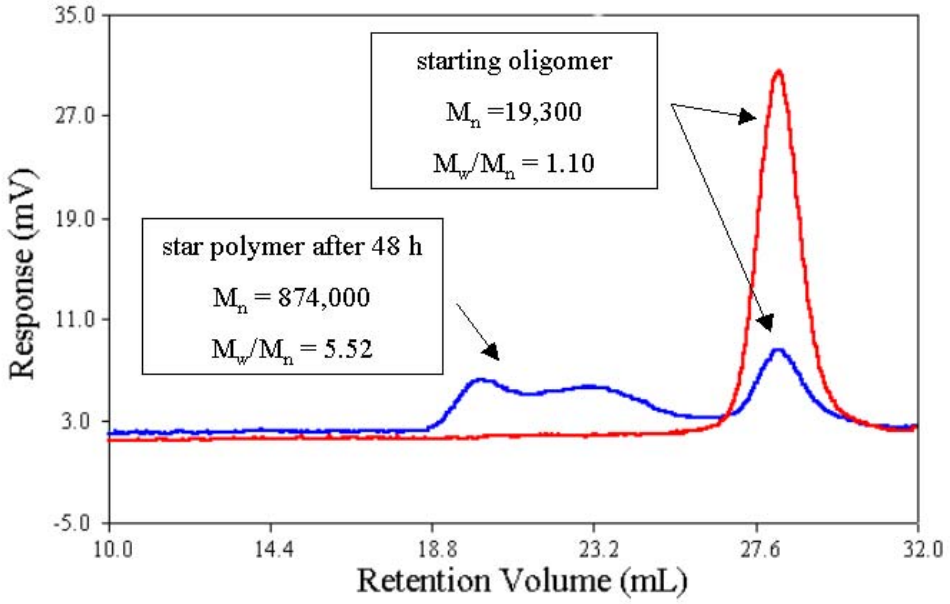

Figure 4.2 Size exclusion chromatographic analysis of precursor arm oligomer and star-shaped polystyrene after 48 h in *m*-xylene at 138 °C.

4.4.5 Control Reaction in Absence of DVB Coupling Component

In order to further support that DVB participated in the formation of the high molecular weight branched products, TEMPO terminated oligomers were heated in the absence of DVB and SEC analysis was utilized to confirm the absence of branching. Figure 4.3 depicts the SEC chromatogram for the precursor TEMPO terminated oligomer

and the product after subjecting the oligomer to coupling reaction conditions in the absence of DVB. The two chromatograms in Figure 4.3 are super-imposable indicating no coupling in the absence of DVB.

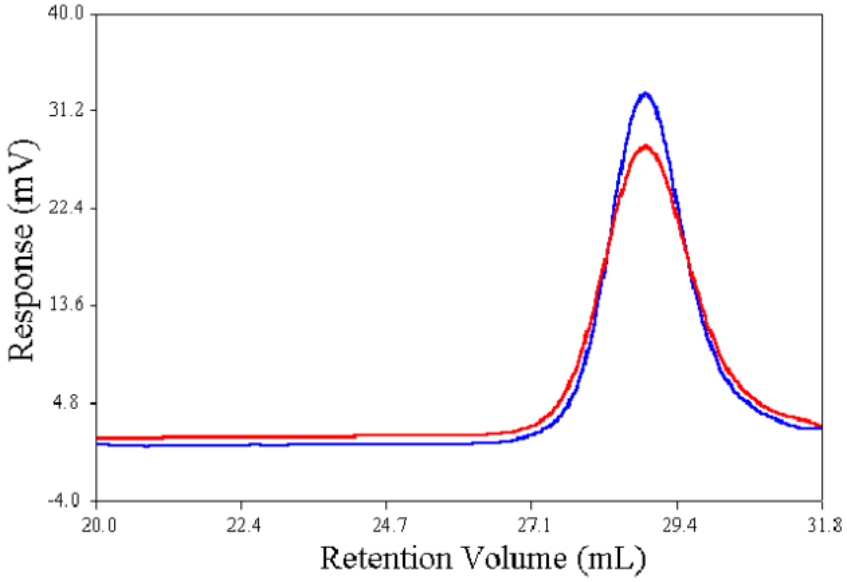

Figure 4.3 Size exclusion chromatographic analysis of precursor arm oligomer before and after 24 h in *m*-xylene at 138 °C.

4.4.6 FTIR Kinetic Analysis of DVB Coupling Reaction via SFRP

In situ mid-FTIR was used to monitor the coupling of TEMPO-terminated polystyrene oligomers with DVB. The ReactIR 1000 reaction analysis system was programmed to collect an infrared spectrum of the reaction contents every 5 min. DVB exhibited two strong infrared absorbances characteristic of the vinyl functional group that were easily monitored (carbon-hydrogen wag (=CH_2) at 907 cm^{-1} and the carbon-hydrogen out-of-plane deformation (=CH) at 983 cm^{-1}). The waterfall plot of the collected spectra showing the =CH_2 absorbance region is illustrated in Figure 4.4. Kinetic analysis of the reaction was performed from the absorbance data obtained using *in situ* mid-FTIR. Figure

4.5 depicts a pseudo-first order kinetic analysis of the DVB coupling reaction. The natural log of the $=CH_2$ absorbance at 907 cm^{-1} was plotted against time (seconds) to produce a straight line whose slope is equal to an observed rate constant (k_{obs} = 3.9 x 10^{-6} s^{-1}) for the coupling reaction, which indicates a controlled first order rate for the solution reaction of DVB with TEMPO-terminated polystyrene oligomers. For comparison, the observed first order rate constant measured for the nitroxide-mediated stable free radical polymerization of styrene was 2.1 x 10^{-5} s^{-1} for the bulk free radical polymerization of styrene in the presence of TEMPO at 132 °C.

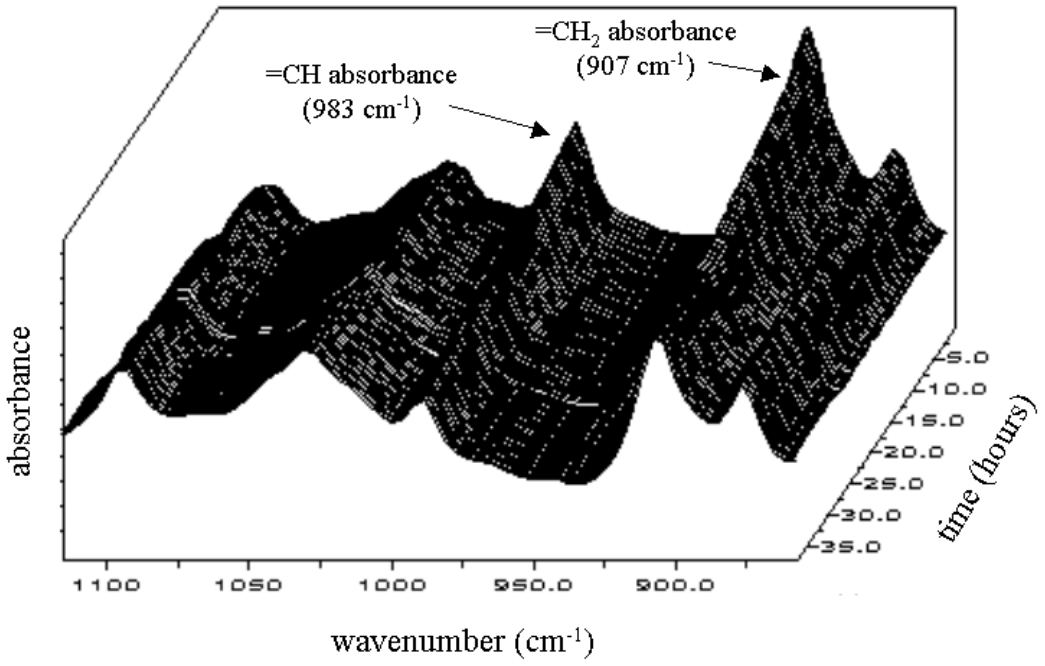

Figure 4.4 Real-time FTIR waterfall plot of DVB $=CH_2$ wag at 907 cm^{-1} and =CH out-of-plane deformation at 983 cm^{-1}.

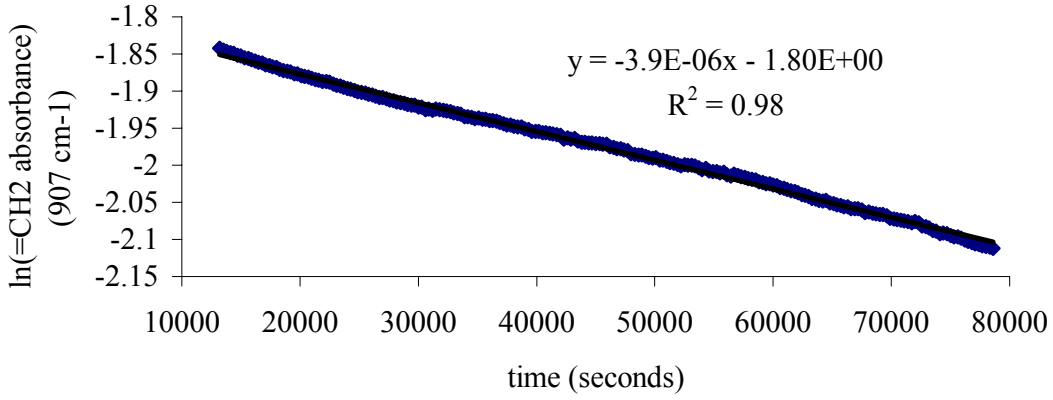

Figure 4.5 First-order kinetic plot for DVB coupling of TEMPO-terminated polystyrene oligomers (determined from the real-time FTIR profile of the DVB $=CH_2$ wag at 907 cm^{-1}).

4.4.7 Viscosity and Light Scattering Analysis

Intrinsic viscosities for branched structures are typically lower than linear macromolecules of equivalent molecular weight. The intrinsic viscosities for the 319,000 g/mol molecular weight branched product (**H**) were measured to be approximately 0.30 dL/g (NMP/0.02M P_2O_5, 60 °C), and theoretical values (calculated from Mark-Houwink-Sakurada relation using parameters obtained from SEC analysis of linear polystyrene) for linear polystyrene with equivalent weight average molecular weights were approximately 0.60 dL/g. The lower solution viscosities were indicative of a branched architecture. Differential scanning calorimetry (DSC) was utilized for the determination of glass transition (T_g) temperatures, and the star polymers exhibited T_g values (100 °C) consistent with high molecular weight polystyrene.

Multiangle laser light scattering (MALLS) was used to determine the root mean square (RMS) radius for the 319,000 g/mol branched products. RMS radius (often called

the radius of gyration) describes the size of a particle in a solution, regardless of its shape. The theory and experimental details of MALLS has been reviewed previously.[22] Typically, the z-average moments for a macromolecular particle are the most accurate for describing and comparing size information. The branched product from reaction **H** has a z-average molecular weight of approximately 1.5 million and a z-average RMS radius of 19 nm via MALLS. In order to estimate the RMS radius for linear polystyrene of equivalent molecular weight, we referred to the experimentally determined relationship between the molecular weight and RMS radius of linear polystyrene in THF solvent (RMS radius = 0.014 x $M^{0.585}$ (nm)) reported by Podzimek.[23] Consequently, the theoretical calculated value for 1.5 million g/mol linear polystyrene is approximately 57 nm using this relationship. The branching ratio (g_M)[24] can then be determined accordingly: $g_M = (RMS_{branched})^2/(RMS_{linear})^2$. The branching ratio for material **H** is then estimated from: $(19)^2/(57)^2 = 0.11$. The branching ratio compares the radii of branched and linear macromolecules of equivalent molecular weight and as branched macromolecules are more compact than linear counterparts, the ratio is always less than 1. A branching ratio of 0.11 suggests that the coupled star-shaped macromolecules reported here have a very dense and compact structure.

4.5 CONCLUSIONS

High molecular weight star-shaped polystyrenes were prepared via the coupling of TEMPO-terminated polystyrene oligomers with divinylbenzene (DVB) in *m*-xylene at 138 °C. Special attention was devoted to the determination of optimum coupling reaction conditions including the determination of the optimum ratio of the coupling solvent to divinylbenzene (9 to 1 by volume). Linear polystyrene oligomers (M_n =19,000 g/mol) were prepared in bulk styrene using benzoyl peroxide in the presence of TEMPO at

---

[22] Wyatt, P. J. *Anal. Chim. Act.* **1993**, *1*, 272.
[23] Podzimek, S. *J. Appl. Polym. Sci.* **1994**, *54*, 91.
[24] Zimm B. H.; Stockmayer, W. H. *J. Chem. Phys.* **1949**, *17*, 1301.

approximately 126 °C under an inert atmosphere. Coupling of the TEMPO terminated oligomers using optimum reaction conditions resulted in products with number average molecular weights exceeding 300,000 g/mol, suggesting the formation of relatively well-defined star-shaped polymers. The stability of the TEMPO terminated oligomers was investigated at coupling reaction conditions in the absence of DVB. SEC chromatograms of the precursor TEMPO terminated oligomer and a sample subjected to the coupling conditions in the absence of DVB were super-imposable indicating the absence of appreciable molecular weight change. In addition, intrinsic viscosity measurements in NMP/0.02M P_2O_5 at 60 °C supported the formation of a star-shaped architecture. The measurement and evaluation of size information via MALLS further supports the formation of compact highly branched star-shaped products. The preliminary results described herein demonstrate the utility of this method to form star-shaped polymers via nitroxide mediated stable free radical polymerization using an arm-first method.

Acknowledgments. Financial support provided by the Jeffress Memorial Trust, Virginia Tech Department of Chemistry, and the National Science Foundation (CRIF CHE-9974632) is gratefully acknowledged. The authors also thank Dr. H. K. Shobba for SEC results.

Recommended future studies:

- Investigation of the effect of starting precursor arm length on the synthesis of star-shaped polymers using nitroxide mediated SFRP.
- Investigate concentration of active TEMPO-capped chains versus "dead" uncapped chains of the precursor arms.
- Investigate SFRP star synthesis using additional monomers (acrylates, methacrylates, dienes, etc.) and other coupling agents.

CHAPTER 5

Determination of Monomer Reactivity Ratios Using *In situ* FTIR Spectroscopy for Maleic Anhydride/Norbornene Free Radical Copolymerization

5.1 ABSTRACT

Monomer reactivity ratios for maleic anhydride (MAH)/norbornene (Nb) free radical copolymerizations were estimated using the linear graphical method, which is based upon the terminal model developed by Mayo and Lewis. Reactions were carried out using optimized reaction conditions that were previously determined for MAH/Nb copolymerizations (3 mol % AIBN initiator, 60 % solids in THF, 65 °C, 24 h). Copolymerization data was collected via *in situ* FTIR to low degrees of conversion (approximately 10 %) for copolymerizations of MAH and Nb. Five different MAH/Nb comonomer feed compositions were analyzed: 40/60, 45/55, 50/50, 55/45, and 60/40. Conversion data measured with *in situ* FTIR was then employed in conjunction with the rearranged copolymer composition equation to estimate MAH and Nb reactivity ratios. Both of the reactivity ratios were estimated using this method to be near zero (r_{MAH} = 0.02, r_{Nb} = 0.01), which was indicative of an alternating copolymerization mechanism.

5.2 INTRODUCTION

The most simple quantitative statistical treatment for the determination of copolymerization composition, which is generally referred to as the terminal model, was first hypothesized by Dostal[1] in 1936 and later elucidated by others.[2] The terminal model is based upon the assumption that the chemical reactivity of a propagating polymer chain is independent of the size or composition of the chain and is only influenced by the terminal propagating repeat unit. Though the terminal model is dependent on several assumptions and may not be the most accurate model to describe a copolymer process, it is relatively simple to apply and provides a facile starting point when evaluating copolymerizations of various monomer pairs. When two monomers, M_1 and M_2 are copolymerized by free radical methods, four reactions are feasible according to the terminal model:

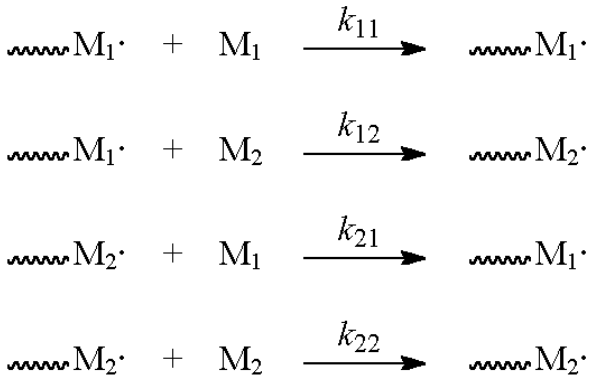

Figure 5.1 Terminal model of copolymerization.

[1] Dostal, H. *Monatsh. Chem.* **1936**, *69*, 424.
[2] Mayo, F. R.; Lewis, F. M. *J. Am. Chem. Soc.* **1944**, *66*, 1594. Alfrey, T., Jr.; Goldfinger, G. *J. Chem. Phys.* **1944**, *12*, 115. Wall, F. T. *J. Am. Chem. Soc.* **1944**, *66*, 2050.

Where k_{11} is the rate constant for the addition of a propagating chain ending in M_1 adding to monomer M_1, k_{12} is the rate constant for the addition of a propagating chain ending in M_1 adding to monomer M_2, and so on. The rate constants can then be expressed in terms of the monomer reactivity ratios, r_1 and r_2, where $r_1 = k_{11}/k_{12}$ and $r_2 = k_{22}/k_{21}$. Monomer reactivity ratios may either be experimentally[3] determined or estimated[4] and for free radical polymerizations are generally independent of initiator and solvent with only slight temperature dependence. The different types of copolymerization behavior can then be described based upon the values of the monomer reactivity ratios. "Random copolymerization" results when $r_1 = r_2 = 1$ due to the equal reactivity of the monomers toward both types of propagating chain ends and the resulting copolymer composition will directly reflect the comonomer feed. When $r_1r_2 = 1$, the two different types of propagating chain ends both add preferentially to one of the monomers, which is described as "ideal copolymerization". The case when r_1 and r_2 are much greater than one results in a tendency to form blocks of both monomers and is appropriately termed "block copolymerization". Alternating copolymerization, which describes the situation when $r_1 = r_2 = 0$, is an example of chain copolymerization where each of the monomers adds preferentially to the other, which results in an alternating monomer sequence distribution along the backbone.[5] Monomers that are difficult to homopolymerize are often found to be capable of undergoing alternating copolymerization. For example, if a strong electron acceptor is added together with a strong electron donor, regular alternating copolymers may result from either spontaneous initiation or a free radical source.[6]

The mechanisms of most typical copolymerizations fall somewhere between the extremes of "ideal copolymerization" and "alternating copolymerization". The mechanism of copolymerization becomes increasingly "alternating" as the r_1r_2 product decreases from

---

[3] *Polymer Handbook,* 3rd ed.; Brandrup, J., Immergut, E. H., Eds.; Wiley & Sons: New York, 1989; Chapter 2, p 153.
[4] Alfrey, T., Jr.; Price, C. C. *J. Polym. Sci.* **1947**, *2*, 101.
[5] Odian, G. *Principles of Polymerization*, 3rd ed.; Wiley & Sons: New York, 1991; Chapter 6.
[6] Cowie, J. M. G. In *Comprehensive Polymer Science*; Allen, G., Bevington, J. C., Eastmond, G. C., Ledwith, A., Russo, S., Sigwalt, P., Eds.; Pergamon: Oxford, England, 1989; Vol. 4, Chapter 22.

one toward zero. For polymerizations where the r_1r_2 product lies somewhere between zero and one, the composition of the copolymer can be controlled to some extent by variation of the monomer feed ratio. However, as r_1r_2 approaches very close to zero, the "alternating" behavior of the polymerization mechanism becomes the dominate factor and a 1:1 alternating copolymer can be formed independent of the monomer feed ratio.

The terminal model also provides a useful means to approximate copolymer compositions that are dependent on such factors as the comonomer feed ratio and the reactivities of the comonomers according to the model. The Mayo-Lewis equation,[7] which is derived from the terminal model using the assumption of the steady-state radical approximation, can be used to describe the instantaneous copolymer composition:

$$\frac{d[M_1]}{d[M_2]} = \frac{[M_1](r_1[M_1]+[M_2])}{[M_2]([M_1]+r_2[M_2])}$$

Figure 5.2 Mayo-Lewis copolymer composition equation.

Where r_1 and r_2 are the respective monomer reactivity ratios. $[M_1]$ and $[M_2]$ describe the starting concentrations in the comonomer feed. The instantaneous mole fractions of the two repeating units in the copolymer are then defined as $d[M_1]/d[M_2]$. The terminal model, therefore, allows one to predict the instantaneous copolymer composition for a given comonomer feed simply on the basis of the comonomer reactivity ratios. Although the terminal model relies on several assumptions and may not be the most reliable model to describe a copolymerization process, it is has the advantages of being simple to apply and very useful as a starting point to study a given copolymerization reaction.

---

[7] Mayo, F. R.; Lewis, F. M. *J. Am. Chem. Soc.* **1944**, *66*, 1594.

Maleic anhydride (MAH) is the most widely studied comonomer for producing alternating copolymers. MAH is a very strong electron acceptor that has been shown to homopolymerize poorly,[8] but will react with a number of electron donating monomers to form alternating copolymers.[9] Of particular interest is that many 1,2-disubstituted and cyclic olefins such as norbornene, that do not homopolymerize by free-radical methods, will form alternating copolymers with maleic anhydride. Recently, main-chain alicyclic macromolecules produced from the alternating free radical copolymerization of MAH with norbornene and norbornene derivatives have received attention as photoresist materials for 193 nm lithography.[10] Cyclic olefins such as norbornene will not homopolymerize to appreciable amounts via free radical methods. However, when cyclic olefins are reacted with maleic anhydride, which is a strong electron acceptor, in the presence of a free radical initiator, copolymerization occurs in an alternating manner. In addition, maleic anhydride also serves to incorporate oxygen into the material, providing necessary adhesion and solubility properties that are required for imaging performance while still retaining sufficient etch resistance to be successfully demonstrated as 193 nm resist materials.[11] The cyclic olefin character of these materials provides for excellent etch resistance, surpassing even currently utilized phenol based resists. Furthermore, the increased etch resistance is of great importance because of the decreasing film thickness necessary for the achievement of increasingly smaller feature sizes. In addition, the ability to modify polymer properties via incorporation of cyclic olefin monomer derivatives has further made this a very attractive route to new materials for 193 nm lithography.

---

[8] For a general review of maleic anhydride homopolymerization, see: Gaylord, N. G. *J. Macromol. Sci. Rev. Macromol. Chem.* **1975**, *13*, 235. Regel, W.; Schneider, C. *Makromol. Chem.* **1981**, *182*, 237.

[9] Walling, C.; Briggs, E. R.; Wolfstirn, K. B.; Mayo, F. R. *J. Am. Chem. Soc.* **1948**, *70*, 1537. Barb, W. G. *J. Polym. Sci.* **1953**, *11*, 117. Seymour, R. B.; Garner, D. P. *Polymer* **1976**, *17*, 21. Block, H.; Cowd, M. A.; Walker, S. M. *Polymer* **1972**, *13*, 549. Gaylord, N. G.; Maiti, S.; Patnaik, B. K.; Takahashi, A. *J. Macromol. Sci., Chem.* **1972**, *A6*, 1459. Gaylord, N. G.; Maiti, S. *J. Macromol. Sci., Chem.* **1972**, *A6*, 1481. Fujimori, K. *J. Macromol. Sci., Chem.* **1975**, *A9*, 495. Caze, C.; Loucheux, C. *J. Macromol. Sci., Chem.* **1975**, *A9*, 29.

[10] Allen, R. D.; Opitz, J.; Larson, C. E.; Wallow, T. I.; Hofer, D. C. *Microlithography World*, *5* (winter 1999).

[11] Houlihan, F. M.; Wallow, T. I.; Nalamasu, O.; Reichmanis, E. *Macromolecules* **1997**, *30*, 6517.

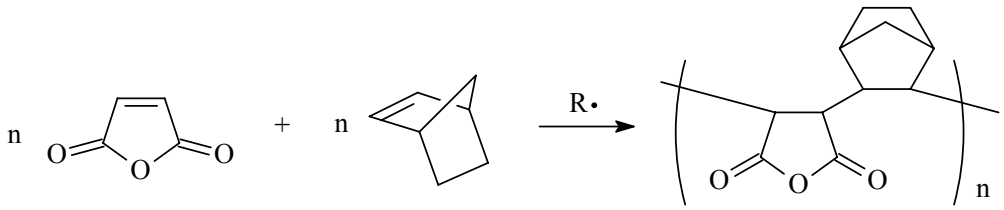

Scheme 5.1 Radical alternating copolymerization of maleic anhydride and norbornene.

Polymerization reaction data is traditionally obtained by careful sampling techniques followed by gravimetric and molecular weight analysis. Alternatively, samples can be withdrawn from the reactor and analyzed for residual monomer in solution at various times by chromatographic or spectroscopic techniques. Sample removal techniques can be very difficult, especially since many reactions are extremely sensitive to oxygen and other impurities that can be introduced during sampling. *In situ* mid-infrared spectroscopy is a desirable alternative, state-of-the-art, real-time, monitoring technique that is well suited to obtain real-time monomer conversion data for polymerization processes. In addition, reactions can be analyzed without complicated reactor modifications or expensive deuterated monomers. Previously, Long *et al*. have utilized *in situ* near-infrared (NIR) (10,000 – 4,000 cm^{-1}) spectroscopy using fiber optic probe technology to obtain solution polymerization kinetics of living anionic processes.[12] More recently, Puskas[13] and Storey[14] have reported the application of *in situ* mid-infrared (4000 - 650 cm^{-1}) spectroscopy to monitor living cationic polymerization processes. In addition, Bradley and Long recently applied *in situ* mid-infrared spectroscopy to study melt-phase acidolysis and ester exchange polymerization mechanisms.[15] Recently, McGrath and Wiles have used *in situ* mid-IR spectroscopy to measure monomer conversion in order to determine the reactivity

---

[12] Long, T. E.; Liu, H. Y.; Schell, D. M.; Teegarden, D. M.; Uerz, D. S. *Macromolecules* **1993**, *26*, 6237.
[13] Puskas, J. E.; Lanzendörfer, M. G.; Pattern, W. E. *Polym. Bull.* **1998**, *40*, 55. Puskas, J. E.; Lanzendörfer, M. G. *Macromolecules* **1998**, *31*, 8684.
[14] Storey, R. F.; Donnalley, A. B.; Maggio, T. L. *Macromolecules* **1998**, *31*, 1523.
[15] Bradley, J. R.; Long, T. E. *Polymer Preprints* **1999**, *40(1)*, 564.

ratios for acrylonitrile/methyl acrylate radical copolymerization[16] via non-linear methodologies first developed by Tidwell and Mortimer.[17] These previous efforts have demonstrated the utility of *in situ* infrared spectroscopy to obtain real-time structural and kinetic information for polymerization processes. Herein, the use of *in situ* FTIR spectroscopy to measure reactivity ratios for norbornene/maleic anhydride radical copolymerization using the Mayo-Lewis graphical method will be described.

5.3 EXPERIMENTAL

5.3.1 Materials

Norbornene (Nb) was purchased from Aldrich and vacuum distilled (0.1 mm Hg) at room temperature from calcium hydride after degassing three times using the traditional freeze-thaw method. After distillation Nb was stored under positive nitrogen pressure as a sealed solution in tetrahydrofuran. Maleic anhydride (MAH) was purchased from Aldrich and purified via sublimation immediately prior to use. Tetrahydrofuran was distilled using the classic sodium/benzophenone ketyl. All other reagents were purchased from Aldrich and used as received.

5.3.2 Characterization

Molecular Weight Characterization

Molecular weights were measured using a Wyatt miniDAWN multiangle laser light scattering (MALLS) detector with a 690 nm laser (Wyatt Technology, Santa Barbara, CA) connected to a Waters SEC (515 pump, 717 autosampler, and 410 refractive index

---

[16] Wiles, K. B., M.S. Thesis, Virginia Polytechnic Institute and State University, Blacksburg, VA, 2002. Wiles, K. B.; Bhanu, V. A.; Pasquale, A. J.; Long, T. E.; McGrath, J. E. *Polym. Prepr. (Am. Chem. Soc., Div. Polym. Chem.)* **2001**, *42*(2), 608.

[17] Tidwell, P. W.; Mortimer, G. A. *J. Polym. Sci., Part A: Polym. Chem.* **1965**, *3*, 369.

detector). The miniDAWN was connected in series after three 5-μm Plgel mixed-bed columns (Polymer Laboratories, Amherst, MA). Measurements were made at 40 °C with THF as the solvent at a flow rate of 1.0 mL/min.

NMR Characterization

^{1}H NMR spectra were obtained using a Varian UNITY 400 spectrometer at 400 MHz in $CDCl_3$ at ambient temperature. ^{13}C NMR spectra were obtained using a Varian UNITY-400 spectrometer at 100 MHz in DMSO-d_6 at ambient temperature.

***In situ* FTIR**

In situ mid-FTIR spectra were collected with a ReactIR 1000 (MCT detector, S/N = 7500, resolution = 4) (ASI Applied Systems, Millersville, MD, www.asirxn.com) reaction analysis system equipped with a light conduit and DiComp (diamond-composite) insertion probe. Reaction data was analyzed using ASI ReactIR software. The details and capabilities of the ReactIR 1000 reaction analysis system based on attenuated total reflectance (ATR) have been described in detail previously.[18]

5.3.3 Example Procedure with *in situ* FTIR for a Maleic Anhydride/Norbornene Copolymerization

In a 100 mL, round-bottomed, three-necked flask that was fitted with the ASI ReactIR 1000 DiComp probe was added a magnetic stir bar, Nb (9.40 g, 100 mmol), MAH (9.80 g, 100 mmol), and tetrahydrofuran (THF) (14.4 mL). A schematic of the copolymerization setup with *in situ* FTIR is illustrated in Figure 5.3. An oil bath at 65 ºC was raised using a jack until the reaction solution was completely immersed in the oil at 65 ºC. Once the temperature of the reaction mixture reached 65 ºC, 2,2-azobisisobutyronitrile (AIBN) (0.984 g, 6.00 mmol) was added to the flask. The flask was immediately purged with

[18] Storey, R. F.; Donnalley, A. B.; Maggio, T. L. *Macromolecules* **1998**, *31*, 1523.

nitrogen for approximately 30 seconds and sealed tightly under positive nitrogen pressure (4-5 psi) with a rubber septum. An oil bath at 65 ºC was raised to the reaction flask and FTIR data collection was started. The ReactIR was programmed to collect an FTIR spectrum of the reaction mixture every minute (64 scans) for the first hour of reaction and then every 5 minutes (256 scans) for the remainder of the reaction (FTIR data up to approximately 5-10 % conversion was used for measuring the reactivity ratios). The reaction was then stirred at 65 ºC for 24 h while collecting FTIR spectra. After 24 h, the oil bath was removed and the reaction contents were allowed to cool to room temperature. After 24 h, the reaction mixture had solidified and was no longer stirring. The DiComp probe was removed from the reaction flask and THF (~ 50 mL) was added to dissolve the solid. The dissolved material was then precipitated into hexanes (~ 500 mL), filtered, and dried overnight under vacuum (0.1 mm Hg) at approx. 75 ºC.

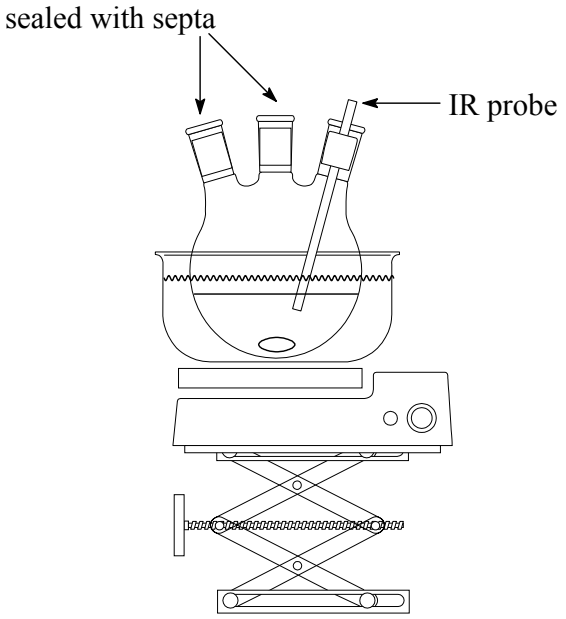

Figure 5.3 Nb/MAH copolymerization setup with *in situ* FTIR monitoring.

5.4 RESULTS AND DISCUSSION

5.4.1 Kinetic Analysis of Nb/MAH Free Radical Copolymerizations using *In situ* FTIR

In situ FTIR was used to instantaneously monitor monomer conversion data in real time for the determination of reactivity ratios for norbornene (Nb)/maleic anhydride (MAH) free radical copolymerization (Scheme 5.1). A reaction flask was specifically designed to permit the introduction of the ATR based infrared probe and attention was devoted to ensure the reactor was sealed to eliminate any volatilization of reaction components. Strong vinylene carbon-hydrogen (=C-H) absorbances of the monomers were observed and allowed for kinetic analysis of the terpolymerizations using *in situ* FTIR. The waterfall plot of the vinylene region for a norbornene (Nb)/maleic anhydride (MAH) (50/50 mol ratio) is illustrated in Figure 5.4. The vinylene carbon-hydrogen absorbance of Nb was observed at 710 cm^{-1}. The vinylene carbon-hydrogen absorbance of MAH was observed at 695 cm^{-1}.

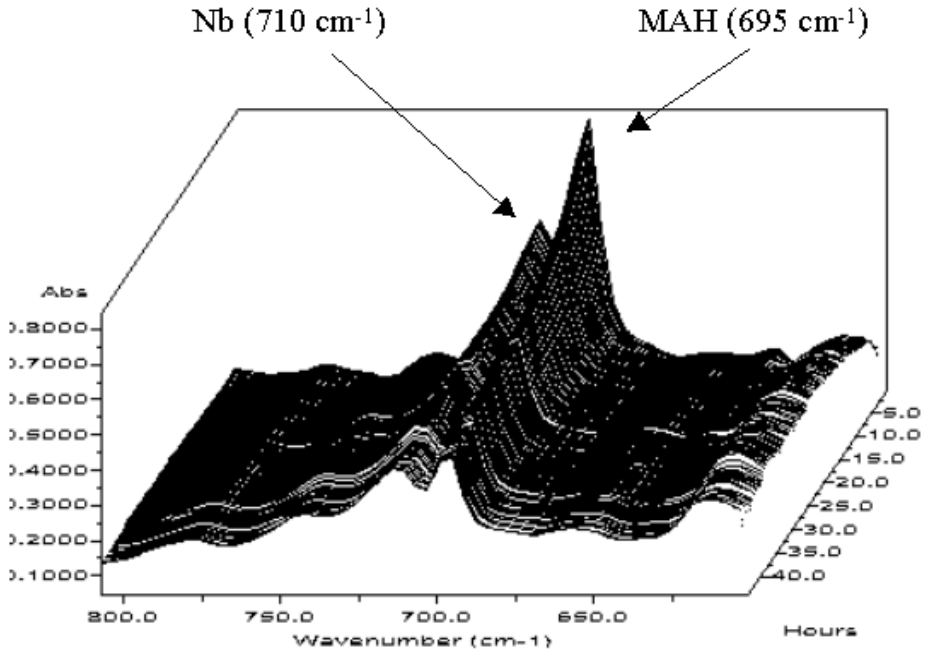

Figure 5.4 Vinylene region of "waterfall" plot for 50/50 Nb/MAH alternating copolymerization.

Pseudo first order kinetic plots were constructed from the data obtained via the *in situ* monitoring of the monomer absorbances. Initial kinetic interpretations have focused on the assumption of pseudo first order kinetics for an alternating polymerization mechanism (Figure 5.6). Excellent agreement was observed using these assumptions and linear kinetic plots were observed. A representative pseudo first order kinetic plot for a Nb/MAH copolymerization constructed from a plot of ln[monomer absorbance (total area from 670 to 725 cm^{-1})] vs. time (50/50 mol ratio, 65 °C k_{obs} = 6.7 x 10^{-5} s^{-1}) is shown in Figure 5.5. As was expected for an alternating copolymerization mechanism, the fastest rate of copolymerization was observed for the 50/50 comonomer feed ratio.

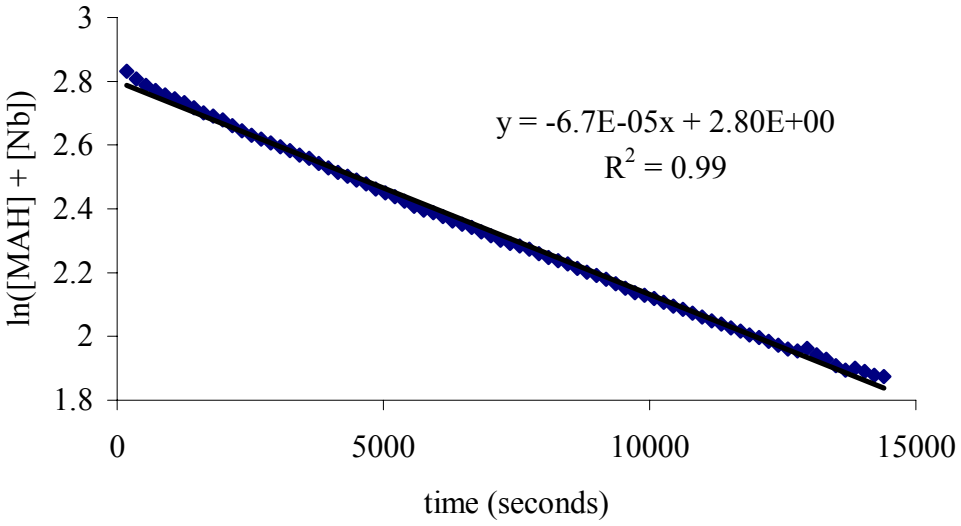

Figure 5.5 Psuedo first order kinetic treatment of Nb and MAH concentration determined via *in situ* FTIR absorbances (total area from 670 to 725 cm^{-1}).

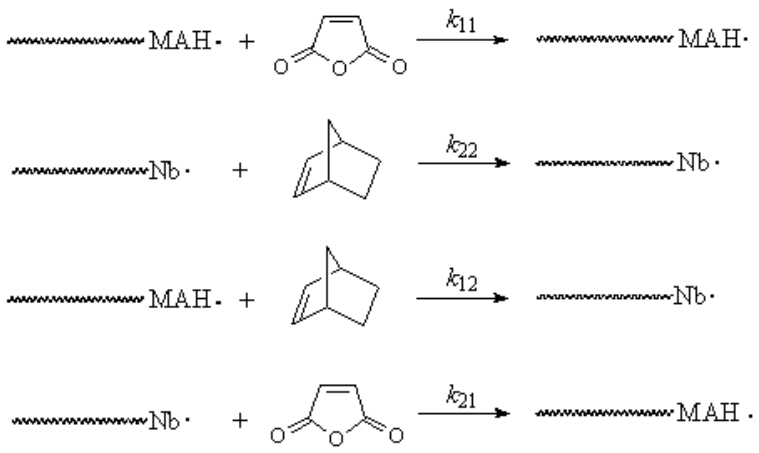

assuming negligible homopolymerization of MAH and Nb, k_{11}=k_{22}=0, overall rate is:

$$\text{rate} = k_{12}[(\text{MAH}\cdot)(\text{Nb})] + k_{21}[(\text{Nb}\cdot)(\text{MAH})]$$

assuming a steady state concentration of radical and alternating polymerization, rate is:

$$\text{rate} = (k_{12} + k_{21})([\text{P}\cdot][\text{M}])$$

where [P·] = conc. of growing polymer radicals and [M] = conc. of MAH or Nb monomer

and therefore an observed rate constant (k_{obs}) is obtained from a plot of ln[M] vs. time

$$\boldsymbol{k_{obs} = (k_{12} + k_{21})[\text{P}\cdot]}$$

Figure 5.6 Pseudo first order alternating kinetic assumptions for a norbornene/maleic anhydride alternating copolymerization.

Table 5.1 Observed rate constants MAH/Nb copolymerizations as a function of starting comonomer feed.

[MAH]/[Nb]	k_{obs} (x 10^5 s^{-1})[a]
40/60	3.9
45/55	5.7
50/50	6.7
55/45	6.3
60/40	5.4

[a] Determined via *in situ* FTIR up to 10 % conversion.

5.4.2 Evaluation of Nb/MAH Reactivity Ratios

Free radical reactivity ratios of Nb and MAH were evaluated via graphical linear analysis of the rearranged copolymer composition equation (Figure 5.7) based upon the terminal model developed by Mayo and Lewis:[19]

$$r_2 = \frac{[M_1]}{[M_2]}\left[\frac{d[M_2]}{d[M_1]}\left(1 + \frac{r_1[M_1]}{[M_2]}\right) - 1\right]$$

Figure 5.7 Rearranged copolymer composition equation.

The graphical linear analysis method relies on measuring the copolymer composition to low degrees of conversion, such that a considerable change in the comonomer feed ratio does not occur.

In situ mid-infrared (mid-IR) spectroscopy was used to collect monomer concentration data to low degrees of conversion (approximately 10 %) in real-time during free radical copolymerizations of norbornene (Nb) and maleic anhydride (MAH). Monomer conversion data collected using *in situ* FTIR was subsequently used to calculate the instantaneous copolymer composition (d[MAH]/d[Nb]), which was calculated according to the terminal model. Infrared absorbances that were due to the vinylene functionality, which decrease as the monomers propagate, were identified for both Nb and MAH. Figure 5.4 illustrates the "waterfall" plot of the vinylene carbon-hydrogen (=C-H) out-of-plane deformations for both MAH (695 cm^{-1}) and Nb (710 cm^{-1}).

---

[19] Mayo, F. R.; Lewis, F. M. *J. Am. Chem. Soc.* **1944**, *66*, 1594.

Copolymerization data was collected via *in situ* FTIR to low degrees of conversion (approximately 10 %) for copolymerizations of MAH and Nb. Five different MAH/Nb comonomer feed compositions were analyzed: 40/60, 45/55, 50/50, 55/45, and 60/40. d[MAH]/d[Nb] values were obtained from plots of the monomer FTIR absorbance peak heights (Figure 5.4), which were multiplied by the corresponding mol fraction in the starting comonomer feed. A representative d[MAH]/d[Nb] plot for the 50/50 MAH/Nb feed composition calculated to 10 % conversion is shown in Figure 5.8. The d[MAH]/d[Nb] values for all five comonomer feed ratios are summarized in Table 5.2. As discussed earlier, the theoretical value of $d[M_1]/d[M_2]$ in the case of a perfectly alternating copolymerization mechanism, where r_{11} and r_{22} are equal to 0, is expected to be 1 regardless of the starting comonomer feed. As expected, the experimentally measured d[MAH]/d[Nb] listed in Table 5.2 for all five different starting concentrations are approximately one within the experimental error of the method. The values randomly ranged from a low of 0.941 for the 40/60 [MAH]/[Nb] comonomer feed to a high of 1.05 for the 45/55 [MAH]/[Nb] comonomer feed.

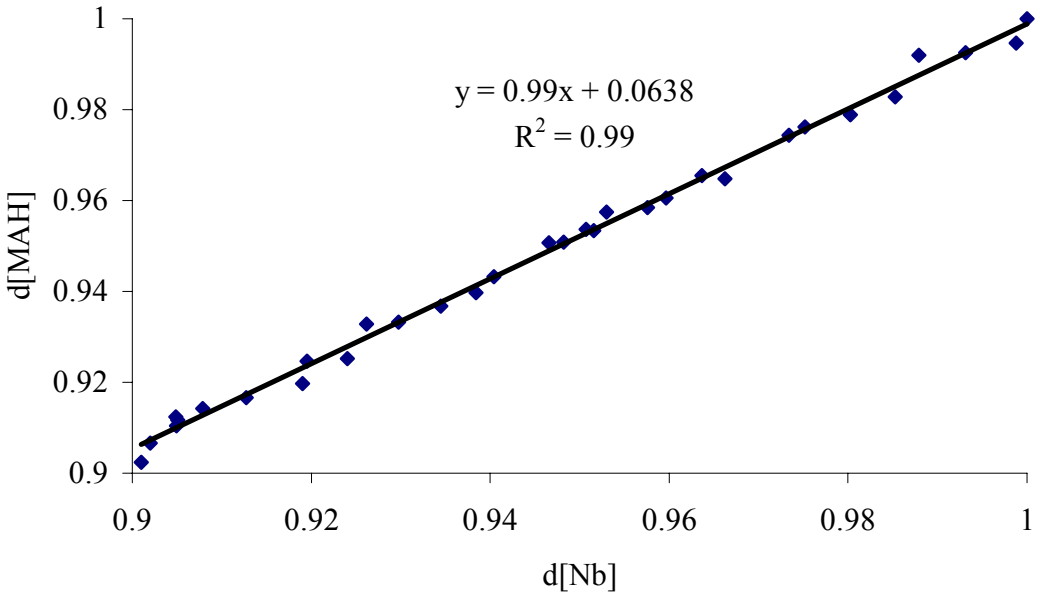

Figure 5.8 Plot of d[MAH] vs. d[Nb] for a 50/50 (mol ratio) MAH/Nb free radical copolymerization measured using *in situ* FTIR.

Table 5.2 Comonomer incorporation as a function of starting comonomer feed.

[MAH]/[Nb] [a]	**d[MAH]/d[Nb]** [b]
40/60	0.96
45/55	1.0
50/50	0.99
55/45	1.0
60/40	0.99

a Starting comonomer feed ratio. *b* Mole fractions incorporated into copolymer (determined via *in situ* FTIR) after approximately 10% conversion.

Next, r_{MAH} and r_{Nb} values for each of the starting comonomer feed ratios were determined. Arbitrary values for one of the reactivity ratios were assumed and then the value for the other reactivity ratio was calculated from the rearranged copolymer composition equation using the known starting comonomer concentrations and the measured d[MAH]/d[Nb] values measured using *in situ* FTIR. For example, r_{MAH} and r_{Nb} values for the 50/50 comonomer feed copolymerization are listed in Table 5.3. Values ranging from –1.0 to 1.0 were chosen for r_{MAH}. r_{Nb} values were then calculated for each of the assumed r_{MAH} values. This process was repeated for all of the copolymerizations at different comonomer feeds. Estimation of the reactivity ratios using the terminal model graphical method was then carried out by means of graphing r_{MAH} vs. r_{Nb} for all of the starting concentrations (Figure 5.9). The average intersection points of the multiple plotted lines were then taken to be the estimated monomer reactivity ratios (r_{MAH} = 0.02, r_{Nb} = 0.01).

Table 5.3 Example calculated r_{Nb} values determined from the rearranged copolymer composition equation and assumed r_{MAH} values for a 50/50 MAH/Nb copolymerization.

r_{MAH}(assumed)	r_{Nb}
-1	-1.00
-0.8	-0.79
-0.6	-0.57
-0.4	-0.36
-0.2	-0.14
0	0.07
0.2	0.28
0.4	0.50
0.6	0.71
0.8	0.93
1	1.14

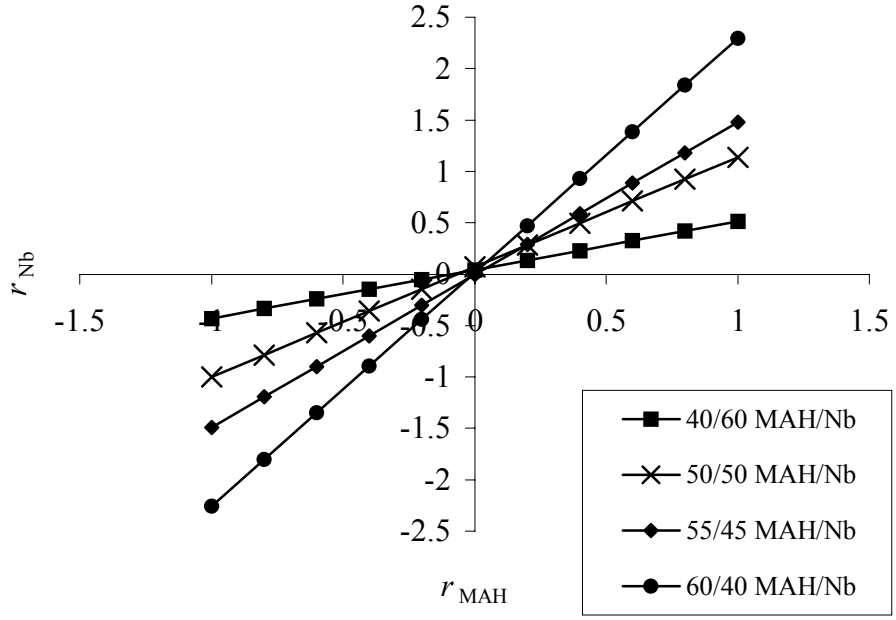

Figure 5.9 Mayo-Lewis linear graphical analysis of MAH and Nb reactivity ratios.

5.5 CONCLUSIONS

Free radical reactivity ratios of Nb and MAH were evaluated via graphical linear analysis of the rearranged copolymer composition equation based upon the terminal model developed by Mayo and Lewis. Copolymerization data was collected via *in situ* FTIR to low degrees of conversion (approximately 10 %) for copolymerizations of MAH and Nb. Copolymer composition data for 40/60, 45/55, 50/50, 55/45, and 60/40 MAH/Nb comonomer feed compositions were measured. Conversion data measured with *in situ* FTIR was then employed in conjunction with the rearranged copolymer composition equation to estimate MAH and Nb reactivity ratios. Both of the reactivity ratios were estimated using this method to be approximately zero (r_{MAH} = 0.02, r_{Nb} = 0.01), which was further indication of an alternating copolymerization.

Acknowledgments. Financial support provided by the Jeffress Memorial Trust, Virginia Tech Department of Chemistry, National Science Foundation (CRIF CHE-9974632), and IBM is gratefully acknowledged. The authors would also like to thank the Center of Adhesive and Sealant Science (CASS) at Virginia Tech and the Adhesive and Sealant Council (ASC) for financial support through an ASC Education Foundation Research Fellowship.

Recommended future studies:

- Application of *in situ* FTIR as a tool for the rapid determination of reactivity ratios for other comonomer systems.
- Validate reactivity analysis using non-linear methods.

CHAPTER 6

Fundamental Investigations of the Free Radical Copolymerization and Terpolymerization of Maleic Anhydride, Norbornene, and Norbornene *t*-Butyl Ester: *In situ* Mid-infrared Spectroscopic Analysis

6.1 ABSTRACT

Various synthetic factors that affect the molecular weight, yield, and composition of maleic anhydride (MAH), norbornene (Nb), and *tert*-butyl 5-norbornene-2-carboxylate (NbTBE) terpolymers were investigated. Pseudo first order kinetic analysis using *in situ* FTIR indicated that the observed rate of reaction (k_{obs}) was a strong function of the Nb/NbTBE ratio with a maximum of 6.7 x 10^{-5} s^{-1} for a 50/0/50 Nb/NbTBE/MAH monomer ratio and a minimum of 1.1 x 10^{-5} s^{-1} for a 0/50/50 Nb/NbTBE/MAH ratio. In addition, polymer yields were also observed to be a function of the Nb/NbTBE ratio and also decreased with increasing NbTBE. Sampling of an Nb/NbTBE/MAH (25/25/50 mol ratio) terpolymerization and subsequent analysis using ^{1}H NMR indicated that the relative rate of Nb incorporation is approximately 1.7 times faster than NbTBE incorporation. Also, the observed rate constant of 4.4 x 10^{-5} s^{-1} calculated using ^{1}H NMR agreed favorably with the k_{obs} determined via *in situ* FTIR (3.8 x 10^{-5} s^{-1}). Terpolymerizations in excess NbTBE and in the absence of solvent resulted in relatively high molecular weight materials (M_n > 20,000) and provided a potential avenue for control of the Nb/NbTBE incorporation into the resulting materials.

6.2 INTRODUCTION

Photolithography using 193 nm (Ar-F laser) light has emerged for the production of the next generation of microelectronic devices.[1] Current technologies (Kr-F laser), including ultraviolet (UV) and deep-UV photolithography, employ aromatic materials based upon phenolic polymers.[2] However, the photon energy of 193 nm light is high enough for aromatic polymers to absorb strongly at this wavelength, resulting in opaque materials that are not practical for 193 nm lithography.[3] Therefore, significant attention has been devoted to the design of materials that are optically transparent at 193 nm and also have the desirable etch-resistant and image-forming properties of phenolic based materials.[4]

A number of approaches to photoresists with high transparency at 193 nm have been reported.[5] Initially, acrylic-based polymers seemed promising as new materials for 193 nm lithography. Acrylates were desirable materials due to only a weak carbonyl absorption at 193 nm, which resulted in good transparency when exposed to this wavelength of light.[6] In 1991, Allen and coworkers described successful 193 nm patterning using an all-acrylic terpolymer composed of methyl methacrylate, *tert*-butyl methacrylate and methacrylic

---

[1] Nozaki, N.; Kaimoto, M.; Takahashi, S.; Takeshi, S.; Abe, N. *Chem. Mater.* **1994**, *6*, 1492. Kunz, R. R.; Palmateer, A. R; Forte, A. R.; Allen, R. D.; Wallraff, G. M.; DiPietro, R. A.; Hofer, D. C. *Proc. SPIE-Int. Soc. Opt. Eng.* **1996**, *2724*, 365. Allen, R. D.; Opitz, J.; Larson, C. E.; Wallow, T. I.; Hofer, D. C. *Microlithography World* **winter 1999**, 5. Jung, M. H.; Jung, J. C.; Lee, G.; Baik, K. H. *Jpn J. Appl. Phys., Part 1* **1998**, *37*, 6889. Nalamasu, O.; Houlihan, R. A.; Cirelli, A. G.; Watson, G. P.; Hutton, R. S.; Kometani, J. M.; Reichmanis, E. *J. Vac. Sci. Technol., B* **1998**, *16*, 3716. Okoroanyanwu, U.; Byers, J.; Shimokawa, T.; Willson, C. G. *Chem. Mater.* **1998**, *10*, 3328.

[2] Ito, H. *Solid State Technol.* **1996**, *36(7)*, 164. Willson, C. G. In *Introduction to Microlithography*, 2nd ed.; Thompson, L. F., Willson, C. G., Bowden, M. J., Eds.; ACS Professional Reference book; American Chemical Society: Washington, DC, 1994; Ch. 3.

[3] Kunz, R. R.; Allen, R. D.; Wallraff, G. M. *Polym. Prepr. (Am. Chem. Soc., Div. Polym. Chem.)* **1994**, *35(2)*, 939.

[4] Allen, R. D.; Wallraff, G. M.; Hofer, D. C.; Kunz, R. R. *IBM J. Res. Dev.* **1997**, *41*, 95.

[5] Nonogaki, S.; Ueno, T.; Ito, T. Chemistry of Photoresist Materials. In *Microlithography Fundamentals in Sumiconductor Devices and Fabrication Technology*; Marcel Dekker: New York, 1999; pp 115-119.

[6] Wallraff, G. M.; Hinsberg, W. D. *Chem. Rev.* **1999**, *99*, 1801.

acid.[7] However, a major disadvantage of acrylic materials was poor reactive-ion etch resistance under the etching conditions used widely in the semiconductor industry.[8] The primary design challenge that has emerged in the development of new materials for 193 nm photolithography is the compromise between imaging performance (broadly defined as resolution, adhesion, sensitivity, and compatibility with industry standard aqueous-base developers) and reactive-ion etch resistance.[4] For the initial acrylic materials, the chemical modifications that were used to tailor imaging performance also deleteriously influenced reactive-ion etch resistance. Previously, it was determined that there is a correlation between increased reactive-ion etch resistance and a high carbon to hydrogen (C/H) ratio.[9] This observation supports the fact that phenolic resist materials, which have a high C/H ratio, exhibit good plasma etch resistance. Therefore, an increase in the C/H ratio has resulted in improved reactive-ion etching properties of acrylic based materials, and a number of acrylic-based materials containing pendant alicyclic adamantane or norbornane substitution have been investigated.[10] Incorporation of the pendant alicyclic functionalities greatly improved the etch resistance of acrylic based materials. However, the increase in etch resistance was also accompanied by decreased image performance. Consequently, 193 nm photolithography acrylic resist materials that possessed both etch resistance and superior image performing properties were not achievable.

---

[7] Allen, R. D.; Wallraff, G. M.; Hinsberg, W. D.; Simpson, L. L. *J. Vac. Sci. Technol., B* **1991**, *9*, 3357.

[8] Wallow, T. I.; Brock, P. J.; Dipietro, R. A.; Allen, R. D.; Opitz, J.; Sooriyakumaran, R.; Hofer, D. C; Meute, J.; Byers, J. D.; Rich, G. K.; McCallum, M.; Schuetze, S.; Jayaraman, S.; Hullihen, K.; Vicari, R.; Rhodes, L. F.; Goodall, B. L.; Shick, R. A. *Proc. SPIE-Int. Soc. Opt. Eng.* **1998**, *3333*, 92.

[9] Gokhan, H.; Esho, S.; Ohnishi, Y. *J. Electrochem. Soc.* **1983**, *130*, 143. Kunz, R. R.; Palmateer, A. R; Forte, A. R.; Allen, R. D.; Wallraff, G. M.; DiPietro, R. A.; Hofer, D. C. *Proc. SPIE-Int. Soc. Opt. Eng.* **1996**, *2724*, 365.

[10] Kaimoto, Y.; Nozaki, K.; Takechi, M.; Abe, N. *Proc. SPIE-Int. Soc. Opt. Eng.* **1992**, *1672*, 66. Nozaki, K.; Kaimoto, Y.; Takahashi, M.; Takechi, Abe, N. *Chem. Mater.* **1994**, *6*, 1492. Takechi, S.; Takahashi, M.; Kotachi, A.; Nozaki, K.; Yano, E.; Hanyu, I. *J. Photopolym. Sci. Technol.* **1996**, *9*, 475. Yamashita, K.; Endo, M.; Sasago, M.; Nomura, N.; Nagano, H.; Mizuguchi, S.; Ono, T.; Sato, T. *J. Vac. Sci. Technol., B* **1993**, *11*, 2692. Nakano, K.; Maeda, K.; Iwasa, S.; Yano, J.; Ogura, Y.; Hasegawa, E. *Proc. SPIE-Int. Soc. Opt. Eng.* **1994**, *2195*, 194. Maeda, K.; Nakano, K.; Ohfuji, T.; Hasegawa, E. *Proc. SPIE-Int. Soc. Opt. Eng.* **1996**, *2724*, 377. Allen, R. D.; Wallraff, G. M.; DiPietro, R. A.; Hofer, D. C.; Kunz, R. R. *J. Photopolym. Sci. Technol.* **1994**, *7*, 507.

An alternative approach to increase the C/H ratio has been to incorporate alicyclic structures directly into the polymer backbone.[6] A variety of synthetic routes for producing resist materials with alicyclic backbones has been investigated, including cyclic olefin alternating free radical copolymerization,[11] metal catalyzed vinyl addition polymerization,[12] and ring opening metathesis polymerization (ROMP) followed by hydrogenation.[13] In recent years, the most promising of these methods that has emerged for synthesizing alicyclic materials for 193 nm lithography is the alternating free radical copolymerization of maleic anhydride with cyclic olefin monomers such as norbornene (Scheme 6.1).[14] Cyclic olefins will homopolymerize poorly via free radical methods. However, norbornene is a cyclic olefin that contains bridged allylic hydrogens that do not chain transfer to an appreciable extent due to the resulting unstable radical.[15] When norbornene is combined with the electron-poor olefin maleic anhydride in the presence of a

---

[11] Allen, R. D.; Wallraff, G. M.; DiPietro, R. A.; Hofer, D. C.; Kunz, R. R. *J. Photopolym. Sci. Technol.* **1994**, *7*, 507. Okoroanyanwu, U.; Shimokawa, T.; Byers, J.; Medeiros, D.; Willson, C. G.; Niu, Q, J.; Fréchet, J. M. J.; Allen, R. D. *Proc. SPIE-Int. Soc. Opt. Eng.* **1997**, *3049*, 92. Okoroanyanwu, U.; Shimokawa, T.; Byers, J.; Willson, C. G. *Chem Mater.* **1998**, *10*, 3319. Nozaki, K.; Yano, E. *J. Photopolym. Sci. Technol.* **1997**, *10*, 545. Patterson, K.; Okoroanyanwu, U.; Shimokawa, T.; Cho, S.; Byers, J.; Willson, C. G. *Proc. SPIE-Int. Soc. Opt. Eng.* **1998**, *3333*, 425. Wallow, T. I.; Houlihan, F. M.; Nalamasu, O.; Chandross, E. A. Neenan, T. X.; Reichmanis, E. *Proc. SPIE-Int. Soc. Opt. Eng.* **1996**, *2724*, 355. Houlihan, F. M.; Wallow, T. I.; Nalamasu, O.; Reichmanis, E. *Macromolecules* **1997**, *30*, 6517. Patterson, K.; Yamchika, M.; Cho, S.; Rager, T.; Yamada, S.; Byers, J.; Willson, C. G. *Polym. Mat. Sci. Eng.* **1999**, *81*, 43. Gabor, A. H.; Dimov, O.; Medina, A. N.; Bowden, M. J.; Neisser, M. O.; Houlihan, F. M.; Cirelli, R. A.; Dabbagh, G.; Hutton, R. S.; Rushkin, I. L.; Sweeney, J. R.; Nalamasu, O.; Reichmanis, E. *Polym. Mat. Sci. Eng.* **1999**, *81*, 41.

[12] Okoroanyanwu, U.; Shimokawa, T.; Byers, J.; Medeiros, D.; Willson, C. G.; Niu, Q, J.; Fréchet, J. M. J.; Allen, R. D. *Proc. SPIE-Int. Soc. Opt. Eng.* **1997**, *3049*, 92. Okoroanyanwu, U.; Shimokawa, T.; Byers, J.; Willson, C. G. *Chem Mater.* **1998**, *10*, 3319. Allen, R. D.; Sooriyakumaran, R.; Opitz, J.; Wallraff, G. M.; DiPietro, R. A.; Breyta, G.; Hofer, D. C. *Proc. SPIE-Int. Soc. Opt. Eng.* **1996**, *2724*, 334. Allen, R. D.; Opitz, J.; Wallow, T. I.; DiPietro, R. A.; Hofer, D. C.; Jayaraman, S.; Hullihan, K. A.; Rhodes, L. F.; Goodall, B. L.; Shick, R. A. *Proc. SPIE-Int. Soc. Opt. Eng.* **1998**, *3333*, 463. Opitz, J.; Allen, R. D.; Wallow, T. I.; Wallraff, G. M.; Hofer, D. C. *Proc. SPIE-Int. Soc. Opt. Eng.* **1998**, *3333*, 571.

[13] Okoroanyanwu, U.; Shimokawa, T.; Byers, J.; Medeiros, D.; Willson, C. G.; Niu, Q, J.; Fréchet, J. M. J.; Allen, R. D. *Proc. SPIE-Int. Soc. Opt. Eng.* **1997**, *3049*, 92. Okoroanyanwu, U.; Shimokawa, T.; Byers, J.; Willson, C. G. *Chem Mater.* **1998**, *10*, 3319.

[14] Okoroanyanwu, U.; Byers, J.; Shimokawa, T.; Willson, C. G. *Chem. Mater.* **1998**, *10*, 3328. Houlihan, F. M.; Wallow, T. I.; Nalamasu, O.; Reichmanis, E. *Macromolecules* **1997**, *30*, 6517.

[15] Koch, V. R.; Gleicer, G. J. *J. Am. Chem. Soc.* **1971**, *93*, 1657.

free radical initiator, copolymerization occurs in an alternating manner.[16] In addition, maleic anhydride also serves to incorporate polar functionality into the polymer, providing necessary adhesion and solubility properties that are required for imaging performance while retaining sufficient etch resistance in 193 nm resist applications.[17] The cyclic olefin character of these materials provides for excellent etch resistance, surpassing even currently utilized phenol based resists. Furthermore, the increased etch resistance is of great importance because of the decreasing film thickness necessary for the achievement of increasingly smaller feature sizes.[18] In addition, the ability to modify the polymer properties via incorporation of cyclic olefin derivatives that improve lithographic performance has resulted in attractive routes to new materials for 193 nm lithography.

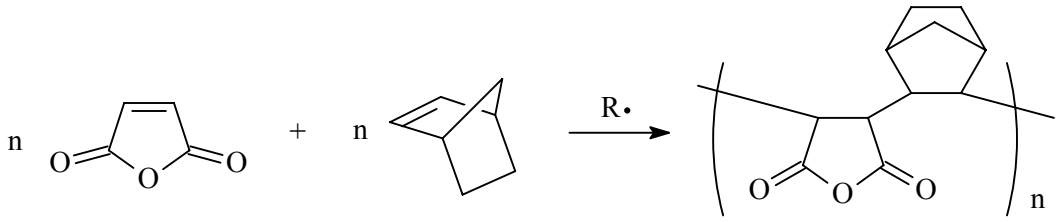

Scheme 6.1 Maleic anhydride and norbornene alternating copolymerization scheme.

Despite the abundance of scientific literature describing the alternating copolymerization of maleic anhydride with electron-rich olefins, multicomponent copolymerizations with norbornene(s) proceed via a complicated polymerization

---

[16] Okoroanyanwu, U.; Shimokawa, T.; Byers, J.; Medeiros, D.; Willson, C. G.; Niu, Q, J.; Fréchet, J. M. J.; Allen, R. D. *Proc. SPIE-Int. Soc. Opt. Eng.* **1997**, *3049*, 92.

[17] Houlihan, F. M.; Wallow, T. I.; Nalamasu, O.; Reichmanis, E. *Macromolecules* **1997**, *30*, 6517. Pasquale, A. J.; Allen, R. D.; Long, T. E. In *Forefront of Lithographic Materials Research: Proceedings of the 12th International Conference on Photopolymers*; Ito, H., Khojasteh, M. M., Li, W., Eds.; Society of Plastics Engineers (SPE); New York, N.Y.; pp 291-297. Pasquale, A. J.; Truong, H.; Allen, R. D.; Long, T. E. *J. Adhes.*, accepted for publication.

[18] Allen, R. D.; Opitz, J.; Larson, C. E.; Wallow, T. I.; Hofer, D. C. *Microlithography World* **winter 1999**, 5.

mechanism resulting in the uncontrolled formation of low molecular weight oligomers.[19] Although these alicyclic copolymers were prepared using a relatively uncontrollable polymerization process, the copolymers were successfully demonstrated as 193 nm imaging materials with improved plasma-etch resistance. Ito and coworkers have recently described an investigation of the copolymerization of norbornene or a *t*-butyl ester substituted norbornene with maleic anhydride using ^{1}H NMR spectroscopy.[20] Monomer consumption studies indicated that copolymerization of a norbornene *tert*-butyl ester with maleic anhydride in dioxane at 84 °C resulted in lower yields (32 %) compared to norbornene (60 %). NMR-scale reactions (< 0.08 g total monomer) did not provide optimized copolymerization conditions, comparative rate constants, or molecular weights and molecular weight distributions. In addition, terpolymerizations of norbornene, norbornene t-butyl ester, and maleic anhydride, which more closely exemplify 193 nm microlithographic applications, were not reported. Our research objectives reported herein have focused on the investigation of synthetic factors that influence the molecular weight, yield, and composition of terpolymers of maleic anhydride (MAH), norbornene (Nb), and *tert*-butyl 5-norbornene-2-carboxylate (NbTBE). This has been achieved using a unique combination of experimental variation, *in situ* infrared spectroscopy, and nuclear magnetic resonance spectroscopy. *In situ* infrared spectroscopy of alternating copolymerizations has not been reported earlier, and this experimental approach is more facile than conventional NMR approaches. This fundamental understanding will provide the basis for the development of a polymerization system that results in more predictable molecular weights and higher polymerization yields. The development of a fundamental understanding of the polymerization mechanism for maleic anhydride with norbornene and norbornene derivatives will result in viable manufacturing processes and improved 193-nm

---

[19] Okoroanyanwu, U.; Shimokawa, T.; Byers, J.; Medeiros, D.; Willson, C. G.; Niu, Q, J.; Fréchet, J. M. J.; Allen, R. D. *Proc. SPIE-Int. Soc. Opt. Eng.* **1997**, *3049*, 92. Houlihan, F. M.; Wallow, T. I.; Nalamasu, O.; Reichmanis, E. *Macromolecules* **1997**, *30*, 6517. Patterson, K.; Yamchika, M.; Cho, S.; Rager, T.; Yamada, S.; Byers, J.; Willson, C. G. *Polym. Mat. Sci. Eng.* **1999**, *81*, 43.

[20] Ito, H.; Miller, D.; Sveum, N.; Sherwood, M. *J. Polym. Sci. Part A: Polym. Chem.* **2000**, *38*, 3521. Ito, H.; Miller, D.; Sherwood, M. *J. Photopolym. Sci. Technol.* **2000**, *13*, 559.

lithographic performance. *In situ* infrared analysis of terpolymerizations containing maleic anhydride, norbornene, and acrylic monomers will also be discussed.

6.3 EXPERIMENTAL

6.3.1 Materials

Norbornene (Nb) was purchased from Aldrich and vacuum distilled (0.1 mm Hg) at room temperature from calcium hydride after degassing three times using the traditional freeze-thaw method. After distillation it was stored under positive nitrogen pressure as a solution in tetrahydrofuran. Maleic anhydride (MAH) was purchased from Aldrich and purified via sublimation immediately prior to use. Tetrahydrofuran was distilled using the classic sodium/benzophenone ketyl. All other reagents were purchased from Aldrich and used as received.

6.3.2 Characterization

Molecular Weight Characterization

Molecular weights were measured using a Wyatt miniDAWN multiangle laser light scattering (MALLS) detector with a 690 nm laser (Wyatt Technology, Santa Barbara, CA) connected to a Waters SEC (515 pump, 717 autosampler, and 410 refractive index detector). The miniDAWN was connected in series after three 5-μm Plgel mixed-bed columns (Polymer Laboratories, Amherst, MA). Measurements were made at 40 °C with THF as the solvent at a flow rate of 1.0 mL/min.

Thermogravimetric Analysis

Thermogravimetric analysis (TGA) was carried out under nitrogen with a TA Instruments TGA 295Thermogravimetric Analyzer at a heating rate of 10 °C/minute.

NMR Characterization

^{1}H NMR spectra were obtained using a Varian UNITY 400 spectrometer at 400 MHz in $CDCl_3$ at ambient temperature. ^{13}C NMR spectra were obtained using a Varian UNITY-400 spectrometer at 100 MHz in DMSO-d_6 at ambient temperature.

***In situ* FTIR**

In situ mid-FTIR spectra were collected with a ReactIR 1000 (MCT detector, S/N = 7500, resolution = 4) (ASI Applied Systems, Millersville, MD, www.asirxn.com) reaction analysis system equipped with a light conduit and DiComp (diamond-composite) insertion probe. Reaction data was analyzed using ASI ReactIR software. The details and capabilities of the ReactIR 1000 reaction analysis system based on attenuated total reflectance (ATR) have been described in detail previously.[21]

6.3.3 Synthesis of *tert*-Butyl 5-Norbornene-2-carboxylate (NbTBE)

Freshly cracked cyclopentadiene (1.45 moles, 96.0 mL) was added drop-wise via addition funnel to a stirred solution of *tert*-butyl acrylate (1.45 moles, 212.0 mL) and 3,5-di-tert-butylphenol (0.00728 moles, 1.5g) in a 500 mL round bottom flask. A water condenser was then inserted into the round bottom flask it was placed into an oil bath at 140 ºC (Figure 6.1). The reaction mixture was then stirred for 5 h at 140 ºC using a magnetic stir bar. The yellow crude liquid reaction mixture was then purified *via* vacuum distillation (40 °C, 0.1 mm Hg) to give a colorless oil (88.0 g, 66 % isolated yield). GC and NMR analysis indicated the product was >99% pure and was obtained as an endo/exo isomer mixture (≅ 75/25) as expected.

---

[21] Storey, R. F.; Donnalley, A. B.; Maggio, T. L. *Macromolecules* **1998**, *31*, 1523.

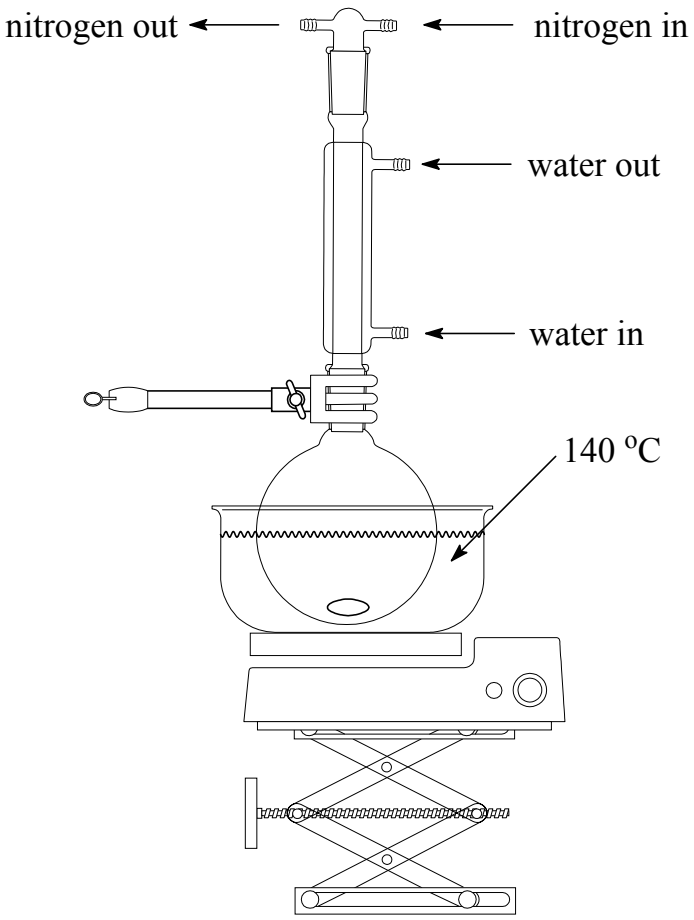

Figure 6.1 Reaction setup for NbTBE synthesis.

6.3.4 Synthesis and *In situ* FTIR of a Nb/NbTBE/MAH Terpolymerization

A typical terpolymerization reaction (Scheme 6.2) with *in situ* FTIR monitoring is described. In a 100 mL, round-bottomed, three-necked flask that was fitted with the ReactIR 1000 DiComp probe was added a magnetic stir bar, norbornene (Nb) (4.79 g, 51 mmol), *tert*-butyl 5-norbornene-2-carboxylate (NbTBE) (9.89 g, 51 mmol), maleic anhydride (MAH) (10.0 g, 102 mmol), 2,2-azobisisobutyronitrile (AIBN) (1.004 g, 6.12 mmol), and THF (16.5 mL). The flask was purged with nitrogen for approximately one minute and sealed tightly under positive nitrogen pressure (4-5 psi) with rubber septa. An oil bath at 65 ºC was raised to the reaction flask and FTIR data collection was started. A

schematic of the reaction setup with *in situ* FTIR probe is shown in Figure 6.2 and a photo of the setup in Figure 6.3. The ReactIR was programmed to collect an averaged FTIR spectrum of the reaction mixture every 5 minutes (256 scans) for the duration of the reaction. The reaction was then stirred at 65 ºC for 24 h while collecting FTIR spectra. The oil bath was removed after 24 h and the reaction contents were allowed to cool to room temperature. After 24 h, the reaction mixture had solidified to a glass and was no longer stirring. The DiComp probe was removed from the reaction flask and THF (~ 50 mL) was added to dissolve the solid glass. After completely dissolving in THF (approx. 24 h), the dissolved material was precipitated into hexanes (~ 500 mL), filtered, washed with isopropyl alcohol (~ 200 mL) and dried overnight under vacuum (0.1 mm Hg) at approx. 75 ºC to give 19.6 g (80 % yield) of white powder. GPC: M_n = 6,700 (M_w/M_n = 1.64). Nb/MAH (50/50) copolymer had a 10% weight loss at 355 ºC (nitrogen) and a glass transition temperature of 275 ºC. A Nb/NbTBE/MAH (25/25/50) terpolymer showed a lower 10% weight loss at 220 ºC (nitrogen) resulting from degradation of the *t*-butyl ester functionality.

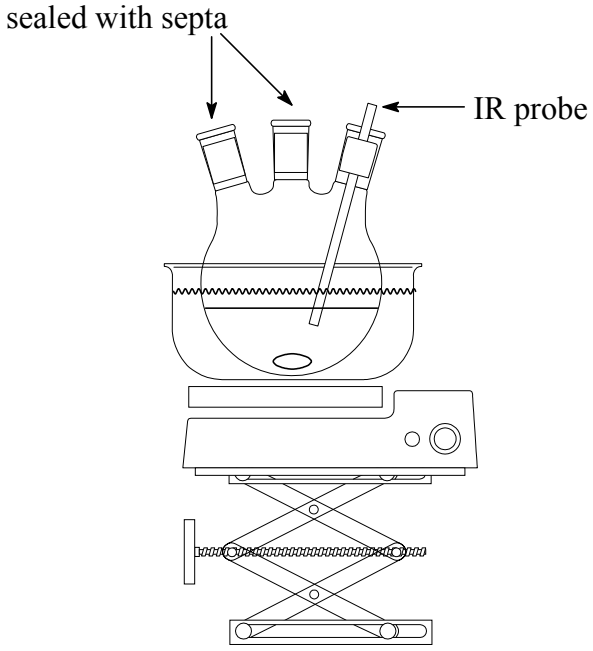

Figure 6.2 Terpolymerization setup with *in situ* FTIR monitoring.

Figure 6.3 Illustration of polymerization reaction with *in situ* FTIR module.

6.4 RESULTS AND DISCUSSION

6.4.1 Nb/MAH Free Radical Alternating Copolymerization Reaction Conditions.

Research efforts were initially focused on developing an understanding of the factors that influence the copolymerization of norbornene and maleic anhydride polymerization processes. Special attention was devoted to the effects of monomer feed ratio, monomer:solvent ratio, and initiator concentration. In addition, particular focus was also directed towards the development of *in situ* infrared spectroscopy techniques for the real

time assessment of polymerization kinetics and conversion.[22] It was demonstrated that the monomer feed ratio did not strongly influence the molecular weight and isolated yield in a significant manner, and products with number average molecular weights ranging from 8,000 to 9,000 and 80-90 % yields were typically obtained. As expected, an increase in initiator concentration resulted in an increase in yield (Figure 6.4**)**. A simultaneous decrease in the number average molecular weight was also observed with increased initiator amount (Figure 6.5).

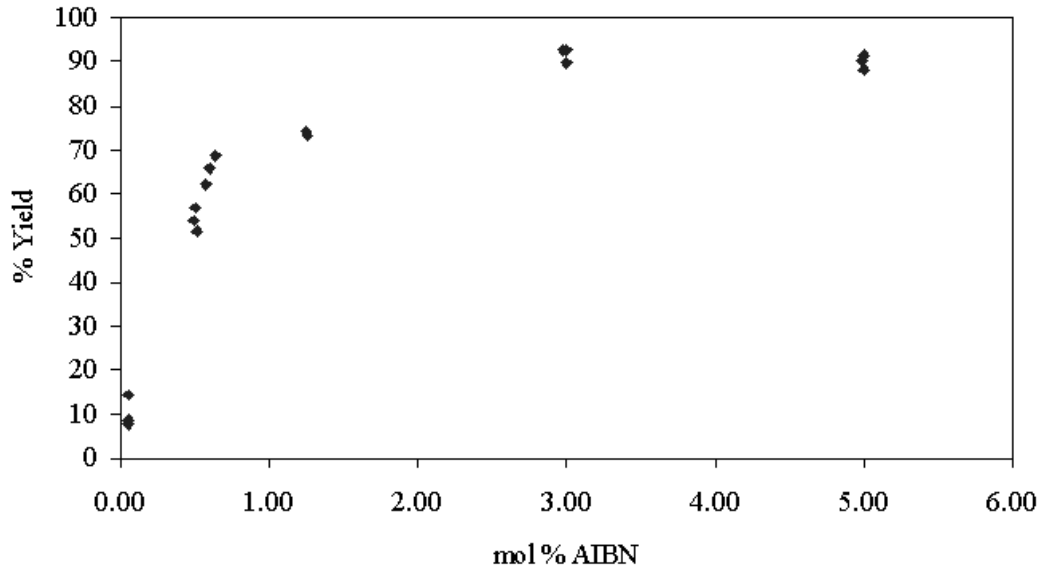

Figure 6.4 Yield (%) versus mol % AIBN (THF, 60 % solids, 65 °C, 24 h).

[22] Pasquale, A. J.; Long, T. E. *Macromolecules* **1999**, *32*, 7954. Pasquale, A. J.; Long, T. E. *Polym. Prepr. (Am. Chem. Soc., Div. Polym. Chem.)* **2000**, *41*(1), 944.. Pasquale, A. J.; Long, T. E. *J. Polym. Sci. Part A: Polym. Chem.* **2001**, *39*, 216.

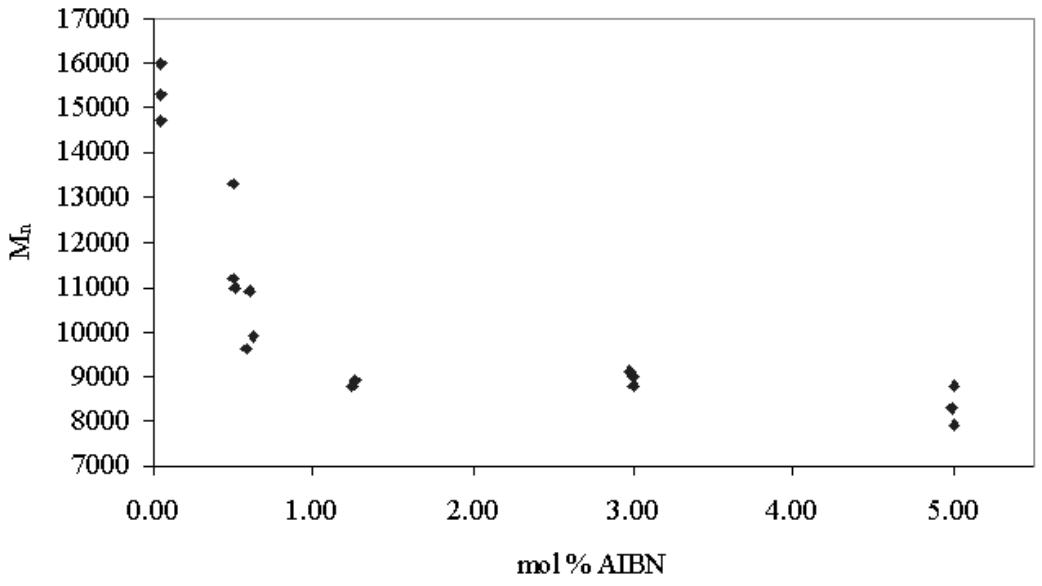

Figure 6.5 Number average molecular weight versus mol % AIBN (THF, 60 % solids, 50/50 Nb/MAH, 65 °C, 24 h).

A maximum in both yield and number average molecular weight was observed at approximately 50-60 % monomer solids in tetrahydrofuran (THF) (Figure 6.6 and Figure 6.7). A maximum is attributed to an expected increase in solution viscosity as the polymerization proceeds, and spectroscopic analyses were performed prior to an appreciable increase in the solution viscosity. Kinetic analyses using monomer conversion were based on spectroscopic analysis during the first 4 hours of polymerization to ensure the absence of viscosity effects. The following optimum reaction conditions were determined from these initial investigations: equimolar feed ratio Nb and MAH, 3 mole percent AIBN (based on total monomer), 60 % solids in THF solvent for 24 h at 65 °C.

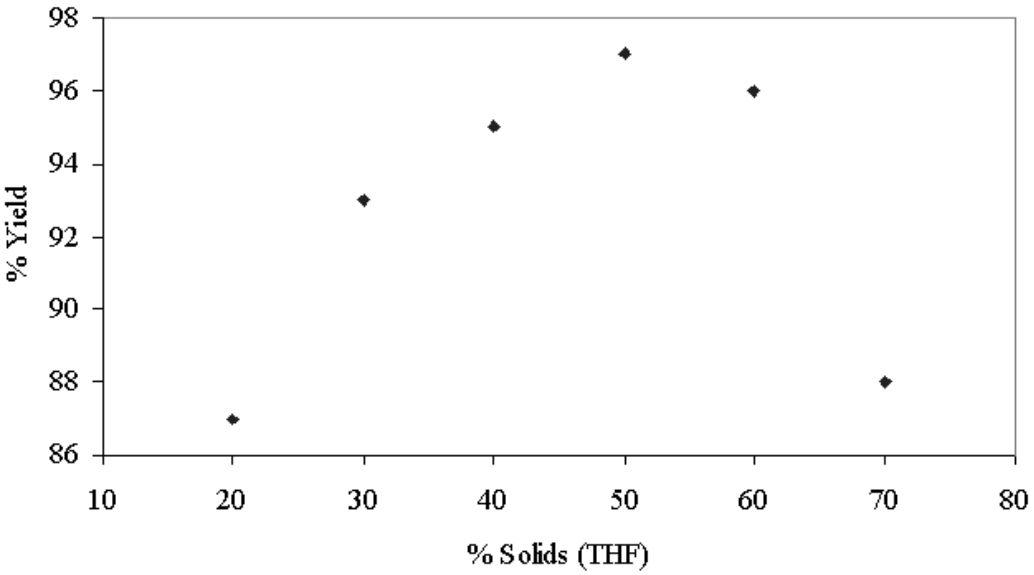

Figure 6.6 Yield (%) versus solids % in THF (3 mol percent AIBN, 50/50 Nb/MAH, 65 °C, 24 h).

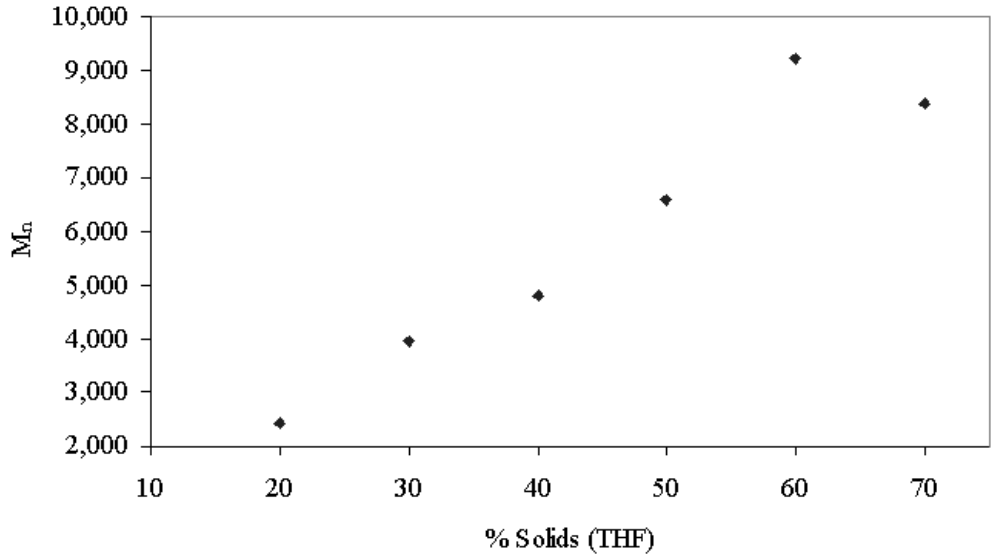

Figure 6.7 Number average molecular weight versus solids % in THF (3 mol percent AIBN, 50/50 Nb/MAH, 65 °C, 24 h).

6.4.2 Kinetic Analysis of Nb/NbTBE/MAH Free Radical Terpolymerization using *In situ* FTIR

A derivative of Nb containing a *t*-butyl ester functionality, NbTBE, was also investigated in copolymerizations with MAH and terpolymerizations with Nb and MAH. In free radical copolymerizations with MAH, NbTBE behaved similarly to Nb and formed an almost perfectly alternating copolymer with MAH. Terpolymers prepared via free radical polymerization of Nb, NbTBE, and MAH (Scheme 6.2) resulted in multicomponent copolymers that theoretically contained alternating sequences of MAH/Nb and MAH/NbTBE (monomer consumption studies of terpolymerizations indicated that 50 mol % of converted monomer was MAH). *In situ* infrared spectroscopy provided real-time changes in monomer absorbances and allowed for comparative kinetic analysis of the Nb/NbTBE/MAH free radical terpolymerization processes.

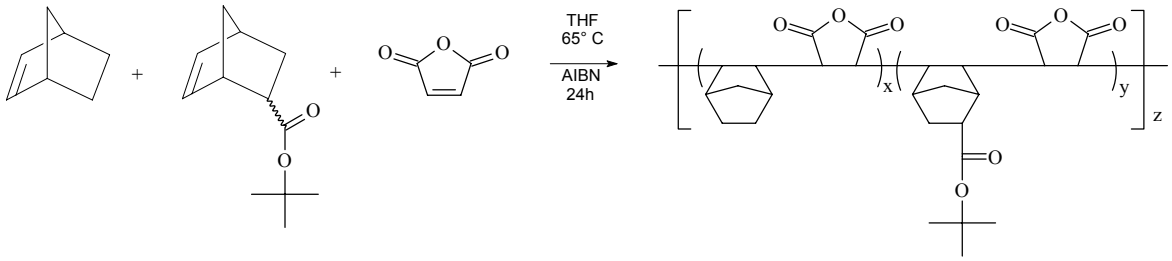

Scheme 6.2 Nb/NbTBE/MAH alternating terpolymerization scheme.

A reaction flask was specifically designed to permit the introduction of the ATR based infrared probe and attention was devoted to ensure the reactor was sealed to eliminate any volatilization of reaction components. Strong vinylene (=C-H) absorbances of the monomers were observed and allowed for kinetic analysis of the terpolymerizations using *in situ* FTIR. The waterfall plot of the vinylene =C-H region for a Nb/NbTBE/MAH

(25/25/50 mol ratio) is illustrated in Figure 6.8. The vinylene absorbances of Nb and NbTBE were not resolved and their combined absorbance was observed at 710 cm^{-1}. The vinylene absorbance of MAH was observed at 695 cm^{-1}.

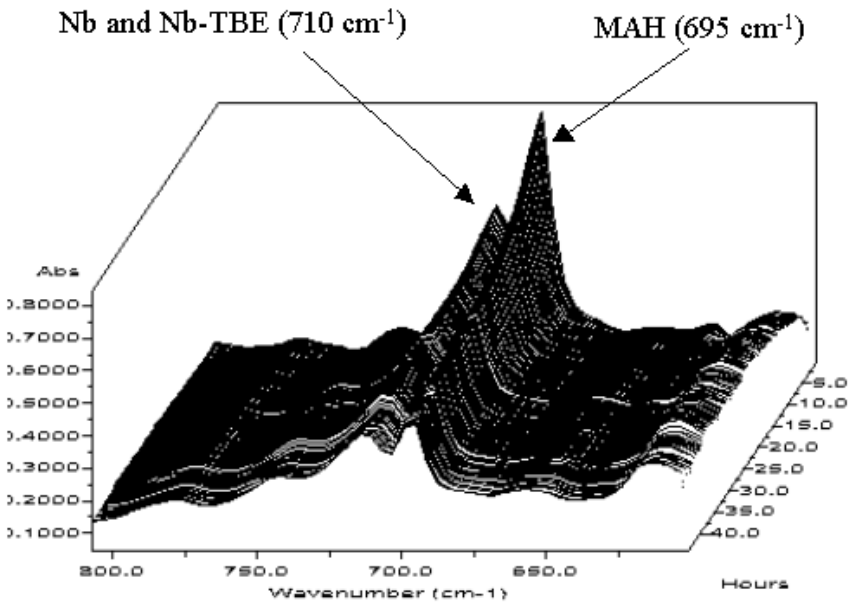

Figure 6.8 Vinylene region of "waterfall plot" for Nb/NbTBE/MAH (25/25/50 mol ratio) terpolymerization (*in situ* FTIR, spectrum acquired every 5 min).

Pseudo first order kinetic plots were constructed from the data obtained via the *in situ* monitoring of the monomer absorbances. Initial kinetic interpretations have focused on the assumption of pseudo first order kinetics for an alternating polymerization mechanism (Figure 6.9). Excellent agreement was observed using these assumptions and linear kinetic plots were observed. A representative kinetic plot of ln[monomer absorbance (total area from 670 to 725 cm^{-1})] vs. time for a Nb/NbTBE/MAH (25/25/50 mol ratio, k_{obs} = 3.8 x 10^{-5} s^{-1}) terpolymerization is shown in Figure 6.10.

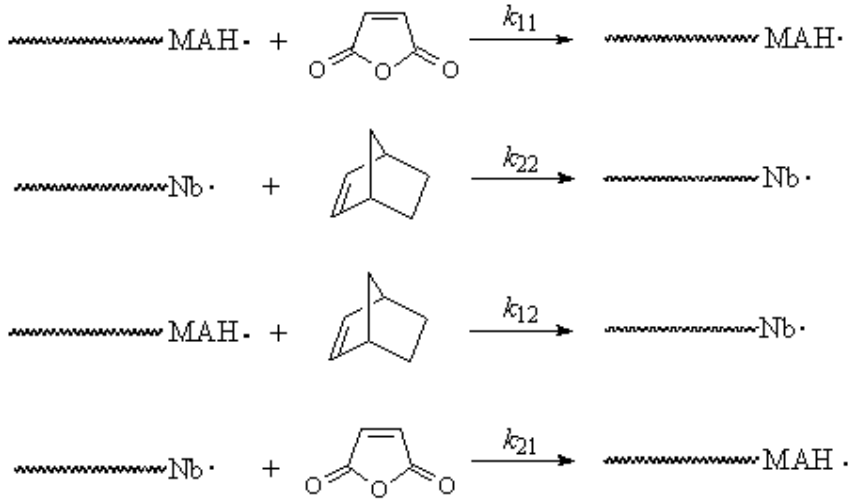

assuming negligible homopolymerization of MAH and Nb, k_{11}=k_{22}=0, overall rate is:

$$\text{rate} = k_{12}[(\text{MAH}\cdot)(\text{Nb})] + k_{21}[(\text{Nb}\cdot)(\text{MAH})]$$

assuming a steady state concentration of radical and alternating polymerization, rate is:

$$\text{rate} = (k_{12} + k_{21})([\text{P}\cdot][\text{M}])$$

where [P·] = conc. of growing polymer radicals and [M] = conc. of MAH or Nb monomer

and therefore an observed rate constant (k_{obs}) is obtained from a plot of ln[M] vs. time

$$\boldsymbol{k_{obs} = (k_{12} + k_{21})[\text{P}\cdot]}$$

Figure 6.9 Pseudo first order alternating polymerization kinetic assumptions.

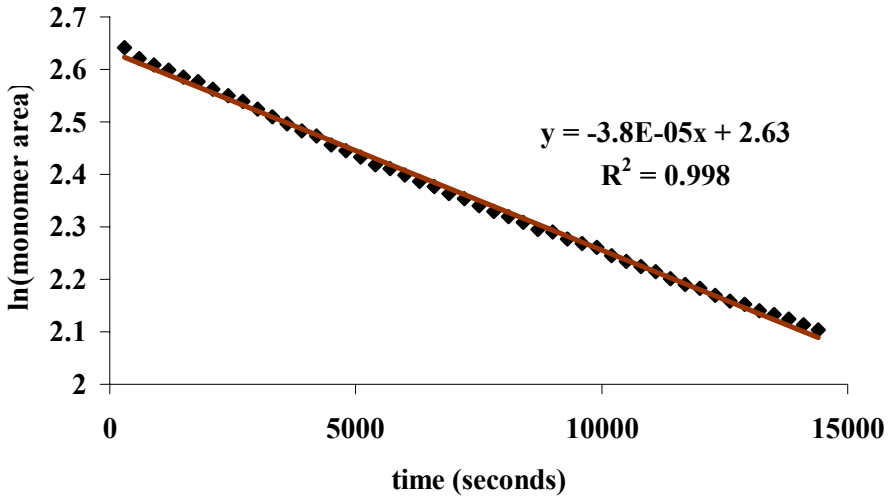

Figure 6.10 Psuedo first order kinetic treatment of convoluted Nb, NbTBE, and MAH (total area from 670 to 725 cm^{-1}) absorbances determined via *in situ* FTIR.

Free radical terpolymerizations of Nb/NbTBE/MAH with various ratios of Nb to NbTBE (while maintaining a 50 % molar feed of maleic anhydride) were performed using previously determined optimum conditions (3 mol % AIBN, THF (60 % solids), 24 h). Terpolymerizations were conducted using the following Nb/NbTBE/MAH monomer feed ratios: 50/0/50, 35/15/50, 25/25/50, 15/35/50, 0/50/50. The observed rate constants determined using *in situ* FTIR, percent yields, molecular weights, and Nb/NbTBE composition in the resulting materials are summarized in Table 6.1. Several trends are apparent from the data analysis. First, the observed reaction rate is a strong function of the monomer feed ratio of Nb/NbTBE with a maximum of 6.7 x 10^{-5} s^{-1} at a 50/0/50 Nb/NbTBE/MAH monomer feed ratio. The observed rate decreases with increasing NbTBE monomer feed to a minimum of 1.1 x 10^{-5} s^{-1} at a 0/50/50 Nb/NbTBE/MAH monomer feed ratio. In addition, percent yield exhibits a similar trend with a maximum yield of 94 % for a 50/0/50 Nb/NbTBE/MAH feed ratio and a minimum yield of 60 %

observed for a 0/50/50 Nb/NbTBE/MAH feed ratio. The observed decrease in rate with increasing NbTBE is proposed to be due to a combination of steric and electronic effects resulting from the *tert*-butyl ester functionality of NbTBE.

Table 6.1 Summary of Nb/NbTBE/MAH terpolymerizations varying the monomer feed ratio of Nb to NbTBE.

Nb/Nb-TBE/MAH	Observed rate (FTIR) x 10^5 s^{-1} [a]	Yield (%)	M_n[b]	M_w/M_n	Nb/Nb-TBE [c]
50/0/50	6.7	94	7,300	1.63	
35/15/50	5.3	87	6,500	1.46	3.2
25/25/50	3.8	80	6,700	1.64	1.4
15/35/50	2.6	75	6,600	1.49	0.68
0/50/50	1.1	60	6,900	1.59	

[a] Determined from first order kinetic plot using MAH/NB peak area via in-situ FTIR for first 4 h of reaction. [b] Wyatt miniDAWN MALLS detector coupled with Waters GPC with external 410 RI detector viscometer, THF solvent at 40 °C and 1.0 mL/min flow rate. [c] Determined using ^{13}C NMR (Varian Unity-400) at 100 MHz, DMSO-d_6, ambient temperature. Ratio calculated from integration of the quaternary carbon of *tert*-butyl ester group (δ 80 ppm) of Nb-TBE to the total carbonyl region (δ 170-176 ppm). For calculation, a 1:1 ratio of MAH to total cyclic olefin (Nb and Nb-TBE) is assumed.

^{13}C NMR analysis of terpolymers prepared from a 25/25/50 Nb/NbTBE/MAH monomer feed ratio further indicated that the terpolymers were enriched in Nb and depleted in NbTBE. The ^{13}C NMR spectrum of a Nb/NbTBE/MAH terpolymer is illustrated in Figure 6.11. The results obtained using ^{13}C NMR are quantitative based upon a carbon relaxation time experiment that was performed to calibrate the recycle delay for a NbTBE/MAH copolymer. The ratio of Nb to NbTBE in the terpolymer was subsequently determined via integration of the quaternary carbon of *tert*-butyl group (δ 80 ppm) to the carbonyl region (δ 170-176 ppm). Assuming a 1:1 molar ratio of MAH to the total cyclic olefin (Nb and NbTBE) incorporated into the terpolymer, the ratio of Nb to NbTBE

incorporated was subsequently determined to be 1.4:1.0 and confirmed that the final polymer composition does not match the monomer feed.

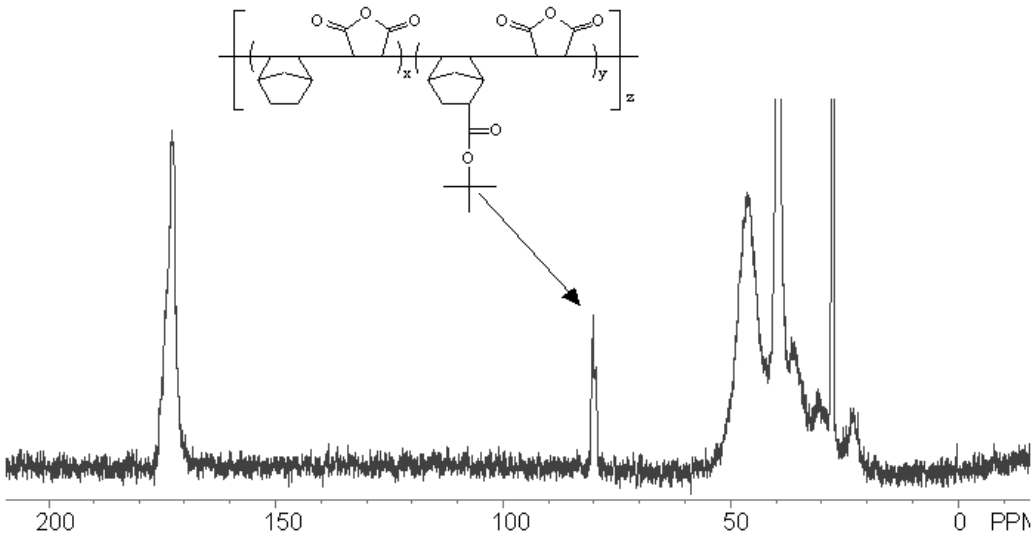

Figure 6.11 ^{13}C NMR (DMSO-d_6) spectra of terpolymer prepared from a 25/25/50 Nb/NbTBE/MAH monomer feed ratio.

6.4.3 Kinetic Analysis of Nb/NbTBE/MAH Free Radical Terpolymerizations via Sampling and ^{1}H NMR Analysis

In parallel with *in situ* real-time monitoring, a 25/25/50 Nb/NbTBE/MAH terpolymerization was sampled with time and subsequently analyzed using ^{1}H NMR at regular intervals for the first eight hours. ^{1}H NMR was a useful method for the spectroscopic separation of the norbornene and norbornene ester monomers. In addition, this technique was used to compare and evaluate the utility of *in situ* FTIR. The ^{1}H NMR spectrum depicting olefinic proton assignments for maleic anhydride, norbornene, and norbornene ester is shown in Figure 6.12. Moreover, it was determined using ^{1}H and ^{13}C NMR that the norbornene ester is a mixture of approximately 74 % endo and 26 % exo

stereoisomers. The assignments for the exo and endo stereoisomers are also shown in Figure 6.12. It is important to note that the ratio of endo to exo isomers did not change within the error of the NMR instrument and was approximately 74/26 throughout the entire polymerization, indicating that neither isomer shows a preference towards polymerization. Ito et al. have also observed that neither the exo or endo isomers of NbTBE show a preference towards polymerization with maleic anhydride under free radical conditions.[37] In contrast, Hennis and Sen have recently shown that exo substituted norbornenes are polymerized more readily than endo substituted norbornenes via palladium catalyzed insertion polymerization.[23] It is also expected for conventional free radical polymerization that exo substituted norbornenes would react faster than endo substituted norbornenes since endo substitution may sterically hinder the norbornene olefinic site. However, since neither isomer shows preference in the free radical copolymerization with maleic anhydride, it is proposed that the lower reactivity of substituted norbornenes is not due solely to steric factors.

[23] Hennis, A. D.; Sen, A. *Polym. Prepr. (Am. Che. Soc., Div. Polym. Chem.)* **2000**, *41*(2), 1933.

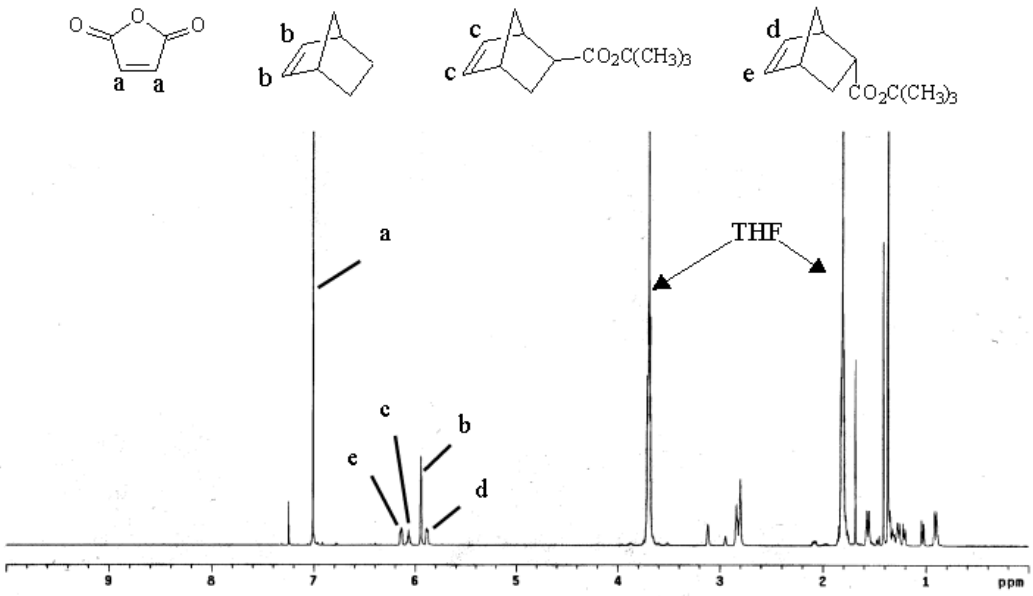

Figure 6.12 ^{1}H NMR ($CDCl_3$) of Nb/NbTBE/MAH (25/25/50 mol ratio) reaction mixture.

Monomer conversion data is typically obtained from the relative integration of monomer and polymer resonances; however, the ^{1}H NMR spectra of the terpolymerization reaction samples were very broad and unresolved, and this conventional approach was not suitable. Thus, in order to determine conversion data for the terpolymerizations, the monomer peaks were integrated relative to the tetrahydrofuran (THF) solvent peak at δ 3.7 ppm. The signal due to THF was presumed to remain at the same relative concentration throughout the reaction since the reactions were performed under positive nitrogen pressure and attention was devoted to ensure that the reactor was sealed tightly to eliminate any volatilization of reaction components. Terpolymerization conversion data for MAH, Nb, and NbTBE data obtained using ^{1}H NMR is summarized in Table 6.2.

Table 6.2 Conversion data for a Nb/NbTBE/MAH (25/25/50 mol ratio) terpolymerization determined from ^{1}H NMR analysis.

	conversion[a]		
time (h)	MAH (%)	Nb (%)	NbTBE (%)
0	0	0	0
1	28	32	9
2	31	44	18
3	54	51	27
4	50	62	32
5	58	68	39
6	64	73	48
7	71	77	53
8	74	80	58

[a] ^{1}H NMR ($CDCl_3$ solvent).

First order kinetic plots constructed from the conversion data of MAH (Figure 6.13), Nb (Figure 6.14) and NbTBE (Figure 6.14) were linear and complimented kinetic analysis using *in situ* FTIR data. Assuming alternating copolymerization of Nb and NbTBE with MAH, first order kinetic analysis of MAH using ^{1}H NMR was directly compared to analysis via *in situ* FTIR. The value obtained using ^{1}H NMR (4.4×10^{-5} s^{-1}, Figure 6.13) correlated well with the value from *in situ* FTIR (3.8×10^{-5} s^{-1}, Figure 6.10). The observed rate constants for both Nb and NbTBE (Figure 6.14) were linear with a ratio in rates of approximately 5:3 (Nb:NbTBE). This result combined with complementary kinetic analysis of copolymerizations using *in situ* FTIR (Table 6.1), which showed that the copolymerization of Nb and MAH was approximately 6 times faster than the copolymerization of NbTBE and MAH, provides an interesting insight to the reaction mechanism. It was previously discussed that the slower reaction rate of the NbTBE

olefinic site was likely due to a combination of steric and electronic effects. However, the presence of NbTBE in a terpolymerization also decreases the rate of Nb propagation.

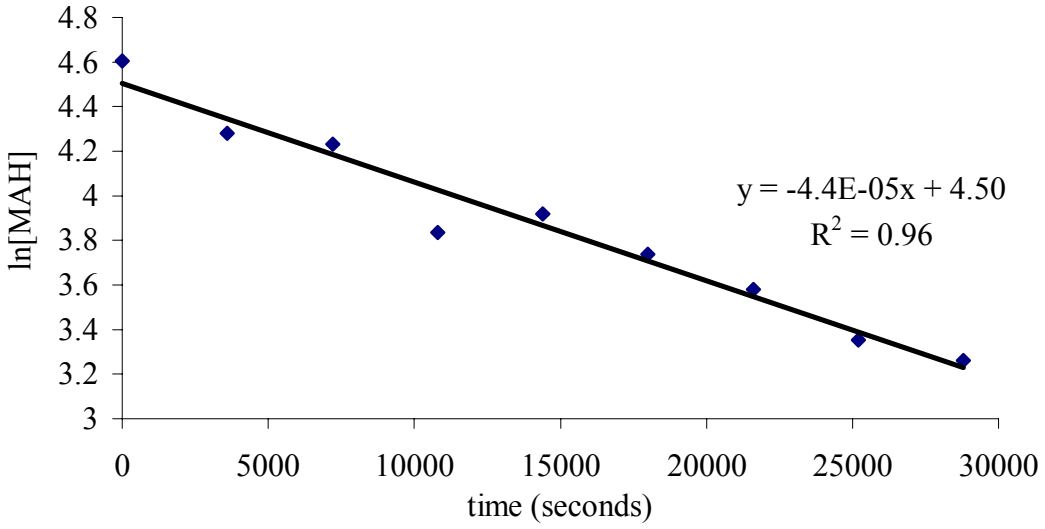

Figure 6.13 First order kinetic analysis of maleic anhydride conversion (determined using ^{1}H NMR analysis of samples taken every hour for the first 8 h).

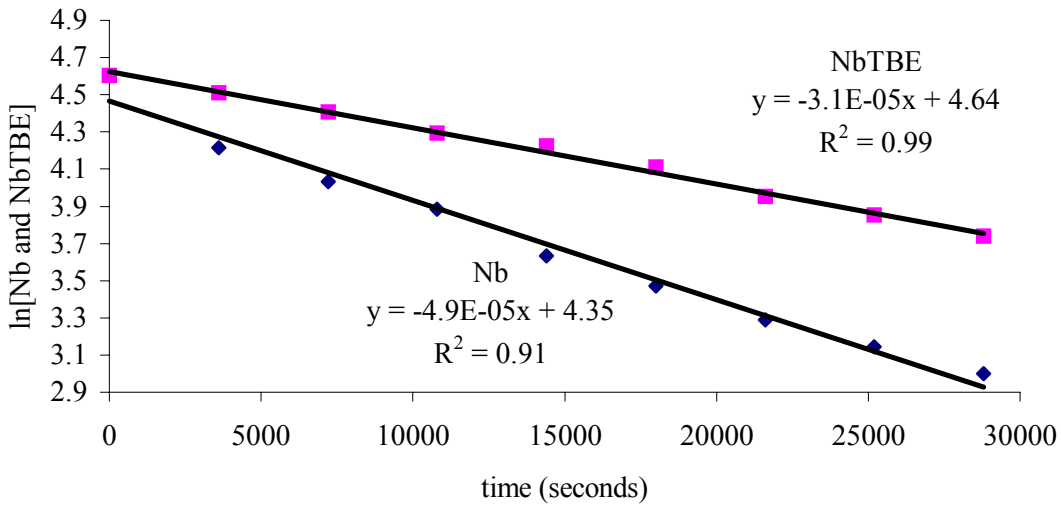

Figure 6.14 First order kinetic analysis of Nb and NbTBE conversion (determined using ^{1}H NMR analysis of samples taken every hour for the first 8 h).

6.4.4 Bulk Nb/NBTBE/MAH Bulk Terpolymerization in Excess NbTBE

Preparation of Nb/NbTBE/MAH terpolymers in the absence of a polymerization solvent is particularly promising since a bulk polymerization provides an economical and environmentally friendly route for these terpolymeriztions. Furthermore, performing the terpolymerizations in excess NbTBE offers the potential to control the incorporation of NbTBE into the terpolymers. All reactions were allowed to proceed for 24 h at 65 °C. The results of the experiments are summarized in Table 6.3. The excess of NbTBE to Nb was varied while maintaining a 1:2 molar charge of Nb to MAH. As one can see in Table 3, relatively high molecular weights for these terpolymerizations were obtained using this methodology. Number average molecular weights close to 20,000 were obtained when the polymerization was performed in excess NbTBE compared to number average molecular weights consistently around 7,000 when the terpolymerizations are performed in THF solvent at 60 % solids. In addition, it was observed that the Nb/NbTBE ratio in the

terpolymers was controllable via changing the excess amount of NbTBE in the monomer feed. The Nb/NbTBE ratio in the terpolymer decreased from a maximum of 1.50 using a 1:1 Nb:NbTBE monomer feed ratio to 0.22 using a 1:4 Nb:NbTBE monomer feed ratio (Table 6.3). *In situ* infrared analysis of the terpolymerizations in excess NbTBE were complicated due to absorbance overlap.

Table 6.3 Summary of bulk Nb/NbTBE/MAH terpolymerizations carried out in excess NbTBE.

excess NbTBE	yield (%)	M_n[a]	M_w/M_n	Nb/NbTBE[b]
1x NbTBE	53	20,200	1.54	1.50
2x NbTBE	85	20,000	1.56	0.66
4x NbTBE	91	17,100	1.53	0.22

[a] Wyatt miniDAWN multiple angle laser light scattering detector in-line with Waters GPC system with 410 RI detector, 40 °C, 1.0 mL/min. [b] Determined using ^{13}C NMR (Varian Unity-400) at 100 MHz, DMSO-d_6, ambient temperature. Ratio calculated from integration of the quaternary carbon of *tert*-butyl ester group (δ 80 ppm) of NbTBE to the total carbonyl region (δ 170-176 ppm). For calculation, a 1:1 ratio of MA to total cyclic olefin (Nb and NbTBE) is assumed.

6.4.5 Nb/MAH Copolymerizations with the Addition of *tert*-Butyl Acrylate (tBA) and *tert*-Butyl Methacrylate (tBMA)

The addition of tBA and tBMA to copolymerizations of Nb and MAH was also studied. Previously, Reichmanis and coworkers have reported that tBA (up to 0.3 mol fraction) can be incorporated in a controlled and predictable manner into free radical alternating copolymerizations of Nb and MAH.[24] *In situ* FTIR was used to follow and evaluate monomer conversion for 50/50 Nb/MAH copolymerizations incorporating 15

mole percent (based upon total Nb and MAH concentration) of either tBA or tBMA. The remaining reaction conditions were based upon previously optimized conditions (3 mol % AIBN, THF, 60 % solids, 65 °C for 24 h under positive nitrogen pressure (5-10 psi)). Normalized monomer conversions that were determined real-time via *in situ* FTIR are illustrated in Figure 6.15 and Figure 6.16. Conversion values were based upon FTIR absorbance peak heights corresponding to each monomer. As one can see, the conversion profiles of monomers were significantly different between the reactions incorporating either tBA or tBMA. Although the free radical homopolymerization rate of an acrylate is expected to be approximately four times faster than a corresponding methacrylate,[25] tBMA reacted much faster than tBA under identical conditions in these systems. In addition, the conversion of Nb and MAH was disrupted more in the presence of tBMA and only low conversion of Nb occurred in the reaction with tBMA. This observation agreed well with results reported by Ito and coworkers, who investigated the same terpolymerization schemes.[26] The yield of the 50/50/15 Nb/MAH/tBA terpolymerization was 83 % with a number average molecular weight of 7,800 (M_w/M_n = 1.74) using MALLS detection. The 50/50/15 terpolymerization of Nb/MAH/tBMA resulted in a lower yield of 68 % with a number average molecular weight of 11,800 (M_w/M_n = 1.60) using MALLS detection. GPC was performed directly on the reaction mixtures after 24 h to ensure the polymers were not fractionated during precipitation.

---

[24] Houlihan, F. M.; Wallow, T. I.; Nalamasu, O.; Reichmanis, E. *Macromolecules* **1997**, *30*, 6517.
[25] *Polymer Handbook*, 4th ed.; Brandrup, J., Immergut, E. H., Grulke, E. A., Eds.; Wiley & Sons: New York, 1999.
[26] Ito, H.; Miller, D.; Sveum, N.; Sherwood, M. *J. Polym. Sci. Part A: Polym. Chem.* **2000**, *38*, 3521.

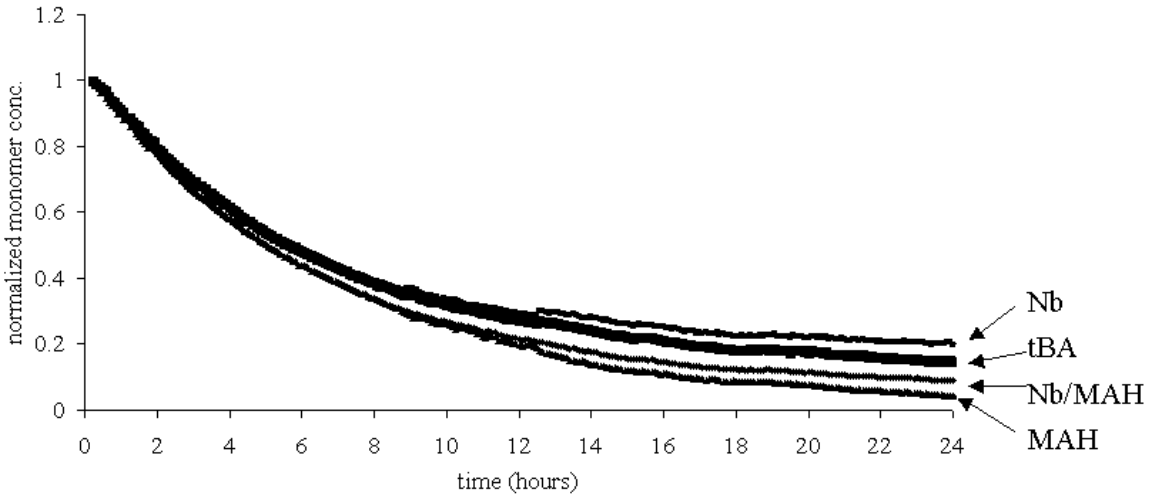

Figure 6.15 Normalized monomer concentrations for a 50/50/15 Nb/MAH/tBA terpolymerization determined using *in situ* FTIR.

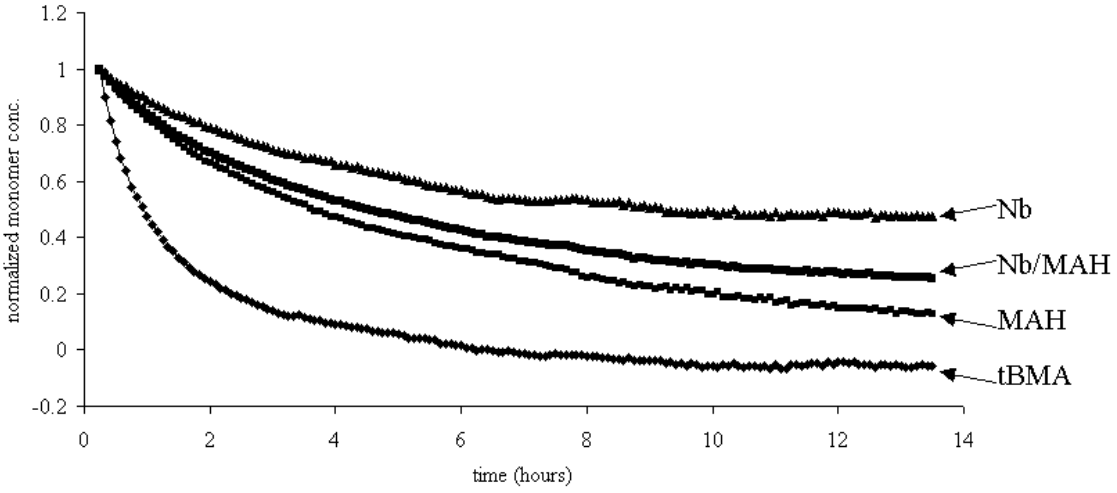

Figure 6.16 Normalized monomer concentrations for a 50/50/15 Nb/MAH/tBMA terpolymerization measured using *in situ* FTIR.

The GPC chromatograms of the terpolymerization reaction mixtures are illustrated in Figure 6.17 and Figure 6.18. The chromatogram of the Nb/MAH/tBA terpolymerization (Figure 6.17) appears to be symmetric and monomodal while the chromatogram of the Nb/MAH/tBMA terpolymerization (Figure 6.18) is slightly bimodal with a high molecular weight shoulder indicating heterogeneity. The irregularity of the Nb/MAH/tBMA chromatogram further suggested that tBA was incorporated more uniformly than tBMA into free radical copolymerizations of Nb and MAH.

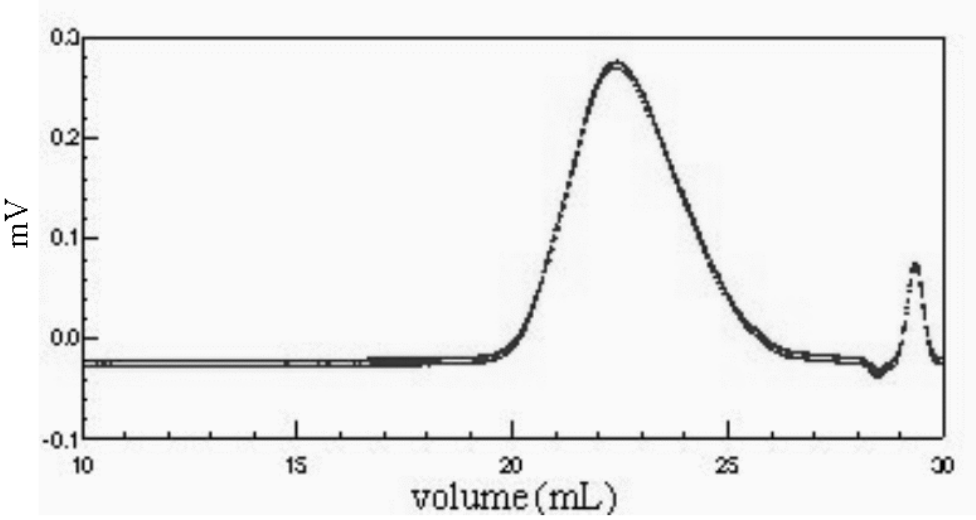

Figure 6.17 GPC chromatogram of 50/50/15 Nb/MAH/tBA terpolymerization.

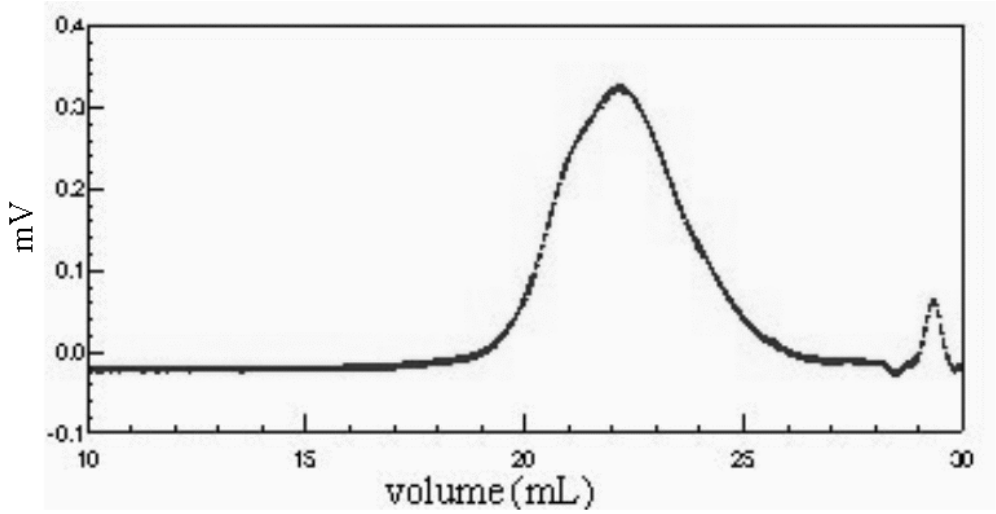

Figure 6.18 GPC chromatogram of 50/50/15 Nb/MAH/tBMA terpolymerization.

6.5 CONCLUSIONS

Synthetic factors that affect the molecular weight, yield, and composition of Nb/NbTBE/MAH terpolymers have been investigated. Efforts have indicated optimum reaction conditions in terms of yield and molecular weight for free radical alternating copolymerizations of Nb and MAH as follows: 60 percent solids in THF, 3.0 mol percent AIBN compared to total monomer amount, a 50:50 molar ratio of Nb:MAH, and 65 °C for 24 h. Real-time monitoring via *in situ* FTIR spectroscopy of alternating terpolymerizations of MAH with Nb and NbTBE was utilized to evaluate the relative rates of varying Nb/NbTBE monomer feed ratios. Pseudo first order kinetic plots constructed from the *in situ* FTIR absorbance data indicated that the rate of reaction was a strong function of the Nb/NbTBE ratio and decreased with increasing NbTBE. In addition, percent yields were also observed to be a function of the Nb/NbTBE ratio and again decreased with increasing NbTBE. Sampling of a Nb/NbTBE/MAH (25/25/50 mol ratio) terpolymerization and subsequent analysis using ^{1}H NMR indicated that the relative rate of Nb incorporation was approximately 1.7 (5/3) times faster than NbTBE incorporation. Terpolymerizations carried out in excess NbTBE in the absence of solvent resulted in higher molecular weights

and provided for a relative amount of control of the Nb/NbTBE incorporation into the resulting materials. Copolymerizations of Nb and MAH with the addition of tBA or tBMA as a third monomer showed that tBMA reacted much faster than tBA under identical conditions in these systems and the conversion of Nb and MAH was disrupted more in the presence of tBMA.

Acknowledgements. Financial support provided by IBM, Jeffress Memorial Trust, Virginia Tech Department of Chemistry, National Science Foundation (CRIF CHE-9974632), and the Center of Adhesive and Sealant Science (CASS) at Virginia Tech and the Adhesive and Sealant Council (ASC) is gratefully acknowledged. The author would also like to thank Thomas Glass at Virginia Tech for assistance with NMR analysis.

Recommended future studies:

- Study rate of MAH copolymerization with Nb ester derivatives containing different size alkyl chains (i.e. methyl, ethyl, isopropyl, t-butyl ester, etc.) in order to more accurately probe the steric contribution to the observed decrease in rate.
- Studies to better determine either the existence or absence of a complexed comonomer system.
- Apply different copolymerization models to MAH/Nb copolymerizations.

CHAPTER 7

Investigations of the Adhesion of Maleic Anhydride/Cyclic Olefin Alternating Copolymers to Silicon Substrates: Improved Materials for 193 nm Lithography

7.1 ABSTRACT

Various synthetic variations that affect the molecular weight, yield, and composition of maleic anhydride (MAH), norbornene (Nb), and tert-butyl 5-norbornene-2-carboxylate (NbTBE) terpolymers have been investigated. The adhesive properties of these polymers were evaluated from work of adhesion (W_{adh}) values to silicon substrates (treated with hexamethyldisilazane) using the method of fractional surface free energy from contact angle measurements of water and methylene iodide on the polymer films and substrate. These measurements showed that W_{adh} values increased as the content of NbTBE in the terpolymers was increased. Calculated work of adhesion values for the Nb/NbTBE/MAH terpolymers were close to those of conventional 248 nm photoresist polymers. Furthermore, 193 nm resist formulations incorporating polymers with high NbTBE content showed increased imaging performance and successfully produced sharp and defined features as small as 110 nm, which was seen via scanning electron microscopy (SEM).

7.2 INTRODUCTION

Photolithography using 193 nm (Ar-F laser) light is the basis for the production of the next generation of microelectronic devices.[1] Current technology (Kr-F laser), including ultraviolet (UV) and deep-UV (DUV) photolithography, employs aromatic materials based upon phenolic polymers.[2] However, the photon energy of 193 nm light is high enough for aromatic polymers to absorb strongly at this wavelength, resulting in opaque materials that are not practical for 193 nm lithography.[3] Therefore, recent years have seen a large effort devoted to the design of materials that are optically transparent at 193 nm and also have the desirable etch-resistant and image-forming properties of phenolic based materials.[4]

A number of approaches to materials with high transparency at 193 nm have been reported.[5] Initially, acrylic-based polymers seemed promising as new materials for 193 nm lithography. Acrylates were desirable polymeric materials due to only a weak carbonyl absorption at 193 nm, which resulted in good transparency when exposed to this wavelength of light.[6] For example, Allen and coworkers described successful 193 nm patterning using an all-acrylic terpolymer made up of methyl methacrylate, *tert*-butyl methacrylate, and methacrylic acid.[7] However, the poor reactive-ion etch resistance of

---

[1] Nozaki, N.; Kaimoto, M.; Takahashi, S.; Takeshi, S.; Abe, N.; *Chem. Mater.* **1994**, *6*, 1492. Kunz, R. R.; Palmateer, A. R,; Forte, A. R.; Allen, R. D.; Wallraff, G. M.; DiPietro, R. A.; Hofer, D. C.; *Proc. SPIE-Int. Soc. Opt. Eng.* **1996**, *2724*, 365. Allen, R. D.; Opitz, J.; Larson, C. E.; Wallow, T. I.; Hofer, D. C. *Microlithography World*, *5* (winter 1999). Jung, M. H.; Jung, J. C.; Lee, G.; Baik, K. H.; *Jpn J. Appl. Phys., Part 1* **1998**, *37*, 6889. Nalamasu, O.; Houlihan, R. A.; Cirelli, A. G.; Watson, G. P.; Hutton, R. S.; Kometani, J. M.; Reichmanis, E. *J. Vac. Sci. Technol., B* **1998**, *16*, 3716. Okoroanyanwu, U.; Byers, J.; Shimokawa, T.; Willson, C. G. *Chem. Mater.* **1998**, *10*, 3328.

[2] Ito, H. *Solid State Technol.* **1996**, *36*(7), 164. Willson, C. G. In *Introduction to Microlithography*, 2nd ed.; Thompson, L. F., Willson, C. G., Bowden, M. J., Eds.; ACS Professional Reference book; American Chemical Society: Washington, DC, 1994; Ch. 3.

[3] Kunz, R. R.; Allen, R. D.; Wallraff, G. M. *Polym. Prepr. (Am. Chem. Soc., Div. Polym. Chem.)* **1994**, *35*(2), 939.

[4] Allen, R. D.; Wallraff, G. M.; Hofer, D. C.; Kunz, R. R.; *IBM J. Res. Dev.* **1997**, *41*, 95.

[5] Nonogaki, S.; Ueno, T.; Ito, T.; In *Microlithography Fundamentals in Sumiconductor Devices and Fabrication Technology*; Marcel Dekker: New York, 1999; pp. 115-119.

[6] Wallraff, G. M.; Hinsberg, W. D. *Chem. Rev.* **1999**, *99*, 1801.

[7] Allen, R. D.; Wallraff, G. M.; Hinsberg, W. D.; Simpson, L. L. *J. Vac. Sci. Technol., (B)* **1991**, *9*, 3357.

acrylics under the etching conditions used widely in the semiconductor industry has limited their application in 193 nm resist materials.[8] The primary design challenge that has emerged in the development of new materials for 193 nm photolithography is the trade off between imaging performance (broadly defined as resolution, adhesion, sensitivity, and compatibility with industry standard aqueous-base developers) and reactive-ion etch resistance.[4] The chemical modifications that were used to tailor the imaging performance of acrylic polymers also detrimentally influenced reactive-ion etch resistance.[8] Previously, it has been determined that there is a correlation between increased reactive-ion etch resistance and a high carbon to hydrogen (C/H) ratio,[9] helping to explain why currently used phenolic materials, which have a high C/H ratio, exhibit good plasma etch resistance. Therefore, in an attempt to improve the reactive-ion etching properties of acrylic based polymers via increasing the C/H ratio, a number of acrylic-based materials containing pendant alicyclic adamantane or norbornane functionality have been investigated.[10] Incorporation of the pendant alicyclic functionalities into the multi-component photoresist acrylic polymeric materials resulted in greatly improved etch resistance. However, the increase in etch resistance was also accompanied by decreased image performance. Consequently, the development of a acrylic 193 nm photoresist polymer material with both etch resistance and image performing properties required for industrial application has not been achieved.

---

[8] Wallow, T. I.; Brock, P. J.; Dipietro, R. A.; Allen, R. D.; Opitz, J.; Sooriyakumaran, R.; Hofer, D. C, Meute, J.; Byers, J. D.; Rich, G. K.; McCallum, M.; Schuetze, S.; Jayaraman, S.; Hullihen, K.; Vicari, R.; Rhodes, L. F.; Goodall, B. L.; Shick, R. A. *Proc. SPIE-Int. Soc. Opt. Eng.* **1998**, *3333*, 92.

[9] Gokhan, H.; Esho, S.; Ohnishi, Y. *J. Electrochem. Soc.* **1983**, *130*, 143. Kunz, R. R.; Palmateer, A. R.; Forte, A. R.; Allen, R. D.; Wallraff, G. M.; DiPietro, R. A.; Hofer, D. C. *Proc. SPIE-Int. Soc. Opt. Eng.* **1996**, *2724*, 365.

[10] Kaimoto, Y.; Nozaki, K.; Takechi, M.; Abe, N. *Proc. SPIE-Int. Soc. Opt. Eng.* **1992**, *1672*, 66. Nozaki, K.; Kaimoto, Y.; Takahashi, M.; Takechi, M.; Abe, N.; *Chem. Mater.* **1994**, *6*, 1492. Takechi, S.; Takahashi, M.; Kotachi, A.; Nozaki, K.; Yano, E.; Hanyu, I. *J. Photopolym. Sci. Technol.* **1996**, *9*, 475. Yamashita, K.; Endo, M.; Sasago, M.; Nomura, N.; Nagano, H.; Mizuguchi, S.; Ono, T.; Sato, T. *J. Vac. Sci. Technol., (B)* **1993**, *11*, 2692. Nakano, K.; Maeda, K.; Iwasa, S.; Yano, J.; Ogura, Y.; Hasegawa, E. *Proc. SPIE-Int. Soc. Opt. Eng.* **1994**, *2195*, 194. Maeda, K.; Nakano, K.; Ohfuji, T.; Hasegawa, E. *Proc. SPIE-Int. Soc. Opt. Eng.* **1996**, *2724*, 377. Allen, R. D.; Wallraff, G. M.; DiPietro, R. A.; Hofer, D. C.; Kunz, R. R. *J. Photopolym. Sci. Technol.* **1994**, *7*, 507.

An alternative approach to increase the C/H ratio in 193 nm photoresist polymers has been to incorporate alicyclic structures directly into the polymer backbone.[6] Recent years have seen the investigation of a variety of synthetic methods for producing 193 nm resist materials with alicyclic backbones.[11] They include the alternating free radical copolymerization of maleic anhydride with cyclic olefins, metal catalyzed vinyl addition polymerization, and ring opening metathesis polymerization (ROMP) followed by hydrogenation. In recent years, the most promising of these methods that has emerged for synthesizing alicyclic photoresist materials for 193 nm lithography is the alternating free radical copolymerization of maleic anhydride with cyclic olefin monomers such as norbornene (Scheme 7.1). Cyclic olefins will homopolymerize poorly via free radical methods. However, when cyclic olefins are reacted with maleic anhydride, which is a strong electron acceptor, in the presence of a free radical initiator, they copolymerize in an alternating manner.[12] In addition, maleic anhydride also serves to incorporate oxygen into the material, providing necessary adhesion and solubility properties that are required for imaging performance while still retaining sufficient etch resistance to be successfully demonstrated as 193 nm resist materials.[13] The cyclic olefin character of these materials provides for excellent etch resistance, surpassing even currently utilized phenol based resists. Furthermore, the increased etch resistance is of great importance because of the

---

[11] Okoroanyanwu, U.; Shimokawa, T.; Byers, J.; Medeiros, D.; Willson, C. G.; Niu, Q, J.; Fréchet, J. M. J.; Allen, R. D. *Proc. SPIE-Int. Soc. Opt. Eng.* **1997**, *3049*, 92. Okoroanyanwu, U.; Shimokawa, T.; Byers, J.; Willson, C. G. *Chem Mater.* **1998**, *10*, 3319. Nozaki, K.; Yano, E. *J. Photopolym. Sci. Technol.* **1997**, *10*, 545. Patterson, K.; Okoroanyanwu, U.; Shimokawa, T.; Cho, S.; Byers, J.; Willson, C. G. *Proc. SPIE-Int. Soc. Opt. Eng.* **1998**, *3333*, 425. Wallow, T. I.; Houlihan, F. M.; Nalamasu, O.; Chandross, E. A.; Neenan, T. X.; Reichmanis, E. *Proc. SPIE-Int. Soc. Opt. Eng.* **1996**, *2724*, 355. Houlihan, F. M.; Wallow, T. I.; Nalamasu, O.; Reichmanis, E. *Macromolecules* **1997**, ***30***, 6517. Patterson, K.; Yamchika, M.; Cho, S.; Rager, T.; Yamada, S.; Byers, J.; Willson, C. G. *Polym. Mat. Sci. Eng.* **1999**, *81*, 43. Gabor, A. H.; Dimov, O.; Medina, A. N.; Bowden, M. J.; Neisser, M. O.; Houlihan, F. M.; Cirelli, R. A.; Dabbagh, G.; Hutton, R. S.; Rushkin, I. L.; Sweeney, J. R.; Nalamasu, O.; Reichmanis, E. *Polym. Mat. Sci. Eng.* **1999**, *81*, 41. Allen, R. D.; Sooriyakumaran, R.; Opitz, J.; Wallraff, G. M.; DiPietro, R. A.; Breyta, G.; Hofer, D. C. *Proc. SPIE-Int. Soc. Opt. Eng.* **1996**, *2724*, 334. Allen, R. D.; Opitz, J.; Wallow, T. I.; DiPietro, R. A.; Hofer, D. C.; Jayaraman, S.; Hullihan, K. A.; Rhodes, L. F.; Goodall, B. L.; Shick, R. A. *Proc. SPIE-Int. Soc. Opt. Eng.* **1998**, *3333*, 463. Opitz, J.; Allen, R. D.; Wallow, T. I.; Wallraff, G. M.; Hofer, D. C.; *Proc. SPIE-Int. Soc. Opt. Eng.* **1998**, ***3333***, 571.

[12] Allen, R. D.; Opitz, J.; Larson, C. E.; Wallow, T. I.; Hofer, D. C.; *Microlithography World*, 5 (winter 1999).

decreasing film thickness necessary for the achievement of increasingly smaller feature sizes.[12] In addition, the ability to modify the polymer properties via incorporation of cyclic olefin monomer derivatives to improve lithographic performance has further made this a very attractive route to new materials for 193 nm lithography.

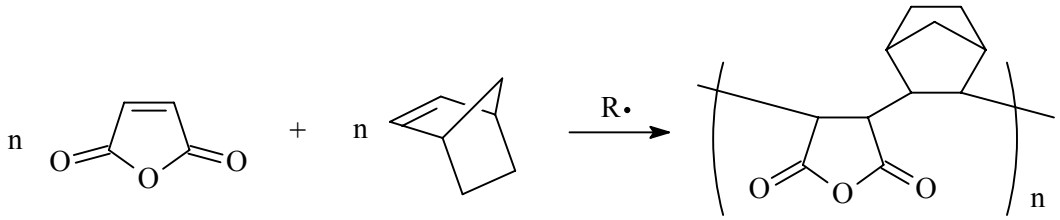

Scheme 7.1 Maleic anhydride and norbornene alternating copolymerization scheme.

The adhesion performance of resist systems will be a critical performance criterion as microelectronic device features are pushed to smaller dimensions. The adhesion properties of chemically amplified resist polymers based on poly(hydroxystyrene) have been very successful in the production of patterned images using UV and DUV lithography. However, as device features are driven to dimensions below 100 nm, the properties of adhesion and resist rigidity become increasingly more important to prevent the collapse of patterned images.[14] Fréchet and coworkers have recently demonstrated the successful use of a hyperbranched polyester as a negative tone chemically amplified resist that produced uniform 100 nm lines via electron-beam exposure.[15] However, the 100 nm features exhibited poor adhesion to the silicon substrate and resulted in random migration of the patterned lines (Figure 7.1). In addition, the issue of adhesion for alternating copolymers of cyclic olefins with maleic anhydride has also been addressed previously. For example, Kim and coworkers have recently investigated the adhesive and lithographic properties of maleic anhydride/norbornene copolymers with the addition of an adhesion promoter to

---

[13] Houlihan, F. M.; Wallow, T. I.; Nalamasu, O.; Reichmanis, E. *Macromolecules* **1997**, *30*, 6517.
[14] Koh, C. W.; Baik, K. H.; *J. Photopolym. Sci. Technol.* **2000**, *13*, 539.
[15] Trimble, A. R.; Tully, D. C.; Fréchet, J. M. J.; Medeiros, D. R.; Angelopoulos, M. *Polym. Prepr. (Am. Chem. Soc., Div. Polym. Chem.)* **2000**, *41*(1), 325.

improve the adhesive properties of the resists.[16] They reported that the addition of hydrophilic 2-(2-methoxyethoxy) ethyl ester groups (Figure 7.2) into their structures resulted in improved adhesion and 150 nm lines and spaces were successfully obtained using an ArF exposure system.

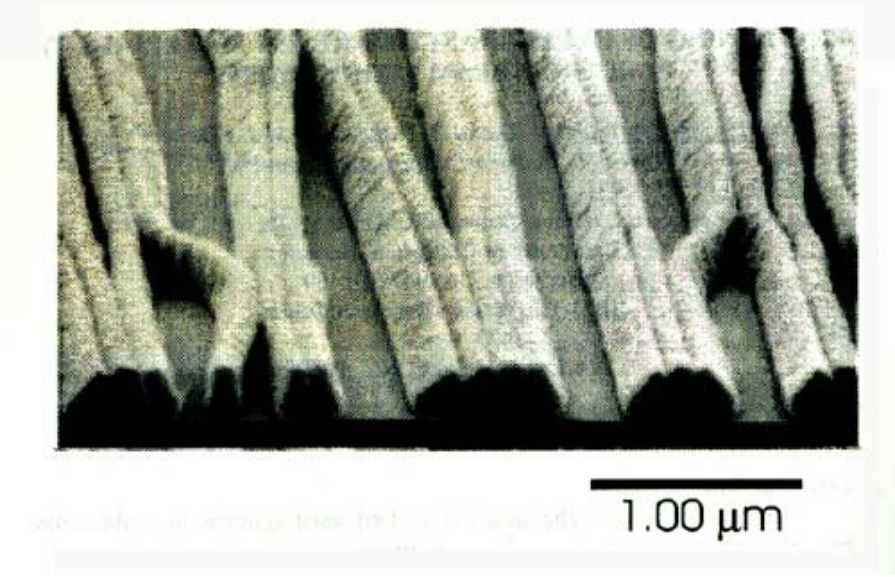

Figure 7.1 SEM of hyperbranched polyester resist material patterned via electron-beam lithography.[15]

[16] Kim, J. B.; Yun, H. J.; Kwon, Y. G.; Lee, B. W. *Polymer* **2000**, *41*, 8035.

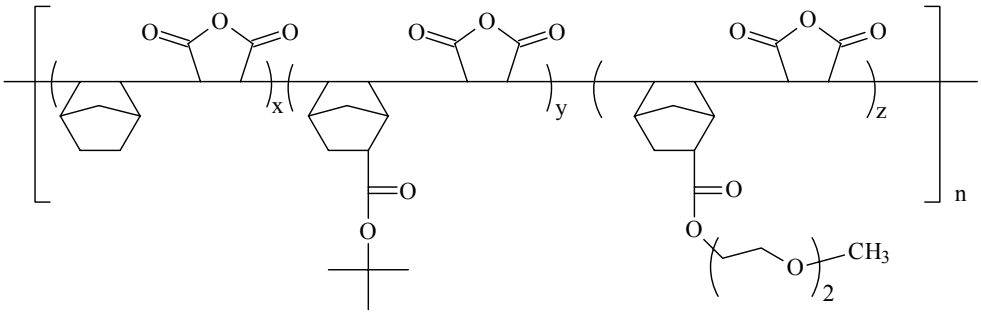

Figure 7.2 Incorporation of adhesion promoter (2-(2-methoxyethoxy) ethyl ester Nb derivative) into cyclic olefin/maleic anhydride photoresist polymer.

The focus of this research has been to investigate the adhesive and imaging properties of terpolymers composed of maleic anhydride (MAH), norbornene (Nb), and a norbornene derivative containing an acid labile *tert*-butyl ester functionality, *tert*-butyl 5-norbornene-2-carboxylate (NbTBE) (Scheme 7.2), which when hydrolyzed to the corresponding carboxylic acid, lends aqueous base solubility. The *tert*-butyl functionality also serves to incorporate additional oxygen, which is anticipated to affect the adhesive properties of the resists. This study will describe the synthesis and characterization of these terpolymers based on MAH, Nb, and NbTBE. Thermodynamic work of adhesion values as a function of the NbTBE incorporation will also be discussed and successful patterning of these resist polymers using 193 nm ArF exposure technology will be demonstrated.

7.3 EXPERIMENTAL

7.3.1 Materials

Norbornene (Nb) was purchased from Aldrich and vacuum distilled (0.1 mm Hg) at room temperature from calcium hydride after degassing three times using the traditional freeze-thaw method. After distillation it was stored under positive nitrogen pressure as a solution in tetrahydrofuran. Maleic anhydride (MAH) was purchased from Aldrich and

purified via sublimation immediately prior to use. Tetrahydrofuran was distilled using the classic sodium/benzophenone ketyl. All other reagents were purchased from Aldrich and used as received.

7.3.2 Characterization

Molecular Weight Characterization

Molecular weights were measured using a Wyatt miniDAWN multiangle laser light scattering (MALLS) detector with a 690 nm laser (Wyatt Technology, Santa Barbara, CA) connected to a Waters SEC (515 pump, 717 autosampler, and 410 refractive index detector). The miniDAWN was connected in series after three 5-μm Plgel mixed-bed columns (Polymer Laboratories, Amherst, MA). Measurements were made at 40 °C with THF as the solvent at a flow rate of 1.0 mL/min.

NMR Characterization

^{1}H NMR spectra were obtained using a Varian UNITY 400 spectrometer at 400 MHz in $CDCl_3$ at ambient temperature. ^{13}C NMR spectra were obtained using a Varian UNITY-400 spectrometer at 100 MHz in DMSO-d_6 at ambient temperature.

***In situ* FTIR**

In situ mid-FTIR spectra were collected with a ReactIR 1000 (MCT detector, S/N = 7500, resolution = 4) (ASI Applied Systems, Millersville, MD, www.asirxn.com) reaction analysis system equipped with a light conduit and DiComp (diamond-composite) insertion probe. Reaction data was analyzed using ReactIR software. The details and capabilities of the ReactIR 1000 reaction analysis system based on attenuated total reflectance (ATR) have been described in detail previously.[17]

---

[17] Storey, R. F.; Donnalley, A. B.; Maggio, T. L. *Macromolecules* **1998**, *31*, 1523.

Contact Angles

Nb/NbTBE/MAH terpolymers were spin coated (4000 rpm) on hexamethyldisilazane (HMDS) treated silicon wafers from 0.25 μm filtered 13 % (w/w) cyclohexanone solutions. The films were baked at 120 °C for approximately 2 min to remove residual solvent. Contact angles of water and methylene iodide on the terpolymer films and silicon substrate were measured using a contact angle goniometer.

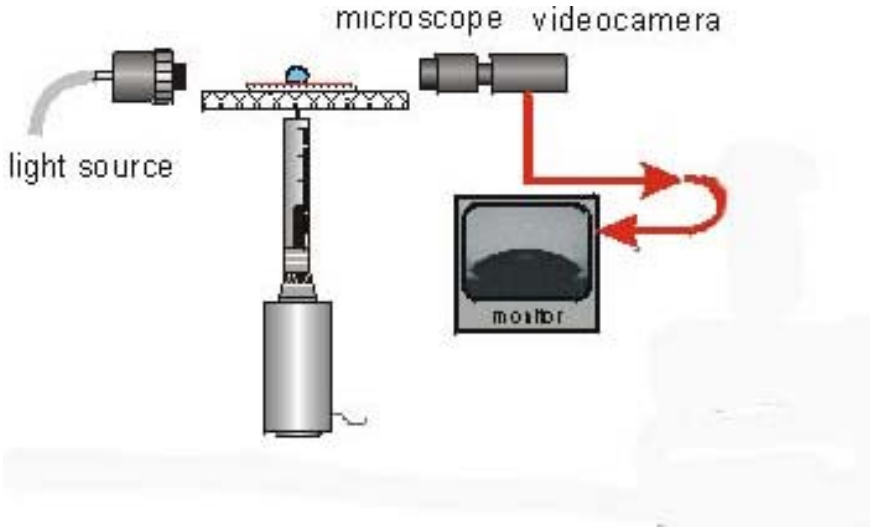

Figure 7.3 Basic schematic of a contact angle goniometer.

7.3.3 Synthesis of *tert*-Butyl 5-Norbornene-2-carboxylate (NbTBE)

Freshly cracked cyclopentadiene (1.45 moles, 96.0 mL) was added drop-wise via addition funnel to a stirred solution of *tert*-butyl acrylate (1.45 moles, 212.0 mL) and 3,5-di-tert-butylphenol (0.00728 moles, 1.5g) in a 500 mL round bottom flask. A water condenser was then inserted into the round bottom flask it was placed into an oil bath at 140 ºC (Figure 7.4). The reaction mixture was then stirred for 5 h at 140 ºC using a magnetic stir bar. The yellow crude liquid reaction mixture was then purified via vacuum

distillation (40 °C, 0.1 mm Hg) to give a colorless oil (88.0 g, 66 % isolated yield). GC and NMR analysis indicated the product was >99% pure and was obtained as an endo/exo isomer mixture (≅ 75/25) as expected.

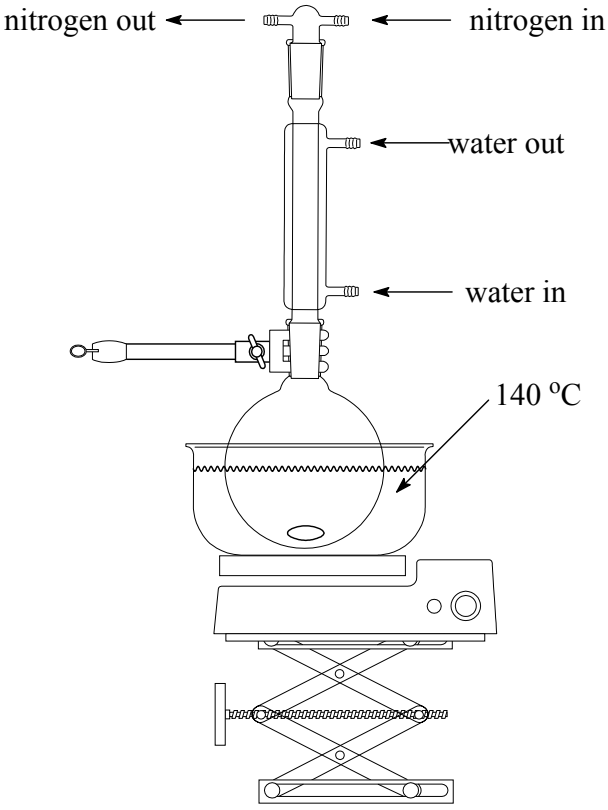

Figure 7.4 Reaction setup for NbTBE synthesis.

7.3.4 Synthesis and *In situ* FTIR of a Nb/NbTBE/MAH Terpolymerization

A typical terpolymerization reaction (Scheme 7.2**)** with *in situ* FTIR monitoring is described. In a 100 mL, round-bottomed, three-necked flask that was fitted with the ReactIR 1000 DiComp probe was added a magnetic stir bar, norbornene (Nb) (4.79 g, 51

mmol), *tert*-butyl 5-norbornene-2-carboxylate (NbTBE) (9.89 g, 51 mmol), maleic anhydride (MAH) (10.0 g, 102 mmol), 2,2-azobisisobutyronitrile (AIBN) (1.004 g, 6.12 mmol), and THF (16.5 mL). The flask was purged with nitrogen for approximately one minute and sealed tightly under positive nitrogen pressure (4-5 psi) with rubber septa. An oil bath at 65 ºC was raised to the reaction flask and FTIR data collection was started. The ReactIR was programmed to collect an averaged FTIR spectrum of the reaction mixture every 5 minutes (256 scans) for the duration of the reaction. The reaction was then stirred at 65 ºC for 24 h while collecting FTIR spectra. The oil bath was removed after 24 h and the reaction contents were allowed to cool to room temperature. After 24 h, the reaction mixture had solidified to a glass and was no longer stirring. The DiComp probe was removed from the reaction flask and THF (~ 50 mL) was added to dissolve the solid glass. After completely dissolving in THF (approx. 24 h), the dissolved material was precipitated into hexanes (~ 500 mL), filtered, washed with isopropyl alcohol (~ 200 mL) and dried overnight under vacuum (0.1 mm Hg) at approx. 75 ºC to give 19.6 g (80 % yield) of white powder. GPC: M_n = 6,700 (M_w/M_n = 1.64). Nb/MAH (50/50) copolymer had a 10% weight loss at 355 ºC (nitrogen) and a glass transition temperature of 275 ºC. A Nb/NbTBE/MAH (25/25/50) terpolymer showed a lower 10% weight loss at 220 ºC (nitrogen) resulting from degradation of the *t*-butyl ester functionality.

7.4 RESULTS AND DISCUSSION

7.4.1 Synthesis and Characterization of Nb/NbTBE/MAH Terpolymers

Free radical alternating terpolymerizations of Nb/NbTBE/MAH with various ratios of Nb to NbTBE (while maintaining a 50 % molar feed of MAH) were performed using previously determined optimum conditions for Nb/MAH alternating copolymerizations (3 mol % AIBN, THF (60 % solids), 24 h). Terpolymerizations were conducted using the following Nb/NbTBE/MAH monomer feed ratios: 50/0/50, 35/15/50, 25/25/50, 15/35/50, 0/50/50.

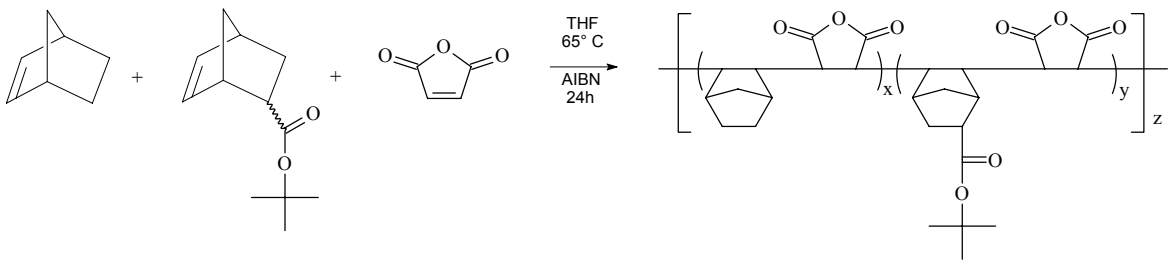

Scheme 7.2 Nb/NbTBE/MAH alternating terpolymerization scheme.

Observed rate constants determined using *in situ* FTIR (Figure 7.5), percent yields, molecular weights, and Nb/NbTBE composition in the resulting materials are summarized in Table 7.1. Several trends were observed from analysis of the data presented in Table 7.1. First, the observed reaction rate is a strong function of the monomer feed ratio of Nb/NbTBE with a maximum of 6.7 x 10^{-5} s^{-1} at a 50/0/50 Nb/NbTBE/MAH monomer feed ratio. The observed rate decreases with increasing NbTBE monomer feed to a minimum of 1.1 x 10^{-5} s^{-1} at a 0/50/50 Nb/NbTBE/MAH monomer feed ratio. In addition, percent yield exhibited a similar trend with a maximum yield of 94 % for a 50/0/50 Nb/NbTBE/MAH feed ratio and a minimum yield of 60 % for a 0/50/50 Nb/NbTBE/MAH feed ratio. The observed decrease in rate with increasing NbTBE is proposed to be due to a combination of steric and polarity effects resulting from the *tert*-butyl ester functionality of NbTBE. ^{13}C NMR analysis of terpolymers prepared from a 25/25/50 Nb/NbTBE/MAH monomer feed ratio further indicated that the terpolymers were enriched in Nb and depleted in NbTBE. The ratio of Nb to NbTBE in the terpolymer was subsequently determined via integration of the quaternary carbon of *tert*-butyl group (δ 80 ppm) to the carbonyl region (δ 170-176 ppm). Assuming a 1:1 ratio of MAH to the total cyclic olefin (Nb and NbTBE) incorporated into the terpolymer, the ratio of Nb to NbTBE incorporated was subsequently determined to be 1.4:1.0.

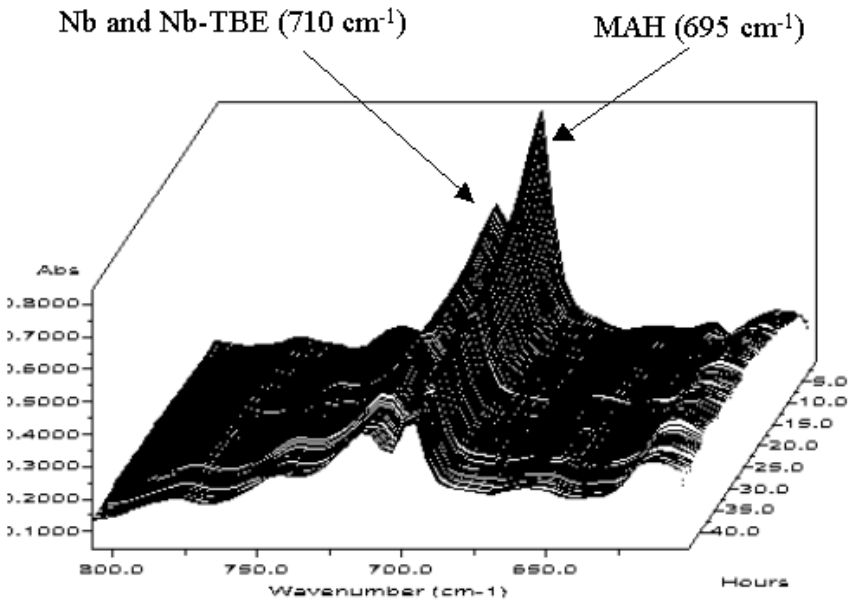

Figure 7.5 Vinylene region of "Waterfall Plot" for Nb/NbTBE/MAH (25/25/50 mol ratio) terpolymerization (*in situ* FTIR, spectrum acquired every 5 min).

Table 7.1 Summary of Nb/NbTBE/MAH terpolymerizations varying the monomer feed ratio of Nb to NbTBE.

Nb/Nb-TBE/MAH	Observed rate (FTIR) x 10^5 s^{-1} [a]	Yield (%)	M_n[b]	M_w/M_n	Nb/Nb-TBE [c]
50/0/50	6.7	94	7,300	1.63	
35/15/50	5.3	87	6,500	1.46	3.2
25/25/50	3.8	80	6,700	1.64	1.4
15/35/50	2.6	75	6,600	1.49	0.68
0/50/50	1.1	60	6,900	1.59	

[a] Determined from first order kinetic plot using MAH/NB peak area via in-situ FTIR for first 4 h of reaction. [b] Wyatt miniDAWN MALLS detector coupled with Waters GPC with external 410 RI detector viscometer, THF solvent at 40 °C and 1.0 mL/min flow rate. [c] Determined using ^{13}C NMR (Varian Unity-400) at 100 MHz, DMSO-d_6, ambient temperature. Ratio calculated from integration of the quaternary carbon of *tert*-butyl ester group (δ 80 ppm) of Nb-TBE to the total carbonyl region (δ 170-176 ppm). For calculation, a 1:1 ratio of MAH to total cyclic olefin (Nb and Nb-TBE) is assumed.

7.4.2 Adhesion and Lithographic Performance

Adhesive properties of the terpolymers were evaluated from calculating the work of adhesion (W_{adh}) between the polymer and an HMDS treated silicon substrate using the method of fractional surface free energy as demonstrated by Owens and Wendt[18] (eqn. 1):

$$W_A = 2(\gamma_1^d \gamma_2^d)^{1/2} + 2(\gamma_2^p \gamma_1^p)^{1/2} \qquad (1)$$

This equation developed by Owens and Wendt is based upon the Fowkes hypothesis of surface energy separation[19] and states that if the dispersion and polar force components of the surface energy are known, the work of adhesion is determined by the sum of the square

[18] Owens, D. K.; Wendt, R. C., *J. Appl. Polym. Sci.* **1969**, *13*, 1741.
[19] Fowkes, F. M. *J. Phys. Chem.* **1962**, *66*, 382.

roots of their products. Kim and coworkers have previously used this approach to study the adhesive properties of alicyclic 193 nm resist polymers.[20] Contact angles of water and methylene iodide and W_{adh} values are summarized in Table 7.2.

Table 7.2 Water and methylene iodide contact angles and W_{adh} values for Nb/NbTBE/MAH terpolymers.

Polymer	contact angle (H_2O) [b]	contact angle (CH_2I_2) [b]	W_{adh}[c]
50/0/50 [a]	94 ± 0.82	68 ± 0.82	58.6
35/15/50 [a]	91 ± 0.92	65 ± 1.2	60.6
25/25/50 [a]	87 ± 1.1	62 ± 1.2	62.5
15/35/50 [a]	85 ± 0.92	60 ± 1.1	63.8
0/50/50 [a]	82 ± 1.0	58 ± 0.70	64.9
Si wafer	94 ± 1.0	47 ± 1.1	

[a] Nb/NbTBE/MAH monomer feed ratio. [b] Measured using a contact angle goniometer. Reported value is the average of ten measurements. [c] Work of adhesion to a HMDS treated silicon wafer (dyne/cm).

It was determined that W_{adh} increased with higher NbTBE composition in the terpolymer with a minimum of 58.6 dyne/cm for a 50/50 Nb/MAH copolymer and a maximum of 64.9 dyne/cm for a 50/50 NbTBE/MAH copolymer. In addition, lithographic evaluation of the terpolymers demonstrated that the 50/50 NbTBE/MAH showed excellent imaging capability at 193 nm. Scanning electron micrographs (SEM) of imaged films for a 50/50 NbTBE/MAH copolymer and a 25/25/50 Nb/NbTBE/MAH terpolymer are

[20] Kim, J. B.; Yun, H. J.; Kwon, Y. G.; Lee, B. W. *Polymer* **2000**, *41*, 8035.

illustrated in Figure 7.6. Semi-dense 110 nm and 120 nm lines (1:1.5 line/space) were printed with sharp and defined features. The imaged 50/50 NbTBE/MAH copolymer resist formulation exhibited vertical and consistent sidewalls. In comparison, the patterned lines produced from the resist formulation using the 25/25/50 Nb/NbTBE/MAH terpolymer had significantly increased line thinning and sloping sidewalls. All of the resist polymer compositions exhibited good adhesion (qualitative observation based upon SEM of patterned images) to the silicon substrate after imaging and no movement of the patterned images was observed. The method discussed above for calculating the W_{adh} values of the resist polymers to the silicon substrates provides a useful technique for the estimation of the adhesive properties of resist polymers to the silicon substrates and it was demonstrated that the calculated W_{adh} increased with increasing NbTBE content. However, the essential performance criterion is whether the final patterned images adhere to the substrate and all of the patterned images produced from the MAH/Nb/NbTBE resist compositions investigated in this study did show good adhesion after exposure and development.

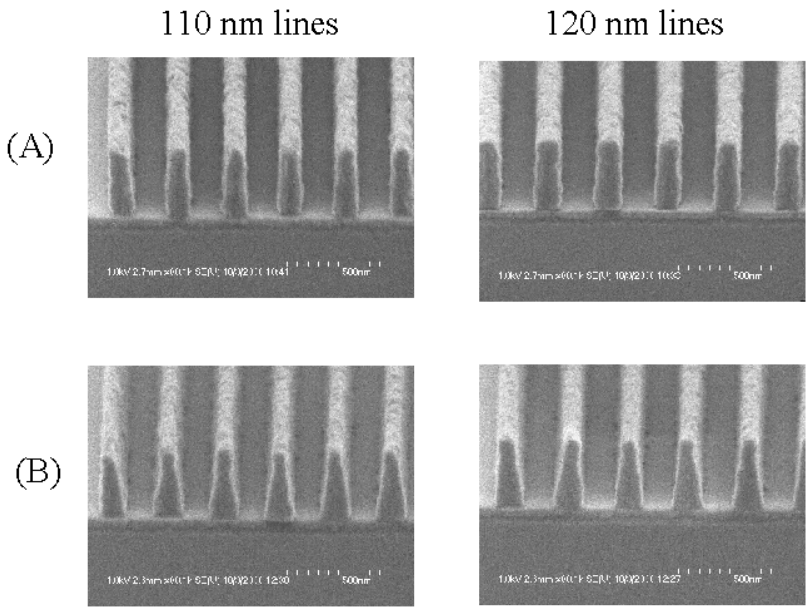

Figure 7.6 Scanning electron micrographs of 110 nm and 120 nm 1:1.5 line/space patterns (ISI Ar-F 193-nm Microstep, NA = 0.6). (A) 50/50 NbTBE/MAH copolymer (at a dose of 19 mJ/cm^2). (B) 25/25/50 Nb/NbTBE/MAH terpolymer (at a dose of 36 mJ/cm^2).

7.5 CONCLUSIONS

Real-time monitoring via *in situ* FTIR spectroscopy of alternating terpolymerizations of MAH with Nb and NbTBE was utilized to evaluate the relative rates of varying Nb/NbTBE monomer feed ratios. Pseudo first order kinetic plots constructed from the *in situ* FTIR absorbance data indicated that the rate of reaction was a strong function of the Nb/NbTBE ratio and decreased with increasing NbTBE. In addition, percent yields were also observed to be a function of the Nb/NbTBE ratio and decreased with increasing NbTBE. Calculated work of adhesion (W_{adh}) values of Nb/NbTBE/MAH terpolymers demonstrated a linear increase in W_{adh} with increased NbTBE composition in the terpolymer. Furthermore, SEM micrographs of developed 193 nm resist formulations showed increased imaging performance in polymers with high NbTBE content.

Acknowledgments. Financial support provided by the Jeffress Memorial Trust, Virginia Tech Department of Chemistry, National Science Foundation (CRIF CHE-9974632), and IBM is gratefully acknowledged. The authors would also like to thank the Center of Adhesive and Sealant Science (CASS) at Virginia Tech and the Adhesive and Sealant Council (ASC) for financial support through an ASC Education Foundation Research Fellowship.

Recommended future studies:

- Investigate adhesive and lithographic properties as a function of molecular weight of Nb/MAH copolymers.
- Investigate adhesive and lithographic properties of copolymers prepared from MAH and Nb derivatives containing additional functionality.
- Using Owens and Wendt method of calculating W_{adh}, quantitate experimentally the required minimum adhesive requirement as a function of feature size.

CHAPTER 8

Application of Design of Experiments and *In situ* FTIR to Probe Catalyst Effects on the Free Radical Copolymerization of Norbornene and Maleic Anhydride

8.1 ABSTRACT

Statistical design of experiments was used to probe the effect of several synthetic variables on free radical alternating copolymerizations of norbornene and maleic anhydride were evaluated using statistical design of experiments. Three variables (% AIBN initiator, % solids (in tetrahydrofuran solvent), and zinc chloride Lewis acid catalyst) were examined using a central composite design response surface for process optimization. Predictive models and 3-dimensional contour plots for yield and molecular weight responses were produced using Stat-Ease statistical software. DOE indicated that zinc chloride did not have a statistically significant contribution to either yield or molecular weight. However, kinetic evaluations of Nb/MAH alternating copolymerizations using *in situ* FTIR demonstrated that the addition of zinc chloride significantly increased the rate of copolymerization, indicating true catalytic behavior.

8.2 INTRODUCTION

Alternating copolymerization is an example of chain copolymerization where each of the monomers adds preferentially to the other.[1] The most widely studied comonomer for producing alternating copolymers is maleic anhydride (MAH). MAH contains an electron poor double bond and has been shown to homopolymerize poorly via free radical methods.[2] However, MAH will copolymerize with a number of electron rich olefins to form alternating copolymers.[3] Many 1,2-disubstituted and cyclic olefins that do not readily homopolymerize using free radical initiators will form alternating copolymers with MAH. This has been attributed to the low radical reactivity of the electron rich 1,2-disubstituted double bond. Recently, main-chain alicyclic macromolecules produced from the alternating free radical copolymerization of MAH with norbornene and norbornene derivatives have received attention as photoresist materials for 193-nm lithography.[4] MAH serves to incorporate the polar carbonyl oxygen, which provides necessary adhesion and solubility that are both required for acceptable imaging performance. In addition, the alicyclic backbone resulting from copolymerization with norbornene provides for excellent etch resistance, surpassing even phenol based materials.

---

[1] Odian, G. *Principles of Polymerization*, 3rd ed.; Wiley & Sons: New York, 1991; Ch 6.

[2] Gaylord, N. G. *J. Macromol. Sci. Rev. Macromol. Chem.* **1975**, *13*, 235. Regel, W.; Schneider, C. *Makromol. Chem.* **1981**, *182*, 237.

[3] Walling, C.; Briggs, E. R.; Wolfstirn, K. B.; Mayo, F. R. *J. Am. Chem. Soc.* **1948**, *70*, 1537. Barb, W. G. *J. Polym. Sci.* **1953**, *11*, 117. Seymour, R. B.; Garner, D. P. *Polymer* **1972**, *13*, 549. Block, H.; Cowd, M. A.; Walker, S. M. *Polymer* **1972**, *13*, 549. Gaylord, N. G.; Maiti, S.; Patnaik, B. K.; Takahashi, A. *J. Macromol. Sci., Chem.* **1972**, *A6*, 1459. Gaylord, N. G.; Maiti, S. *J. Macromol. Sci., Chem.* **1972**, *A6*, 1481. Fujimori, K. *J. Macromol. Sci., Chem.* **1975**, *A9*, 495. Case, C.; Loucheux, C. *J. Macromol. Sci., Chem.* **1975**, *A9*, 495.

[4] Allen, R. D.; Opitz, J.; Larson, C. E.; Wallow, T. I.; Hofer, D. C. *Microlithography World* **winter 1999**, 5. Ito, H.; Miller, D. C.; Sherwood, M. *J. Photopolym. Sci. Technol.* **2000**, *13*, 559. Okoroanyanwu, U.; Byers, J.; Shimokawa, T.; Willson, C. G. *Chem. Mater.* **1998**, *10*, 3328. Jung, M. H.; Jung, J. C.; Lee, G.; Baik, K. H. *Jpn. J. Appl. Phys., Part 1* **1998**, *37*, 6889. Houlihan, F. M.; Wallow, T. I.; Nalamasu, O.; Reichmanis, E. *Macromolecules* **1997**, *30*, 6517.

The addition of a Lewis acid catalyst such as $ZnCl_2$ to the free radical alternating copolymerization of maleic anhydride with electron rich monomers is expected to have a marked effect on the kinetics of copolymerization.[5] Hirooka and coworkers first reported the use of a Lewis acid (ethylaluminum dichloride) to synthesize alternating copolymers of propylene and acrylonitrile.[6] Subsequently, a significant amount of research has been devoted to the preparation of alternating copolymers in the presence of Lewis acids. It has been shown that the addition of Lewis acids to free radical copolymerizations of acrylic, methacrylic, maleic, or fumaric monomers with donor monomers such as styrene, butadiene, or isoprene leads to copolymers with almost perfectly alternating structures.[5] Furthermore, the addition of Lewis acids to free radical polymerizations of acrylic and methacrylic monomers has been shown to increase the polymerization rates as a function of added Lewis acid.[7]

Optimization and control of polymerization processes requires a strong knowledge of how experimental variables can affect the properties of the resulting macromolecules. Statistical design of experiments (DOE) is a very useful and powerful tool that provides for the efficient and rapid development of experimental models that have predictive capacity for polymerization methods. For example, Daroux et al. have previously described process optimization of industrial bulk styrene polymerizations using statistical DOE.[8] Another beneficial feature of statistical DOE is that it can provide for the detection interactions of multiple factors that are not typically elucidated from empirically examining the effect of one variable at a time. The discovery of novel macromolecular architecture and controlled polymerization processes also can be facilitated using DOE. For instance, Williamson and Long have recently integrated statistical DOE with in-parallel synthetic strategies to

---

[5] Bamford, C. H. In *Alternating Copolymers*; Cowie, J. M. G., Ed.; Plenum Press: New York, 1985; Ch. 3.
[6] Hirooka, M.; Yabuuchi, H.; Morita, S.; Nakaguchi, K. *J. Polym. Sci. B* **1967**, *5*, 47.
[7] Bamford, C. H.; Jenkins, A. D.; Johnston, R. *Proc. R. Soc. London A* **1957**, *241*, 364. Imoto, M.; Otsu, T.; Harada, Y. *Makromol. Chem.* **1963**, *65*, 174.
[8] Daroux, M.; Zamani, H.; Greffe, J. L.; Bordet, J. *Chem. Eng. J.* **1981**, *22*, 125.

rapidly probe anionic polymerizations of 1,3-cyclohexadiene for the future design of novel architectures based on this monomer.[9]

8.3 EXPERIMENTAL

8.3.1 Materials

Norbornene (Nb) was purchased from Aldrich and vacuum distilled (0.1 mm Hg) at room temperature from calcium hydride after degassing three times using the traditional freeze-thaw method. After distillation it was stored under positive nitrogen pressure as a solution in tetrahydrofuran. Maleic anhydride (MAH) was purchased from Aldrich and purified via sublimation immediately prior to use. Tetrahydrofuran was distilled using the classic sodium/benzophenone ketyl. All other reagents were purchased from Aldrich and used as received.

8.3.2 Characterization

Molecular Weight Characterization

Molecular weights were measured using a Wyatt miniDAWN multiangle laser light scattering (MALLS) detector with a 690 nm laser (Wyatt Technology, Santa Barbara, CA) connected to a Waters SEC (515 pump, 717 autosampler, and 410 refractive index detector). The miniDAWN was connected in series after three 5-μm Plgel mixed-bed columns (Polymer Laboratories, Amherst, MA). Measurements were made at 40 °C with THF as the solvent at a flow rate of 1.0 mL/min.

NMR Characterization

---

[9] Williamson, D. T.; Long, T. E. *Polymer Preprints* **2001**, *42*(2), 634.

^{1}H NMR spectra were obtained using a Varian UNITY 400 spectrometer at 400 MHz in $CDCl_3$ at ambient temperature. ^{13}C NMR spectra were obtained using a Varian UNITY-400 spectrometer at 100 MHz in DMSO-d_6 at ambient temperature.

***In situ* FTIR**

In situ mid-FTIR spectra were collected with a ReactIR 1000 (MCT detector, S/N = 7500, resolution = 4) (ASI Applied Systems, Millersville, MD, www.asirxn.com) reaction analysis system equipped with a light conduit and DiComp (diamond-composite) insertion probe. Reaction data was analyzed using ReactIR software. The details and capabilities of the ReactIR 1000 reaction analysis system based on attenuated total reflectance (ATR) have been described in detail previously.[10]

8.3.3 Design of Experiments

Stat-Ease Design-Expert (version 6.0.1) statistical software was used to perform design of experiment statistical analysis of the effect of experimental variables on maleic anhydride/norbornene free radical alternating copolymerizations. Three variables (% AIBN initiator, % solids (in tetrahydrofuran solvent), and zinc chloride Lewis acid catalyst) were examined using a central composite design response surface. The design required twenty experiments: each variable was varied over 5 levels, plus and minus alpha (axial points), plus and minus 1 (factorial points) and the center point.

---

[10] Storey, R. F.; Donnalley, A. B.; Maggio, T. L. *Macromolecules* **1998**, *31*, 1523.

8.3.4 Norbornene/Maleic Anhydride Alternating Copolymerization in the Presence of Zinc Chloride Lewis Acid Catalyst

In a 100 mL, round-bottomed, three-necked flask that was fitted with the ASI ReactIR 1000 DiComp probe was added a magnetic stir bar, norbornene (Nb) (9.40 g, 100 mmol), maleic anhydride (MAH) (9.80 g, 100 mmol), zinc chloride ($ZnCl_2$) (3.40 g, 25 mmol), and tetrahydrofuran (THF) (14.4 mL). A schematic of the copolymerization setup with *in situ* FTIR is illustrated in Figure 5.3. An oil bath at 65 ºC was raised using a jack until the reaction solution was completely immersed in the oil at 65 ºC. Once the temperature of the reaction mixture reached 65 ºC, 2,2-azobisisobutyronitrile (AIBN) (0.984 g, 6.00 mmol) was added to the flask. The flask was immediately purged with nitrogen for approximately 30 seconds and sealed tightly under positive nitrogen pressure (4-5 psi) with a rubber septum. The ReactIR was programmed to collect an FTIR spectrum of the reaction mixture every minute (64 scans) for the first hour of reaction and then every 5 minutes (256 scans) for the remainder of the copolymerization. The reaction was then stirred at 65 ºC for 24 h while collecting FTIR spectra. After 24 h, the oil bath was removed and the reaction contents were allowed to cool to room temperature. After 24 h, the reaction mixture had solidified and was no longer stirring. The DiComp probe was removed from the reaction flask and THF (~ 50 mL) was added to dissolve the solid. The dissolved material was then precipitated into hexanes (~ 500 mL), filtered, and dried overnight under vacuum (0.1 mm Hg) at approx. 75 ºC.

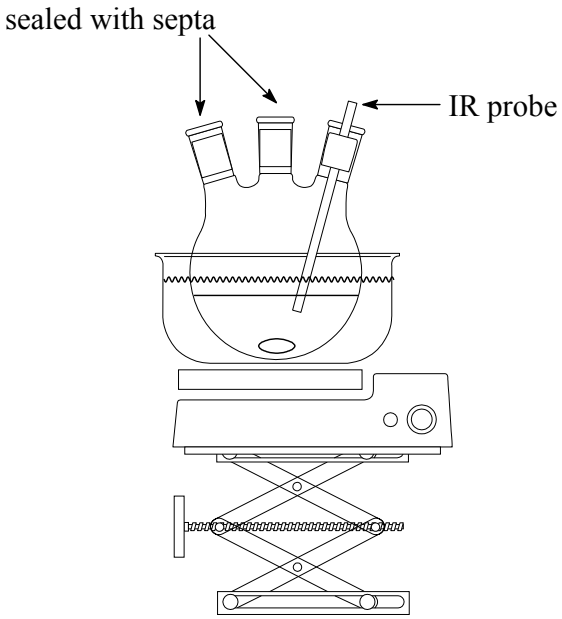

Figure 8.1 Nb/MAH copolymerization setup with *in situ* FTIR monitoring.

8.4 RESULTS AND DISCUSSION

8.4.1 Nb/MAH Copolymerization Design of Experiments

Statistical design of experiments (DOE) was used to probe the effect of synthetic variables on the free radical copolymerization of norbornene (Nb) and maleic anhydride (MAH) (Scheme 8.1). Three variables (% AIBN initiator, % solids (in tetrahydrofuran solvent), and zinc chloride Lewis acid catalyst) were examined using a central composite design response surface for process optimization.

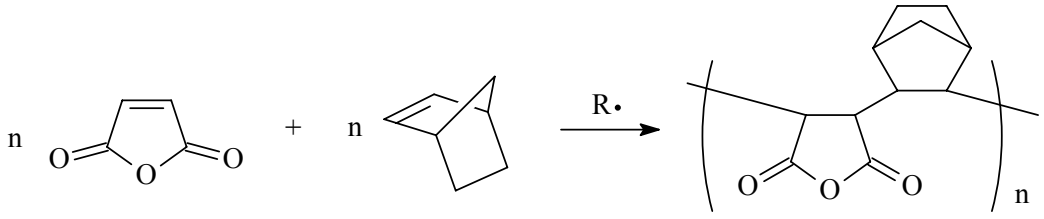

Scheme 8.1 Free radical alternating copolymerization of norbornene and maleic anhydride.

Stat-Ease Design-Expert (version 6.0.1) statistical software was used for DOE statistical analysis and to produce the mathematical models based upon the response data. The responses measured were isolated yield and number average molecular weight. The design required twenty experiments: each variable was varied over 5 levels, plus and minus alpha (axial points), plus and minus 1 (factorial points) and the center point. Initiator concentration was varied from 0.1 mol percent to 4.0 mol percent of the total comonomer concentration. Solids percent was varied from 10-75 %. Zinc chloride Lewis acid catalyst was varied from 0-67 mol percent compared to MAH. Variables that were assumed to remain constant included the comonomer feed (50/50 mol ratio), stir rate, solvent (THF), temperature (65 °C), and time (24 h). A summary of the experimental variables and resulting responses are presented in Table 8.1.

Table 8.1 Variables and responses for Nb/MAH free radical copolymerization DOE experiments.

STD	Run	Factor 1: Initiator %	Factor 2: Solids %	Factor 3: Zinc Chloride	Response 1: % yield	Response 2: M_n
8	1	3.260	61.82	53.45	90	3140

9	2	2.080	42.50	33.52	82	5430
2	3	3.260	23.18	13.59	69	1254
3	4	0.908	61.82	13.59	68	6030
11	5	2.080	42.50	33.52	89	3270
1	6	0.908	23.18	13.59	48	3260
5	7	0.908	23.18	53.45	49	4620
12	8	2.080	42.50	33.52	82	2990
6	9	3.260	23.18	53.45	75	2590
4	10	3.260	61.82	13.59	83	2260
7	11	0.908	61.82	53.45	54	14800
10	12	2.080	42.50	33.52	79	4960
13	13	0.101	42.50	33.52	31	6310
20	14	2.080	42.50	33.52	82	4840
15	15	2.080	10.00	33.52	33	2010
16	16	2.080	75.00	33.52	42	3480
14	17	4.070	42.50	33.52	84	5560
19	18	2.080	42.50	33.52	81	4500
17	19	2.080	42.50	0.00	77	5610
18	20	2.080	42.50	67.04	78	6530

Mathematical models were prepared from the response data using the Stat-Ease statistical software. 3-Dimensional surface plots illustrating % yield and number average molecular weight are shown in Figure 8.2 and Figure 8.3, respectively. The models for both the yield and molecular weight responses had significant F-values with high confidence levels and low standard deviations. DOE analysis did not detect a statistical effect of the zinc chloride variable on either the yield or molecular weight response and therefore the responses are shown as a function of the other two variables (initiator % and solids %). The contour plots visually illustrate that a maximum in molecular weight occurs at the highest percent solids and lowest initiator percent as is expected for a free radical solution polymerization. Yield, however, showed an intermediate maximized response at approximately 50 %. As expected, yield continuously increased with higher % initiator. It is anticipated that a maximum in yield occurred at 50 % solids from competing propagation rate and reaction viscosity effects. The affect was not observed to be dramatic and only varied from about 66 – 89 % yield over the entire solids range shown in Figure 8.2. The statistical model agreed well with previously determined optimum conditions (using conventional one-factor-at-a-time methodology) of 3 mol percent initiator and 60 % solids.

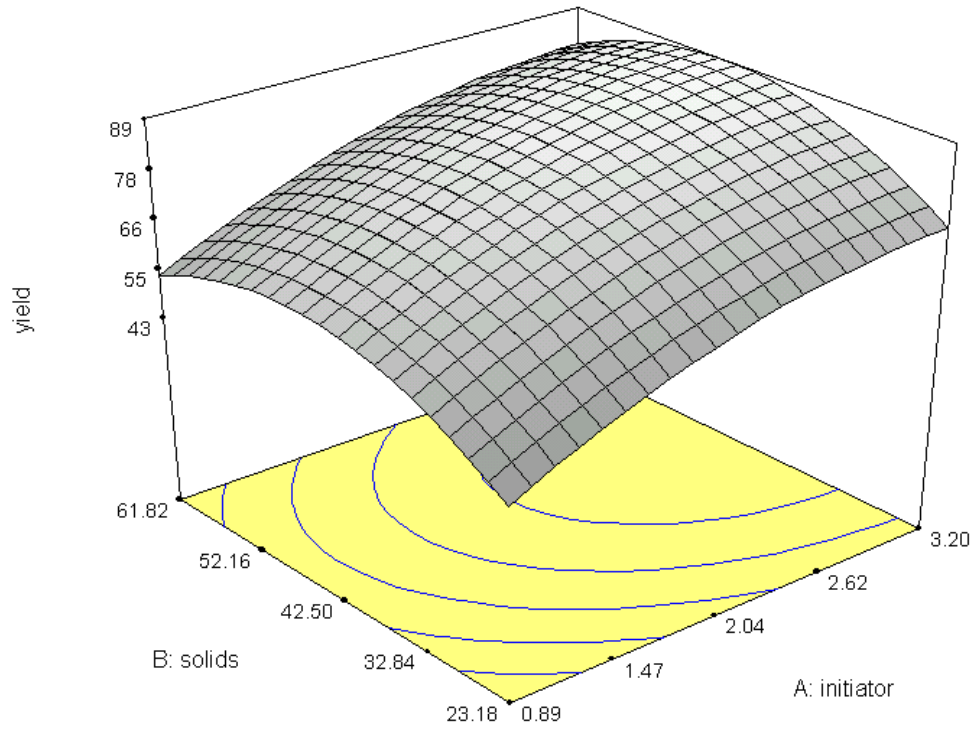

Figure 8.2 3-Dimensionl surface plot of yield response as a function of % solids and mol % initiator.

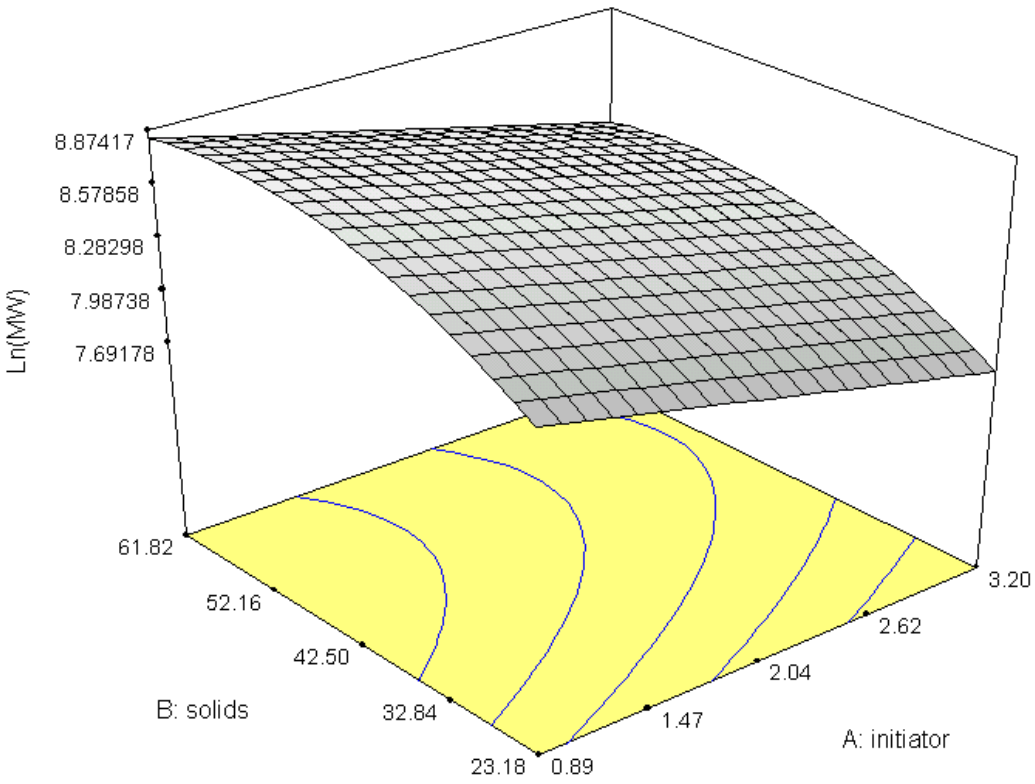

Figure 8.3 3-Dimensional surface plot of number average molecular weight response as a function of solids % and mol % initiator.

8.4.2 Effect of Zinc Chloride on the Rate of Maleic Anhydride and Norbornene Free Radical Copolymerization

The effect of zinc chloride on the copolymerization rate of maleic anhydride and norbornene was investigated via measuring the observed copolymerization rate ($k_{obs}=k_p[M][P\cdot]$) at various amounts of zinc chloride using *in situ* FTIR spectroscopy. The kinetic effects of Lewis acids on free radical polymerization was first reported by Bamford and coworkers, who investigated the solution free radical polymerization (DMF) of

acrylonitrile in the presence of lithium salts.[11] Increases in both the rate and the degree of polymerization were observed in the presence of lithium chloride. A mechanistic understanding of Lewis acids effects on kinetics and the enhancement of the alternating tendency of comonomer pairs has received significant attention and several theories have been proposed.[12] One such proposed mechanism is the coordination of the Lewis acid metal halide to H-bond acceptor groups such as carbonyls. For example, the copolymerization scheme of MAH and Nb in the presence of complexed zinc chloride (to MAH) is presented in Scheme 8.2.

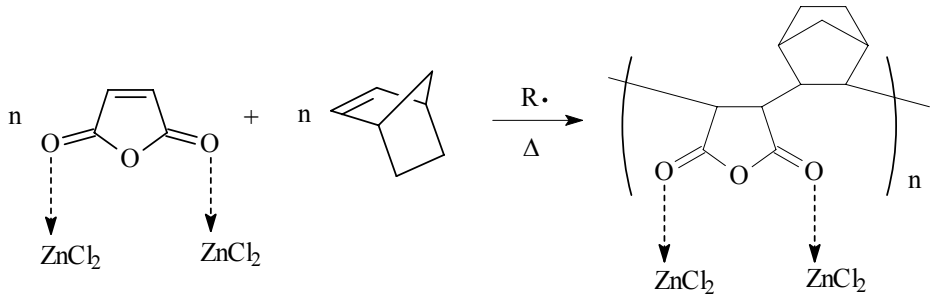

Scheme 8.2 Norbornene/maleic anhydride alternating copolymerization in the presence of zinc chloride.

In situ mid-FTIR was used to collect monomer conversion data for the copolymerization of Nb and MAH in the presence of zinc chloride. *In situ* infrared spectroscopy provided real-time changes in monomer absorbances and allowed for comparative kinetic analysis of the Nb/MAH free radical copolymerization processes. A previous publication has described in more detail the kinetic analysis of Nb/MAH free

[11] Bamford, C. H.; Jenkins, A. D.; Johnston, R. *Proc. R. Soc. London A* **1957**, *241*, 364.
[12] Bamford, C. H. In *Alternating Copolymers*; Cowie, J. M. G., Ed.; Plenum Press: New York, 1985; Ch. 3.

radical co- and terpolymerizations using *in situ* FTIR spectroscopy.[13] A reaction flask was specifically designed to permit the introduction of the ATR based infrared probe and attention was devoted to ensure the reactor was sealed to eliminate any volatilization of reaction components. Strong vinylene (=C-H) absorbances of the monomers were observed and allowed for kinetic analysis of the copolymerizations using *in situ* FTIR. The waterfall plot of the vinylene =C-H region for a Nb/MAH (50/50 mol ratio) copolymerization is illustrated in Figure 8.4. Infrared absorbances that are due to the olefinic functionality, which decrease as the monomers propagate, were identified for both Nb and MAH (MAH at 695 cm^{-1} and Nb at 710 cm^{-1}). Conversion data was collected via *in situ* FTIR to low degrees of conversion (approximately 10 %).

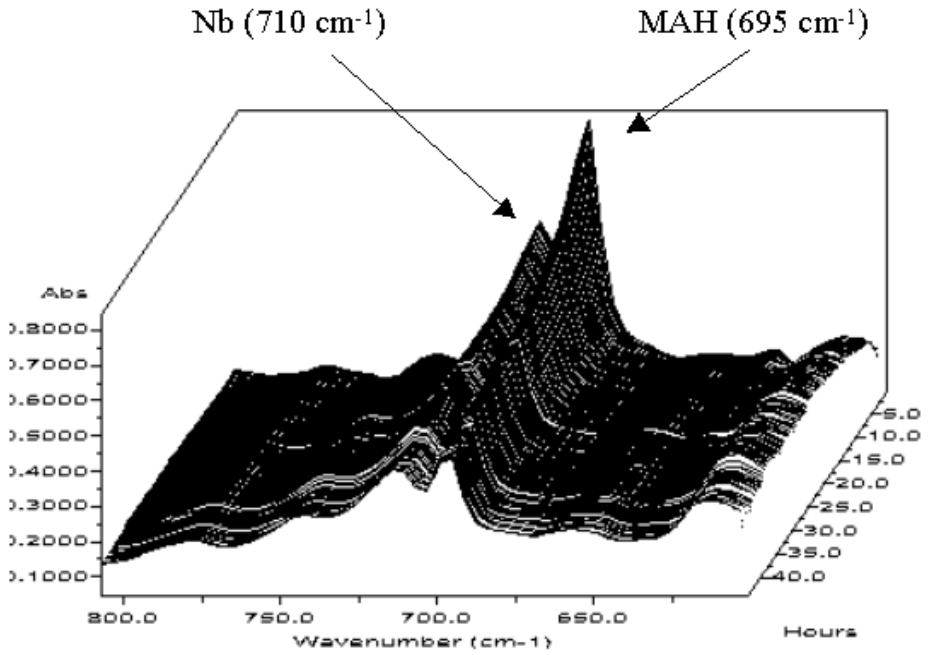

Figure 8.4 Vinylene region of "waterfall" plot for 50/50 Nb/MAH alternating copolymerization.

[13] Pasquale, A. J.; Allen, R. D.; Long, T. E. *Macromolecules* **2001**, *34*, 8064.

Psuedo first order observed rate constants were constructed using monomer conversion data for Nb/MAH copolymerizations in the presence of varying zinc chloride amounts (0.0, 0.10, 0.25, and 0.50 molar equivalents to maleic anhydride) and are shown in Figure 8.5. Higher concentrations of zinc chloride were not investigated as the addition of zinc chloride in amounts greater than 0.50 molar equivalents to maleic anhydride resulted in incomplete solubility under optimized solvent concentration (60% solids in THF). The observed rate constant for Nb/MAH free radical copolymerizations systematically increased from 7.0×10^{-5} s^{-1} in the absence of zinc chloride to 1.8×10^{-4} s^{-1} at 0.50 equivalents. Such a result suggests that there is a very strong electronic effect introduced upon addition of a Lewis acid to the copolymerization of Nb and MAH. It is presumed that the Lewis acid enhances the electron withdrawing nature of MAH via complexation with the conjugated carbonyl (Scheme 8.2). The rate of alternating copolymerization, which is occurring between an electron-rich (Nb) and electron-poor (MAH) comonomer pair, is increased as a result of the decreased electron density of the MAH carbon-carbon double bond. An appreciable effect on the molecular weights or yields of these copolymerizations resulting from the addition of zinc chloride catalyst was not observed, which agreed favorable with DOE statistical analysis.

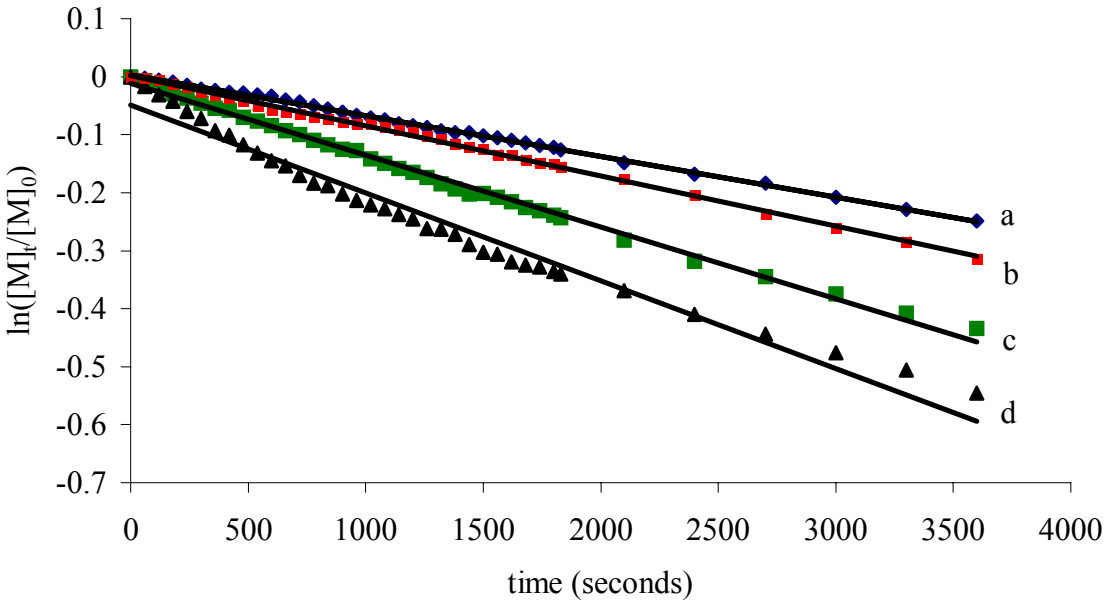

Figure 8.5 Norbornene/maleic anhydride copolymerization observed rate constant as a function of zinc chloride (molar equiv. to MAH): (a) 0.0, k_{obs}=7.0 x 10^{-5} s^{-1}; (b) 0.10, k_{obs}=8.6 x 10^{-5} s^{-1}; (c) 0.25, k_{obs}=1.4 x 10^{-4} s^{-1}; (d) 0.50, k_{obs}=1.8 x 10^{-4} s^{-1}.

8.4.3 Effect of Chain Transfer on the Molecular Weight of MAH/Nb Alternating Copolymers

MAH/Nb copolymerizations conducted in ethyl acetate (EtOAc) solvent resulted in higher molecular weights than copolymerizations prepared in tetrahydrofuran (THF). Consistently, number average molecular weights of MAH/Nb copolymers prepared in EtOAc were close to 50% higher than number average molecular weights of the same copolymers prepared in THF. As THF is far more susceptible to chain transfer during a free radical process than is EtOAc, a series of experiments were carried out to probe the effect of chain transfer on the resulting molecular weights. Solvent transfer constants (C_S) were taken from the slope of the line prepared from a plot of $1/\overline{X}_n$ vs. [S]/[M] (where S =

solvent and M = monomer), which is taken from the Mayo equation.[14] Copolymerizations with [S]/[M] ratios of 1/1, 2/1, 3/1, and 4/1 were carried out for both THF and EtOAc solvents using previously optimized reaction conditions (3 mol % AIBN at 65 °C). Copolymerizations were taken to approximately 10 % conversion isolated by means of precipitation into isopropanol. Number average molecular weights were measured using SEC with a MALLS detector. The kinetic chain length ($\overline{X}_n$) was taken as the number average molecular weight determined using SEC/MALLS divided by the weight of the repeat unit (192 amu, combined mass of both a MAH and Nb monomer was used under assumption of perfect alternation). The graph of $1/\overline{X}_n$ vs. [S]/[M] for both THF and EtOAc is shown in Figure 8.6. C_S values were taken from the slopes of the lines and were 0.0096 for THF and 0.0025 for EtOAc. The higher C_S for THF (approximately 4 times higher) quantitatively provided a measure to account for the lower molecular weights that were obtained when the copolymerizations were carried out in THF. Knowledge of the effect of chain transfer lends itself as a convenient route to control the molecular weight of MAH/Nb copolymerizations. Another classical means to control molecular weight in free radical polymerizations is to add a chain transfer agent such as a thiol. To probe the effect of a chain transfer agent on MAH/Nb copolymer molecular weights, copolymerizations were carried out in the presence of small amounts of n-butane thiol (Table 8.2). A plot of $1/\overline{X}_n$ vs. [S]/[M] using the data in Table 8.2 results in a C_S value (taken from the slope) of 4.9 for n-butane thiol.

[14] Mayo, F. R. *J. Am. Soc.* **1943**, *65*, 2324.

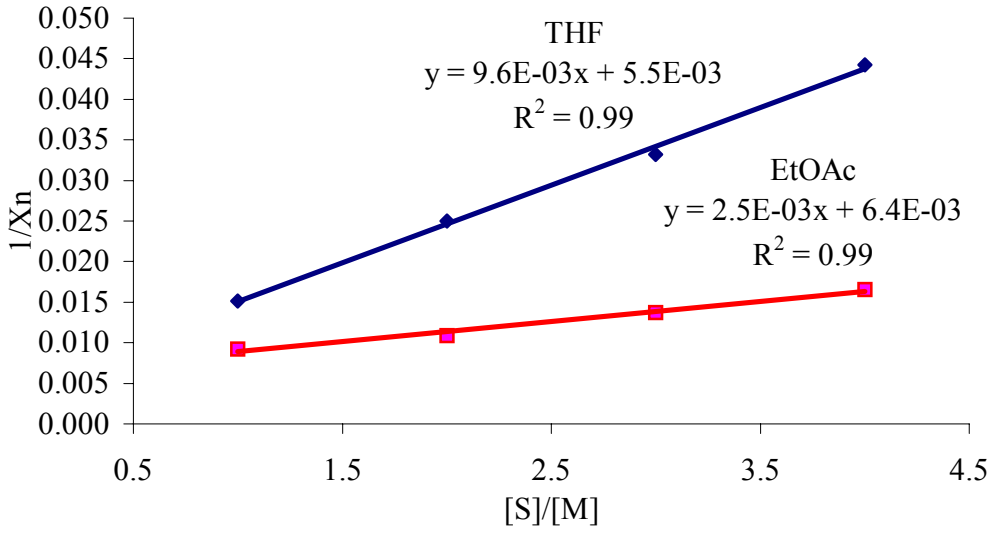

Figure 8.6 Plot of $1/\overline{X}_n$ vs. [S]/[M] for MAH/Nb copolymerizations (3 mol % AIBN, 65 °C) in both THF and EtOAc solvents.

Table 8.2 Molecular weights of MAH/Nb copolymers as a function of n-butane thiol chain transfer agent.

n-BuSH (mol %)	M_n [a]	M_w/M_n [a]
0	15,300	1.44
0.1	12,300	1.56
0.2	11,200	1.65
0.3	7,150	1.62
0.4	6,070	1.85

[a] Wyatt miniDAWN multiple angle laser light scattering detector in-line with Waters SEC system (410 RI detector). THF solvent at 40 °C and 1.0 mL/min flow rate.

8.5 CONCLUSIONS

The effect of several synthetic variables on free radical alternating copolymerizations of norbornene and maleic anhydride were evaluated using statistical design of experiments. Three variables (% AIBN initiator, % solids (in tetrahydrofuran solvent), and zinc chloride Lewis acid catalyst) were examined using a central composite design response surface for process optimization. Predictive models and 3-dimensional contour plots for yield and molecular weight responses were produced using Stat-Ease statistical software. The results of statistical DOE analysis agreed favorably with previously determined optimum conditions (using one-factor-at-a-time methods) for norbornene/maleic anhydride alternating copolymerization. Zinc chloride was not detected by DOE to affect either yield or molecular weight. However, zinc chloride was observed to have a marked effect on the copolymerization rate, which indicated it behaved as a true catalyst by increasing the rate of reaction while having no appreciable effect on the yield or molecular weight.

Acknowledgements. Financial support provided by the Jeffress Memorial Trust, Virginia Tech Department of Chemistry, National Science Foundation (CRIF CHE-9974632), and IBM is gratefully acknowledged. The authors would also like to thank the Center of Adhesive and Sealant Science (CASS) at Virginia Tech and the Adhesive and Sealant Council (ASC) for financial support through an ASC Education Foundation Research Fellowship.

Recommended future studies:

- Application of statistical DOE to optimize reaction conditions for various polymerization processes.
- $ZnCl_2$ studies in EtOAc solvent.
- Examination of other Lewis acid such as trialkyl aluminum compounds.

CHAPTER 9

Synthesis of Norbornene Derivatives via Diels-Alder Cycloadditions and Copolymerization with Maleic Anhydride

9.1 ABSTRACT

Several norbornene (Nb) derivatives were synthesized via facile Diels-Alder cycloaddition reactions of cyclopentadiene with α-olefins containing electron withdrawing groups. The Diels-Alder adducts were subsequently copolymerized with maleic anhydride (MAH) using free radical polymerization conditions previously determined for maleic anhydride/norbornene copolymerizations. Further functionality was introduced into the copolymers through acid catalyzed hydrolysis of poly(Nb-*alt*-MAH) and poly(NbCN-*alt*-MAH) copolymers. FTIR confirmed hydrolysis of the anhydrides to acid functionalities and indicated no appreciable hydrolysis of the nitrile functionality. Observed copolymerization rates (k_{obs}) were measured using *in situ* FTIR and a dramatic decrease in the rate of copolymerization was observed for the Nb comonomers that contained a strong electron-withdrawing functionality, which indicated a significant electronic influence on the free radical copolymerization rate with maleic anhydride due to the electron withdrawing strength of the Nb substituents.

9.2 INTRODUCTION

Maleic anhydride (MAH) is the most widely studied comonomer for producing alternating copolymers. MAH is a very strong electron acceptor that has been shown to homopolymerize poorly,[1] but will react with a number of electron donating monomers to form alternating copolymers.[2] Of particular interest is that many 1,2-disubstituted and cyclic olefins such as norbornene, that do not homopolymerize by free-radical methods, will form alternating copolymers with maleic anhydride. Recently, main-chain alicyclic macromolecules produced from the alternating free radical copolymerization of MAH with norbornene and norbornene derivatives have received attention as photoresist materials for 193 nm lithography.[3] Cyclic olefins such as norbornene will not homopolymerize to appreciable amounts via free radical methods. However, when cyclic olefins are reacted with maleic anhydride in the presence of a free radical initiator, they copolymerize in an alternating manner (Scheme 9.1). In addition, maleic anhydride also serves to incorporate oxygen into the material, providing necessary adhesion and solubility properties that are required for imaging performance while still retaining sufficient etch resistance to be successfully demonstrated as 193 nm resist materials.[4] The cyclic olefin character of these materials provides for excellent etch resistance, surpassing even currently utilized phenol based resists. Furthermore, the increased etch resistance is of great importance because of the decreasing film thickness necessary for the achievement of increasingly smaller feature sizes. In addition, the ability to modify the polymer properties via incorporation of cyclic

---

[1] (a) For a general review of maleic anhydride homopolymerization, see: Gaylord, N. G. *J. Macromol. Sci. Rev. Macromol. Chem.* **1975**, *13*, 235. (b) Regel, W.; Schneider, C. *Makromol. Chem.* **1981**, *182*, 237.

[2] Walling, C.; Briggs, E. R.; Wolfstirn, K. B.; Mayo, F. R. *J. Am. Chem. Soc.* **1948**, *70*, 1537. Barb, W. G. *J. Polym. Sci.* **1953**, *11*, 117. Seymour, R. B.; Garner, D. P. *Polymer* **1976**, *17*, 21. Block, H.; Cowd, M. A.; Walker, S. M. *Polymer* **1972**, *13*, 549. Gaylord, N. G.; Maiti, S.; Patnaik, B. K.; Takahashi, A. *J. Macromol. Sci., Chem.* **1972**, *A6*, 1459. Gaylord, N. G.; Maiti, S. *J. Macromol. Sci., Chem.* **1972**, *A6*, 1481. Fujimori, K. *J. Macromol. Sci., Chem.* **1975**, *A9*, 495. Caze, C.; Loucheux, C. *J. Macromol. Sci., Chem.* **1975**, *A9*, 29.

[3] Allen, R. D.; Opitz, J.; Larson, C. E.; Wallow, T. I.; Hofer, D. C. *Microlithography World*, *5* (winter 1999).

[4] Houlihan, F. M.; Wallow, T. I.; Nalamasu, O.; Reichmanis, E. *Macromolecules* **1997**, *30*, 6517.

olefin monomer derivatives to improve lithographic performance has further made this a very attractive route to new materials for 193 nm lithography.

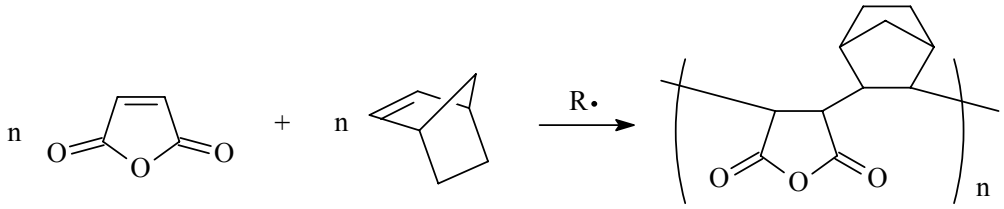

Scheme 9.1 Radical alternating copolymerization of maleic anhydride and norbornene.

The alternating copolymerization of cyclic olefins with maleic anhydride offers exceptional versatility in the compositional design of new macromolecules due to both inherent polarity and potential reactivity of the anhydride functionality. Previous studies have focused on the investigations of various experimental factors that affect the molecular weight, yield, and composition of maleic anhydride (MAH), norbornene (Nb), and an acid cleavable ester functionalized norbornene, *tert*-butyl 5-norbornene-2-carboxylate (NbTBE).[5] In addition, the adhesive and lithographic properties of these co- and terpolymers were evaluated as a function of the amount of ester Nb derivative that was incorporated using work of adhesion (W_{adh}) values to silicon substrates (treated with hexamethyldisilazane) employing the method of fractional surface free energy.[6]

Facile Diels-Alder reactions of cyclopentadiene with functional olefins offer further versatility due to the potential to synthesize a number of norbornene derivatives that can be copolymerized with maleic anhydride.[7] Further polymer modification of the anhydride functionality provides for a myriad of structures that can be produced via this strategy

---

[5] Pasquale, A. J.; Allen, R. D.; Long, T. E. *Macromolecules* **2001**, *34*, 2108.
[6] Pasquale, A. J.; Truong, H.; Allen, R. D.; Long, T. E. *J. Adhes.* **2002**, *78*, 1.
[7] Sauer, J.; Sustmann, R. *Agnew. Chem. Int. Ed. Engl.* **1980**, *19*, 779.

(Figure 9.1). For example, hydrolysis of the anhydride functionality yields two acid functionalities per anhydride repeat unit.[8]

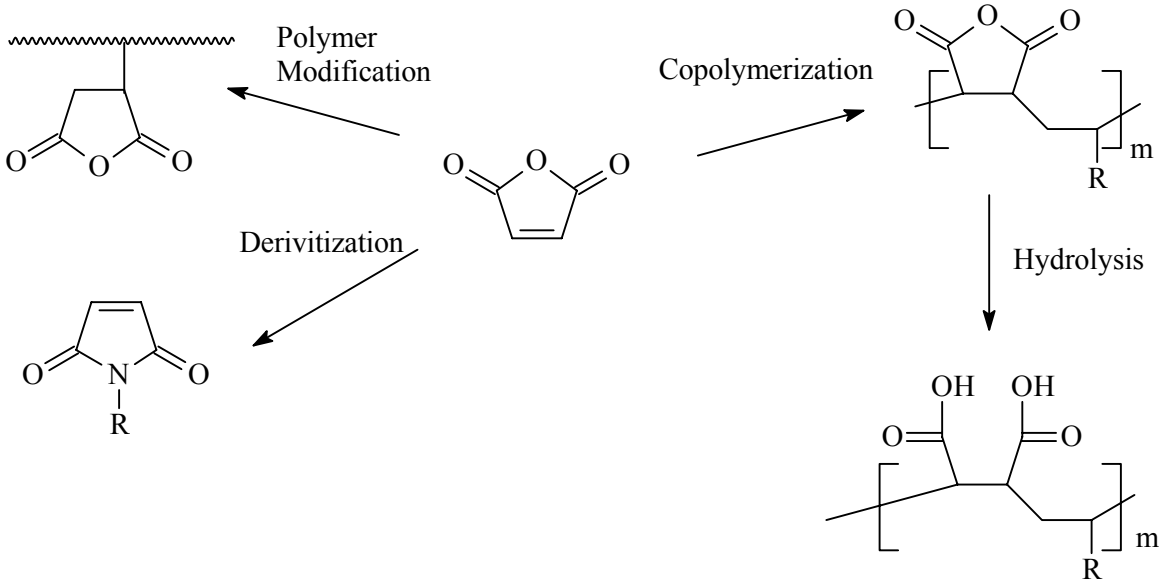

Figure 9.1 Potential maleic anhydride modifications.

9.3 EXPERIMENTAL

9.3.1 Materials

Norbornene (Nb) was purchased from Aldrich and vacuum distilled (0.1 mm Hg) at room temperature from calcium hydride after degassing three times using the traditional freeze-thaw method. After distillation, it was stored under positive nitrogen pressure as a solution in tetrahydrofuran. Maleic anhydride (MAH) was purchased from Aldrich and purified via sublimation immediately prior to use. Tetrahydrofuran was distilled using the classic sodium/benzophenone ketyl. Cyclopentadiene was obtained from cracking

[8] Rim, P. B.; O'Connor, K. M. *J. Appl. Polym. Sci.* **1986**, *32*, 4679.

dicyclopentadiene (Scheme 9.2) at approximately 160 °C. All other reagents were purchased from Aldrich and used as received.

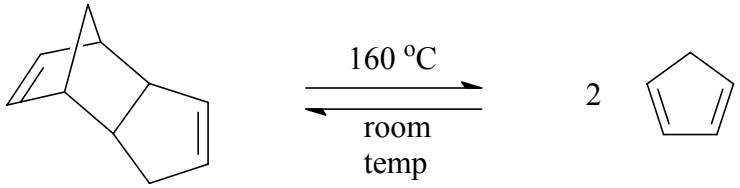

Scheme 9.2 Reverse Diels-Alder cracking reaction of dicyclopentadiene.

9.3.2 Characterization

Molecular Weight Characterization

Molecular weights were measured using a Wyatt miniDAWN multiangle laser light scattering (MALLS) detector with a 690 nm laser (Wyatt Technology, Santa Barbara, CA) connected to a Waters SEC (515 pump, 717 autosampler, and 410 refractive index detector). The miniDAWN was connected in series after three 5-μm Plgel mixed-bed columns (Polymer Laboratories, Amherst, MA). Measurements were made at 40 °C with THF as the solvent at a flow rate of 1.0 mL/min.

Thermogravimetric Analysis

Thermogravimetric analysis (TGA) was carried out under nitrogen with a TA Instruments TGA 295Thermogravimetric Analyzer at a heating rate of 10 °C/minute.

NMR Characterization

^{1}H NMR spectra were obtained using a Varian UNITY 400 spectrometer at 400 MHz in $CDCl_3$ at ambient temperature. ^{13}C NMR spectra were obtained using a Varian UNITY-400 spectrometer at 100 MHz in DMSO-d_6 at ambient temperature.

In situ FTIR

In situ mid-FTIR spectra were collected with a ReactIR 1000 (MCT detector, S/N = 7500, resolution = 4) (ASI Applied Systems, Millersville, MD, www.asirxn.com) reaction analysis system equipped with a light conduit and DiComp (diamond-composite) insertion probe (Figure 9.2). Reaction data was analyzed using ReactIR software. The details and capabilities of the ReactIR 1000 reaction analysis system based on attenuated total reflectance (ATR) have been described in detail previously.[9]

Figure 9.2 ASI ReactIR 1000 *in situ* FTIR instrument.

Contact Angles

[9] Storey, R. F.; Donnalley, A. B.; Maggio, T. L. *Macromolecules* **1998**, *31*, 1523.

Cyclic olefin/maleic anhydride copolymers were spin coated (2000 rpm) on hexamethyldisilazane (HMDS) treated silicon wafers from 0.25 μm filtered 13 % (w/w) cyclohexanone solutions. The films were baked at 120 °C for approximately 2 min to remove residual solvent. Contact angles of water on the polymer films were measured using a contact angle goniometer (Figure 9.3). Reported values are the average of eight measurements.

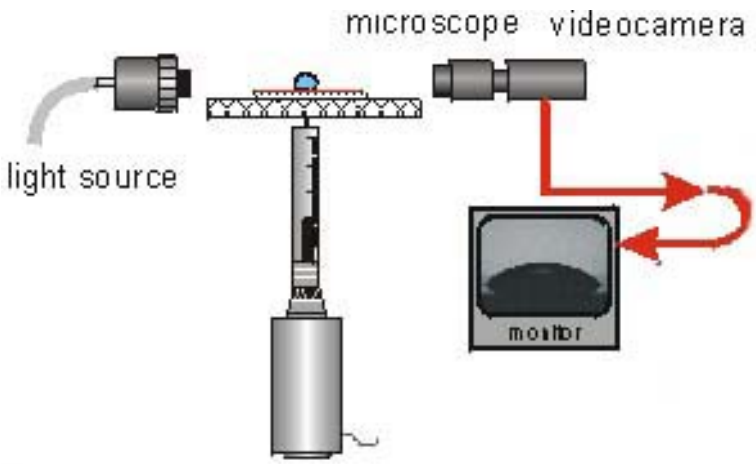

Figure 9.3 Basic schematic of a contact angle goniometer.

9.3.3 tert-Butyl 5-Norbornene-2-carboxylate (NbTBE) (Scheme 9.3)

Freshly cracked cyclopentadiene (1.45 moles, 96.0 mL) was added drop-wise via addition funnel to a stirred solution of *tert*-butyl acrylate (1.45 moles, 212.0 mL) and 3,5-di-tert-butylphenol (0.00728 moles, 1.5g) in a 500 mL round bottom flask. A water condenser was then inserted into the round bottom flask it was placed into an oil bath at 140 ºC (Figure 9.4). The reaction mixture was then stirred for 5 h at 140 ºC using a magnetic stir bar. The yellow crude liquid reaction mixture was then purified via vacuum

distillation (40 °C, 0.1 mm Hg) to give a colorless oil (88.0 g, 66 % isolated yield). GC and NMR analysis indicated the product was >99% pure and was obtained as an endo/exo isomer mixture (≅ 75/25).

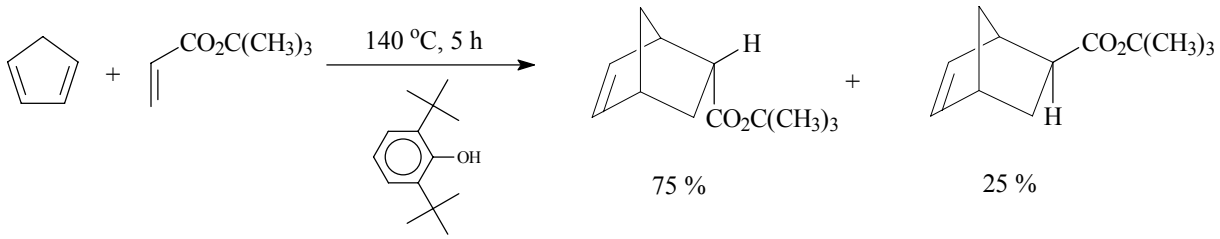

Scheme 9.3 Diels-Alder synthesis of *tert*-butyl 5-nborbornene-2-carboxylate (NbTBE).

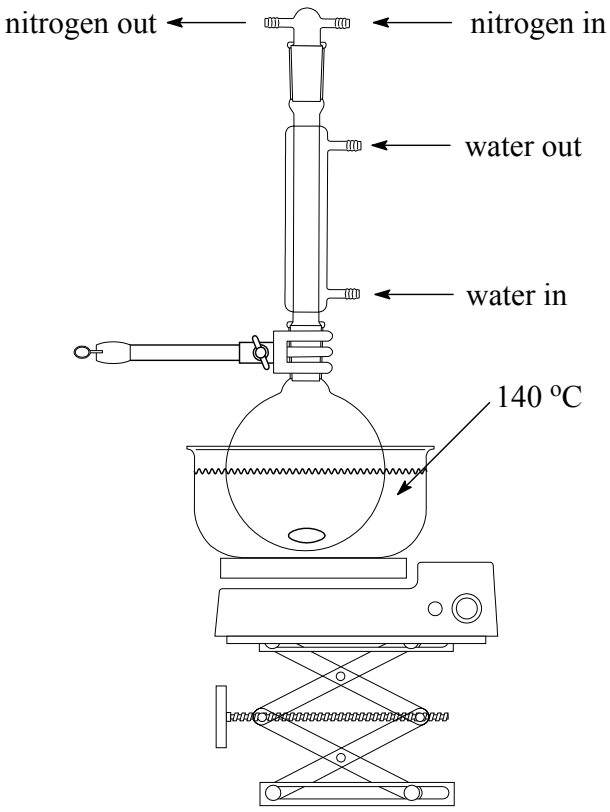

Figure 9.4 Reaction setup for Diels-Alder synthesis of *tert*-butyl 5-nborbornene-2-carboxylate (NbTBE).

9.3.4 5-Cyanobicyclo[2.2.1]hept-2-ene (NbCN) (Scheme 9.4)

Freshly cracked cyclopentadiene (1.21 moles, 80.0 g, 100 mL) was added drop-wise via addition funnel to a stirred solution of acrylonitrile (1.21 moles, 64.1 g, 80 mL) in a 500 mL round bottom flask at 0 °C (ice-water bath). After addition the ice-water bath was removed from the flask. The flask was capped with a septa and stirred using a magnetic stir bar for 24 h at room temperature (Figure 9.5). The yellow crude liquid reaction mixture was then purified via distillation at 170 °C using a water aspirator to give a slightly yellow oil (105 g, 73 % isolated yield). GC and NMR analysis indicated the product was >99% pure and was obtained as an endo/exo isomer mixture (≅ 50/50).

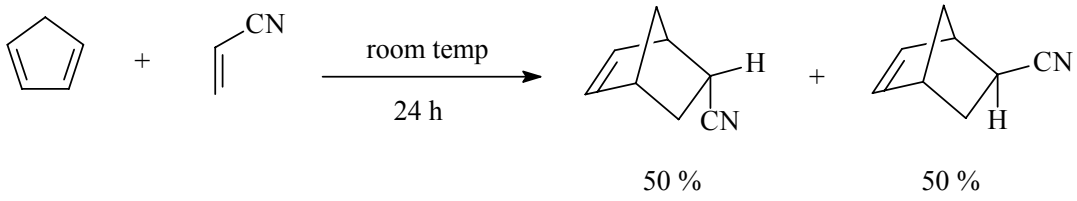

Scheme 9.4 Diels-Alder synthesis of 5-cyanobicyclo[2.2.1]hept-2-ene (NbCN).

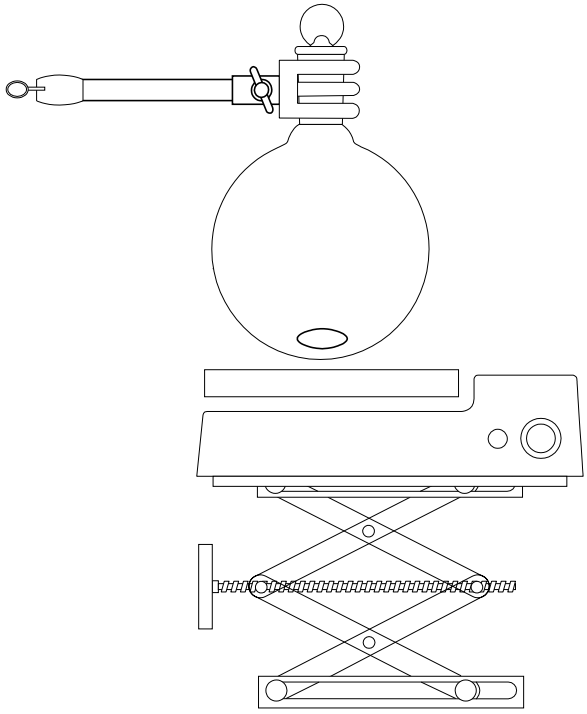

Figure 9.5 Reaction setup for Diels-Alder synthesis of 5-cyanobicyclo[2.2.1]hept-2-ene (NbCN).

9.3.5 5-Norbornene-2-phosphonate ($NbPO_3Et_2$) (Scheme 9.5)

Freshly cracked cyclopentadiene (0.152 moles, 10.1 g, 12.6 mL) was added drop-wise via addition funnel to a stirred solution of diethyl vinyl phosphonate (0.152 moles, 25 g) and 3,5-di-tert-butylphenol (0.00062 moles, 0.157 g) in a 100 mL round bottom flask. A water condenser was then inserted into the round bottom flask it was placed into an oil bath at 160-170 ºC (Figure 9.6). The reaction mixture was then stirred for 17 h at 160-170 ºC using a magnetic stir bar. The yellow crude liquid reaction mixture was then purified via vacuum distillation (70 °C, 0.1 mm Hg) to give a yellow oil (25.6 g, 74 % isolated yield). GC and NMR analysis indicated the product was >99% pure and was obtained as an endo/exo isomer mixture (≅ 53/47).

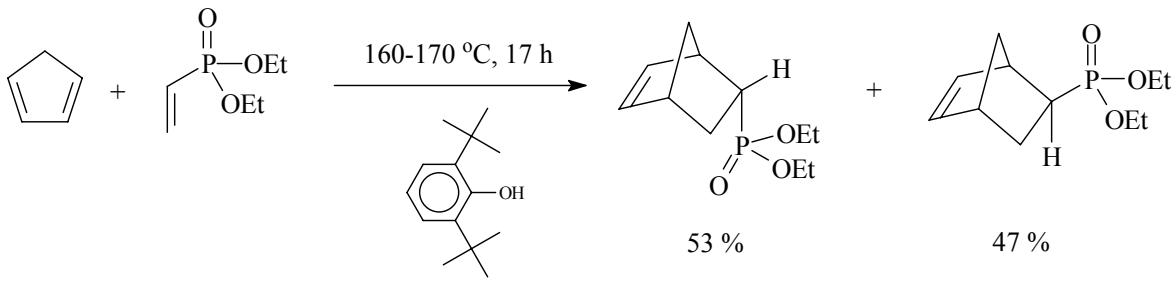

Scheme 9.5 Diels-Alder synthesis of 5-norbornene-2-phosphonate ($NbPO_3Et_2$).

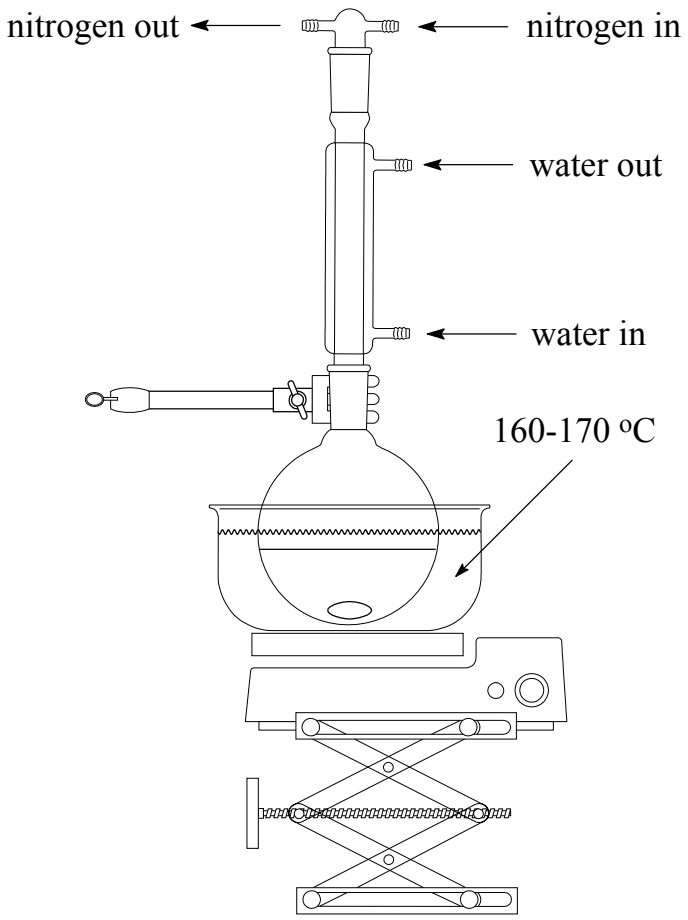

Figure 9.6 Reaction setup for Diels-Alder synthesis of 5-norbornene-2-phosphonate ($NbPO_3Et_2$).

9.3.6 Poly(NbTBE-*alt*-MAH) (Scheme 9.6)

In a 100 mL, round-bottomed, three-necked flask that was fitted with the ReactIR 1000 DiComp probe was added a magnetic stir bar, *tert*-butyl 5-norbornene-2-carboxylate (NbTBE) (102 mmol, 19.78 g, 20.08 mL), maleic anhydride (MAH) (102 mmol, 10.0 g), 2,2-azobisisobutyronitrile (AIBN) (6.12 mmol, 1.004 g), and THF (19.85 mL). The flask was purged with nitrogen for approximately one minute and sealed tightly under positive nitrogen pressure (4-5 psi) with rubber septa. An oil bath at 65 ºC was raised to the reaction flask and FTIR data collection was started. A schematic of the reaction setup with

in situ FTIR probe is shown in Figure 9.7. The ReactIR was programmed to collect an averaged FTIR spectrum of the reaction mixture every 5 minutes (256 scans) for the duration of the reaction. The reaction was then stirred at 65 ºC for 24 h while collecting FTIR spectra. The oil bath was removed after 24 h and the reaction contents were allowed to cool to room temperature. After 24 h, the reaction mixture had solidified to a glass and was no longer stirring. The DiComp probe was removed from the reaction flask and THF (~ 50 mL) was added to dissolve the solid glass. After completely dissolving in THF (approx. 24 h), the dissolved material was precipitated into hexanes (~ 500 mL), filtered, washed with isopropyl alcohol (~ 200 mL) and dried overnight under vacuum (0.1 mm Hg) at approx. 75 ºC to give 18.0 g (60 % yield) of white powder. GPC: M_n = 6,960 (M_w/M_n = 1.60).

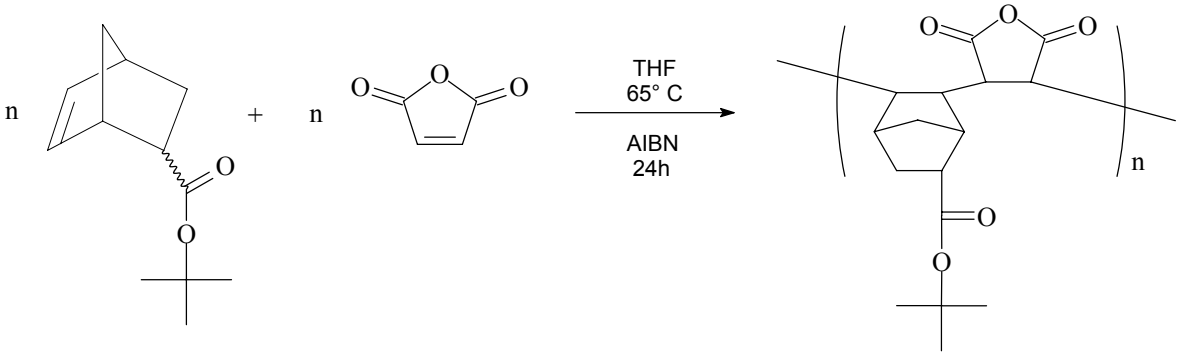

Scheme 9.6 NbTBE/MAH alternating copolymerization scheme.

9.3.7 Poly(NbCN-*alt*-MAH) (Scheme 9.7)

In a 100 mL, round-bottomed, three-necked flask that was fitted with the ReactIR 1000 DiComp probe was added a magnetic stir bar, 5-cyanobicyclo[2.2.1]hept-2-ene (NbCN) (102 mmol, 12.14 g, 12.14 mL), maleic anhydride (MAH) (102 mmol, 10.0 g), 2,2-azobisisobutyronitrile (AIBN) (6.12 mmol, 1.004 g), and THF (16.6 mL). The flask was purged with nitrogen for approximately one minute and sealed tightly under positive

nitrogen pressure (4-5 psi) with rubber septa. An oil bath at 65 ºC was raised to the reaction flask and FTIR data collection was started. A schematic of the reaction setup with *in situ* FTIR probe is shown in Figure 9.7. The ReactIR was programmed to collect an averaged FTIR spectrum of the reaction mixture every 5 minutes (256 scans) for the duration of the reaction. The reaction was then stirred at 65 ºC for 24 h while collecting FTIR spectra. The oil bath was removed after 24 h and the reaction contents were allowed to cool to room temperature. The DiComp probe was removed from the reaction flask and THF (~ 50 mL) was added to dissolve the viscous reaction mixture. After completely dissolving in THF (approx. 24 h), the dissolved material was precipitated into hexanes (~ 500 mL), filtered, washed with isopropyl alcohol (~ 200 mL) and dried overnight under vacuum (0.1 mm Hg) at approx. 75 ºC to give 5.55 g (25 % yield) of white powder. GPC: M_n = 3,100 (M_w/M_n = 1.20).

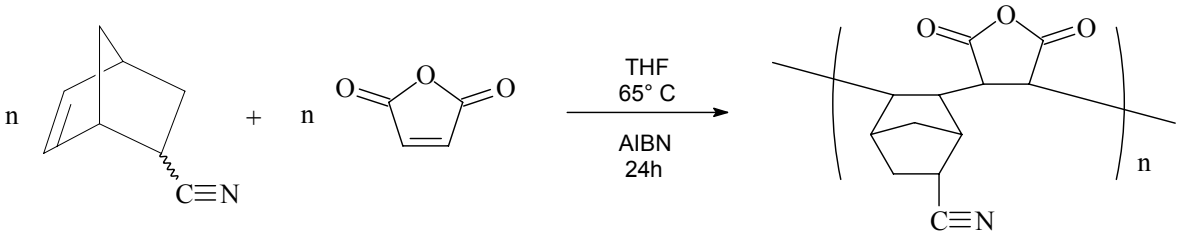

Scheme 9.7 NbCN/MAH alternating copolymerization scheme.

9.3.8 Poly($NbPO_3Et_2$-*alt*-MAH) (Scheme 9.8)

In a 100 mL, round-bottomed, three-necked flask that was fitted with the ReactIR 1000 DiComp probe was added a magnetic stir bar, 5-norbornene-2-phosphonate ($NbPO_3Et_2$) (50 mmol, 11.5 g, 10.5 mL) maleic anhydride (MAH) (50 mmol, 4.9 g), 2,2-azobisisobutyronitrile (AIBN) (3.0 mmol, 0.492 g), and THF (12.3 mL). The flask was purged with nitrogen for approximately one minute and sealed tightly under positive nitrogen pressure (4-5 psi) with rubber septa. An oil bath at 65 ºC was raised to the

reaction flask and FTIR data collection was started. A schematic of the reaction setup with *in situ* FTIR probe is shown in Figure 9.7. The ReactIR was programmed to collect an averaged FTIR spectrum of the reaction mixture every 5 minutes (256 scans) for the duration of the reaction. The reaction was then stirred at 65 ºC for 24 h while collecting FTIR spectra. The oil bath was removed after 24 h and the reaction contents were allowed to cool to room temperature. The DiComp probe was removed from the reaction flask and THF (~ 50 mL) was added to dilute the viscous reaction mixture. After completely dissolving in THF (approx. 24 h), the solution was precipitated into hexanes (~ 500 mL), filtered, washed with isopropyl alcohol (~ 200 mL) and dried overnight under vacuum (0.1 mm Hg) at approx. 75 ºC to give 8.0 g (49 % yield) of white powder. GPC: M_n = 1,280 (M_w/M_n = 1.38).

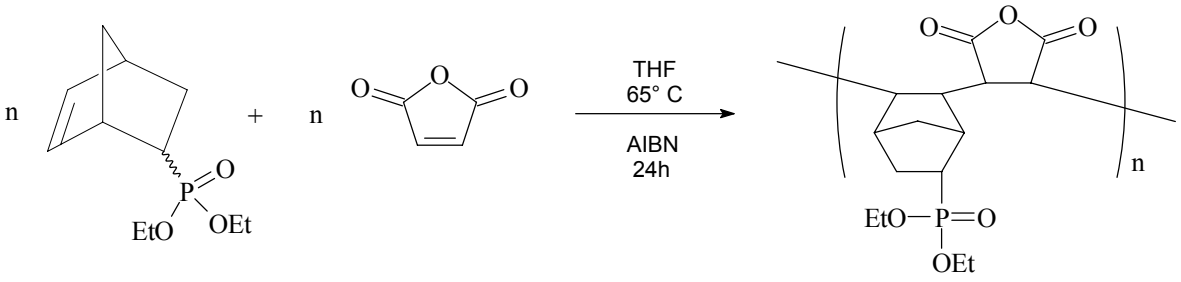

Scheme 9.8 $NbPO_3Et_2$/MAH alternating copolymerization scheme.

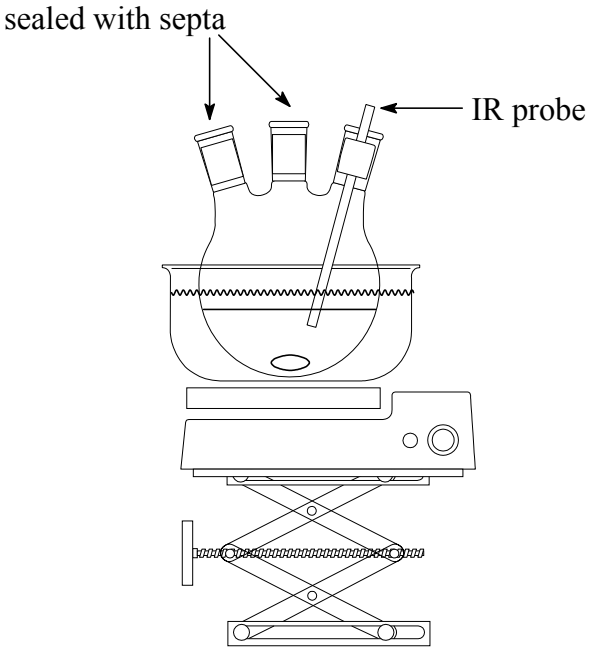

Figure 9.7 Terpolymerization setup with *in situ* FTIR monitoring.

9.3.9 Poly(Nb-alt-MAH) Hydrolysis

In a 50 mL round-bottomed flask poly(Nb-*alt*-MAH) (5.0 g) was dissolved in THF/water (40 mL/5.0 mL). Concentrated HCl (5.0 mL) (approximately 2.0 equivalents per anhydride unit) was then added dropwise to the solution at room temperature. After complete addition of HCl, the homogeneous reaction was stirred for 24 h at 50 °C. The reaction mixture was precipitated into hexanes (200 mL), filtered, and dried under vacuum at 60 °C to give 5.9 g (94% yield assuming complete hydrolysis).

9.4 RESULTS AND DISCUSSION

9.4.1 Diels-Alder Synthesis of Nb Derivatives

Diels-Alder cycloaddition reactions are very useful in the synthesis of small organic compounds due to their high yield and high stereospecificity.[10] The Diels-Alder cycloaddition involves the 1,4-addition of a conjugated diene in the *cis* conformation to an alkene (dienophile) in which two new sigma bonds are formed from two pi bonds. The reaction is not polar and no charged or radical intermediates are involved. It is known as a concerted reaction, where the bonds are broken and formed simultaneously (Scheme 9.9). The reaction works best when there is an appreciable difference between the electron densities in the diene and the dienophile. Typically, the dienophile contains electron-withdrawing groups while the diene is electron rich. The resulting adduct is a six-membered cycloalkene.

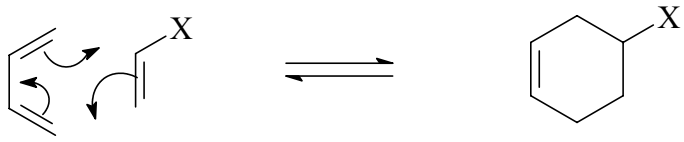

X = electron withdrawing group

Scheme 9.9 Diels-Alder concerted cycloaddition reaction.

Cyclopentadiene is an electron-rich, conjugated diene that is very useful for Diels-Alder cycloaddition reactions. The resulting Diels-Alder adducts formed from the reaction of cyclopentadiene with α-olefins are norbornene derivatives that can subsequently be copolymerized with maleic anhydride in order to introduce further functionality into the copolymer backbone. The synthesis of several functionalized norbornene derivatives was achieved from the reaction of cyclopentadiene and various α-olefins (Scheme 9.10).

---

[10] Solomons, T. W. G. *Organic Chemistry*, 6th ed.; Wiley & Sons: New York, 1996; Ch 12.

Cyclopentadiene was obtained from the reverse Diels-Alder cracking reaction of the stable dimer, dicyclopentadiene, which is the Diels-Alder adduct from two molecules of the diene (Scheme 9.2). Cyclopentadiene and the α-olefins were reacted together in equimolar amounts. The reactions involving *tert*-butyl acrylate and diethyl vinyl phosphonate required high heat for reaction and were carried out in the presence of a free radical inhibitor, 3,5-di-*tert*-butylphenol. The reaction with acrylonitrile, which contains a very strong electron withdrawing group, was carried out at room temperature. The reaction mixtures were purified using vacuum distillation to give the Diels-Alder adducts as mixtures of endo and exo isomers. The resulting yields and endo/exo isomer ratios are summarized in Table 9.1.

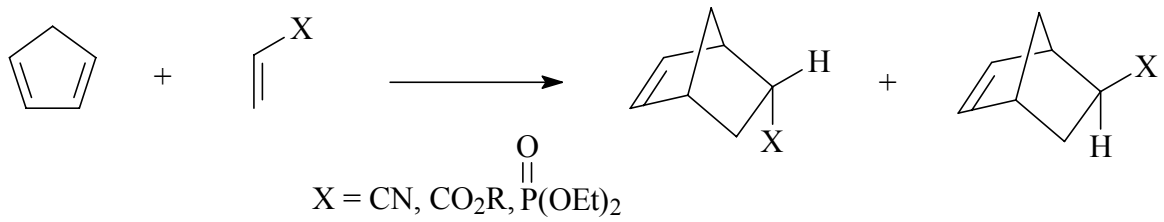

Scheme 9.10 Nb derivatives synthesized via Diels-Alder Cycloadditions.

Table 9.1 Summary of cycloaddition reactions to synthesize norbornene derivatives.

X	rxn temp. (°C)	yield (%)	endo/exo
$CO_2C(CH_3)_3$	25	66	75/25
CN	140	73	50/50
PO_3Et_2	160-170	74	53/47

9.4.2 Alternating Copolymerization of Norbornene Derivatives with Maleic Anhydride

Norbornene (Nb) derivatives were copolymerized with maleic anhydride (MAH) using optimized reaction conditions that were determined earlier for Nb/MAH alternating copolymerization (*i.e.* 3.0 mole percent AIBN, THF (60% solids), 65 ºC.[11] Typically, very high yields (>90%) are obtained from alternating copolymerizations of MAH and norbornene (Nb) under these conditions. However, lower yields consistently resulted from copolymerizations of MAH with the Nb derivatives. In addition, number average molecular weights were also lower for copolymers of MAH with the derivatives than the typical number average molecular weight for poly(Nb-*alt*-MAH) copolymers (≅ 7,000 g/mol). Yields, number average molecular weights, and molecular weight distributions for copolymerizations of MAH with Nb and the Nb derivatives are summarized in Table 9.2.

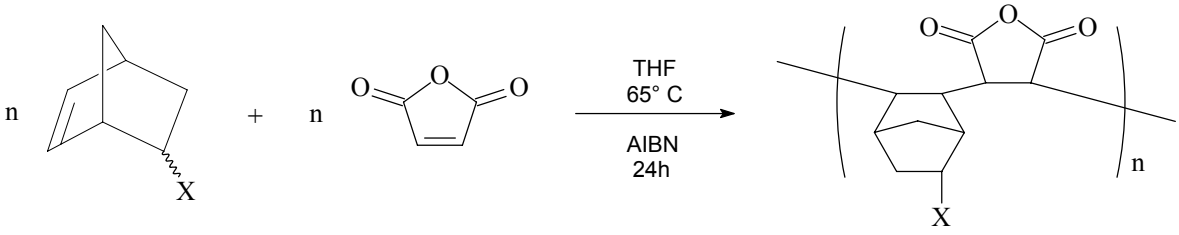

Scheme 9.11 Copolymerization of norbornene derivatives with maleic anhydride.

[11] Pasquale, A. J.; Karro, R.; Allen, R. D.; Long, T. E. *Polym. Prepr. (Am. Chem. Soc., Div. Polym. Chem.)* **2000**, *41*(2), 1931.

Table 9.2 Summary of free radical copolymerizations of maleic anhydride with norbornene.

X	yield (%) [a]	M_n [b]	M_w/M_n [b]
H	94	7,400	1.9
$CO_2C(CH_3)_3$	60	6,960	1.6
CN	25	3,100	1.2
PO_3Et_2	49	1,280	1.4

[a] Isolated yield. [b] Wyatt miniDAWN multiple angle laser light scattering detector in-line with Waters SEC system (410 RI detector), THF solvent at 40 °C and 1.0 mL/min flow rate.

9.4.3 Poly(Nb-*alt*-MAH) Hydrolysis

The hydrolysis of poly(Nb-*alt*-MAH) polymers were carried out using acidic reaction conditions and is outlined in Scheme 9.12. Approximately 2.0 equivalents of HCl per anhydride unit were added to a stirred solution of the copolymer dissolved in a THF/water mixture. After complete addition of the HCl, the mixture was heated to 50 °C and stirred for 24 h. The resulting product was precipitated into hexanes, dried, and characterized using GPC, FTIR, and NMR spectroscopy.

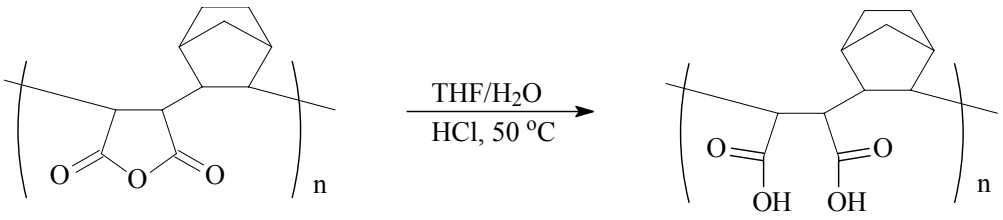

Scheme 9.12 Acid catalyzed hydrolysis of poly(Nb-*alt*-MAH).

The carbonyl region of the infrared spectrum for poly(Nb-*alt*-MAH) and the corresponding hydrolyzed polymer, poly(Nb-*alt*-MA(maleic acid)) is illustrated in Figure 9.8. The hydrolysis of the anhydride is indicated by the decrease in the absorbance of the characteristic anhydride peaks at 1760 and 1850 cm^{-1} and the increase of the carboxylic acid carbonyl absorbance at 1710 cm^{-1}. In addition, residual anhydride absorbances in the spectrum of poly(Nb-*alt*-MAH) indicated that approximately 80 % conversion of the anhydride to acid was achieved. Figure 9.9 illustrates the characteristic nitrile functional group absorbance at 2230 cm^{-1} for the three copolymers. The poly(Nb-*alt*-MAH) control shows no absorbance as expected while both poly(NbCN-*alt*-MAH) and poly(NbCN-*alt*-MA) exhibited similar nitrile absorbances, which indicated that selective hydrolysis of the anhydride functionality was possible in the presence of the nitrile functional group.

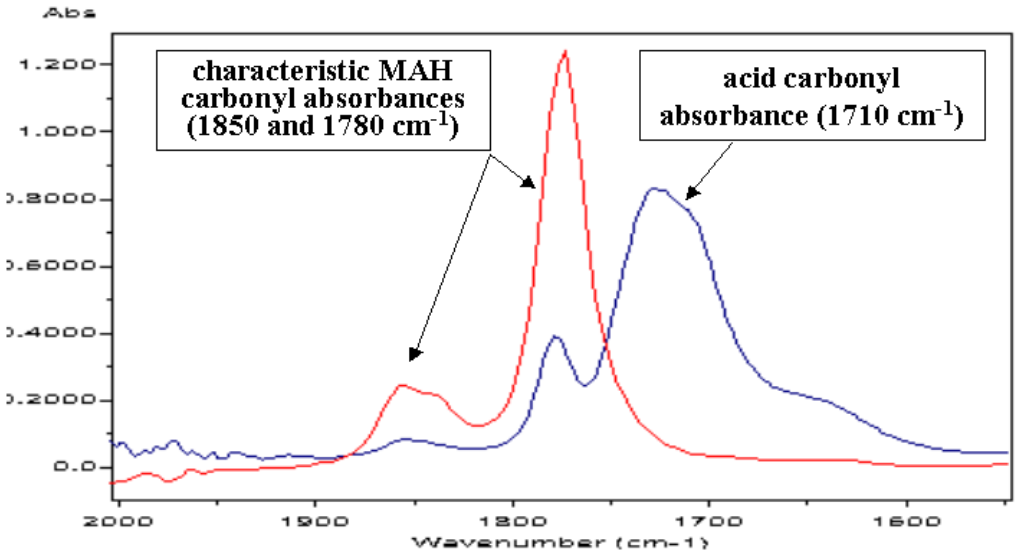

Figure 9.8 Maleic anhydride FTIR carbonyl region illustrating acid catalyzed hydrolysis of the anhydride functionality.

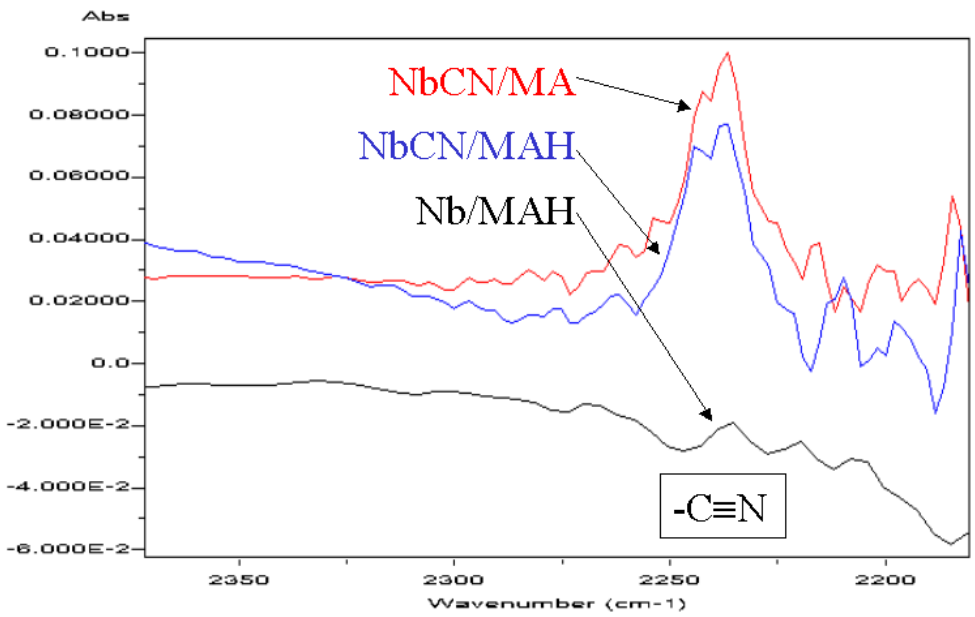

Figure 9.9 FTIR nitrile region showing toleration of nitrile functionality to acid hydrolysis reaction conditions.

The surface properties of the copolymers were evaluated from the measurement of water contact angles on films that were spin coated (2000 rpm) on hexamethyldisilazane (HMDS) treated silicon wafers from 0.25 μm filtered 13 % (w/w) cyclohexanone solutions. The resulting contact angles are summarized in Figure 9.10. The contact angle gives an estimation of the polarity for the surface of the copolymer film. As was expected, the measured contact angle was lower for the hydrolyzed material and the copolymers containing the polar nitrile and phosphine oxide functionalities.

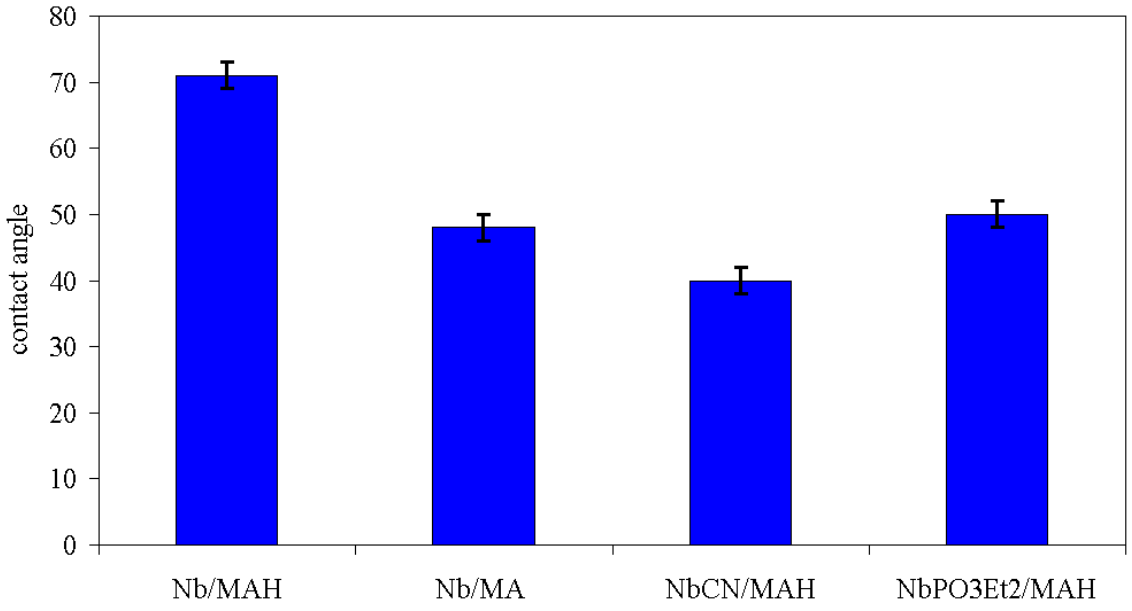

Figure 9.10 Water contact angles on alternating copolymer films.

9.4.4 Copolymerization Rates of Nb Derivatives with MAH

In situ mid-FTIR was used to collect monomer conversion data for the copolymerization of MAH with Nb derivatives. *In situ* infrared spectroscopy provided real-time changes in monomer absorbances and allowed for comparative kinetic analysis of the free radical copolymerization of MAH with Nb derivatives. A reaction flask was specifically designed to permit the introduction of the ATR based infrared probe and attention was devoted to ensure the reactor was sealed to eliminate any volatilization of reaction components. Strong vinylene (=C-H) absorbances of the monomers were observed and allowed for kinetic analysis of the copolymerizations using *in situ* FTIR. The waterfall plot of the vinylene =C-H region for a Nb/MAH (50/50 mol ratio) copolymerization is illustrated in (Figure 9.11**)**. Infrared absorbances that were due to the olefinic functionality, which decreases as the monomers propagate, were identified for both Nb and MAH (MAH at 695 cm^{-1} and Nb and Nb derivatives at 710 cm^{-1}).

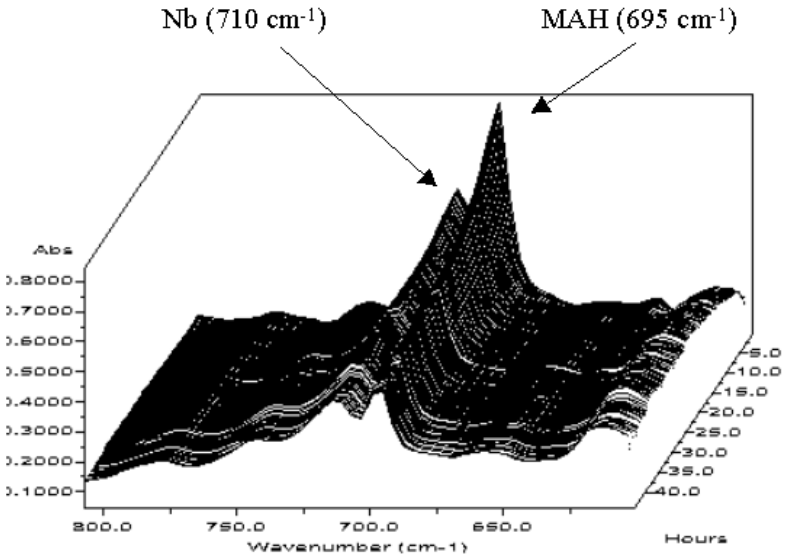

Figure 9.11 Vinylene region of *in situ* FTIR "waterfall" plot for 50/50 Nb/MAH alternating copolymerization.

Kinetic studies of free radical alternating copolymerizations of MAH with Nb derivatives indicate that there is a strong electronic effect of the Nb substituents on the rate of copolymerization with MAH. Observed rates (k_{obs}) for copolymerization of MAH with Nb derivatives containing electron-withdrawing substituents (X=CN and X=$CO_2C(CH_3)_3$) were measured using *in situ* FTIR. Pseudo first order kinetic plots were constructed from the data obtained using *in situ* monomer absorbance profiles. Kinetic interpretations have been based on the assumption of pseudo first order kinetics for an alternating polymerization mechanism (Figure 9.12). Excellent agreement was observed using these assumptions and linear kinetic plots were observed. First order kinetic plots constants for Nb, NbCN, and NbTBE are illustrated in Figure 9.13. A dramatic decrease in the rate of copolymerization was observed with Nb comonomers containing electron-withdrawing functionality. The k_{obs} decreased from 6.7 x 10^{-5} s^{-1} for a Nb/MAH copolymerization to 1.1 x 10^{-5} s^{-1} for NbTBE/MAH copolymerization and to 3.2 x 10^{-6} s^{-1} for NbCN/MAH

copolymerization. The pendant groups increase the bulkiness of the Nb comonomer, and one could the reduced rate to be primarily due to steric effects. However, the Nb containing the nitrile functionality, which is much less bulky than the *tert*-butyl ester group, copolymerized with MAH significantly slower than NbTBE. In addition, it is interesting to note that neither the endo or exo isomers of either derivative showed a preference for copolymerization. These results suggested that the predominant factor resulting in slower rates of copolymerization is due to the polar influence of the substituent. Unfortunately, ^{13}C NMR ($CDCl_3$) of Nb monomers did not exhibit appreciable differences in the olefinic carbon chemical shifts that could be quantitated as a function of electron withdrawing functionality.

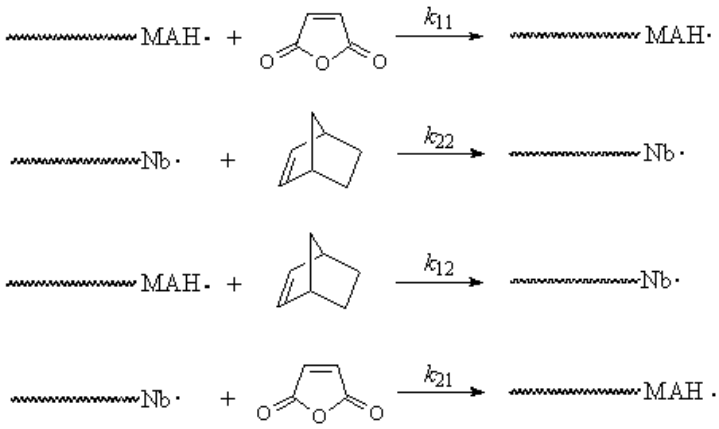

assuming negligible homopolymerization of MAH and Nb, k_{11}=k_{22}=0, overall rate is:

$$\text{rate} = k_{12}[(\text{MAH}\cdot)(\text{Nb})] + k_{21}[(\text{Nb}\cdot)(\text{MAH})]$$

assuming a steady state concentration of radical and alternating polymerization, rate is:

$$\text{rate} = (k_{12} + k_{21})([\text{P}\cdot][\text{M}])$$

where [P·] = conc. of growing polymer radicals and [M] = conc. of MAH or Nb monomer

and therefore an observed rate constant (k_{obs}) is obtained from a plot of ln[M] vs. time

$$\boldsymbol{k_{obs} = (k_{12} + k_{21})[\text{P}\cdot]}$$

Figure 9.12 Pseudo first order alternating kinetic assumptions for a norbornene/maleic anhydride alternating copolymerization.

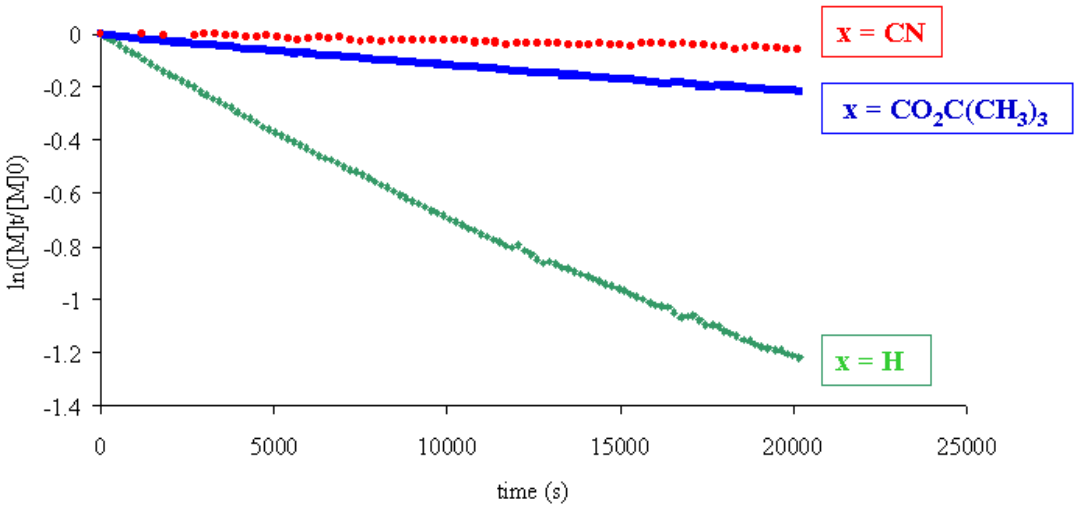

Figure 9.13 Psuedo first order kinetic plots for the free radical copolymerization of maleic anhydride with various norbornene derivatives.

9.5 CONCLUSIONS

Several norbornene derivatives were synthesized via facile Diels-Alder cycloaddition reactions of cyclopentadiene with α-olefins containing an electron withdrawing groups. Maleic anhydride (MAH) was copolymerized with the substituted norbornene derivatives using free radical solution polymerization conditions previously optimized for copolymerizations of norbornene and maleic anhydride. Further functionality was introduced from acid catalyzed hydrolysis of poly(Nb-*alt*-MAH) and poly(NbCN-*alt*-MAH) copolymers, which resulted in selective hydrolysis of the anhydride functionality. FTIR confirmed hydrolysis of the anhydrides to acid functionalities and indicated no appreciable hydrolysis of the nitrile functionality. Observed rates (k_{obs}) for copolymerization of MAH with Nb derivatives containing electron-withdrawing substituents (X=CN and X=$CO_2C(CH_3)_3$) were measured using *in situ* FTIR. A significant decrease in the rate of copolymerization was observed for the Nb derivatives that contained the strongly electron-withdrawing functionalities, which indicated there is a significant

electronic influence on the free radical copolymerization rate with maleic anhydride due to the electron withdrawing strength of the Nb substituents.

Acknowledgements. Financial support was provided by IBM, the Jeffress Memorial Trust, and the National Science Foundation (CRIF CHE-9974632) and is gratefully acknowledged. The authors would also like to thank the Center for Adhesive and Sealant Science (CASS) at Virginia Tech and the Adhesive and Sealant Council (ASC) for financial support through an ASC Education Foundation Research Fellowship.

Recommended future studies:

- Rate studies with additional derivatives to quantitate the polar influence on the rate of copolymerization.
- Explore feasibility of using the water soluble hydrolyzed copolymers as metal particle stabilizers in aqueous media.
- Synthesize series of Nb ester derivatives containing different size alkyl groups to probe more accurately steric vs. polar effects on the rate of copolymerization.
- NMR studies in THF-d_8 to probe chemical shift of olefinic carbons in a polar solvent.

Summary

Linear polystyrene oligomers (M_n = 19,300 g/mol, M_w/M_n = 1.10) were prepared in bulk styrene using benzoyl peroxide in the presence of 2,2,6,6-tetramethyl-1-piperidinyloxy (TEMPO) at approximately 130 °C. *In situ* mid-infrared spectroscopy was successfully utilized to follow initiation, monomer conversion, and polymer formation. Real-time data allowed for the determination of apparent rate constants ($k_{app}=k_p[P_n\bullet]$) of (2.1 ± 0.02) x 10^{-5} s^{-1} at 132 °C and (1.2 ± 0.02) x 10^{-5} s^{-1} at 126 °C from the profile of the decaying styrene vinyl carbon-hydrogen (=CH_2) absorbance at 907 cm^{-1}. High molecular weight star-shaped polystyrenes were prepared via the coupling of TEMPO terminated polystyrene oligomers with divinylbenzene (DVB) in *m*-xylene at 138 °C. The optimum ratio of the coupling solvent (*m*-xylene) to divinylbenzene coupling agent was empirically determined to be 9 to 1 based on volume. Coupling of the TEMPO terminated oligomers under optimum conditions resulted in a compact and dense product with a number average molecular weight exceeding 300,000 g/mol (M_w/M_n = 3.03) after 24 h, suggesting the formation of relatively well-defined star-shaped polymers. The stability of the TEMPO terminated oligomers was investigated at coupling reaction conditions in the absence of DVB. SEC chromatograms of the precursor TEMPO terminated oligomer and a sample subjected to the coupling conditions in the absence of DVB were super-imposable indicating the absence of appreciable molecular weight change. The intrinsic viscosities and RMS radius of the star-shaped products were lower than calculated values for linear analogs of equivalent molecular weight, which further supported the formation of compact, star-shaped architectures.

Synthetic factors that affect the molecular weight, yield, and composition of maleic anhydride (MAH), norbornene (Nb), and *tert*-butyl 5-norbornene-2-carboxylate (NbTBE) terpolymers were investigated. Pseudo first order kinetic analysis using *in situ* FTIR indicated that the observed rate of reaction (k_{obs}) was a strong function of the Nb/NbTBE ratio with a maximum of 6.7 x 10^{-5} s^{-1} for a 50/0/50 Nb/NbTBE/MAH monomer ratio and a minimum of 1.1 x 10^{-5} s^{-1} for a 0/50/50 Nb/NbTBE/MAH ratio. Sampling of a

Nb/NbTBE/MAH (25/25/50 mol ratio) terpolymerization and subsequent analysis using ^{1}H NMR indicated that the relative rate of Nb incorporation was approximately 1.7 (5/3) times faster than NbTBE incorporation. Calculated work of adhesion values (W_{adh}) values for Nb/NbTBE/MAH terpolymers were observed to increase as the content of NbTBE was increased. In addition, 193 nm photoresist formulations incorporating polymers with high NbTBE content showed increased imaging performance using 193 nm light and successfully produced sharp and defined features as small as 110 nm, which was seen via scanning electron microscopy (SEM). Copolymerizations of Nb and MAH with the addition of tBA or tBMA as a third monomer showed that tBMA reacted much faster than tBA under identical conditions in these systems and the conversion of Nb and MAH was disrupted more in the presence of tBMA. Polymer yields were also observed to be a function of the Nb/NbTBE ratio and also decreased with increasing NbTBE.

Free radical reactivity ratios of Nb and MAH were evaluated via graphical linear analysis of the rearranged copolymer composition equation based upon the terminal model developed by Mayo and Lewis. Copolymerization data was collected via *in situ* FTIR to low degrees of conversion (approximately 10 %) for copolymerizations of MAH and Nb. Five different MAH/Nb comonomer feed compositions were analyzed: 40/60, 45/55, 50/50, 55/45, and 60/40. Conversion data measured with *in situ* FTIR was then employed in conjunction with the rearranged copolymer composition equation to estimate MAH and Nb reactivity ratios. Both of the reactivity ratios were estimated using this method to be approximately zero, which was further indication of an alternating copolymerization mechanism.

The effect of several synthetic variables on free radical alternating copolymerizations of norbornene and maleic anhydride were evaluated using statistical design of experiments. Three variables (% AIBN initiator, % solids (in tetrahydrofuran solvent), and zinc chloride Lewis acid catalyst) were examined using a central composite design response surface for process optimization. Predictive models and 3-dimensional contour plots for yield and molecular weight responses were produced using Stat-Ease statistical software. The results of statistical DOE analysis agreed favorably with previously determined optimum conditions (using one-factor-at-a-time methods) for norbornene/maleic anhydride

alternating copolymerization. Zinc chloride was not detected by DOE to affect either yield or molecular weight. However, kinetic evaluations of Nb/MAH alternating copolymerizations using *in situ* FTIR demonstrated that the addition of zinc chloride significantly increased the rate of copolymerization, indicating true catalytic behavior.

Several norbornene (Nb) derivatives synthesized via facile Diels-Alder cycloadditions were subsequently copolymerized with maleic anhydride (MAH). Observed copolymerization rates (k_{obs}) were measured using *in situ* FTIR and a dramatic decrease in the rate of copolymerization was observed for Nb comonomers that contained a strong electron-withdrawing functionality, which indicated a significant electronic influence on the free radical copolymerization rate with maleic anhydride due to the electron withdrawing strength of the Nb substituents. Further functionality was introduced into the copolymers through acid catalyzed hydrolysis of poly(Nb-*alt*-MAH) and poly(NbCN-*alt*-MAH) copolymers. FTIR confirmed hydrolysis of the anhydrides to acid functionalities and indicated no appreciable hydrolysis of the nitrile functionality.

Vita

Anthony (A.J.) Joseph Pasquale, son of Dominic and Sharon Pasquale, was born on October 11, 1972 in Logansport, Indiana. He was raised in Canadian Lakes, Michigan and Normal, Illinois. He graduated from Normal Community High School in May of 1990. In August of the same year, he began his undergraduate studies at the University of Illinois in Urbana, Illinois. In 1992 he transferred to Illinois State University in Normal, Illinois and graduated from there in May of 1994 with a B.S. degree in Chemistry. He began employment in June of that year with Procter & Gamble in Cincinnati, Ohio as a Research Associate in Beauty Care Product Research and Development. In August of 1995, he left Procter & Gamble and entered graduate school in the Department of Chemistry at Iowa State University in Ames, Iowa. He graduated from Iowa State in December of 1998 with an M.S. degree in Organic Chemistry. In January of 1999 he entered the Ph.D. program in Chemistry at Virginia Tech. Upon completion of his Ph.D. degree in April of 2002, he will be employed with DuPont as a Division Chemist in Fluoroproducts Technology at Parkersburg, West Virginia.